

Downloaded from UvA-DARE, the institutional repository of the University of Amsterdam (UvA)
<http://hdl.handle.net/11245/2.172983>

File ID uvapub:172983
Filename Thesis
Version final

SOURCE (OR PART OF THE FOLLOWING SOURCE):

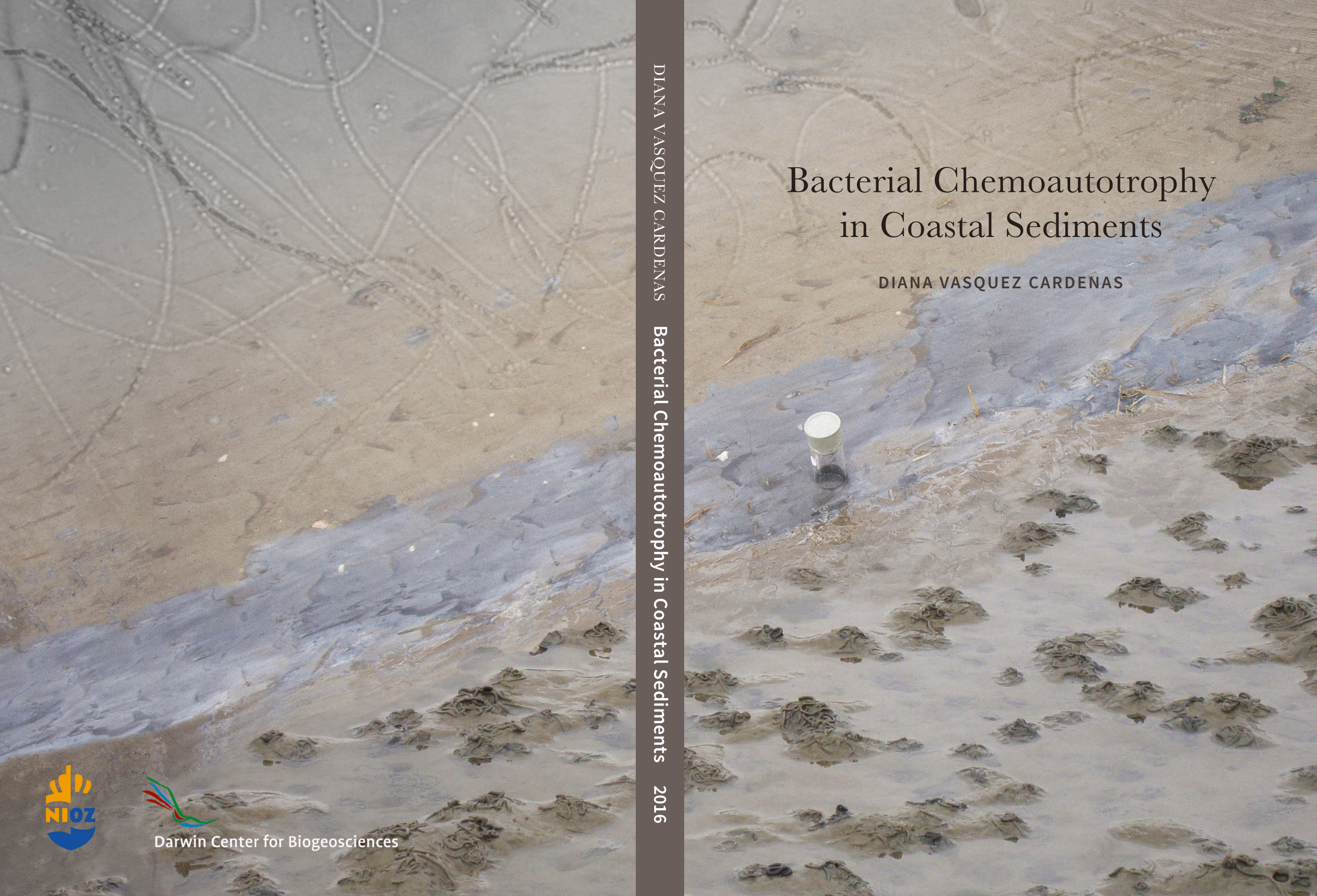
Type PhD thesis
Title Bacterial chemoautotrophy in coastal sediments
Author(s) D. Vasquez Cardenas
Faculty FNWI
Year 2016

FULL BIBLIOGRAPHIC DETAILS:

<http://hdl.handle.net/11245/1.531841>

Copyright

It is not permitted to download or to forward/distribute the text or part of it without the consent of the author(s) and/or copyright holder(s), other than for strictly personal, individual use, unless the work is under an open content licence (like Creative Commons).

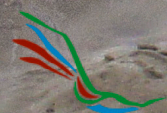
The background image shows a coastal sediment site. In the foreground, there is a shallow, muddy area with a small, clear plastic vial with a white cap, containing a dark liquid. The sediment is a mix of brown and grey, with some darker, more organic-looking patches. The overall scene is a natural, somewhat desolate coastal environment.

Bacterial Chemoautotrophy in Coastal Sediments

DIANA VASQUEZ CARDENAS

DIANA VASQUEZ CARDENAS

Bacterial Chemoautotrophy in Coastal Sediments 2016



Darwin Center for Biogeosciences

Vasquez-Cardenas D, 2016. Bacterial Chemoautotrophy in Coastal Sediments
PhD thesis, University of Amsterdam

The research presented in this thesis was carried out at the Departments of Marine Microbiology and Ecosystem Studies of the Royal Netherlands Institute for Sea Research (NIOZ and Utrecht University) in Yerseke, The Netherlands. The investigations were supported by the project “Present and past role of chemoautotrophy in marine sediments” funded by the Darwin Centre for Geoscience (grant 142.16.3060).

ISBN: 978-94-91407-33-8

Design and editing by: Alexandra Vasquez Cardenas | alexandradiseno.com

Printed by: Wöhrmann Print Service, Zutphen, the Netherlands

*Bacterial Chemoautotrophy
in Coastal Sediments*

DIANA VASQUEZ CARDENAS

Bacterial Chemoautotrophy in Coastal Sediments

ACADEMISCH PROEFSCHRIFT

ter verkrijging van de graad van doctor
aan de Universiteit van Amsterdam
op gezag van de Rector Magnificus
prof. dr. D.C. van den Boom

ten overstaan van een door het College voor Promoties ingestelde commissie,

in het openbaar te verdedigen in de Agnietenkapel

op donderdag 12 mei 2016, te 10:00 uur

door Diana Vasquez Cardenas

geboren te Santa Fe de Bogotá, Colombia

PROMOTIECOMMISSIE:

Promotor:	Prof. dr. L.J. Stal	Universiteit van Amsterdam
Copromotores:	Dr. ir. H.T.S. Boschker Prof. dr. ir. F.J.R. Meysman	NIOZ NIOZ, Vrije Universiteit Brussel
Overige Leden:	Prof. dr. J. Huisman Prof. dr. C.P.D Brussaard Prof. dr. G. Muijzer Dr. H.G. van der Geest Dr. M. Mußmann Prof. dr. K. Jürgens Dr. L. Villanueva	Universiteit van Amsterdam Universiteit van Amsterdam Universiteit van Amsterdam Universiteit van Amsterdam University of Vienna Leibniz Institute for Baltic Sea Research NIOZ

Contents

CHAPTER 1 <i>Introduction</i>	9
CHAPTER 2 <i>Chemoautotrophic carbon fixation rates and active bacterial communities in intertidal marine sediments</i>	31
CHAPTER 3 <i>Microbial carbon metabolism associated with electrogenic sulfur oxidation in coastal sediments</i>	52
CHAPTER 4 <i>Impact of seasonal hypoxia on activity, diversity and community structure of chemoautotrophic bacteria in a coastal sediment (Lake Grevelingen, The Netherlands)</i>	78
CHAPTER 5 <i>Species-specific effects of two bioturbating polychaetes on sediment chemoautotrophic bacteria</i>	122
CHAPTER 6 <i>Bacterial chemoautotrophy in coastal sediments</i>	144
CHAPTER 7 <i>Discussion</i>	173
<i>Summary</i>	184
<i>Samenvatting</i>	188
<i>References</i>	192
<i>Acknowledgements</i>	212
<i>Curriculum vitae</i>	214

Introduction

More than 200 years ago Sergei Winogradsky discovered a novel microbial process by which filamentous bacteria (*Beggiatoa*) could grow in the dark in media solely enriched with inorganic compounds, a process latter defined as chemosynthesis. Chemoautotrophic micro-organisms are unlike photoautotrophs given that they use the chemical energy derived from reoxidation reactions (chemo-) rather than using light energy (photo-) to fix inorganic carbon (-autotrophs). Within the chemoautotrophic micro-organisms an additional distinction is made between electron donors which can either be inorganic (chemolitho-) or organic (chemoorgano-) compounds (Jørgensen 2006).

In the late 1970s with the discovery of deep sea hydrothermal vents, a great diversity of different chemoautotrophic microbes were found to be the primary producers of these deep sea systems, both as free-living microbes and as symbionts of animals (Jannasch & Mottl 1985; Wirsén et al., 1993; Nakagawa & Takai 2008). In recent decades, carbon and sulfur cycling associated to chemoautotrophic microbes in chemoclines of hypoxic basins have also received much attention (Tuttle & Jannasch 1973; Glaubitz et al., 2009; Lavik et al., 2009). However, in coastal sediments photoautotrophic organisms are the main source of labile organic matter, and thus chemoautotrophic production is considered to be negligible given the low growth yield (Jørgensen & Nelson 2004). At the start of this thesis work, only three studies directly examined chemoautotrophy in coastal sediments (Enoksson & Samuelsson 1987; Thomsen & Kristensen 1997; Lenk et al., 2010), and these showed that chemoautotrophic production in typical coastal sediments may be much higher than previously thought. This thesis therefore aimed at 1) increasing the number of chemoautotrophy observations in coastal sediments, 2) identifying key chemoautotrophic bacteria, 3) determining possible environmental factors that regulate chemoautotrophic activity, and 4) evaluating the importance of chemoautotrophy in the carbon cycle of coastal sediments.

1.1 MINERALIZATION AND REOXIDATION IN SEDIMENTS

In coastal marine sediments (e.g. intertidal areas, estuaries, continental shelf) oxygen penetrates only millimeters deep into the sediment, and hence degradation of organic matter mostly occurs anaerobically (Howarth 1984). Anaerobic mineralization pathways include the respiration of NO_3^- , FeOOH , MnO_2 , and SO_4^{2-} that follow a vertical redox zonation in the sediment that reflects the potential energetic gain (Jørgensen 2006, Fig. 1). These processes result in the production of a large reservoir of reduced compounds, such as ferrous iron (Fe^{2+}), ammonium (NH_4^+) and reduced sulfur species (H_2S , S^0 , FeS) that are reoxidized by chemoautotrophic bacteria following the redox cascade of electron donors and acceptors in the sediment (Fig. 1). The most important anaerobic pathway of organic matter degradation is sulfate reduction which on average accounts for half of the mineralization rate occurring in coastal sediments (Jørgensen 2006). Given the high production rate of reduced sulfur via sulfate reduction, the potential chemoautotrophic activity through sulfur oxidation in coastal sediments is large and in fact much greater than in hydrothermal vents (Howarth 1984).

Microbial mediated chemical reactions gain highly variable amounts of energy. The energy yield of a reaction is given by the Gibbs free energy (ΔG_0) and indicates the change in energy released per mol of reactant, which is available for metabolic processes (Jørgensen 2006). A net decrease in free energy ($-\Delta G_0$) indicates that the reaction may proceed spontaneously or can be catalyzed biologically, while a net increase ($+\Delta G_0$) indicates an endergonic reaction that requires energy in the form of ATP to drive the reaction. Most

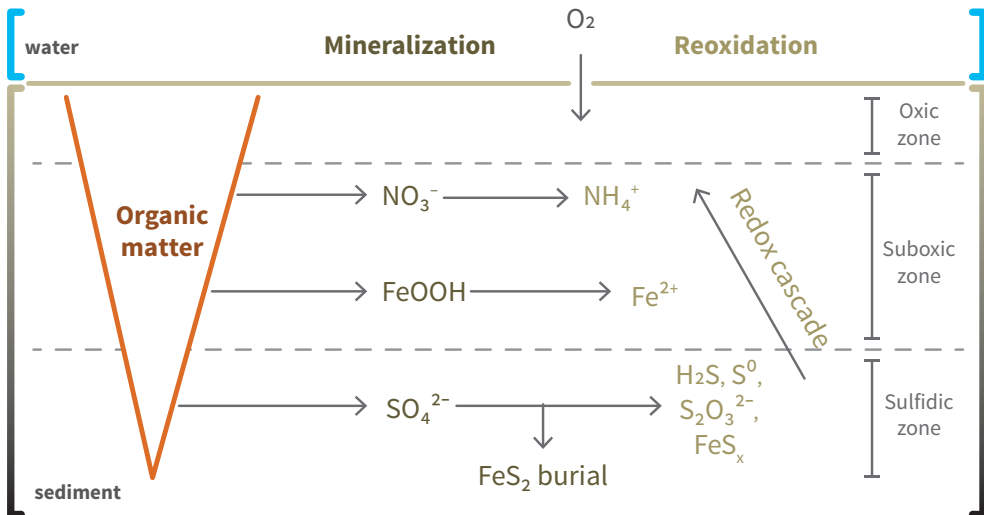
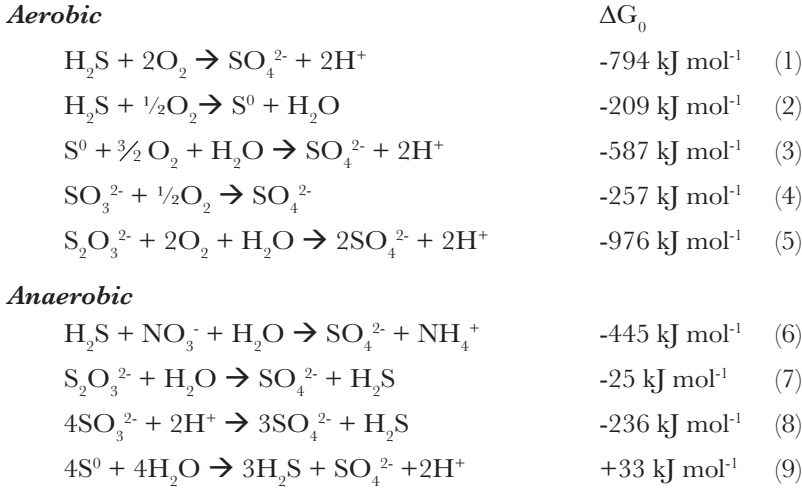


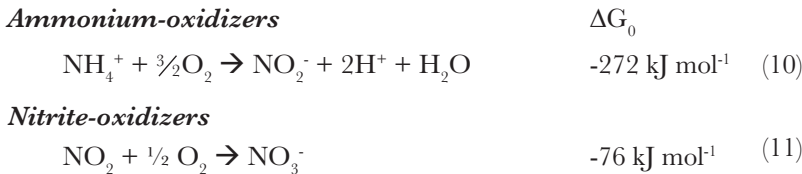
Figure 1. Simplified scheme of mineralization and reoxidation pathways in marine sediments and their relation to geochemical zonation.

of the reoxidation reactions performed by chemoautotrophic bacteria in marine sediments depend on the oxidation of reduced sulfur species which encompass high energy yielding reactions both under oxic and anoxic conditions:



The last reaction describes the disproportionation of elemental sulfur which is an endergonic process under standard conditions, however if the produced sulfide is efficiently removed (sulfide concentration ~1 mM) the reaction becomes exergonic (Jørgensen 2006; Canfield et al., 2005).

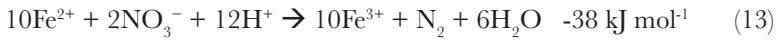
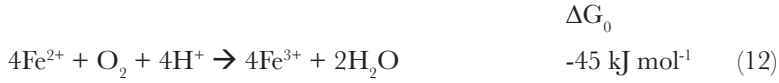
Despite the prevalence of reduced sulfur in marine sediments chemoautotrophic bacteria gain energy from several other reoxidation pathways. One of the more thermodynamically favorable reactions is the reoxidation of ammonium produced from the degradation of organic matter, however given the typical C:N ratio of 8 in marine organic matter, there will be much less ammonium than sulfide production during anaerobic mineralization. This reoxidation occurs via a two-step process performed by nitrifying bacteria:



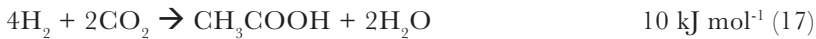
Complete nitrification has however been recently identified to occur in one micro-organism (van Kessel et al., 2015). Nitrification accounts for a large percentage of the ammonium turn over in sediments but the bacteria involved generally present

low growth yields of 0.1 mole of carbon fixed per mole of ammonium oxidized, or 0.02 mole of carbon fixed per mole of nitrite oxidized (Belsler 1984). Hence this particular group of chemoautotrophs may contribute more to the N-cycling than to C-cycling in coastal sediments.

Reduced iron formed through iron respiration is also an energetically favorable electron donor for chemoautotrophs in sediments. Iron oxidizing bacteria compete with chemical reactions under oxic conditions and as such these chemoautotrophs generally grow in micro-aerobic or acidic environments, and in the absence of O₂ use NO₃⁻ as an electron acceptor (Canfield et al., 2005):



Other inorganic reactions that support chemoautotrophic bacteria in marine sediments include aerobic hydrogen oxidization (Equation 14) which under anaerobic conditions it is coupled to sulfate reduction (Equation 15); anaerobic ammonium oxidization (anammox) (Equation 16), and acetate formation by acetogens (Equation 17) (Banfield & Nealson 1997; Canfield et al., 2005; Lever 2012):



1.2 SULFUR CYCLING IN COASTAL SEDIMENTS

In sediments layers below the oxygen penetration depth, sulfate reduction occurs producing sulfide which diffuses upwards. In most marine sediments, sulfide does not reach the sediment surface but rather reacts with oxidized iron minerals in the suboxic zone (*i.e.* sediment layer devoid of oxygen and free-sulfide in pore water) and precipitates in the form of iron sulfide (FeS) and pyrite (Fe₂S) (Zopf et al., 2004; Jørgensen & Nelson 2004, Fig. 2):



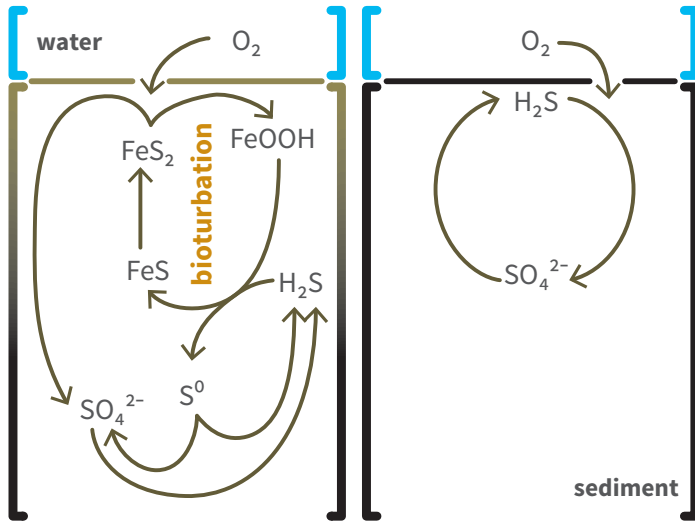
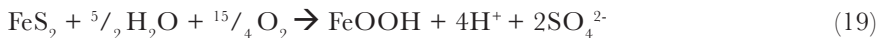


Figure 2. Simplified scheme of sulfur cycling in bioturbated (left panel) and non-bioturbated sulfide-rich sediments (right panel). See Section 1.2 for detailed explanation.

These iron compounds are then cycled in the sediment by biological mixing of sediment particles by bioturbating fauna that functions as a “conveyor belt” (Jørgensen & Nelson 2004; Fig. 2). Iron sulfide and pyrite are transported up to the sediment surface where they are reoxidized to iron (hydro)oxide:



Iron (hydro)oxide is mixed downward resulting in the formation of elemental sulfur and the replenishment of iron in deeper sediments where the cycle starts again. The elemental sulfur formed can then be disproportionated by bacteria into both reduced (sulfide) and oxidized sulfur (sulfate), (Equations 7, 8, 9; Bak & Pfennig 1987) or react further to form pyrite (FeS_2). Sulfur disproportionation therefore serves as a shunt in the sulfur cycle whereby newly formed HS^- can be reoxidized to sulfur intermediates by metal oxides in the suboxic zone.

In sediments with high mineralization rates, a second scenario of sulfur cycling may occur when the sulfide production rate surpasses the availability of iron (hydro) oxides. Under such conditions the pool of iron (hydro)oxides is exhausted and precipitated as a large reservoir of iron sulfide and pyrite that can easily be detected by the black coloration of sediment surface (Fig. 2). Consequently, reduced sulfur freely

diffuses up towards the sediment surface creating an O_2 - H_2S interface where high rates of aerobic sulfur oxidation occur chemically or microbially (Jørgensen & Nelson 2004; Zopfi et al., 2004). These high concentrations of free sulfide in pore water, in general, are toxic for animals (Vaquer-Sunyer & Duarte 2008) and thus sulfur cycling coupled to iron cycling that depends on bioturbation is not ongoing. Overall, most of the sulfide produced in the top centimeters of marine sediments is eventually oxidized back to sulfate via intermediate sulfur compounds in a network of competing chemical and biological reactions.

1.3 SULFUR-OXIDIZING BACTERIA

Sulfur oxidizing bacteria range from free-living single cells to symbionts of invertebrates to mat forming multi-cellular microbes, most of which are related to the Gamma-, Epsilon- and Deltaproteobacteria in marine environments (Ghosh & Dam 2009; Swan et al., 2011; Hügler & Sievert 2011; Pjevac et al., 2014). These diverse groups of bacteria comprise four main sulfur oxidizing scenarios (Fig. 3): canonical sulfur oxidation at O_2 - H_2S interfaces, nitrate-storing Beggiatoaceae, electrogenic sulfur oxidation by cable bacteria, and coupled to iron-cycling by bioturbating fauna. The last three scenarios have one particular characteristic in common which is the formation of a suboxic zone in the sediment, *i.e.*, a zone devoid of both oxygen and free sulfide in the top centimeters of the sediment.

1.3.1 Canonical sulfur oxidation

Canonical sulfur oxidation entails the direct oxidation of sulfide and reduction of oxygen within the same location where both the donor and acceptor overlap, *i.e.* at the O_2 - H_2S interface (Meysman et al., 2015; Fig. 3a). Large, non-vacuolate filamentous bacteria from the Beggiatoaceae family (Gammaproteobacteria) are commonly found forming mats at the O_2 - H_2S interface in hypoxic systems (Williams & Reimers 1983; Thamdrup & Canfield 1996), in hydrothermal vents (Wirsen et al., 1993; Perner et al., 2007) and in cold seeps (Lichtsschlag et al., 2010; Grünke et al., 2011). These bacteria contain light refracting sulfur globules which gives a whitish color to the mats (Jørgensen, 1982). Sulfur oxidation by these filamentous bacteria can account for up to 90% of the oxygen respiration in sediments (Jørgensen 1982). Most representatives of the Beggiatoaceae grow as chemoautotrophs but some species can also use organic substrates for growth (Mußmann et al., 2003; Jørgensen & Nelson 2004).

In addition, colorless sulfur-oxidizing bacteria from the Epsilonproteobacteria may also carry out canonical sulfur oxidation (e.g. *Arcobacter*, *Sulfurimonas*). These bacteria have high metabolic versatility and growth yields that confer rapid adaptability to

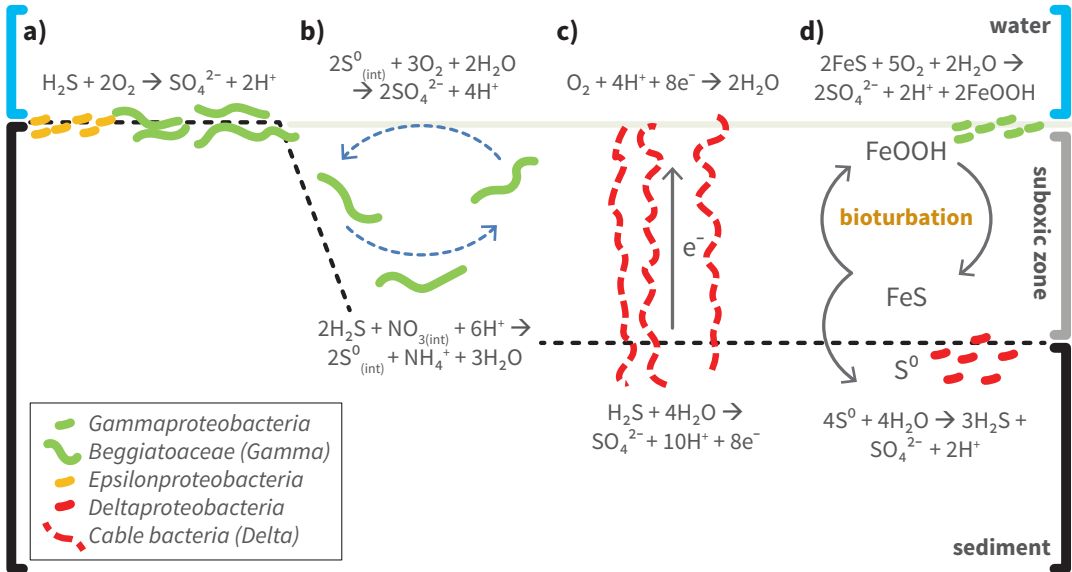


Figure 3. Schematic representation of the four main microbially-mediated sulfur oxidation mechanisms occurring in the top 5 cm of marine sediments: a) canonical sulfur oxidation, b) sulfur oxidation by nitrate-storing *Beggiatoaceae* (trajectory is represented by the broken blue line), c) electrogenic sulfur oxidation by cable bacteria, d) sulfur oxidation promoted by iron cycling via bioturbation (grey arrows). See Section 1.3 for description of processes. Black area represents sulfidic sediments, grey area represents the suboxic zone, and light grey area represents oxic sediments.

changing geochemical conditions (Campbell et al., 2006). Epsilonproteobacteria constitute a major component of the chemoautotrophic community at the oxic-anoxic interface of deep sea sediments, in sulfidic cave springs and in chemoclines where they oxidize sulfide, thiosulfate or elemental sulfur with oxygen or nitrate as electron acceptor (Engel et al., 2003; Nakagawa & Takai 2008; Grote et al., 2012). Epsilonproteobacteria related to the genera *Sulfurimonas* and *Sulfurovum* are also important sulfur-oxidizers in sulfidic sand flats and tidal pools (Pjevac et al., 2014).

1.3.2 Nitrate-storing *Beggiatoaceae*

Large, motile, often filamentous, Gammaproteobacteria of the *Beggiatoaceae* family (*Beggiatoa*, *Thioploca*, *Thiomargarita*) which are capable of intracellular redox shuttling between the oxic and sulfidic horizons (Schulz & Jørgensen 2001; Jørgensen & Nelson 2004; Sayama et al., 2005), can thus live outside of the oxic-anoxic interface (described above) and live in deep anoxic sediments (Mußmann et al., 2003; Preisler et al., 2007). These organisms first capture nitrate at the sediment surface and store it into a large central vacuole before diving into the deeper, sulfide rich, anoxic sediment.

At the H_2S -horizon they oxidize sulfide to elemental sulfur using the stored nitrate. The elemental sulfur is stored in globules and carried back to the surface of the sediment to complete the oxidization to sulfate (Fig. 3b). This cyclic movement and the associated transport of redox compounds, creates a thick suboxic zone in the sediments. This two-step sulfur oxidation via stored nitrate also creates a specific pH signature in the sediment, whereby a pH maximum is created by the consumption of protons when sulfide is oxidized to elemental sulfur in the deep sediment, and a pH minimum is formed at the sediment surface by the production of protons associates to the final oxidation of sulfur to sulfate (Sayama et al., 2005; Seitaj et al., 2015).

1.3.3 Electrogenic sulfur oxidation

Long filamentous Deltaproteobacteria closely related to *Desulfobulbus propionicus*, the so called cable bacteria capable of electrogenic sulfur oxidization (e-SOx) were only described recently (Pfeffer et al., 2012). This bacterium oxidizes sulfide in two spatially separate redox half-reactions over centimeter-distances, *i.e.*, anodic sulfide oxidation which occurs throughout the suboxic zone as well as in the top of the sulfidic zone and cathodic oxygen reduction which occurs within the oxic zone (Fig. 3c). The necessary redox coupling between these two half reactions is ensured by transporting electrons from cell to cell along their longitudinal axis (Nielsen et al., 2010; Pfeffer et al., 2012; Meysman et al., 2015). The exact mechanism by which they transport electrons is at present not known. Geochemically this sulfur-oxidation pathway creates a very distinct pH signature in the sediment which serves to distinguish e-SOx from other sulfur-oxidizing mechanisms such as the aforementioned nitrate-storing Beggiatoaceae. A pH maximum is formed by the consumption of protons due to the reduction of oxygen at the sediment surface, while in deeper sediment the production of protons from the oxidation of sulfide creates a pH minimum (Meysman et al., 2015; Seitaj et al., 2015). Cable bacteria form dense networks that extend throughout the suboxic zone with doubling times of 20 hours (Schauer et al., 2014) however it was unknown whether they use organic (chemo-organo-autotrophs) or inorganic carbon (chemo-litho-autotrophs) substrates for growth.

1.3.4 Iron cycling by bioturbating fauna

Mixing of solid sediment particles by bioturbating fauna promotes iron cycling, by stimulating the two-way conversion between iron sulfides (FeS) and iron (hydro)oxides (FeOOH) (See Section 1.2). This downward transport of iron (hydro)oxides to be reduced in combination with the upward transport of iron sulfides to be oxidized, maintains a centimeter thick suboxic zone in the sediment where free-sulfide is absent

in pore water (Canfield et al., 2005; Seitaj et al., 2015). The upward mixing of iron sulfides into the oxic zone potentially supplies reduced sulfur substrate for chemoautotrophs (Fig. 3d), although microbial oxidation of iron sulfides at circum-neutral pH has not been well studied (Schippers 2004). Alternatively, the reduction of iron (hydro)oxide with sulfide produces elemental sulfur (Equation 18) which may be used by chemoautotrophic Deltaproteobacteria associated to sulfate reducers capable of sulfur disproportion in the anoxic sediments (Bak & Pfennig 1987, Fig. 3d). For example, *Desulfocapsa sulfoexigens* can grow exclusively by disproportionating sulfur under anoxic conditions (Finster et al., 1998) whereas *Desulfobulbus propionicus* can disproportionate both elemental sulfur and thiosulfate (Fuseler & Cypionka 1995).

Additionally, in bioturbated intertidal sediments, single-cell sulfur-oxidizing Gammaproteobacteria appear to be the most abundant chemoautotrophs, accounting up to 45% of all 16S rRNA gene sequences and 40-70% of the total dark carbon fixation (Lenk et al., 2010; Dykema et al., 2016). Gammaproteobacteria are mostly aerobic sulfide-oxidizers and thus characterize surface sediments (Fig. 3d) but they can also couple the oxidization of reduced sulfur compounds to nitrate reduction in deeper anoxic sediments (Ghosh & Dam 2009).

1.4 CARBON FIXATION PATHWAYS

Chemoautotrophic micro-organisms, from diverse Bacteria and Archaea clades, can use one of six known carbon fixation pathways for biosynthesis (Fig.4): Calvin Benson-Bassham cycle, 3-hydroxypropionate pathway, 3-hydroxypropionate/4-hydroxybutyrate pathway, reductive tricarboxylic acid cycle, dicarboxylate/4-hydroxybutyrate cycle, and the reductive acetyl-CoA pathway. The less energy-efficient pathways predominate in oxidized environments (Calvin Benson-Bassham cycle, 3-hydroxypropionate, and 3-hydroxypropionate/4-hydroxybutyrate pathways) whereas the more energy-efficient cycles tend to prevail under oxygen-depleted or anoxic conditions (reductive tricarboxylic acid cycle, dicarboxylate/4-hydroxybutyrate cycle, and reductive acetyl-CoA pathway). The most well studied pathway is the Calvin Benson-Bassham cycle (CBB) although the reductive tricarboxylic acid cycle (rTCA) has received increasing attention in the last decades as it is found in Epsilonproteobacteria (Campbell et al., 2006).

The CBB cycle can be found in eukaryotes (algae and plants), and is the most widespread pathway amongst chemoautotrophic bacteria. The CBB cycle evolved in photo- and chemoautotrophic Alpha-, Beta-, and Gammaproteobacteria that use O_2 or NO_3^- as electron acceptors. The key enzyme in this carbon fixation cycle is ribulose 1,5-bisphosphate carboxylase/oxygenase (RuBisCO) which was used in phylogenetic analysis to study the composition of the CBB-using microbial community in diverse sediments (Nigro & King 2007; Schippers et al., 2012). The second most studied cycle is the reductive tricarboxylic

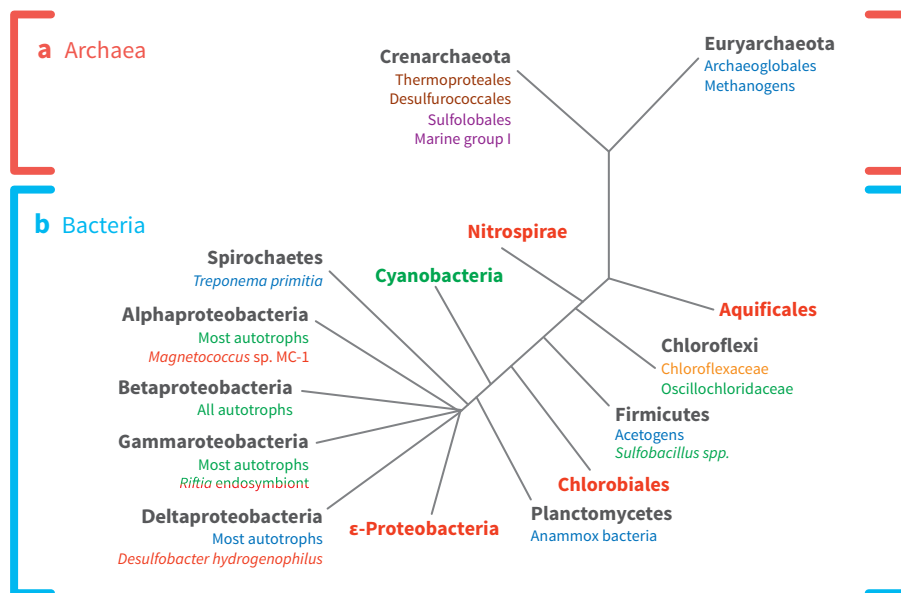


Figure 4. Phylogenetic classification of autotrophic Archaea and Bacteria. Colors indicate the type of carbon fixation used by each clade: green for Calvin Benson-Bassham cycle, red for reductive tricarboxylic acid cycle, blue for the reductive acetyl-CoA cycle, orange for 3-hydroxypropionate bicycle, purple for 3-hydroxyprpionate/4-hydrocybutyrate cycle, brown for the dicarboxylate/4-hydroxybutyrate cycle. Figure modified from Hugler & Sievert (2011).

acid cycle (rTCA), which in essence is a reversal of the Krebs cycle used by heterotrophs. The rTCA is restricted to anaerobic and micro-aerobic conditions and has been found in most Epsilonproteobacteria, some Deltaproteobacteria, Chlorobiales (green sulfur bacteria), Aquificales and magnetotactic Alphaproteobacteria. The characteristic reaction of the rTCA cycle is the ATP-dependent cleavage of citrate into acetyl-CoA and oxaloacetate which is catalyzed by the citryl-CoA synthetase (CCS), the citryl-CoA lyase (CCL) enzymes, and the citrate lyase (ACL). These enzymes have been studied to determine diversity and activity of mostly Epsilonproteobacteria in hydrothermal vent systems (Campbell & Craig Cary 2004; Takai et al., 2005; Perner et al., 2007). At present, no functional gene approaches exists to specifically assess organisms utilizing the other carbon fixation pathways and thus the prevalence of those pathways is poorly known. For a detailed description of all carbon fixation pathways see Berg (2011) and Hügler & Sievert (2011).

1.5 ENERGY EFFICIENCY BY SULFUR-OXIDIZING CHEMOAUTOTROPHS

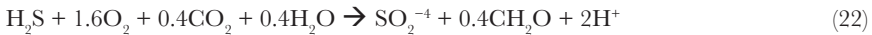
As explained above each reoxidation reaction produces a specific amount of free energy (ΔG_0) which varies depending on the redox pair in question. A fraction of the energy gained is used for synthesizing biomass (growth), while most of the energy is allocated to reduce the terminal electron acceptor for the production of ATP (Kelly 1999; Klatt & Polerecky 2015). In the case of aerobic sulfur-oxidizers, the free energy released from the reoxidation of sulfide generates -794 kJ mol^{-1} (Equation 1; Jørgensen 2006) whereas the amount of energy needed to fix CO_2 via the CBB cycle is $+113 \text{ kJ mol CO}_2^{-1}$ based on the CO_2 reaction (Kelly 1999):



Higher energy requirements for carbon fixation via the CBB cycle of $470 \text{ kJ mol CO}_2^{-1}$ have been calculated based on the overall reaction (Kelly 1999):



The ratio of the free energy used in CO_2 fixation versus the free energy gained in reoxidation is known as energy efficiency. Therefore the theoretical energy efficiency of aerobic sulfide-oxidizers can range between 0.14 and 0.59 per mole of substrate oxidized (*i.e.* $470 \text{ kJ mol CO}_2 / 794 \text{ kJ mol}^{-1}$). Dark carbon fixation observed in batch cultures can vary between 0.35 and 0.46 mol of CO_2 fixed per mole of sulfide oxidized for *Beggiatoa* spp. and *Thiobacillus* spp. (Nelson et al., 1986; Kelly 1999). Assuming an average $\text{CO}_2:\text{H}_2\text{S}$ yield of 0.40, and combining Equation 16 with Equation 18, a general model of chemoautotrophy coupled to sulfur oxidation can be obtained:



The molar ratio of CO_2 fixed to electron donor usage ($\text{CO}_2:\text{O}_2$ yield) varies accordingly, presenting a $\text{CO}_2:\text{O}_2$ yield equal to 0.09 - 0.40 for aerobic thiosulfate-oxidizers, 0.21 - 0.56 for filamentous sulfur-oxidizers (*Beggiatoa*), and up to 1.67 for highly specialized aerobic sulfur oxidizing symbionts of the deep sea worm *Riftia pachyptila* (Klatt & Polerecky 2015).

1.6 BENTHIC CHEMOAUTOTROPHIC PRODUCTION

To determine the contribution of chemoautotrophy to the carbon budget in sediments one can relate the chemoautotrophic production of carbon to the total carbon

mineralized in sediments (CO_2 fixation efficiency). This can be done by directly comparing dark carbon fixation and mineralization rates. However, mineralization rates are difficult to obtain in sediments and thus often lacking in the literature, instead, oxygen consumption rates may be used as a proxy for total organic carbon degradation (Glud 2008). The few studies that experimentally quantify dark carbon fixation in coastal sediments (temperate intertidal flats, brackish lagoons, and tropical freshwater lakes) indicate that CO_2 fixation efficiencies can vary between 0.01 and 0.26 (Enoksson & Samuelsson 1987; Thomsen & Kristensen 1997; Lenk et al., 2010; Santoro et al., 2013).

Alternatively, CO_2 fixation efficiencies can be calculated considering three main factors (Jørgensen & Nelson 2004): 1) the production efficiency of electron donor (mostly sulfide), which scales the production rate of electron donor to the mineralization rate, 2) the reoxidation efficiency of the electron donor (percent of reduced compound used for microbial respiration rather than abiotic oxidation), 3) the molar ratio of CO_2 fixed per mole of electron donor ($\text{CO}_2:\text{H}_2\text{S}$ yield). In a typical coastal sediment sulfate reduction accounts on average for $\sim 50\%$ of the organic carbon oxidation in coastal sediment, and 90% of the H_2S produced is available for reoxidation (on average 10% is buried as pyrite). Thus 45% of the benthic oxygen consumption can be attributed to sulfide oxidation in part mediated by chemoautotrophic sulfur-oxidizers. Taking into account the abovementioned $\text{CO}_2:\text{H}_2\text{S}$ yield of 0.40 (0.35-0.46), and recognizing that only 0.5 mole of sulfide is produced per mole of carbon mineralized in sulfate reduction, then the estimated CO_2 fixation efficiency of chemoautotrophy via sulfide oxidation can be calculated as $0.50 \times 0.90 \times 0.50 \times 0.40 = 0.09$ or 9% of the benthic carbon budget in coastal sediments (Fig. 5). This CO_2 fixation efficiency has been hypothesized to vary however between coastal sediments with 0.03-0.06 in continental shelf sediments, 0.07-0.13 in estuarine sediments and 0.10-0.18 in salt marsh sediments (Howarth 1984), as the prevalence of sulfate reduction varies between these sediments.

Accordingly, there appears to be a substantial and unexplained variability between sites and habitats, and other environmental factors controlling chemoautotrophic activity at a given site may explain the observed variation in the CO_2 fixation efficiency. At present only one study has assessed the possible correlations between several environmental factors and chemoautotrophy rates in twelve lakes from temperate and tropical latitudes (Santoro et al., 2013). The results of these authors show that bacterial production, benthic oxygen consumption, salinity, pH, organic carbon and nitrogen content, nor water content were significantly correlated with dark carbon fixation.

Bioturbation by fauna can also affect reoxidation processes. Hence, chemoautotrophic activity in sediments is affected by burrow irrigation and maintenance as well as through feeding and particle reworking (Aller 1988; Kristensen & Kostka 2005; Fig. 6). For example, Reichardt (1988) found that the strong irrigation activity and particle reworking of lugworm *Arenicola marina* can enhance chemoautotrophic

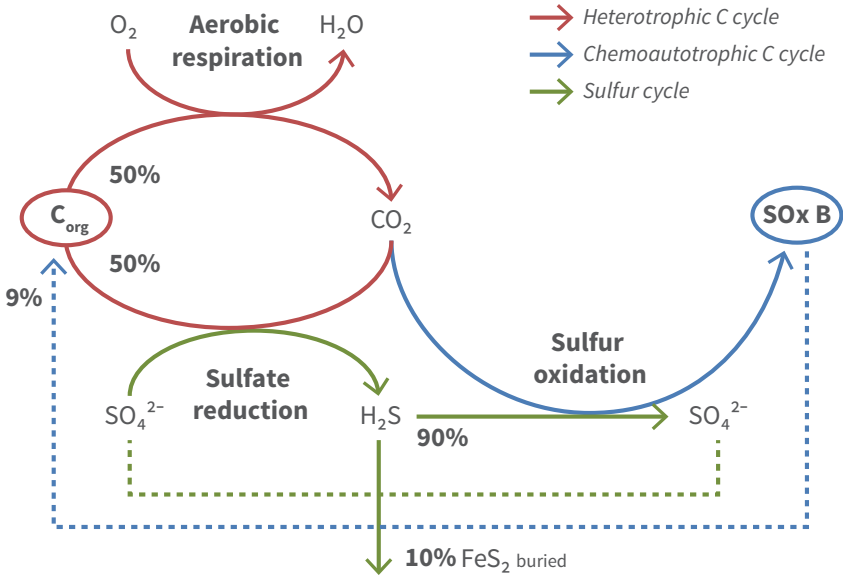


Figure 5. Idealized scheme of the carbon and sulfur cycles in a coastal sediment and the potential role of chemoautotrophic CO_2 assimilation in the overall carbon budget. For simplicity, the burial of organic carbon is ignored and respiration is assumed to be the only source of CO_2 production (no carbonate dissolution). Corg: detrital organic carbon, SOx B: organic C in biomass of sulfur-oxidizing chemoautotrophic bacteria. Modified from Jørgensen & Nelson (2004).

activity in burrow structures relative to surface and subsurface sediments. Studies of eleven faunal species also showed that nine of the species enhanced nitrification potential in burrow walls and tubes in comparison to surface sediment by factors of 1.5 to 60 (Kristensen & Kostka 2005). Moreover, bioturbating fauna potentially has different effects on the microbial community depending on the functional traits of the fauna involved (Papasprou et al., 2006; Bertics & Ziebis 2009; Laverock et al., 2010). Chemoautotrophy rates in coastal sediments can therefore be affected by a number of biogeochemical factors, which are highly understudied and should be addressed systematically.

1.7 METHODS FOR STUDYING CHEMOAUTOTROPHY

The few studies on benthic chemoautotrophy rate measurements implement either radioactive labeling or stable isotope probing (SIP). The incorporation of radioactive carbon (^{14}C -bicarbonate) into particulate organic carbon measured through scintillation counting has been broadly used to quantify benthic chemoautotrophic activity in near shore areas (0.4 - $5 \text{ mmol m}^{-2} \text{ d}^{-1}$, Enoksson & Samuelsson 1987; Thomsen & Kristensen 1997; Lenk et al., 2010), hydrocarbon seeps (0.02 - $1 \text{ mmol m}^{-2} \text{ d}^{-1}$, Bauer et al., 1988), marine lakes (1 - $1.5 \text{ mmol m}^{-2} \text{ d}^{-1}$, Santoro et al., 2013) and methane seeps (12 mmol

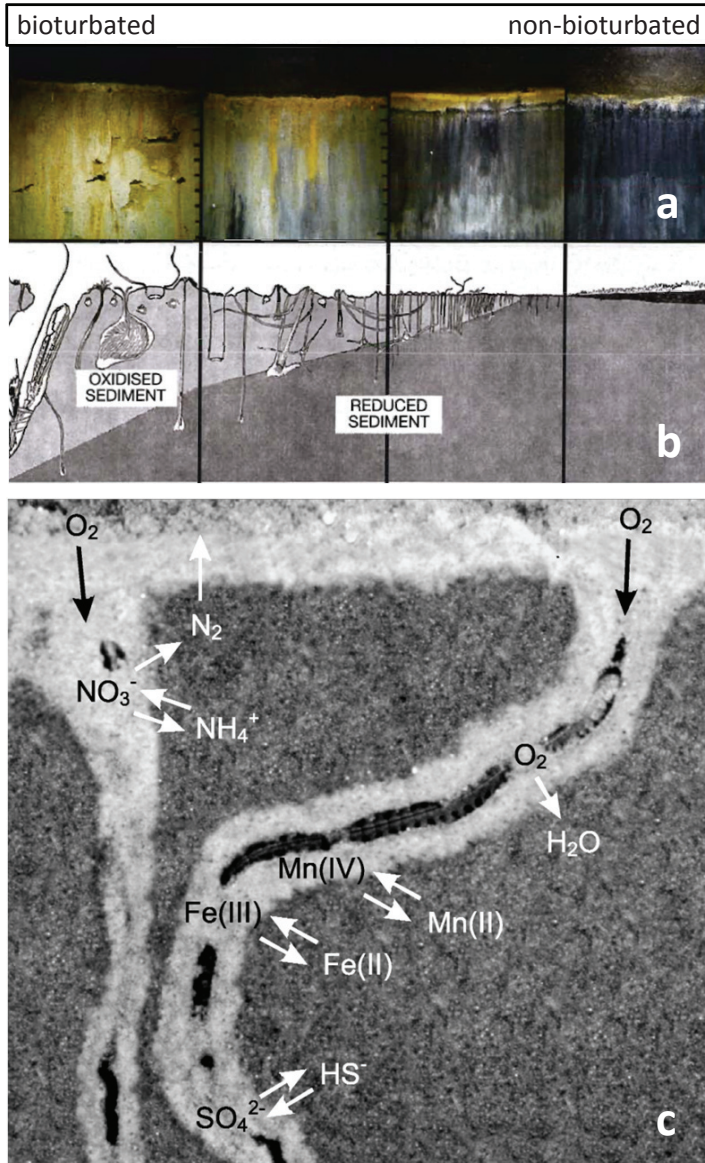


Figure 6. Geochemical impact of bioturbation on coastal sediments. Sediment-profile images (a) and conceptual models (b) are shown along a gradient of decreasing bioturbation intensity. Oxidized sediment is rust-brown, and reduced sediment grey or black. Modified from Nilsson & Rosenberg (2000). (c) Burrow structure of *Nereis (Hediste) diversicolor*. The polychaete itself is visible as the black elongated structure in the middle of the burrow. The light areas represent the oxidized zone at the sediment water interface and around the burrow wall, dark areas represent the reduced zones of the sediment. Arrows show various transport and reaction processes near the burrow wall. Image taken from Kristensen & Kostka (2005).

$\text{m}^{-2} \text{d}^{-1}$, Dale et al., 2010). This technique offers bulk activity measurements but no taxonomic resolution. A recent study however used ^{14}C -labeling in combination with flow-cytometer sorting of specific groups of bacteria labeled through fluorescent *in situ* hybridization (FISH) to quantify dark carbon fixation by Gammaproteobacteria from various sediments (Dyksma et al., 2016). Alternatively, linking activity with identity of bacterial communities has been achieved through the quantification of ^{13}C -incorporation into membrane-bound phospholipid derived fatty acids (PLFA-SIP; Box 1; Boschker et al., 1998). PLFA concentrations are group-specific (examples of PLFA signatures are listed in Table 1) hence differences or shifts in community composition can be identified based on the PLFA profiles (Vestal & White 1989; Boschker & Middelburg 2002; Evershed et al., 2006). This method is highly sensitive and allows the study of low carbon incorporation from environmental samples. However, PLFA-SIP analysis does not offer high taxonomic resolution and as such parallel DNA and RNA based approaches are recommended.

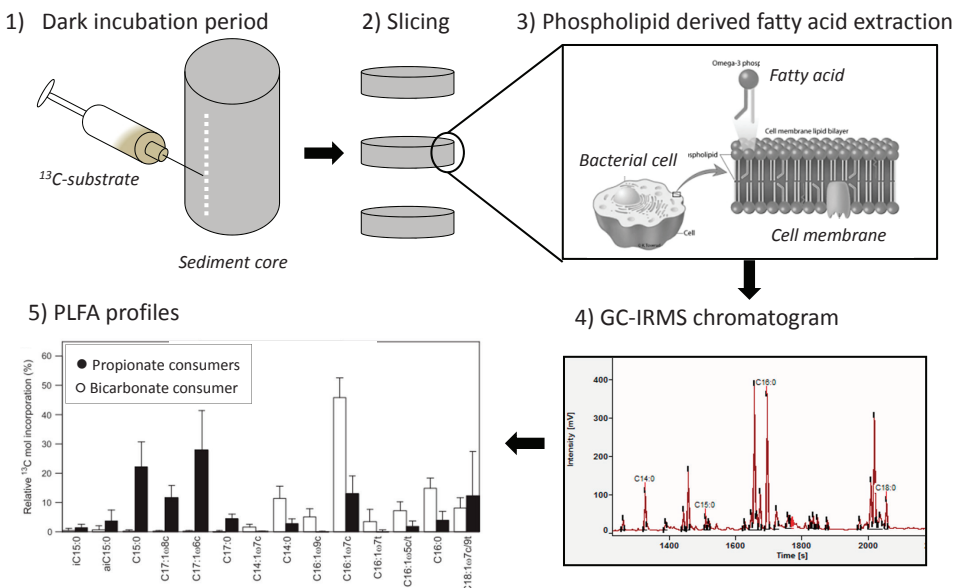
Functional gene approaches are powerful tools to assess the diversity, as well as the abundance and activity of organisms with specific functions. Studying the carboxylation enzymes from the different carbon fixation pathways offers a high taxonomic resolution of autotrophic organisms. However, the study of specific enzymes has its limitation given that only one group of organisms can be quantified at a time thus overlooking the diversity and activity of other groups. The detection of genes coding for subunits of RuBisCO have been broadly used to characterize the autotrophic community using the CBB cycle. In an intertidal mudflat and in lake sediments phylogenetic analysis of genes encoding for RuBisCO showed distinct chemoautotrophic communities with mat forming sulfur-oxidizers dominating the mudflats and H_2 -oxidizers characterizing lake sediments (Nigro & King 2007). Quantification of the *cbb* gene for RuBisCO enzyme in subsurface sediments in upwelling areas was assessed through qPCR (Schippers et al., 2012). The diversity of the rTCA cycle has also been studied in free-living micro-organisms at hydrothermal vents indicated a dominance of Epsilonproteobacteria (Campbell & Craig Cary 2004). Others have assessed the phylogeny of chemoautotrophic bacteria in hydrothermal vent sediments via the *cbb* and *acl* genes (CBB and rTCA cycle, respectively) encountering Gammaproteobacteria related to *Thiomicrospira* using the CBB cycle and Epsilonproteobacteria related to *Arcobacter* and *Sulfurimonas* containing the rTCA cycle (Takai et al., 2005; Perner et al., 2007). Nonetheless, no functional gene approaches have been used to specifically assess organisms utilizing the reductive acetyl-CoA pathway or the 3-HP/4-HB and DC/4-HB cycles.

Alternatively, nanometer-scale secondary ion mass spectrometry (NanoSIMS, Box 2) combined with stable isotope probing allows both the identification and quantification of isotopically enriched bacterial cells. Cell activity can be further linked to the phylogenetic identity by implementing rRNA-based FISH techniques as shown by Orphan et al., (2001)

BOX 1. PLFA-SIP

Isotopes are different forms of the same element that vary in the number of neutrons (e.g. ^{12}C , ^{13}C , ^{14}C). There are radioactive (^{14}C) and stable carbon isotopes (^{12}C , ^{13}C) in nature, the second do not decay and unlike the radioactive isotopes do not pose any health hazard. Stable isotopes are present in nature in different abundances with the low mass isotope (“light isotope”) representing more than 98% (in the case on C, H, O, N) and the high mass isotope (“heavy isotope”) less than 2% (Fry 2006). This difference in abundance is what makes it possible to track the cycling of elements in the environments through stable isotope probing (SIP).

The PLFA-SIP technique comprises the incubation of an environmental sample with substrates enriched in heavy isotopes (e.g. ^{13}C -propionate, ^{13}C -bicarbonate) for a determined period of time. At the end of the incubation samples are collected and the membrane-bound lipids of all cells are extracted. These lipids are analyzed as fatty acid methyl esters (FAME) by GC-c-IRMS (gas chromatography combustion isotope ratio mass spectrometry). The resulting chromatogram indicates the concentration of the different fatty acids present and the amount of heavy isotope (^{13}C) incorporated in each fatty acid. The PLFA profiles between C_{12} and C_{20} can be compared with PLFA signatures from cultured micro-organisms to identify the microbial composition of the sample or to show differences in active bacterial community between sites. Total rates of carbon incorporation are calculated based on the ^{13}C enrichment and concentrations of the fatty acids as described in Boschker & Middelburg (2002) and Evershed et al., (2006).



to reveal the involvement of archaea ANME-2 in the anaerobic oxidation of methane in a consortium with sulfate reducing bacteria related to *Desulfosarcina*. Moreover, Behrens and colleagues (2008) used catalyzed reporter deposition (CARD)-FISH in combination with NanoSIMS to track the fate of C and N in microbial aggregates and describe the interrelationship of these cells. The same technique demonstrated that anaerobic phototrophic bacteria in a lake metalimnion show differential metabolic rates between species and between cells of the same species indicative of heterogeneous metabolic status in a population (Musat et al., 2008). Metabolic activity of deep-subsurface sediment microbes has also been demonstrated with N and C assimilation by both Bacteria and Archaea (Morono et al., 2011).

Table 1. PLFA signatures of the main groups of chemoautotrophic bacteria in marine sediments. The relative contributions of the main fatty acids to the total PLFA composition are listed. The complete PLFA signatures as well as further details on the specific micro-organisms are given in the references.

Metabolism	PLFA signature	Range %	Reference
Mat forming sulfur oxidizers (Gammaproteobacteria)	14:0 16:1 ω 7c 16:1 ω 7t 16:0 18:1 ω 7c	1-6 17-54 3-13 8-12 11-16	(Zhang et al. 2005; Li et al. 2007)
Sulfur oxidizers (Epsilonproteobacteria)	14:0 16:1 ω 7c 16:0 18:1 ω 7c	5-8 20-45 19-37 9-37	(Inagaki et al. 2003; Takai et al. 2006; Donachie et al. 2005)
Nitrite oxidizers	16:1 ω 7c 16:0 18:1 ω 7c	11-54 3-30 42-92	(Lipski et al. 2001; Blumer et al. 1969)
Ammonium oxidizers	16:1 ω 7c 16:0	59-74 26-39	(Blumer et al. 1969)
Iron and Sulfur oxidizers	16:1 ω 7c 16:0 cy17:0 cy19:0	6-46 15-47 5-15 25-31	(Knief et al. 2003)
Sulfate reducers (Deltaproteobacteria)	14:0 15:0 i15:0 16:1 ω 7c 16:0 i17:1 ω 7c 17:1 ω 6c 18:1 ω 7c	2-23 2-28 10-58 0.3-27 3-44 0.2-40 11-51 2-27	(Taylor & Parkes 1983; Edlund et al. 1985; Suzuki et al. 2007; Pagani et al. 2011)

BOX 2. NANOSIMS

Nano-scale secondary ion mass spectrometry (NanoSIMS) is a single-cell technique with high sensitivity and a maximum resolution of 50 nm (Gutierrez-Zamora & Mane-field 2010; Musat et al., 2012). This method involves the bombardment of the bacterial cells in a sample with ions (e.g. Cs^+ or O^-) that sputters a thin layer of the sample away. The secondary ions emitted by the sample are then separated according to mass and detected. Multiple elements or isotopes of these elements can be measured simultaneously and this technique can be used with SIP techniques. Consequently, NanoSIMS provides information about elemental, isotopic and molecular characteristics of a sample from which the activity of single cells may be quantified. The disadvantage of this method apart from the high running costs are sample preparation, and the time involved in fine tuning the instrument to a specific sample.

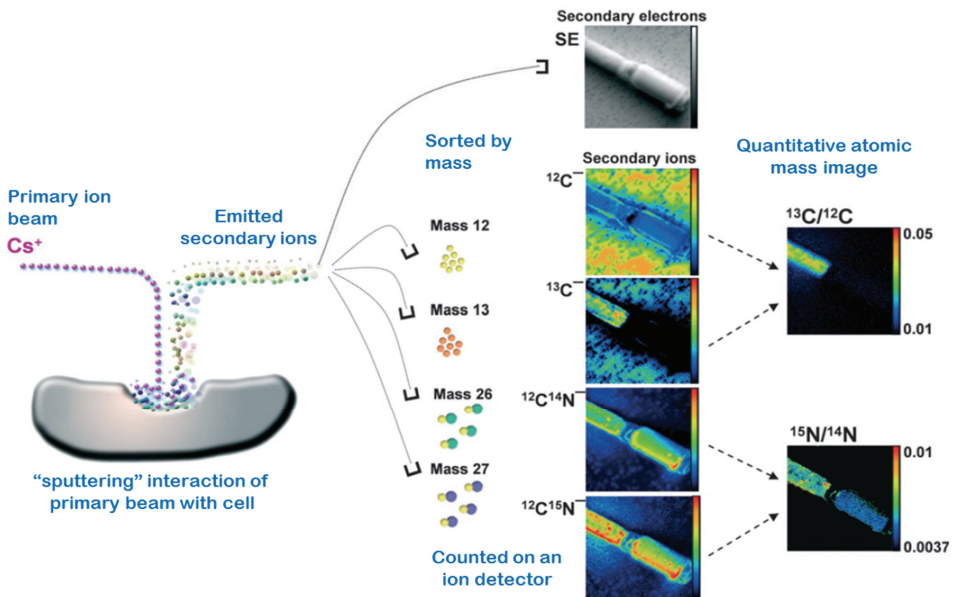


Image taken and modified from Musat et al., 2012

1.8 THESIS RATIONALE AND OUTLINE

The goal of this thesis is to provide an overview of the chemoautotrophic production in coastal sediments and to investigate the factors that control this process and identify the microbial players involved. In order to improve our understanding of the

role of chemoautotrophy in coastal carbon cycling experiments were carried out in the field as well as under controlled conditions in the laboratory. The first objective was to quantify benthic chemoautotrophic carbon fixation rates through the PLFA-SIP. Secondly, chemoautotrophy sediment profiles were assessed to determine possible environmental factors that affect the total chemoautotrophy and depth distribution of activity in a range of coastal sediments. Lastly, the active chemoautotrophic community was characterized through PLFA profiles in combination with DNA/RNA based techniques and NanoSIMS.

CHAPTER 2 – *Chemoautotrophic carbon fixation rates and active bacterial communities in intertidal marine sediments*

I started by selecting two active intertidal areas (an oyster bed and a salt marsh) with contrasting sulfur chemistry in order to measure the rates of dark carbon fixation and to identify the microbial community involved. The results show that salt marsh sediments with high free sulfide in the pore water exhibited higher activity than sediments from the oyster bed area that had limited free sulfide in the pore water. PLFA patterns were site-specific which was supported by differences in the phylogenetic composition of the CBB-using microbial community. Sulfur-oxidizers such as *Beggiatoa* were present in the sulfidic sediments while anaerobic hydrogen oxidizing or S-disproportionating bacteria related to sulfate reducers characterized the non-sulfidic site. Moreover, chemoautotrophy production was similar to carbon mineralization rates in the top layer of the sulfidic marsh sediment which suggest that chemoautotrophy can be a major process in carbon cycling in active coastal sediments.

CHAPTER 3 – *Microbial carbon metabolism associated with electrogenic sulfur oxidation in coastal sediments*

Secondly, I targeted the recently described e-SO_x process to unravel the carbon metabolism of the associated cable bacteria. This chapter describes the development of e-SO_x through microprofiling of the sediment and follows the growth of the cable bacteria network through FISH. Dark carbon fixation rates increased with depth in unison with the development of e-SO_x. NanoSIMS was implemented with ¹³C-bicarbonate and ¹³C-propionate labeling to specifically determine the carbon metabolism of the cable bacteria, which showed propionate over bicarbonate incorporation. The carbon assimilation by the filamentous cable bacteria explained ~50% of the observed growth yields showing that the cable bacteria, although involved in sulfur oxidation, were primarily heterotrophs. The high chemoautotrophic production associated with e-SO_x was further studied through manipulation experiments, which

revealed a tight association between the cable bacteria and chemoautotrophic bacteria from the Gamma- and Epsilonproteobacteria at cm-depth. It is suggested that the cable bacteria can work in a consortium with chemoautotrophic sulfur-oxidizing bacteria to perform electrogenic sulfur oxidation.

CHAPTER 4 – *Impact of seasonal hypoxia on activity, diversity and community structure of chemoautotrophic bacteria in a coastal sediment (Lake Grevelingen, The Netherlands)*

This chapter dives into the seasonally hypoxic marine Lake Grevelingen in order to address the variation in activity and composition of chemoautotrophic bacteria community before and during hypoxia. During the oxic period in spring, geochemical profiles of the three stations studied showed two distinct sulfur oxidation mechanisms: electrogenic sulfur oxidation by cable bacteria or nitrate-storing Beggiatoaceae. In both cases chemoautotrophic activity penetrated deep into the sediment whereby motile nitrate-storing Beggiatoaceae were directly responsible for most of the chemoautotrophy in one station, while at the other two stations chemoautotrophic Gamma- and Epsilonproteobacteria apparently rely on the cable bacteria network as an electron acceptor similar as found in Chapter 3. In summer during hypoxia, chemoautotrophic activity decreased sharply and canonical sulfur oxidation was the main mechanism that took place at the sediment surface where high sulfide and low oxygen concentrations were present. Functional gene analysis showed that Gamma- and Epsilonproteobacteria both decreased in numbers during hypoxia, accompanied by an increase of Deltaproteobacteria 16S rRNA gene sequences related to sulfate reducing bacteria. The results suggest a complex niche partitioning amongst sulfur-oxidizing bacteria regulated by the seasonal availability of O₂ and NO₃⁻ and sulfur species.

CHAPTER 5 – *Species-specific effects of two bioturbating polychaetes on sediment chemoautotrophic bacteria*

A distinguishing characteristic of coastal sediments is the presence of bioturbating fauna that alter the biogeochemistry of the sediments. The degree to which fauna alters the sediments largely depends on the functional traits of the species involved. Hence two functionally different bioturbating polychaetes (*Nereis diversicolor* and the invasive *Marenzelleria viridis*) were selected that noticeably affect the ecology and biogeochemistry of the sediments. Laboratory incubations indicated that the strong ventilation and low bio-irrigation of *N. diversicolor* promoted aerobic chemoautotrophy

whereas the slow ventilation and high bio-irrigation by *M. viridis* fostered anaerobic chemoautotrophic communities. Thus the effects observed were fauna species-specific, mainly controlled by burrow structure, burrow residence time, ventilation and bio-irrigation capacities of the polychaetes.

CHAPTER 6 – *Bacterial chemoautotrophy in coastal sediments*

Finally, to evaluate the importance of chemoautotrophy in coastal carbon cycling the PLFA-SIP technique was used to determine dark carbon fixation rates from 7 coastal marine sediments. In addition, all known data on chemoautotrophy rates in coastal sediments were collected from the literature. A broad range of chemoautotrophic activity is reported from 0.07 to 36 mmol C m⁻² d⁻¹ for diverse coastal sediments. Chemoautotrophy rates presented a power-law relation with benthic oxygen consumption and were inversely correlated to water depth. Mineralization rates and pore water transport mechanisms were linked to the chemoautotrophy activity gradient whereby dark carbon fixation activity was low in permeable sediments (advective flux-driven) and high in cohesive sediments (diffusive flux-driven) presenting high mineralization rates. An additional distinction between the main sulfur oxidation pathways served to ultimately describe five unique depth-distribution patterns of chemoautotrophy in the sediment including cm-deep enhancement of dark carbon fixation in the presence of cable bacteria, nitrate-storing Beggiatoaceae and bioturbating fauna. Average CO₂ fixation efficiency of chemoautotrophs was used to estimate the global chemoautotrophic production for near-shore and continental shelf sediments which together constituted 0.06 Pg C y. This global estimate for coastal sediments is more than two-times lower than previous calculations (0.15 Pg C y) but still one order of magnitude higher than the chemoautotrophic activity of deep sea hydrothermal vents.

CHAPTER 7 – *Discussion*

This chapter synthesizes the collective findings of this research and points out unresolved issues regarding the main objectives of the thesis: key chemoautotrophic bacterial players, regulatory factors of bulk activity and depth distribution, and the importance of chemoautotrophy in coastal sediments.

HENRICUS T.S. BOSCHKER, DIANA VASQUEZ-CARDENAS, HENK BOLHUIS,
TANJA W.C. MOERDIJK-POORTVLIET AND LEON MOODLEY

PLoS One (2014) 9(7):e101443.

*Chemoautotrophic carbon fixation
rates and active bacterial communities
in intertidal marine sediments*

ABSTRACT

Chemoautotrophy has been little studied in typical coastal marine sediments, but may be an important component of carbon recycling as intense anaerobic mineralization processes in these sediments lead to accumulation of high amounts of reduced compounds, such as sulfides and ammonium. We studied chemoautotrophy by measuring dark-fixation of ^{13}C -bicarbonate into phospholipid derived fatty acid (PLFA) biomarkers at two coastal sediment sites with contrasting sulfur chemistry in the Eastern Scheldt estuary, the Netherlands. At one site where free sulfide accumulated in the pore water right to the top of the sediment, PLFA labeling was restricted to compounds typically found in sulfur and ammonium oxidizing bacteria. At the other site, with no detectable free sulfide in the pore water, a very different PLFA labeling pattern was found with high amounts of label in branched i- and a-PLFA besides the typical compounds for sulfur and ammonium oxidizing bacteria. This suggests that other types of chemoautotrophic bacteria were also active, most likely Deltaproteobacteria related to sulfate reducers. Maximum rates of chemoautotrophy were detected in first 1 to 2 centimeters of both sediments and chemosynthetic biomass production was high ranging from 3 to 36 mmol C m⁻² d⁻¹. Average dark carbon fixation to sediment oxygen uptake ratios were 0.22 ± 0.07 mol C (mol O₂)⁻¹, which is in the range of the maximum growth yields reported for sulfur oxidizing bacteria indicating highly efficient growth. Chemoautotrophic biomass production was similar to carbon mineralization rates in the top of the free sulfide site, suggesting that chemoautotrophic bacteria could play a crucial role in the microbial food web and labeling in eukaryotic poly-unsaturated PLFA was indeed detectable. Our study shows that dark carbon fixation by chemoautotrophic bacteria is a major process in the carbon cycle of coastal sediments, and should therefore receive more attention in future studies on sediment biogeochemistry and microbial ecology.

2.1 INTRODUCTION

Reoxidation of reduced intermediates like sulfide and ammonium formed during anaerobic mineralization processes is an important process in coastal marine sediments. Oxygen is typically only found in the top millimeters of these sediments and along macrofauna burrows (Glud 2008), and carbon mineralization proceeds in general by anaerobic processes primarily sulfate reduction. This results in the production and accumulation of large amounts of reduced compounds such as various forms of reduced sulfur and ammonium (Jørgensen 1978). In typical coastal sediments, free sulfide in the pore water is however often only detected below a couple of centimeters as it quickly reacts with iron hydroxides forming iron sulfide (FeS) or pyrite (FeS₂) (Jørgensen & Nelson 2004). Only in very active sediments or sediments containing little reactive iron, free sulfide can be found near the oxic top layer (Jørgensen & Nelson 2004). Long term burial of reduced compounds is thought to be a minor process (Jørgensen & Nelson 2004) and they are mostly transported to more oxidized horizons by either diffusion or bioturbation (Meysman et al., 2006). Oxygen is eventually the main oxidant of these reduced compounds although intermediate reoxidation steps by a variety of anaerobic pathways using nitrate or iron and manganese oxides may also be important (Jørgensen & Nelson 2004). It is estimated that reoxidation processes on average explain 70% of the sediment oxygen flux in shelf sediments (Soetaert et al., 1996) and this value is expected to be higher in active intertidal areas as anaerobic mineralization will be more important.

Many of the known prokaryotes involved in reoxidation processes are chemo(litho) autotrophs that use the energy gained from inorganic reactions to grow by fixing inorganic carbon in the dark (Kelly & Wood 2006). Chemoautotrophic carbon fixation has been shown to be an important process in, for instance, extreme marine ecosystems such as hydrothermal vents (Jannasch & Wirsén 1979; Cavanaugh 1983) and in the chemocline of anoxic marine basins (Sorokin 1972; Tuttle & Jannasch 1979). The current consensus is however that chemoautotrophy is a relatively minor process in coastal sediments due to the relatively low growth yields of chemoautotrophic organisms and the competition with chemical oxidation reactions (Jørgensen & Nelson 2004). In addition, true chemoautotrophic bacteria have to compete with mixotrophic and heterotrophic bacteria that are able to oxidize reduced sulfur compounds (Robertson & Kuenen 2006), which could be relevant especially in active coastal sediments receiving large amounts of organic matter. Studies where chemoautotrophy was actually quantified by determining dark carbon fixation rates are rare for typical coastal marine sediments and we have only been able to locate four studies: two on shallow subtidal sediments from the Baltic (Enoksson & Samuelsson 1987; Thomsen & Kristensen 1997), one study on an intertidal sand flat in the German Wadden Sea (Lenk et al., 2010) and a recent study on three brackish coastal

lake sediments in Brazil (Santoro et al., 2013). However, recent estimates suggest that up to 0.29 Pg C y^{-1} could be potentially fixed by chemoautotrophic micro-organisms in near shore and shelf sediments worldwide compared to 0.92 Pg C y^{-1} of mineralization (Middelburg 2011), suggesting a major role in the sediment carbon cycle. Finally, the dominant chemoautotrophic bacteria involved in sulfur oxidation are not well known in coastal marine sediments. A recent study identified an uncultured group of Gammaproteobacteria as important players (Lenk et al., 2010), but there may be many other groups involved in the diversity of reoxidation processes that occur in marine sediments.

We studied chemoautotrophy in two intertidal sites with contrasting sulfur chemistry: a site where free sulfide was not detected in the top few centimeters of the sediment and a very active site where high concentrations of free sulfide were found right to the top of the sediment. The main substrates driving chemoautotrophy are therefore expected to be different at both sites, namely free sulfide at the very active site versus iron sulfides in the more typical coastal sediment. Chemoautotrophy rates were determined by incubating sediment cores with stable isotope labeled ^{13}C -bicarbonate and measuring labeling in phospholipid derived fatty acids (PLFA). This method both yields estimates of total chemoautotrophy rates and provides an indication of the active bacterial community (Knief et al., 2003; de Bie et al., 2002; Glaubitz et al., 2009). The diversity of Ribulose-1,5-bisphosphate carboxylase/oxygenase (RuBisCO) genes was studied to further indicate possible active chemoautotrophs that use the Calvin cycle for carbon fixation. Finally chemoautotrophy rates were compared with diffusive oxygen fluxes and carbon mineralization rates.

2.2 MATERIALS & METHODS

2.2.1 Description of field sites

Two field sites in the Eastern Scheldt estuary (The Netherlands) were selected, which were expected to show high mineralization rates and have major differences in sulfur chemistry. The site in the Zandkreek area ($51^{\circ}32'41''\text{N}$, $3^{\circ}53'22''\text{E}$) was situated next to a Pacific oyster (*Crassostrea gigas*) bed and was sampled in April 2005 (abbreviation ZK05) and October 2007 (ZK07). The Pacific oyster is an invasive species in the area that was introduced in the Eastern Scheldt around 1970. It stimulates sedimentation and sediment carbon mineralization either by decreasing water currents over the sediment or via pseudo-feces production and biodeposition (Smaal et al., 2009). Sediments were non-sulfidic in the top 5 centimeters in 2005 and slightly sulfidic below 2 centimeter in 2007 (See Result).

The Rattekaai site ($51^{\circ}26'21''\text{N}$, $4^{\circ}10'11''\text{E}$) was situated at the entrance of a salt marsh creek where macroalgal debris (mainly *Ulva* derived) accumulates and is buried

during winter. The sediment was highly sulfidic right to the top and samples were taken from patches where the sediment was covered with a whitish layer in April 2005 (RK05) and May 2006 (RK06). Based on microscopy, typical *Beggiatoa*-like sulfur-oxidizing bacteria were abundant in the top few millimeters of the Rattekaai sediment, especially in 2005 and to a lesser degree in 2006.

2.2.2 Sediment sampling

Undisturbed sediments were sampled with two sizes of polycarbonate core liners. The smaller cores (internal diameter 4.6 cm) contained silicon-filled injection ports at every 0.5 centimeter and were used for measuring chemoautotrophy rates. The larger cores (internal diameter 6 cm) were used for additional measurements of pore water profiles and sediment characteristic, and for measuring mineralization rates. Sediments were sampled at low tide and therefore did not have overlying water. Cores were processed the same day for chemoautotrophy rate measurements and other analyses.

2.2.3 Chemoautotrophy rates

Chemoautotrophy rate measurements were started by injecting 100 μl of 20 mM $\text{NaH}^{13}\text{CO}_3$ (99% ^{13}C ; Cambridge Isotope Laboratories, Andover, MA, USA) horizontally into the sediment cores at 0.5 cm depth intervals by using the line-injection method (Jørgensen 1978). The ^{13}C -label was dissolved in artificial seawater lacking calcium or magnesium in order to avoid precipitation (Kester et al., 1967). The label was made oxygen free by bubbling with nitrogen gas shortly before injection. Sediment cores were incubated in the dark within 2 $^\circ\text{C}$ of the *in situ* temperature (see Table 1) for various periods of up to 4 days, and were ventilated daily by removing the top stopper for one minute (ZK) or incubated without top stoppers (RK) to circumvent the development of suboxic condition in the headspace. After incubation, sediment cores were sliced to a depth of 5 cm and sediment slices were quickly centrifuged (4500 rpm, 5 min) to collect pore water for concentration and ^{13}C analysis of dissolved inorganic carbon (DIC). Sediments were subsequently frozen at -20 $^\circ\text{C}$ and lyophilized before further analysis. Unlabeled, control cores were also processed.

2.2.4 PLFA analysis and calculation of chemoautotrophy rates

Lyophilized sediments were analyzed for PLFA concentrations and ^{13}C -labeling as described before (Boschker et al., 1998; Boschker et al., 2004). In short, PLFA were extracted according to standard protocols and were analyzed by gas chromatography – isotope ratio mass spectrometry (GC-IRMS, Thermo, Bremen, Germany) on an

apolar analytical column (HP5-MS, Agilent, Santa Clara, CA, USA). Stable carbon isotope ratios are reported as $\delta^{13}\text{C}$ ratios on the VPDB scale. Excess ^{13}C in individual PLFA was calculated as in Boschker et al (1998) and divided by the atom percent excess ^{13}C in the DIC pool to calculate actual PLFA synthesis rates. Only very minor labeling was found in poly-unsaturated PLFA typical for Eukarya (see Results) suggesting that PLFA labeling was primarily by Bacteria. We therefore used the labeling data for all common bacterial PLFA in the 12:0 to 20:0 range in our calculations and not just the specific bacterial biomarker PLFA (Middelburg et al., 2000). Total bacterial chemoautotrophy rates were determined by summing synthesis rates in all PLFA typically found in bacteria and converted to chemoautotrophic biomass production by dividing by the typical PLFA content of aerobic bacteria (55 mmol PLFA-C (mol biomass C)⁻¹ (Middelburg et al., 2000; Brinch-Iversen & King 1990). To study the differences in active chemoautotrophic bacterial communities, we performed a principle component analysis (PCA) on log-transformed PLFA ^{13}C -labeling data (in Mol%) using the Statistica software package (StatSoft, Tulsa, USA).

2.2.5 Additional measurements

Oxygen profiles were determined with oxygen microelectrodes (Unisense Ox100, Aarhus, Denmark), which were lowered with a micromanipulator into the sediment until no oxygen was detected. Two profiles were recorded for each duplicate sediment core (four profiles total), which were kept within 2°C of the *in situ* temperature. Oxygen fluxes into the sediment were calculated as described in Van Frausum et al., (2010) with sediment tortuosity estimated from sediment porosity as in Boudreau & Meysman (2006).

Sediment pore water was sampled by slicing duplicate sediment cores in an anaerobic glove-box filled with 3% hydrogen in nitrogen gas (Coy Laboratory Products, Ann Arbor, MI, USA) and slices were centrifuged at 4500 rpm for 10 min at *in situ* temperature. Samples for sulfide analysis were immediately fixed in zinc acetate and analyzed according to Cline (1969). Samples for ammonium and anion analysis were frozen, and analyzed on a QuAAtro segmented flow analyzer (Seal Analytical, Norderstedt, Germany) and suppressed high performance ion chromatography on a Dionex Ionpac AS-14 column (Thermo, Sunnyvale, CA, USA), respectively. Samples for ^{13}C -DIC were added to head-space vials (10 ml) and after acidification analyzed for DIC concentrations and ^{13}C -content by elemental analyzer - IRMS (Moodley et al., 2005).

Sediment carbon mineralization rates were determined using the jar method (Kristensen et al., 1999). Sediment cores were sliced as above and were incubated in completely filled centrifuge tubes. Centrifuge tubes containing the sediment were sealed in air-tight incubation bags filled with nitrogen gas to keep them strictly anaerobic and were incubated within 2°C of the *in situ* temperature for up to 6 days. Sediment pore water was collected

and analyzed as described above. Mineralization rates were calculated from DIC and ammonium production with time and ammonium production was converted to carbon mineralization rates by using the sediment C/N ratio (Table 1).

2.2.6 RuBisCO type IA clone libraries

To further study the diversity of chemoautotrophic bacteria that utilize the Calvin cycle for carbon dioxide fixation, RuBisCO clone libraries were constructed for both sites in March 2008. Sediments were sampled as described above, and the top 0.5 cm of the cores showing the highest chemoautotrophy rates was collected and immediately frozen at -80°C. Total community DNA was extracted from 0.5 g of wet sediment using the MoBio UltraClean Soil DNA Isolation kit according to protocol (MoBio, Carlsbad, CA, USA).

We developed a new degenerative primer set to specifically amplify RuBisCO type IA as this group contains most of the true chemoautotrophic bacteria involved in sulfur and ammonium oxidation (Tabita 1999; Nigro & King 2007). The new primer set also targets *Beggiatoa*-like RuBisCO sequences (Mußmann et al., 2007), which was important as *Beggiatoa*-like bacteria were found at the RK site but were not covered by previously published primer sets developed for chemoautotrophic bacteria. The primer set also targets some of the lower branching Type 1B sequences found in unicellular cyanobacteria, and consists of forward primer 571 (GAY-TTYACCAARGAYGAYG) and reversed primer 898E (ACRCGGAARTGRATRCC). The primer set was first tested against a positive control (*Thioalkalimicrobium aerophilum* kindly provided by Gerhard Muyzer, Delft Technical University, The Netherlands) and PCR conditions were subsequently optimized to specifically amplify the target sequences from sediment DNA extracts.

The final PCR reaction mixture contained: 2.5 µl 10x standard Taq reaction buffer (without Mg), 3.0 mmol L⁻¹ Mg²⁺, 0.2 mmol L⁻¹ dNTPS, 0.2 µmol L⁻¹ of each primer (571 and 898E), 2 U of NEB Taq DNA polymerase, 5% v/v DMSO, 0.2% w/v BSA and 16 µl autoclaved demi water. The PCR cycling intervals were established as follows: preheating at 94 °C for 5 minutes, followed by 40 cycles of denaturation step at 94°C for 1 minute, annealing step at 51 °C for 30 seconds and extension at 72 °C for 30 seconds. The PCR reaction was finished with a final extension time of 7 minutes at 72 °C. PCR products for each sample (RK and ZK) were cloned into *Escherichia coli* Top10 cells using TOPO TA cloning kit (Invitrogen, Carlsbad, CA, USA). Sequencing was performed by a genetic analyzer (Applied Biosystems 3130 Genetic Analyzer, Carlsbad, CA, USA). Editing of the obtained sequences was carried out using the BioEdit software package (<http://jwbrown.mbio.ncsu.edu/>

Table 1. Sediment *in situ* temperature, sediment characteristics, oxygen consumption rates, carbon mineralization rates, chemoautotrophy rates and yields (averages \pm standard deviations, N = 2) for the coastal marine sediments in this study.

Site/Year	Temp. °C	POC ¹ (%)	C/N ¹	O ₂ penetration depth (mm)	O ₂ flux (mmol m ⁻² d ⁻¹)	C mineralization ² (mmol m ⁻² d ⁻¹)	Chemoautotrophy ² (mmol C m ⁻² d ⁻¹)	Yield C/O ₂ (mol C (mol O ₂) ⁻¹)
RK05	14	—	—	0.45 \pm 0.10	17.2 \pm 3.0	—	5.5 \pm 1.9	0.32 \pm 0.11
RK06	17	2.0	10.9	0.23 \pm 0.06	192 \pm 41	197 \pm 36	36.3 \pm 4.8	0.19 \pm 0.03
ZK05	14	—	—	1.7 \pm 0.1	15.0 \pm 0.4	—	2.6 \pm 0.3	0.17 \pm 0.02
ZK07	13	0.6	7.7	0.95 \pm 0.06	15.5 \pm 1.6	105.9 \pm 19.1	2.9 \pm 0.2	0.18 \pm 0.01

¹ Data for 0-1 cm sediment depth. ² Data integrated over 0-5 cm sediment depth.

Bio-Edit/bioedit.html). Primer sequences (T3, T7, 571, 898E) were removed from sequences, then translated to protein sequences, and compared to known sequences using BLAST. Protein sequence alignments and phylogenetic analysis was done in MEGA V (Tamura et al., 2011). Sequences have been deposited in the GenBank database under accession numbers JQ659214 to JQ659253.

2.3 RESULTS

In spring 2005, both sites (RK05 and ZK05) were studied in an initial test to determine if chemoautotrophy rates could be quantified by ^{13}C -DIC labeling of PLFA in the dark. Sites were sampled again in spring 2006 (RK06) and autumn 2007 (ZK07), when a more extensive sampling program was executed.

2.3.1 Sediment biogeochemistry

Oxygen penetrated significantly deeper in ZK sediment (1-2 mm) than RK sediment (0.2-0.5 mm, Table 1). At RK06, high concentrations of free sulfide were found in the very top layer of the sediment, whereas sulfide only started to accumulate below 2 cm sediment depth at ZK07 (Fig. 1). Sulfide and ammonium concentrations were more than 10 times higher for RK06 than for ZK07 throughout the sediment column (Fig. 1). In 2005, pore water samples were also taken at both sites and analyzed for sulfide, but samples were taken two weeks before chemoautotrophy measurements and not at exactly the same location, which is especially important for the RK site due to its patchy nature. However, the contrast between the RK and ZK sites was similar with high concentrations of free sulfide at RK05 right to the top of the sediment core and no detectable sulfide in top 5 cm of the ZK05 sediment (results not shown). Pore water concentrations of DIC and SO_4^{2-} showed little variation with depth for ZK07 strongly indicating bio-irrigation, whereas DIC increased and SO_4^{2-} decreased with depth for RK06 indicating carbon mineralization by sulfate reduction (Fig. 1).

Diffusive sediment oxygen consumption rates as determined from microelectrode profiles were very high for RK06 with $192 \text{ mmol m}^{-2} \text{ d}^{-1}$ and were approximately $15 \text{ mmol m}^{-2} \text{ d}^{-1}$ for all other samplings (Table 1). The difference between the two RK samplings is probably due to the patchy nature of the site, even though visually similar black sediments with a whitish top layer were sampled in both years. For RK06, anaerobic carbon mineralization rates were about twice as high in the top centimeter ($6.8 \pm 0.5 \text{ } \mu\text{mol C cm}^{-3} \text{ d}^{-1}$) than in the 1-5 cm layer ($3.2 \pm 0.8 \text{ } \mu\text{mol C cm}^{-3} \text{ d}^{-1}$), whereas both sediment layers showed similar carbon mineralization rates for ZK07 (0-1 cm, $1.6 \pm 0.9 \text{ } \mu\text{mol C cm}^{-3} \text{ d}^{-1}$; 1-5 cm, $2.3 \pm 0.3 \text{ } \mu\text{mol C cm}^{-3} \text{ d}^{-1}$). Integrated over the upper 5 cm, anaerobic carbon mineralization rates were 197 and 106 mmol

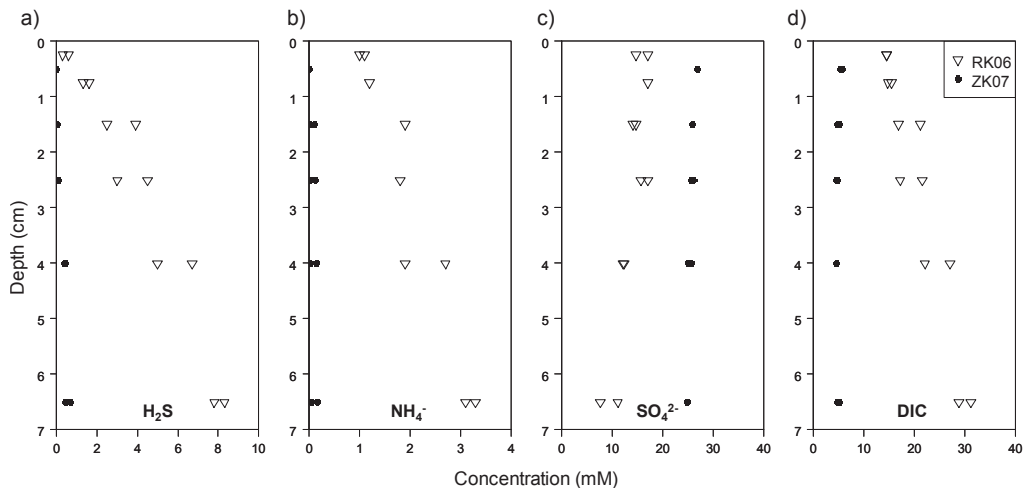


Figure 1. Porewater concentrations for the RK06 and ZK07 sediments. Shown are data for sulfide (a), ammonium (b), sulfate (c) and DIC (d).

C m⁻² d⁻¹ at RK06 and ZK07, respectively (Table 1). Ammonium production-based mineralization rates agreed with carbon mineralization rates at all sediment depths and ammonium-based mineralization rates in the top layer (0-1 cm) were 8.0 ± 2.0 and 1.1 ± 0.3 $\mu\text{mol C cm}^{-3} \text{d}^{-1}$ for RK06 and ZK07, respectively.

2.3.2 Chemoautotrophy rates

Dynamics of PLFA labeling with ¹³C-bicarbonate were studied in detail for RK06. Substantial labeling could already be detected in the 0-0.5 cm horizon after 4 hours of incubation and, although there was some variation, total PLFA labeling increased linearly with time for up to 4 days ($R^2 = 0.77$, $n = 8$). Similar results were obtained for RK05 and ZK05 as calculated chemoautotrophy rates were similar after 2 and 4 days of incubation (data not shown). For RK06, the ¹³C-enrichment in the DIC pool in the 0-0.5 cm of the sediment decreased from 1800 ± 120 ‰ $\Delta\delta^{13}\text{C}$ (¹³C enrichment of the DIC pool of 1.9‰) approximately after 4 hours to 550 ± 110 ‰ $\Delta\delta^{13}\text{C}$ (0.5‰ ¹³C) after four days, probably because of exchange with atmospheric carbon dioxide and dilution with DIC produced during organic matter mineralization. Cores from RK06 could not be kept closed at the top because sub-oxic conditions developed within one day due to the very high oxygen consumption rates. The reported chemoautotrophy rates have been corrected for this change in DIC labeling with incubation time.

Chemoautotrophy was generally limited to the top centimeter of the sediment especially at the RK site (Fig. 2). For RK06, the main activity ($95 \pm 1\%$) was found in the top 0-0.5 cm horizon, which contains the oxic top layer, and below 1 cm depth

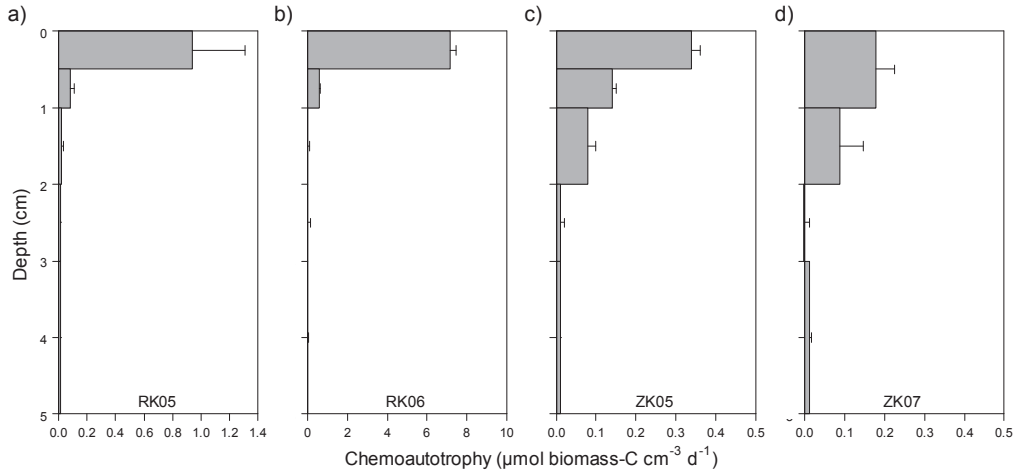


Figure 2. Depth distribution of chemoautotrophy as estimated from ^{13}C -DIC PLFA labeling in dark incubations for the RK and ZK sediments.

no activity could be detected. Similar results were obtained for RK05 when depth profiles were determined after 2 and 4 days. Interestingly, chemoautotrophy rates recorded in the top layer of RK06 were similar ($7.2 \mu\text{mol C cm}^{-3} \text{d}^{-1}$, Fig.2) to the anaerobic carbon mineralization rates ($6.8 \mu\text{mol C cm}^{-3} \text{d}^{-1}$, see above), suggesting balanced CO_2 production and consumption. For the ZK sediment, highest chemoautotrophy rates were also found in the top layer of the sediment, but activity remained relatively high down to 2 cm depth for both sampling dates.

Depth integrated (0-5 cm), whole-core chemoautotrophy rates ranged from 3 – 36 $\text{mmol C m}^{-2} \text{d}^{-1}$ (Table 1). Rates measured at RK06 were very high, about 6 times higher than for RK05, which is probably due to the patchy nature of the site and differences between years (Table 1). Rates for ZK05 and ZK07 were however in the same range and always lower than for the RK site. Whole-core chemoautotrophy rates generally scaled with diffusive oxygen uptake rates and whole sediment chemoautotrophy to oxygen consumption ratios were relatively similar for all sites ranging from 0.17 to 0.32 $\text{mol C (mol O}_2\text{)}^{-1}$ (Table 1).

2.3.3 Active chemoautotrophic bacterial communities

As we determined ^{13}C -dark fixation rates into biomarker PLFA, the results can also be used to describe and compare active communities of chemoautotrophic bacteria. As an example, Fig. 3 shows the PLFA concentration and labeling data as obtained during this study after one day of incubation for the top layer (0-0.5 cm)

of RK06. The PLFA detected were typical for intertidal sediments with high amounts of both bacterial and eukaryote-specific biomarkers; the latter were probably mainly derived from the diatoms growing on the sediment surface as they were dominated by 20:4 ω 6 and 20:5 ω 3 that occur in high amounts in diatoms (Dijkman & Kromkamp 2006; Fig. 3a). Detection of PLFA labeling is based on the increase in $\delta^{13}\text{C}$ ratios and these were well above detection limits in many PLFA (Fig. 3b; 0.6 to 2‰ $\Delta\delta^{13}\text{C}$ detection limit depending on compound). The $\Delta\delta^{13}\text{C}$ ratios were highly variable between PLFA ranging for instance from 0 to 110‰ after one day (Fig. 3b), suggesting that a specific sub-group of the total bacterial community was active. At RK06, PLFA that gained most ^{13}C label were 14:0, 16:1 ω 7c, 16:1 ω 5, 16:0 and 18:1 ω 7c together explaining $83 \pm 4\%$ of the total incorporation into PLFA (Fig. 3c). There were also minor amounts of label recovered in 14:1, 15:1, 15:0, 17:1 ω 8 and cy17:0. Branched, i- and a-PLFA and eukaryote PLFA like 20:4 ω 6 and 20:5 ω 3 gained very little label even though they were a dominant feature in the PLFA concentration pattern (Fig. 3a, c).

The PLFA labeling pattern for the two ZK samplings was very different from the RK site strongly suggesting that different chemoautotrophic communities were active at the two sites. For comparison, the labeling pattern of ZK05 is also presented in Fig. 3d as it showed the largest differences from RK06. Main differences were a much higher labeling in all branched i- and a-PLFA and in several mono-unsaturated PLFA (15:1, 16:1 ω 7t, 17:1 ω 8c, 18:1 ω 9c and 18:1 ω 5) and uneven numbered saturated PLFA (15:0, cy17:0 and 17:0) for both ZK samplings.

To study the differences in PLFA labeling patterns further we performed a PCA analysis for all sediment layers where significant chemoautotrophy was detected (depth ranges RK 0-1 and ZK 0-2 cm; Fig. 4). The first PCA axis explained 42 % of the variation found in the data set, whereas the second axis added another 15%. Clustering was mainly based on 16:1 ω 7c versus 15:0, 17:0, 17:1 ω 8c, 18:0 and all branched PLFA for the first axis similarly as seen in Fig. 3 and 16:0 and 16:1 ω 7t versus 14:0, 14:1 and cy17:0 for the second axis. Clustering of sediment samples was mostly determined by sampling site and sampling year with both RK samplings clustering closely together and more dispersal amongst the samples from the ZK site was observed (Fig. 4a). Some additional variation was found with sediment depth but only for ZK06, where the top layer data (0-1 cm) clustered more closely together with the RK data whereas the deeper layers were shifted towards the ZK05 samples (Fig. 4a). Distribution of label among PLFA did not change substantially with incubation time, suggesting that active chemoautotrophic communities remained similar for up to 4 days. The PCA analysis therefore also showed major difference in active chemoautotrophic bacterial communities between the high free-sulfide RK and low free-sulfide ZK sediments.

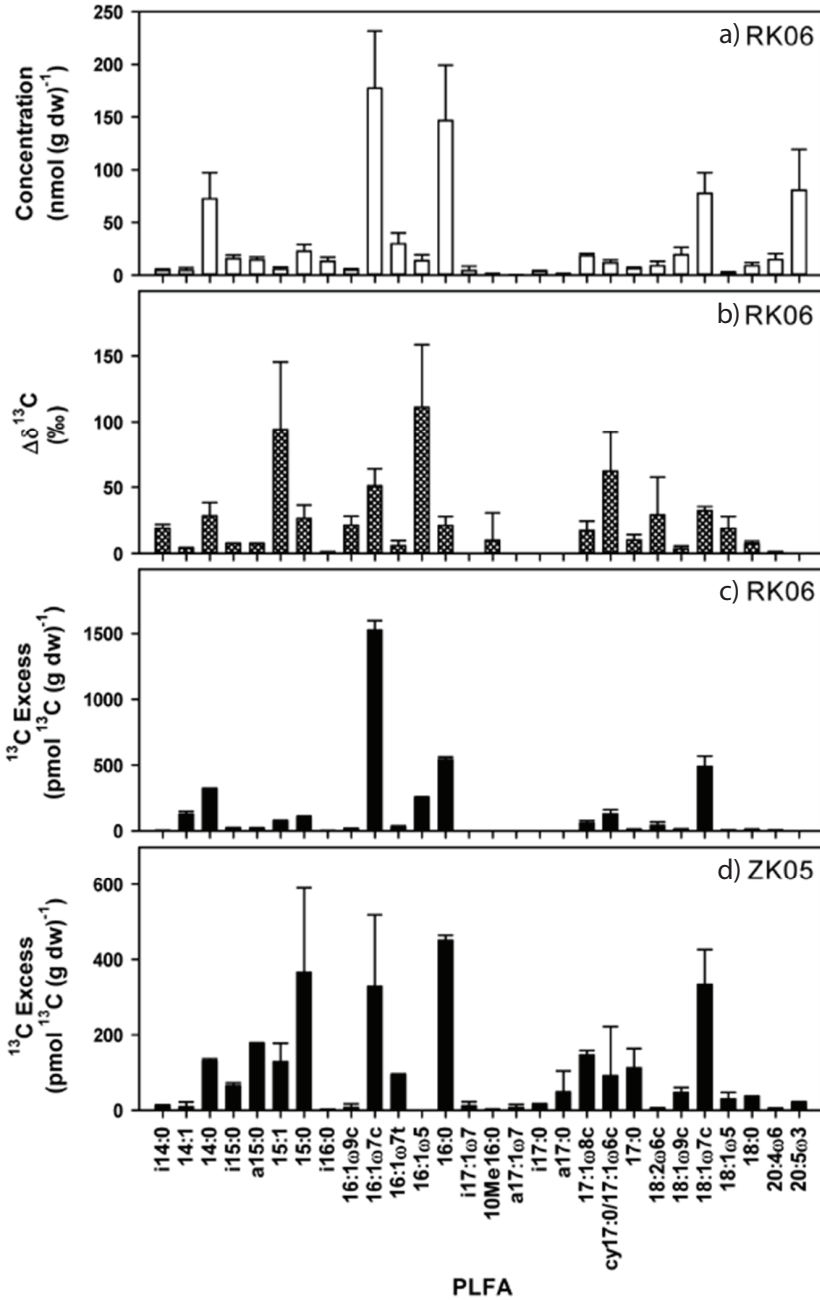


Figure 3. PLFA concentrations (a), $\Delta\delta^{13}\text{C}$ ratios (b) and excess- ^{13}C (c) for RK06 (0-0.5 cm horizon) after 1 day of incubation with ^{13}C -DIC. The excess- ^{13}C PLFA data for ZK05 (0-0.5 sediment horizon) after 2 day of incubation are also shown for comparison d).

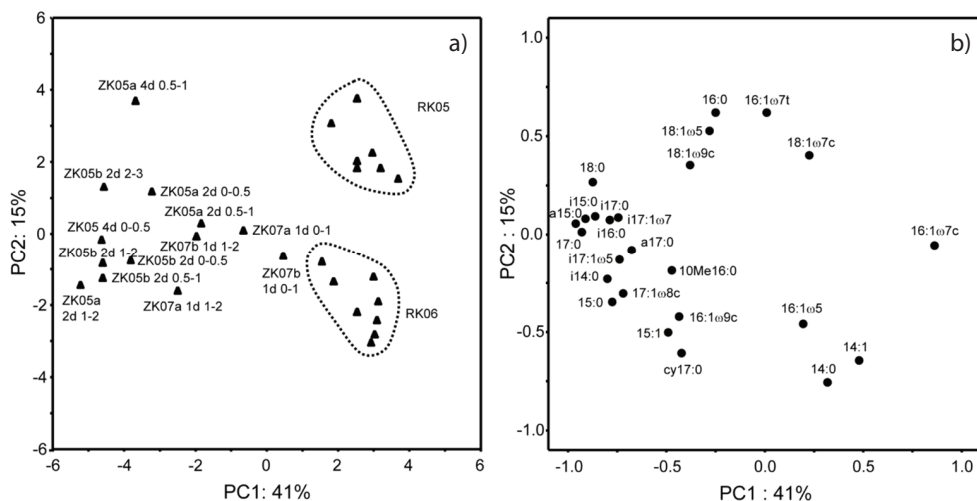


Figure 4. Results of the PCA analysis of the ^{13}C -labeling patterns in PLFA for all samples with detectable chemoautotrophy showing the site scores (a) and variable scores (b) for the two PCA axes that explained most of the variance.

There was also indirect evidence of transfer of dark-fixed carbon to fauna: some ^{13}C -labeling was detected in bulk sediment PLFA characteristic of Eukarya and therefore fauna, 18:2 ω 6c for both sites and 20:4 ω 6 and 20:5 ω 3 for the ZK site (Fig.3c, d).

2.3.4 RuBisCO type IA diversity

To further characterize the chemoautotrophic community, we used a novel primer set to construct clone libraries for the RuBisCO Type IA large-subunit gene for both sites in 2008. For the RK site, 17 clones related to Type IA RuBisCO were recovered and site ZK yielded 23 clones. We also found a limited number of clones related to unicellular cyanobacteria derived type IB RuBisCO especially for the RK site (not shown).

The phylogenetic relationship for the clones from both sites, together with other environmental clones and related micro-organisms is shown in Fig. 5. Type IA clones were found in two main clades labeled type IA 1 and IA 2. RuBisCO type IA 1 clones were most closely related to uncultured faunal endosymbionts belonging to the Gammaproteobacteria and marine sediment clones from a variety of other studies. Whereas sequences in clade IA 2 were related to various chemoautotrophic sulfur and ammonium oxidizing bacteria and also to other environmental sediment clones. *Beggiatoa* RuBisCO type IA also clustered in clade IA 2, but although clones from both RK and ZK were found in this clade they were not closely related to *Beggiatoa* suggesting

that they belonged to other groups of chemoautotrophic bacteria. In general rather similar sequences were recovered from both sites, although ZK clones were relatively more abundant in clade IA 1 and RK clones dominated clade IA 2. The results suggest that chemoautotrophic communities, which use the Calvin cycle for carbon fixation, were relatively similar at both sites and that *Beggiatoa* could not be detected at least for the 2008 sampling.

2.4 DISCUSSION

2.4.1 Rates of chemoautotrophic carbon fixation

We detected very high rates of chemoautotrophic dark fixation in the top layers of two intertidal sediments especially for the RK06 sediment. Volumetric chemoautotrophy rates detected in the top of the RK sediment were comparable to some of the highest sulfate reduction rates detected in marine sediments (Skyring 1987). These high rates are in part explained because reduced substrates produced by mineralization processes are released throughout the active sediment column whereas the reoxidation by chemoautotrophic bacteria is concentrated in the top of the sediment. Dark fixation rates as measured in our study also includes anapleurotic reactions by heterotrophic bacteria, which may account for up to 5 to 10% of the biomass produced by in all bacteria including heterotrophs (Romanenko 1964; Dijkhuizen & Harder 1985; Feisthauer et al., 2008). However, chemoautotrophy rates detected in the top-layer of the RK06 sediment were actually similar to carbon mineralization rates (Fig. 2 and see Results), suggesting that the role of anapleurotic reactions was minimal explaining at most about 5 % of the measured dark-fixation rates if one assumes a relatively high heterotrophic growth efficiency of 50% (del Giorgio & Cole 1998). An additional advantage of measuring dark fixation through ^{13}C -labeling of PLFA is that carbon fixed through anapleurotic reactions is not directly utilized in the synthesis of lipids such as fatty acids (Feisthauer et al., 2008; Wuchter et al., 2003). Based on oxygen consumption rates and assuming a coupled system, chemoautotrophy explained between 18% (RK06) and 32% (RK05) of the sediment carbon cycling, which would make chemoautotrophy the second or third most important biological carbon cycling process after anaerobic carbon mineralization and possibly photosynthesis by benthic diatoms in these intertidal sediments.

Sulfur oxidizing bacteria are expected to be the main chemoautotrophs in these intertidal sediments; the contribution from ammonium oxidizing bacteria should be less important because about 6 times more sulfide than ammonium is produced during anaerobic carbon mineralization given the typical C:N ratio for marine organic matter (Redfield 1958). In addition, nitrifying prokaryotes also tend to have lower

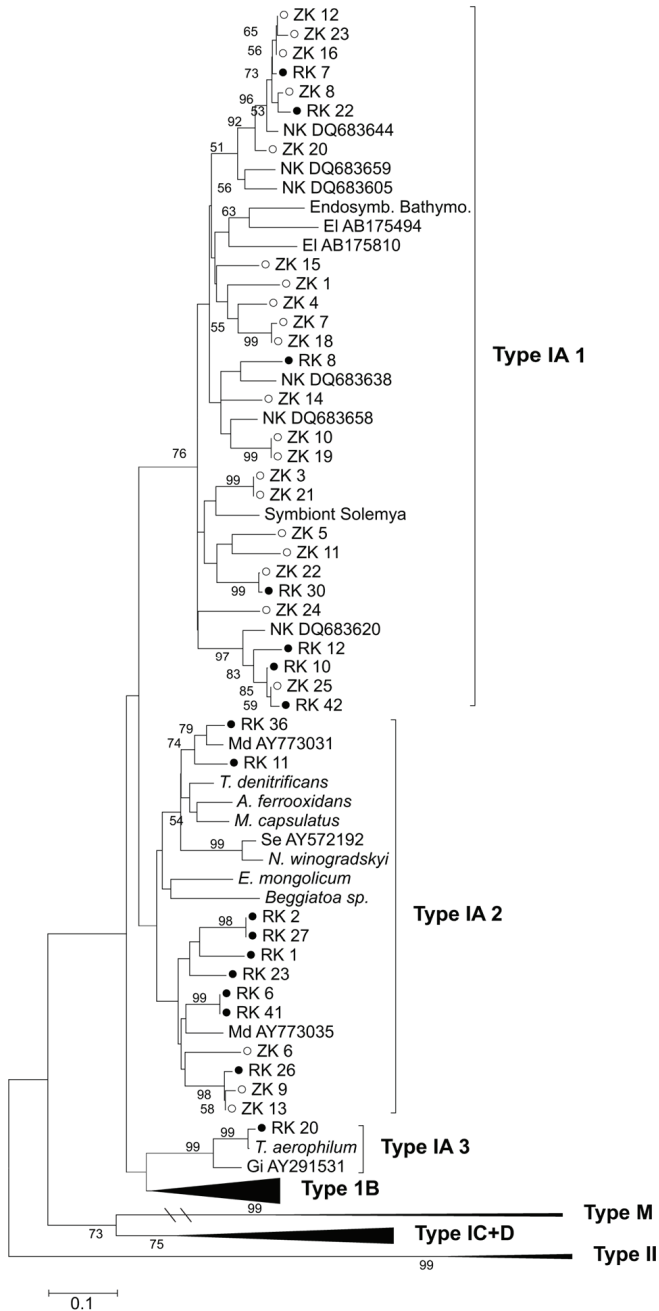


Figure 5. Phylogenetic relationships between RuBisCO Type IA clones recovered from the high free-sulfide RK and low free-sulfide ZK site in 2008 together with relevant sequences of environmental clones from other studies and chemoautotrophic prokaryotes retrieved from Genbank (EI: Elsaied et al., 2007; NK: Nigro & King 2007; Gi: Giri et al., 2004; Md: Madrid et al., unpublished). The Neighbor-Joining tree is based on amino acid sequence and bootstrap values are based on 1000 times replication.

growth yields per mol of substrate oxidized than sulfur-oxidizers (Prosser 1989). The chemoautotrophy data from our study scaled well with measured diffusive oxygen fluxes with an average whole system yield (\pm SD) of 0.22 ± 0.07 mol C (mol O₂)⁻¹ (Table 1), which is very similar to the typically reported maximum growth yields for aerobic sulfur oxidizing bacteria of 0.23 ± 0.11 mol C (mol O₂)⁻¹ (Hempflin & Vishniac 1967; Timmer-Ten 1981; Nelson & Jannasch 1983; Nelson et al., 1986; Odintsova et al., 1993; Hagen & Nelson 1996; Kelly 1999). The similarity in C:O₂ yield between intertidal sediments and sulfur oxidizing bacterial cultures can only be explained if most of the sediment oxygen consumption was indeed used for reoxidation of reduced sulfur and if reoxidation was predominantly performed by obligate sulfur-oxidizing chemoautotrophic bacteria growing close to their maximum reported yields. In addition, chemoautotrophic bacteria should have effectively competed with chemical oxidation processes such as the oxidation of free sulfide with oxygen, as has been shown in gradient systems where oxygen and sulfide are found in close proximity similar to the RK site (Jørgensen & Nelson 2004). Furthermore, even though these coastal sediments receive very high organic matter inputs, our data suggest that the activity by heterotrophic and mixotrophic sulfur-oxidizing bacteria was also limited as this should have led to lower C:O₂ yields. Competition between autotrophic and heterotrophic or mixotrophic sulfur oxidizing bacteria depends to a large extent on the sulfur/organic substrate ratio with low ratios supporting heterotrophic sulfur oxidation (Gottschal et al., 1979; Robertson & Kuenen 2006), but this apparently didn't play a role in the studied sediments possibly due to strong competition for organic substrates by other heterotrophic bacteria. Our results suggest that dark fixation rates as determined by ¹³C-bicarbonate labeling of PLFA yield realistic chemoautotrophy rates in relation to sediment biogeochemistry and that chemoautotrophic bacteria were growing with high efficiency independent of sediment sulfur chemistry.

Chemoautotrophy rate data are available from only four other studies on coastal marine sediments, all of which measured total dark fixation rates by determining ¹⁴C-DIC incorporation into POC (Enoksson & Samuelsson 1987; Thomsen & Kristensen 1997; Lenk et al., 2011; Santoro et al., 2013). It should be noted that two of these studies are based on laboratory incubations with homogenized sediments (Thomsen & Kristensen 1997; Santoro et al., 2013). Thomsen and Kristensen (1997) reported maximum rates of approximately $0.35 \mu\text{mol C cm}^{-3} \text{d}^{-1}$ (averaged over the same depth as in the present study) similar to site ZK, whereas rates found by Enoksson and Samuelsson (1987) and Lenk et al., (2011) are lower at about $0.12 \mu\text{mol C cm}^{-3} \text{d}^{-1}$. The data collected by Thomsen and Kristensen (1997) yield a C:O₂ ratio of 0.24 mol C (mol O₂)⁻¹ similar to our data, whereas the chemoautotrophy rates reported by Enoksson and Samuelsson (1987) are substantially higher than expected from their oxygen consumption rates (C:O₂ ratio about 1.2 mol C (mol O₂)⁻¹). The C:O₂

ratios from Enoksson and Samuelsson (1987) cannot be readily explained in relation to the reported growth yields of sulfur reducing bacteria (Hemphlin & Vishniac 1967; Timmer-Ten 1981; Nelson & Jannasch 1983; Nelson et al., 1986; Odintsova et al., 1993; Hagen & Nelson 1996; Kelly 1999), suggesting that the chemoautotrophy rates for this sediment may have been substantially overestimated possibly due to the incomplete removal of ^{14}C -DIC label. Santoro et al., (2013) found much lower yields of about $0.025 \text{ mol C (mol O}_2\text{)}^{-1}$ for three brackish coastal lake sediments. Lenk et al., (2011) also reported ^{14}C -POC based chemoautotrophy rates of $4.16 \pm 0.03 \text{ mmol C m}^{-2} \text{ d}^{-1}$ for an intertidal flat consisting of permeable sands, which related well to sediment sulfide fluxes (Jansen et al., 2009; Lenk et al., 2011). Lenk et al., did not report oxygen consumption rates. However, potential oxygen fluxes of approximately $70 \text{ mmol O}_2 \text{ m}^{-2} \text{ d}^{-1}$ have been reported for the same sand flat (Billerbeck et al., 2006), suggesting a relatively low C: O_2 yield of about $0.06 \text{ mol C (mol O}_2\text{)}^{-1}$. Oxygen fluxes may have been overestimated because they are potential rates based on aerobic incubations with sediments from different horizons that may not always be oxic. The depth distributions of chemoautotrophy of Enoksson and Samuelsson (1987) and Lenk et al., (2011) were different from our study as they both found substantial rates deeper in the sediment up to a depth of 10 cm. Lenk et al., (2011) studied a permeable sediment where oxidants such as oxygen are transported deep into the sediment by advective pore water flows (Billerbeck et al., 2006), which may explain the high chemoautotrophy rates deeper in the sediment. The chemoautotrophy rates in our study at the RK06 (3.2 to $6.8 \text{ } \mu\text{mol C cm}^{-3} \text{ d}^{-1}$) are the highest reported so far for coastal marine sediments.

Furthermore, our results suggest that chemoautotrophically fixed carbon may also be an important food source in the microbial food web in these typical coastal sediments. Chemoautotrophy rates were similar to carbon mineralization rates in the top layer of the RK06 sediment (Fig. 2 and Results). Net consumption of DIC related to the chemoautotrophy has been indicated in the top layer of active coastal sediments (Aller & Yingst 1985; Thomsen & Kristensen 1997). This suggests that the production by chemoautotrophs dominated the microbial food web and that heterotrophic bacterial secondary production was less important (if one assumes a growth efficiency of 50% for heterotrophic bacteria). Santoro et al., (2013) measured growth of both chemoautotrophic and heterotrophic bacteria in three brackish lakes and found that chemoautotrophy could explain up to 50% of the heterotrophic bacterial growth. Additionally, chemosynthetically produced biomass may potentially be an important source of energy fueling the benthic food web. We indeed detected limited labeling in eukaryotic fauna-derived PLFA for both sediments (Fig.3c, d), which suggests that sediment fauna may in part be feeding on chemoautotrophic bacteria. Chemoautotrophic bacteria support the food web in many extreme marine ecosystems like hydrothermal vents and

mud volcanoes with limited organic matter inputs (Cavanaugh 1983; Van Gaever et al., 2009). Based on our results, the role of chemoautotrophic carbon fixation in the benthic food web of coastal marine sediments should receive more attention.

2.4.2 Communities of chemoautotrophic bacteria

We detected clear difference in PLFA labeling patterns for the ZK and RK sediments suggesting that the active chemoautotrophic bacterial communities were substantially different (Fig. 3 and 4). The classical sulfur and ammonium oxidizing bacteria predominantly contain even-numbered saturated and mono-unsaturated PLFA such as 14:0, 16:1 ω 7c, 16:0 and 18:1 ω 7c (Blumer et al., 1969; Kerger et al., 1986; Lipski et al., 2001; Knief et al., 2003; Zhang et al., 2005; Sakata et al., 2008; Van Gaever et al., 2009). For the RK sediment, most of the label was indeed recovered in these typical PLFA and the PLFA labeling pattern for instance closely resembles the PLFA composition of *Beggiatoa* especially for RK05 (Fig. 3 and Zhang et al., 2005; Van Gaever et al., 2009). Some types of sulfur oxidizing thiobacilli also contain uneven numbered PLFA like cy17:0 (Kerger et al., 1986; Knief et al., 2003), and label was indeed recovered in these PLFA especially at both ZK samplings and at RK06 suggesting that these groups may also be active in coastal sediments. In view of the high free sulfide and ammonium concentrations in the pore water, the PLFA labeling at the RK site was therefore in agreement with the activity of typical chemoautotrophic sulfur and ammonium oxidizing bacteria.

In contrast, major amounts of label were also found in branched i- and a-PLFA at the ZK site, which have not been reported in the classical chemoautotrophic sulfur oxidizing and nitrifying bacteria. However, several groups of sulfate reducing bacteria contain large amounts of branched PLFA (Elferink et al., 1998; Edlund et al., 1985; Taylor & Parkes 1983). In addition, significant amounts of label were recovered in i17:1 ω 7, a17:1 ω 7, 17:1 ω 8c and cy17:0/17:1 ω 6c that have been suggested as specific biomarkers for certain groups of sulfate reducing bacteria (Elferink et al., 1998; Edlund et al., 1985; Taylor & Parkes 1983), suggesting that sulfate reducing bacteria may be important chemoautotrophs in the ZK sediment. Chemoautotrophic growth can be found in two groups of sulfate reducing bacteria namely those that use hydrogen gas as substrate (Rabus et al., 2006) and sulfur disproportionating bacteria that gain energy from inorganic fermentation of substrates such as thiosulfate and elemental sulfur to sulfate and sulfide (Finster et al., 1998; Bak & Pfennig 1987). Both hydrogen turnover and disproportionation reactions have been shown to be important processes in anaerobic marine sediments (Hoehler et al., 1998; Jørgensen & Bak 1991) and they have been indicated to possibly support chemoautotrophy in coastal sediments (Thomsen & Kristensen 1997). For the ZK07 sediment, the labeling

in these branched PLFA became progressively more important with depth (Fig. 4), suggesting that it may indeed be associated with these anaerobic processes. Branched PLFA have also been found in anammox bacteria (Damste et al., 2005), but these also contain 10Me16:0 which showed no or limited labeling in our study (Fig. 3) suggesting that they were not important as chemoautotrophs. This is in agreement with studies that found that denitrification and not anammox is the dominant nitrate consuming process in active coastal sediments (Trimmer et al., 2003; Risgaard-Petersen et al., 2003). The high labeling in branched PLFA as detected at the low free-sulfide ZK site therefore indicates that anaerobic chemoautotrophy most likely by bacteria related to sulfate reducers may be important in coastal sediments.

We also studied the diversity of chemoautotrophic bacteria that use the Calvin cycle for carbon fixation by constructing clone libraries of the RuBisCO type IA gene. Clones detected fell in two main clades: one related to uncultured endosymbiotic sulfur-oxidizing Gammaproteobacteria (clade IA 1) and another related to free living chemoautotrophic sulfur and ammonium oxidizing bacteria (clade IA 2, Fig. 5). Although clade IA 1 sequences were most closely related to endosymbionts, they are also commonly found in related uncultured free-living bacteria (Aida et al., 2008; Lenk et al., 2010). These two RuBisCO clades are usually also detected in other environmental studies on marine sediments (Nigro & King 2007; Elsaied et al., 2007). Lenk et al., (2011) also showed that that free-living Gammaproteobacteria related to sulfur-oxidizing endosymbionts were important for dark carbon fixation in a permeable tidal flat sediment. The differences in RuBisCO clone distribution between the two sediments are most likely due to differences in the availability of reduced sulfur compounds namely free sulfide at the RK site and iron sulfides at the ZK site. However, it seems unlikely that these differences in clone distribution explain the contrasting PLFA labeling patterns from the two sites. First, the differences in RuBisCO clone distribution appear to be less site-dependent compared to the PLFA labeling patterns that showed major differences between sites. Second, the detected clones are related to bacteria that typically do not contain i- and a-branched PLFA as found for the chemoautotrophs from the ZK site. As discussed before, the PLFA composition of both the typical chemoautotrophic sulfur and ammonium-oxidizers in clade IA 2 and Gammaproteobacteria like the ones detected in clade IA 1 is usually dominated by straight saturated and un-saturated compounds similar to the labeling patterns at the RK site (Kerger et al., 1986; Lipski et al., 2001; Knief et al., 2003). Third, sulfate reducing bacteria typically fix inorganic carbon by either the reversed TCA-cycle or the reductive acetyl-CoA pathway (Rabus et al., 2006) and are therefore not targeted in our RuBisCO assay. The dominance of Gammaproteobacteria among the RuBisCO clones is therefore also agreement with the PLFA labeling patterns especially for RK and to lesser degree for ZK.

2.5 CONCLUSION

To conclude, we detected very high rates of chemoautotrophy in two active intertidal sediments and our results indicate that chemoautotrophic carbon fixation is an important part of the carbon cycle of coastal sediments. Clear differences were found in active chemoautotrophic bacterial communities probably caused by differences in reduced sulfur compounds available in the two sediments. Our study suggests that anaerobic bacteria related to sulfate reducers played an important role at the low-sulfide ZK site while typical sulfur-oxidizers, probably Gammaproteobacteria, were more important at the free-sulfide RK site. Chemoautotrophic Archaea such as the ammonium-oxidizing Crenarcheoata widely found in marine sediments (Giri et al., 2004) were not considered in the present study, but their activity could be studied by determining ^{13}C labeling in Archaeal ether-lipids (Wuchter et al., 2003). The number of coastal sediments where chemoautotrophic carbon fixation rates have been determined is still very low especially compared to studies on other aspects of the sedimentary carbon cycle. Besides our study we are aware of only four other studies where chemoautotrophy rates were quantified in coastal marine and brackish lake sediments (Enoksson & Samuelsson 1987; Thomsen & Kristensen 1997; Lenk et al., 2010; Santoro et al., 2013). Hence, chemoautotrophy in coastal marine sediments as driven by reoxidation processes should receive more attention in future studies given its importance in the carbon cycle of coastal sediments and the potential role in the benthic food web.

ACKNOWLEDGEMENTS

WE THANK ANTON TRAMPER, PETER VAN BREUGEL AND MARCO
HOUTEKAMER FOR TECHNICAL AND ANALYTICAL SUPPORT.

THIS IS PUBLICATION NUMBER DW_20141005 OF THE
DARWIN CENTER FOR BIOGEOSCIENCES.

DIANA VASQUEZ-CARDENAS, JACK VAN DE VOSSENBERG, LUBOS
POLERECKY, SAIRAH Y. MALKIN, REGINA SCHAUER, SILVIA HIDALGO-
MARTINEZ, VERONIQUE CONFURIUS, JACK J. MIDDELBURG, FILIP J.R.
MEYSMAN, HENRICUS T.S. BOSCHKER

ISME J. (2015) 9, 1966–1978

*Microbial carbon metabolism
associated with electrogenic sulfur
oxidation in coastal sediments*

ABSTRACT

Recently, a novel electrogenic type of sulfur oxidation was documented in marine sediments, whereby filamentous cable bacteria (*Desulfobulbaceae*) are mediating electron transport over centimetre-scale distances. These cable bacteria are capable of developing an extensive network within days, which implies a highly efficient carbon acquisition strategy. Presently the carbon metabolism of cable bacteria is unknown, so we adopted a multi-disciplinary approach to study the carbon substrate utilization of both cable bacteria and associated microbial community in sediment incubations. Fluorescence *in situ* hybridization showed rapid downward growth of cable bacteria, concomitant with high rates of electrogenic sulfur oxidation, as quantified by micro-electrode profiling. We studied heterotrophy and autotrophy by following ^{13}C -propionate and -bicarbonate incorporation into bacterial fatty acids. This biomarker analysis showed that propionate uptake was limited to fatty acid signatures typical for the genus *Desulfobulbus*. NanoSIMS analysis confirmed heterotrophic rather than autotrophic growth of cable bacteria. Still high bicarbonate uptake was observed in concert with the development of cable bacteria. Clone libraries of 16S cDNA showed numerous sequences associated to chemoautotrophic sulfur-oxidizing Epsilon- and Gammaproteobacteria while ^{13}C -bicarbonate biomarker labeling suggested that these sulfur-oxidizing bacteria were active far below the oxygen penetration. A targeted manipulation experiment demonstrated that chemoautotrophic carbon fixation was tightly linked to the heterotrophic activity of the cable bacteria down to centimetres depth. Overall, results suggest that electrogenic sulfur oxidation is performed by a microbial consortium, consisting of chemo-organotrophic cable bacteria and chemo-lithoautotrophic Epsilon- and Gammaproteobacteria. The metabolic linkage between these two groups is presently unknown and needs further study.

3.1 INTRODUCTION

The traditional view of diffusion-controlled redox zonation in marine sediments has recently been challenged by the observation that micro-organisms are capable of transporting electrons over centimetre-scale distances (Nielsen et al., 2010). This long-distance electron transport is mediated by filamentous cable bacteria belonging to the Desulfobulbaceae that are proposed to catalyse a new electrogenic form of sulfur oxidation (Pfeffer et al., 2012). Cable bacteria have recently been found in a wide range of marine sediment environments (Malkin et al., 2014), and seem to be competitively successful, because they can harvest electron donors (sulfide) at centimetres depth in the sediment while still utilizing thermodynamically favourable electron acceptors, such as oxygen and nitrate (Nielsen et al., 2010; Marzocchi et al., 2014) which are only available in the first millimetres of coastal sediments.

The current conceptual model of electrogenic sulfur oxidation (e-SOx) envisions a new type of metabolic cooperation between cells, where different cells from the same multicellular filament perform distinct redox half reactions. Anodic cells located in suboxic and anoxic sediment zones obtain electrons from sulfide and liberate protons (anodic half-reaction: $\frac{1}{2} \text{H}_2\text{S} + 2\text{H}_2\text{O} \rightarrow \frac{1}{2} \text{SO}_4^{2-} + 4\text{e}^- + 5\text{H}^+$). These electrons are then transported along the longitudinal axis of the filament to cells located near the sediment-water interface (Pfeffer et al., 2012). At the thin oxic layer near the sediment surface, cathodic cells reduce oxygen and consume protons (cathodic half-reaction: $\text{O}_2 + 4\text{e}^- + 4\text{H}^+ \rightarrow 2\text{H}_2\text{O}$). The two half-reactions leave a distinct geochemical fingerprint in the sediment consisting of a shallow oxygen penetration depth, a centimetre wide suboxic zone separating the oxic and sulfidic sediment horizons, and a characteristic pH depth profile, defined by a sharp pH maximum within the oxic zone and a deep and broader pH minimum at the bottom of the suboxic zone (Nielsen et al., 2010).

Laboratory time-series experiments (Schauer et al., 2014; Malkin et al., 2014) show that a network of cable bacteria can rapidly (< 10 days) develop in sediments, reaching high filament densities (> 2000 meter of filaments per cm^2 after 21 days; Schauer et al., 2014) with fast generation times of ~ 20 hours. Furthermore, the progressive downward growth of the cable bacteria closely correlates with the widening of the suboxic zone and a strong increase in biogeochemical rates, such as sedimentary oxygen consumption (Schauer et al., 2014, Malkin et al., 2014). One could hypothesize that cable bacteria may have a similar metabolism to their closest cultured relative *Desulfobulbus propionicus* (Pfeffer et al., 2012) that can efficiently grow as a chemo-organotroph in propionate-rich media while obtaining metabolic energy from oxidation of sulfide to elemental sulfur

followed by sulfur disproportionation (Widdel & Pfennig 1982; Dannenberg et al., 1992; Fuseler & Cypionka 1995; Pagani et al., 2011). It is presently unclear whether they are organotrophs (heterotrophs) or lithoautotrophs (chemoautotrophs).

Here, we adopted a multi-disciplinary approach to characterize the carbon metabolism in coastal sediments with e-SOx activity, resolving the carbon substrate uptake of both cable bacteria as well as their associated microbial community. We conducted a series of laboratory incubations, starting in March 2012, to track the temporal development of the cable bacteria network by microsensor profiling and fluorescence *in situ* hybridisation (FISH), while quantifying inorganic carbon fixation at various time points through stable isotope labeling and biomarker analysis (PLFA-SIP). In August 2012 we studied both inorganic carbon and propionate uptake by PLFA-SIP. In both months, we examined the linkage between carbon metabolisms and e-SOx activity through targeted manipulation treatments. The active microbial community in the March and August experiments was characterized by 16S cDNA clone libraries. The final experiment in May 2013 quantified the carbon tracer uptake of both inorganic (bicarbonate) and organic (propionate) substrates by individual cable bacteria filaments using nanoscale secondary ion mass spectrometry (nanoSIMS).

3.2 MATERIALS & METHODS

3.2.1 Sediment collection and incubation

Sediment was collected from a seasonally hypoxic coastal basin (marine Lake Grevelingen, the Netherlands; 51°44'50.04"N, 3°53'24.06"E; water depth 32 m) using a gravity corer (UWITEC, Germany). At the sampling site, e-SOx activity and associated cable bacteria were previously documented under field conditions (Malkin et al., 2014). The top 20 cm of the sediment was collected, homogenized, and repacked into PMMA acrylic cores (15 cm height; 4 cm inner diameter). Sediment cores were subsequently incubated at 16°C (± 1) in a darkened incubation tank with filtered (0.2 μm) seawater (salinity 30). During incubations, the overlying water was kept at 100% air saturation by continuous air bubbling. Three sediment incubation experiments were conducted: in March 2012, we documented the bacterial community structure and substrate utilization during the temporal development of e-SOx and performed initial targeted manipulation experiments; in August 2012, we performed targeted manipulation experiments on cores in which e-SOx had established; and finally in May 2013, we picked individual cable bacteria filaments from sediments with e-SOx for nanoSIMS analysis after stable isotope labeling.

3.2.2 *Microsensor profiling*

Microsensor profiling (O_2 , pH, H_2S) was performed as described in Malkin et al., (2014) to determine the geochemical fingerprint of the e-SOx process, and hence, the developmental state of e-SOx in the incubated sediments. One set of microsensor profiles was taken per core and 3 to 6 replicate cores were analysed per time point (March: day 1, 2, 3, 6, 8, 9, 10, 13, August: day 12; May: day 20). Two biogeochemical rates were calculated from microsensor profiles: the diffusive oxygen uptake (DOU) of the sediment, which provides a proxy for the activity of the whole microbial community, and the cathodic oxygen consumption (COC), which is a part of the DOU that can be attributed to the cathodic half-reaction of e-SOx and which reflects the activity of the cable bacteria (details on calculation are given in S.I.).

3.2.3 *PLFA-SIP analysis*

Biomarker analysis of phospholipid-derived fatty acids combined with stable isotope probing allows linking bacterial identity and activity (PLFA-SIP, Boschker et al., 1998). In the March and August 2012 experiments, carbon incorporation was assessed by addition of ^{13}C -bicarbonate and ^{13}C -propionate. Stock solutions of 20 mM of ^{13}C -bicarbonate and 1.7 mM of ^{13}C -propionate (both 99% ^{13}C ; Cambridge Isotope Laboratories, Andover, Ma, USA) were prepared in calcium- and magnesium-free artificial seawater to prevent carbonate precipitation and shortly before use bubbled with nitrogen gas shortly before use to remove oxygen.

In the March experiment, only ^{13}C -bicarbonate was used as substrate, and additions were performed after 1, 9 and 13 days. In the August experiment, both ^{13}C -bicarbonate and ^{13}C -propionate were used as substrates (addition at day 12 of incubation). All labeling experiments were conducted in duplicate cores. ^{13}C -carbon substrates were added to the sediment cores with the line injection method (Jørgensen 1978), adding label via vertically aligned side ports in the core liners. For further details on injections and incubation setup see S.I. After 24 hours of incubation with labeled substrate, cores were sectioned in four layers: 0-0.3 cm, 0.3-0.8 cm, 0.8-1.5 cm, 1.5-3.0 cm.

Biomarker extractions were performed on freeze dried sediment as in Guckert et al., (1985) and Boschker et al., (1998) and ^{13}C -incorporation into PLFA was analysed by gas chromatography – isotope ratio mass spectrometry (GC-IRMS, Thermo, Bremen, Germany) on an apolar analytical column (ZB5-MS Phenomenex). Label incorporation was calculated from the product of the concentration of each fatty acid and the increase in ^{13}C abundance relative to the background ^{13}C abundance (Boschker & Middelburg 2002). Total carbon incorporation with propionate and bicarbonate was corrected for dilution of ^{13}C -substrates in pore water (see S.I. for details). Bacterial PLFA

Table 1. Total inorganic carbon and propionate incorporation rates calculated from PLFA-SIP analysis from the top 3 cm. Dissolved oxygen uptake (DOU) was calculated from microsensor profiles. Averages (\pm SD) are listed. NA = not analysed.

Date	Treatment	Cable bacteria biomass (mmol C m^{-2})	Propionate incorporation ($\text{mmol C m}^{-2} \text{d}^{-1}$)	Inorganic carbon incorporation ($\text{mmol C m}^{-2} \text{d}^{-1}$)	DOU ($\text{mmol O}_2 \text{m}^{-2} \text{d}^{-1}$)	
March	1	Control	6	NA	1.6 ± 0.5	51 ± 4
	9	Control	130	NA	9.6 ± 2.4	45 ± 3
		Control	166	NA	10.9 ± 0.9	76 ± 4
	13	Anoxic	NA	NA	0.5 ± 0.1	NA
		0.3 cm cut	NA	NA	7.3 ± 0.5	64 ± 15
August	12	Control	229	16.7 ± 3.7	7.3 ± 2.2	78 ± 18
		Anoxic	NA	2.0 ± 0.2	NA	NA
		0.3 cm cut	NA	9.7 ± 5.7	6.5 ± 1.9	57 ± 23
		0.8 cm cut	NA	9.4 ± 0.9	6.0 ± 1.9	28 ± 6

(12:0 to 20:0) were summed and converted to biomass production assuming an average PLFA carbon contribution of 5.5% of total bacterial carbon (Brinch-Iversen & King 1990, Middelburg et al., 2000).

To determine which biomarkers characterize the bicarbonate and propionate consuming bacterial communities in the sediment, we performed a principal component analysis using R free statistical software (PCA, prcomp{stats} module). PLFA incorporation data (pmol C per gram dry weight) were first normalized to total ^{13}C incorporation and then $\log(x+1)$ transformed. Samples for PCA analysis were selected based on the presence of filaments (minimum 100 m of cable bacteria cm^{-3}), and sufficient ^{13}C -mol incorporation in fatty acids (only samples with more than 1% of the total sediment activity were included).

3.2.4 NanoSIMS

In the May 2013 experiment, microsensor profiling showed that the e-SOx process was fully established at 21 days after the start of the incubation. NanoSIMS analysis was used to visualize and quantify ^{13}C -bicarbonate and ^{13}C -propionate uptake by individual cells within cable bacteria filaments. Stock solutions of ^{13}C -labeled substrate were prepared as for PLFA-SIP, but with higher label concentrations (bicarbonate, 62 mM; propionate, 11 mM), given the lower ^{13}C -sensitivity of the nanoSIMS technique. In total, 500 μl was injected using the line injection method, starting from 5 cm depth up to the sediment surface (10 parallel injections in a 1 cm^2 area). Sediment cores were subsequently incubated for 24 hours in the dark at 16°C. Core sectioning depths were based on microsensor profiling results: a first slice contained the oxic zone (0 to 0.2 cm) and a second slice spanned the suboxic zone (0.4 to 2.0

cm). Individual filaments were picked under a microscope with fine glass hooks made from Pasteur pipettes, and washed several times in artificial seawater to remove sediment particles with a final wash in milliQ to eliminate salt. Isolated filaments were subsequently transferred to gold-sputtered glass slides (0.5 cm diameter, 10 nm gold coating), and dried in a desiccator prior to analysis. Filaments from the sulfidic layer were not included in the study given that not enough filaments could be collected from below 2.0 cm in all treatments. Filaments were retrieved in a similar manner from cores without label addition and served as controls.

NanoSIMS analysis was performed with a nanoSIMS 50L instrument (Cameca) at Utrecht University as described in the S.I. The counts of ^{12}C and ^{13}C from individual filaments were measured and used to calculate the relative ^{13}C fraction as $^{13}\text{C}/(^{12}\text{C}+^{13}\text{C})$. Overall, between 3 and 6 different filaments were analysed from each sample, consisting in total of 39 cells for natural ^{13}C -abundance Controls (oxic zone), 75 cells for ^{13}C -propionate uptake (oxic and suboxic zone) and 53 cells for ^{13}C -bicarbonate label uptake (oxic and suboxic zone). For further calculation of C uptake the average relative ^{13}C abundance of the treated filaments were subtracted from those of the Controls and for final concentrations of ^{13}C -labeled substrates in pore water, as mentioned above for the PLFA-SIP analysis. Abundance of cable bacteria from FISH counts was used to convert ^{13}C enrichment to carbon incorporation rates. Differences in initial ^{13}C -label substrate concentrations and volume of ^{13}C -labeled substrate injected into the sediment were taken into account to compare carbon uptake rates estimated from nanoSIMS results with those obtained from PLFA-SIP analysis.

3.2.5 Manipulation experiments

To further investigate the relationship between e-SOx activity and carbon metabolism, we conducted two types of sediment manipulations in combination with the two ^{13}C -labeled substrates for PLFA-SIP analysis for both the March and August experiments. For the first manipulation we induced anoxia by depleting the overlying water of oxygen, thus impeding all forms of aerobic sulfide oxidation, including e-SOx (Nielsen et al., 2010). The second treatment involved a horizontally cutting of the sediment with a thin nylon thread (60 μm diameter), which selectively disrupts the e-SOx process by interrupting the electron transport by the cable bacteria (Pfeffer et al., 2012). We used two cutting depths: a shallow cut below the oxic zone at 0.3 cm depth and deeper cut in the middle of the suboxic zone at 0.8 cm (see Table 1 for experimental setup). All cores were microprofiled prior to the experiment and only those cores which showed an e-SOx signature were selected for manipulation. Substrate injections were done as for PLFA-SIP analysis. All treatments were done in duplicate cores.

For the anoxic treatment, cores were incubated in nitrogen bubbled overlying water. Cutting was done by fixing a ring on top of the core liner with a height equivalent to the cutting depth. The sediment was subsequently pushed up slowly with a plunger until the top of the ring. Once the sediment was in place, a nylon thread was passed through the sediment guided by the slit between the core liner and the ring, the slit was later sealed with water-proof adhesive tape. Sediment cores with less than one day of incubation were used as control sediment (*i.e.* without e-SOx). These controls were examined 1 to 3 hours after the cut as well as 24 hours after manipulation which showed that the cutting treatment had no effect on microsensors profiles (Fig. S1).

3.2.6 Fluorescence in situ Hybridization (FISH)

The depth distribution of cable bacteria was quantified via FISH analysis performed on one sediment core for each of the three time points in March and at the end of the incubation in August. Sediment cores were sliced in the same four layers as described for PLFA-SIP. The FISH procedure was performed according to Schauer et al., (2014) with probe DSB706 (Manz et al., 1992).

At each time point the total filament length per unit of sediment volume (m cm^{-3}) was calculated (Schauer et al., 2014) as well as the areal density of cable bacteria (m cm^{-2}) by depth integration over all four sediment layers. Number of cells, $3 \mu\text{m}$ in length, was estimated from filaments lengths and converted to biovolume (μm^3) with measured cell diameter. Biovolume was then converted to carbon biomass by adopting the allometric scaling formula $B = 435 V^{0.86}$ ($B = \text{fg C } \mu\text{m}^{-3}$; $V = \mu\text{m}^3$, Romanova and Sazhin 2010) assuming a cylindrical cell shape and a carbon content equal to 50% of the dry weight.

3.2.7 16S cDNA libraries

To describe the active community composition 16S cDNA clone libraries were constructed per sediment layer at day 13 March (354 clones total) and day 12 August (301 clones total). Methods and data analysis were as described in Malkin et al., (2014), where 16S cDNA was amplified by PCR using general bacterial primers Bac F968 (AACGCGAAGAACCTTAC) and Bac R1401 (CGGTGTGTACAAGRCCCG-GGAACG). Sequences have been submitted to GenBank database under accession no BankIt1781572: KP265396–KP265657.

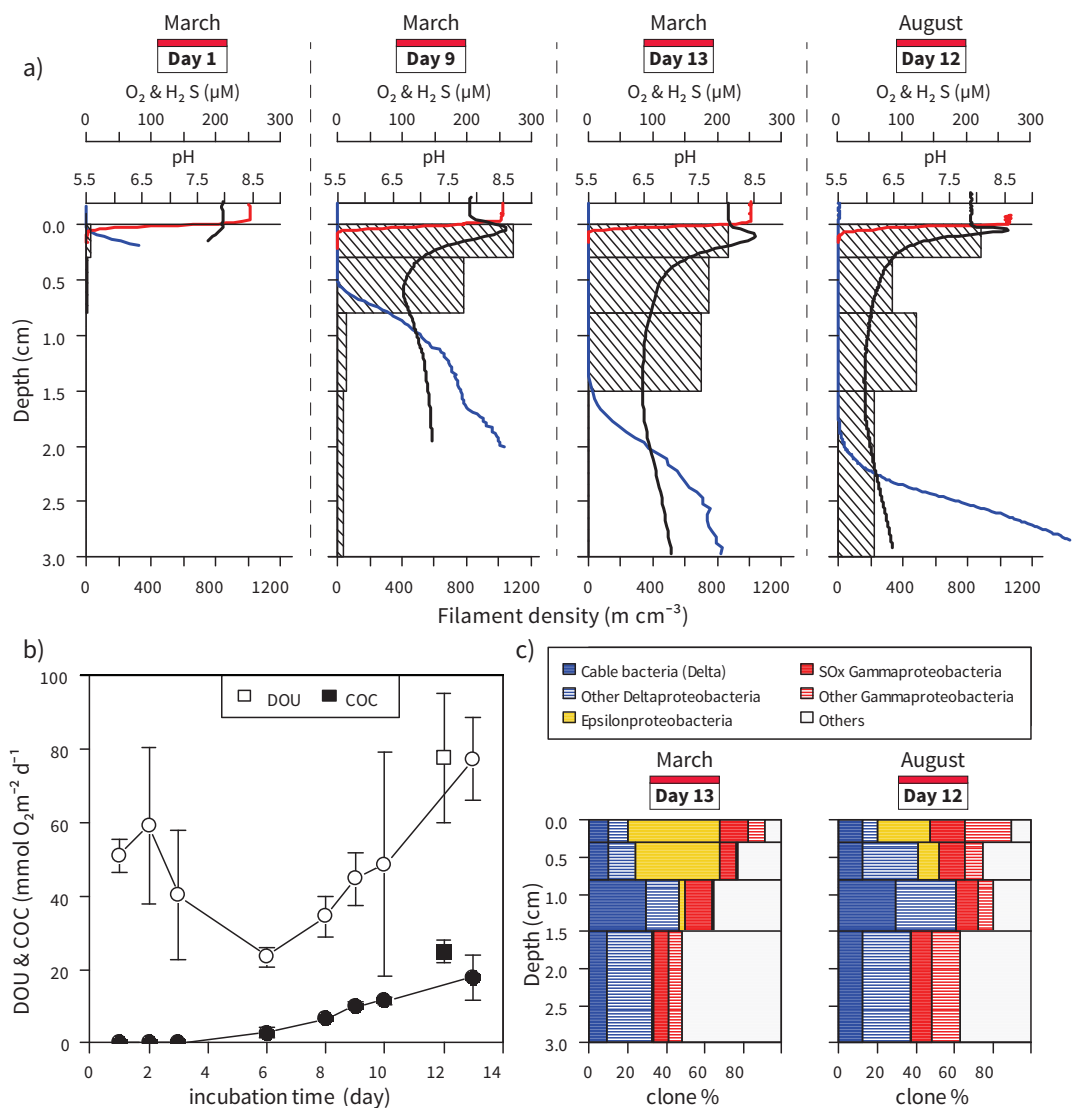


Figure 1. Development of electrogenic sulfur oxidation (e-SOx) and abundance of the associated cable bacteria. a) Microsensor profiles (H_2S , O_2 , pH) that show the geochemical e-SOx signature and the density of cable bacteria (bars). b) Temporal variation of dissolved oxygen uptake (DOU) and cathodic oxygen consumption (COC) calculated from the microsensor profiles. Circles represent data from March 2012 experiment while squares indicate values for the August 2012 incubation. c) Relative contribution of 16S cDNA sequences related to cable bacteria and other main phylogenetic groups for sediment with strong e-SOx signal (day 13 March and day 12 August). In the legend SOx stands for sulfur-oxidizing bacteria. A detailed phylogenetic tree of all OTUs is included in S.I. (Fig. S2).

3.3 RESULTS

3.3.1 Development of electrogenic sulfur oxidation

On day 1 of the March experiment there was no suboxic zone present with sulfide accumulating right below the millimetre deep oxygen penetration. The geochemical fingerprint of e-SOx became apparent after 6 days (not shown), and by day 9, there was a pronounced subsurface pH maximum and a ~ 5 mm wide separation between the O₂ and H₂S horizons, indicative of developing e-SOx activity (Fig. 1a). This suboxic zone progressively widened over the following days (Fig. 1a) reaching a width of ~ 15 mm at day 13. In August, the sediment biogeochemistry showed a very similar development, showing a ~ 18 mm wide suboxic zone accompanied by the typical subsurface pH maximum after 12 days of incubation.

FISH counts for March showed that cable bacteria progressively grew from the sediment surface towards the deeper layers in unison with the widening of the suboxic zone (Fig. 1a). Depth integrated filament length increased 90 fold from day 1 (13 m cm⁻²) to day 13 (1131 m cm⁻²), providing a final cable biomass of 166 mmol C m⁻² (Table 1). The mean biomass accumulation rate over the whole 13-day experiment amounted to 13 mmol C m⁻² d⁻¹. The filament density at the end of the August experiment reached 1095 m cm⁻² with a corresponding biomass of 229 mmol C m⁻², resulting in a mean biomass accumulation rate of 19 mmol C m⁻² d⁻¹. For both experiments filament diameter progressively increased downwards in the oxic zone 0.97 ± 0.10 μm , in the suboxic zone 1.23 ± 0.17 μm and in the sulfidic zone 1.47 ± 0.22 μm .

Over the first 6 days of the March experiment, the DOU of the sediment gradually decreased (Fig. 1b). This has been previously observed in similar incubations, and was attributed to transient oxidation of reduced compounds initially present in the top of the homogenized sediment (Schauer et al., 2014, Malkin et al., 2014). After day 6, when the e-SOx signature became first visible, the DOU increased steeply, reaching a maximum value of 80 mmol m⁻² d⁻¹ on day 13 (Fig. 1b, Table 1). The cathodic oxygen consumption (COC), as derived from the alkalinity balance calculations (see S.I.), represented 13% of the total DOU on day 6 and reached a maximum of 32% by day 13. However, the observed increase in DOU between day 6 and 13 was much higher (54 mmol m⁻² d⁻¹) accounting for 70% of the DOU at day 13. This higher contribution of e-SOx to the overall oxygen consumption is consistent with subsequent manipulation experiments (see below) suggesting that the alkalinity balance procedure may underestimate the true COC.

3.3.2 Microbial community structure

Clone libraries of 16S cDNA from both the March and August incubations revealed three main classes known to be involved in sulfur cycling. Deltaproteobacteria sequences constituted the first class (35% of total clones), of which on average of 45% were highly similar (>97% sequence identity) to previously reported sequences for cable bacteria (Fig. S2). Cable bacteria sequences were found up to 3 cm depth (Fig. 1c) and formed two operational taxonomic units each dominated by sequences from the two different experiments (Fig. S2). The second predominant clade (21% of total clones) was composed of Gammaproteobacteria, which were present throughout the sediment (March 56 clones and August 82 clones, Fig. 1c), and of which 40% were closely related to chemoautotrophic sulfur-oxidizers (candidate *Parabeggiatoa communis*, *Thiomicrospira frisia*, and *T. halophila*) in addition to chemoautotrophic endosymbionts of bivalves, oligochaetes and ciliates (Fig. S2). The third class (17% of total clones) contained chemoautotrophic sulfur-oxidizing Epsilonproteobacteria from the *Sulfurimonas*, *Sulfurovum* and *Arcobacter* genera (Fig. S2). These clones were present in the top 1.5 cm of sediment in March and top 0.8 cm in August sediment (Fig. 1c). The remaining sequences (27%) belonged to a variety of phylogenetic groups related to Verrucomicrobia, Nitrospirae, candidate division OP8, Planctomycetes and some Cyanobacteria.

3.3.3 Carbon isotope labeling

PLFA-SIP analysis revealed a clear distinction between bicarbonate and propionate consuming bacterial populations (Fig. 2). Biomarker fingerprints from the inorganic carbon assimilating community were similar to those of sulfur-oxidizing Gamma- and Epsilonproteobacteria (Inagaki et al., 2004; Donachie et al., 2005; Zhang et al., 2005; Takai et al., 2006, Fig. 2a), characterized by ^{13}C -uptake in 16:1 ω 7c, 16:0, 14:0, 18:1 ω 7c, and 16:1 ω 5c PLFA. In contrast, propionate incorporation was differentiated by high ^{13}C -labeling in 17:1 ω 6c, 15:0, 16:1 ω 7c, and 17:1 ω 8c which resemble the PLFA fingerprint of the genus *Desulfobulbus* spp. (Fig. 2b). Depth integrated carbon incorporation rates for each substrate are listed in Table 1.

NanoSIMS analysis confirmed the preferential uptake of ^{13}C -propionate over ^{13}C -bicarbonate by individual cable bacteria filaments (Fig. 3). Depth integrated carbon incorporation rate determined by nanoSIMS, combined with filament densities determined by FISH (oxic: 10 $\mu\text{mol C cm}^{-3}$ and suboxic: 18 $\mu\text{mol cm}^{-3}$) show that ^{13}C -enrichment in filaments for ^{13}C -bicarbonate incubations was only ~20% of ^{13}C -enrichment with ^{13}C -propionate. Carbon uptake rates yielded a doubling time of filament biomass for propionate (20 hours) that was 3.5 times faster than for bicarbonate (71 hours),

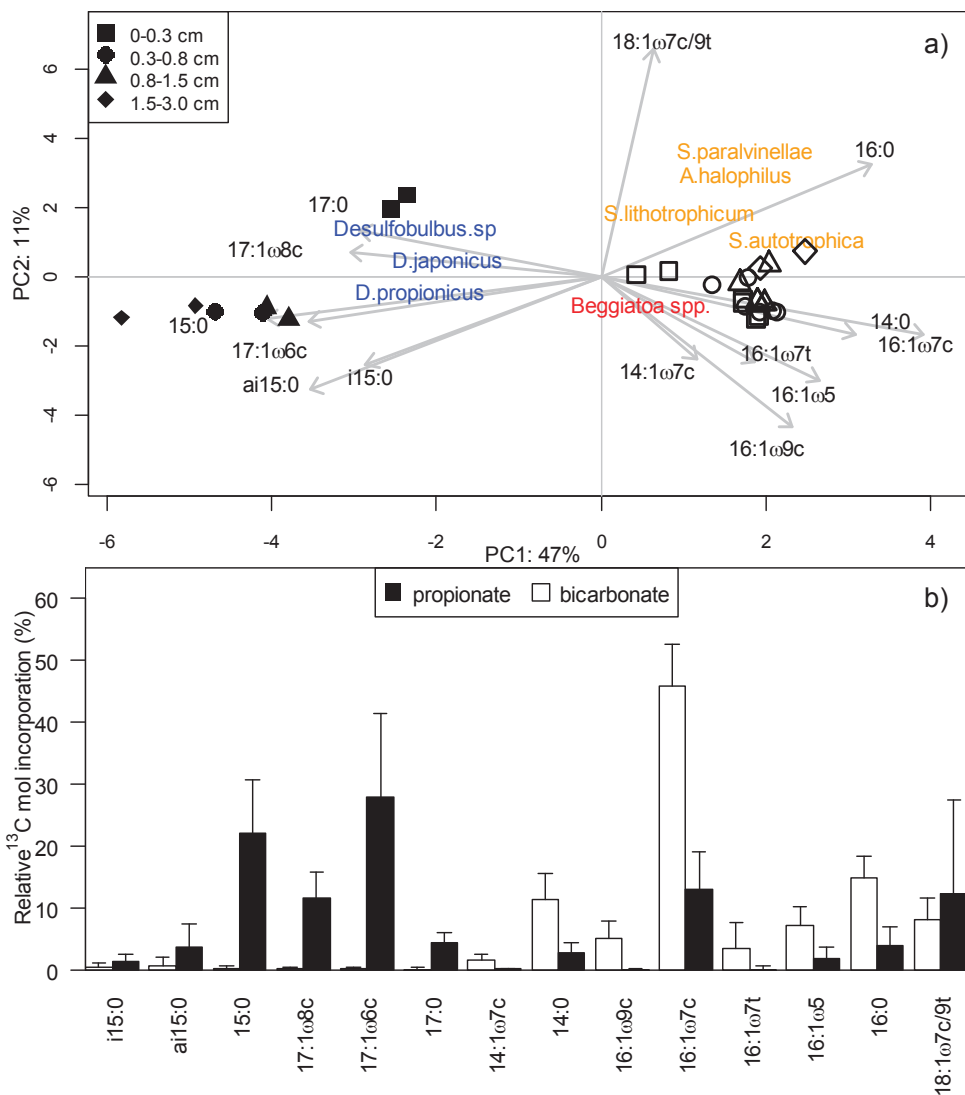


Figure 2. a) Principal component analysis of ^{13}C -substrate incorporation ($\mu\text{mol gram}^{-1}$ dry weight) normalized to mol% and log transformed prior to analysis. The first two axis of the PCA explained 58% of the variance amongst samples. Grey arrows represent the proportion of total variance explained by each fatty acid. Filled symbols indicate samples treated with ^{13}C -propionate, open symbols are samples treated with ^{13}C -bicarbonate, and shapes indicate sediment layers as shown in legend. Only sediment layers with high cable bacteria densities were included in the analysis (see methods). Reference bacteria were added to PCA: *Desulfobulbus* spp. (blue), sulfur-oxidizing Gammaproteobacteria (red), and sulfur-oxidizing Epsilonproteobacteria (yellow, for references see methods). b) Average (\pm SD) percent of total ^{13}C -incorporation for each PLFA in all layers included in PCA plot for both substrate additions (black: propionate n=8, white: bicarbonate n=20).

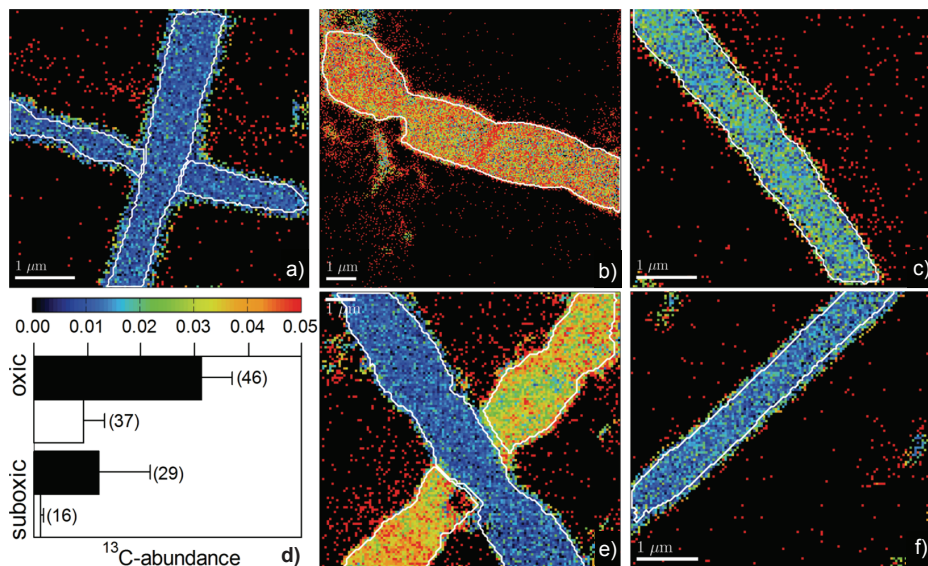


Figure 3. Shown are example images of the relative ^{13}C -abundance ($^{13}\text{C}/(^{13}\text{C}+^{12}\text{C})$) in individual cable bacteria measured by nanoSIMS: natural ^{13}C -abundance Controls a), ^{13}C -propionate incorporation b),e), and ^{13}C -bicarbonate uptake c), f). Filaments are outlined in white. Images in top row are from the oxic layer (0-0.2 cm) while bottom row images are from the suboxic layer (0.4-2.0 cm). Colour scale shows natural ^{13}C -abundance (0.01) in blue and ^{13}C -enrichment increases towards red (0.05). d) Average (\pm SD) values of relative ^{13}C -abundance in filaments from different sediment layers and for different ^{13}C -labeled substrates (black: propionate, white: bicarbonate) are shown. Red dotted line indicates the value for the Control filaments. Number of cells analysed are in parenthesis.

suggesting cable bacteria cannot maintain rapid growth on an autotrophic metabolism. Carbon uptake rates of $7 \text{ mmol m}^{-2} \text{ d}^{-1}$ for propionate and $2 \text{ mmol m}^{-2} \text{ d}^{-1}$ for bicarbonate were comparable to the depth integrated rates for the propionate and bicarbonate consuming bacterial communities obtained with PLFA-SIP (Table 1). Interestingly, incorporation of ^{13}C -propionate by filaments in surface sediment was higher and more homogenous among cells (Fig. 3b) than in deeper sediment horizons where some filaments showed little ^{13}C -enrichment while others had high ^{13}C -enrichment (Fig. 3e).

Experiments revealed substantial rates of organic and inorganic carbon assimilation that extended to centimetres depth into the sediment (Fig. 4). Remarkably, in March bicarbonate uptake expanded in synchrony with the development of the cable bacteria network and the deepening of the sulfide horizon (Fig. 4a-c), resulting in an almost even distribution throughout the oxic and suboxic zone by day 13 (Fig. 4a-c). In August (day 12) inorganic carbon fixation was also present down to 3 cm deep, but the maximum activity was found in the oxic zone (Fig. 4d). Propionate uptake was highest in the top millimetres and extended below the sulfide horizon (Fig. 4e).

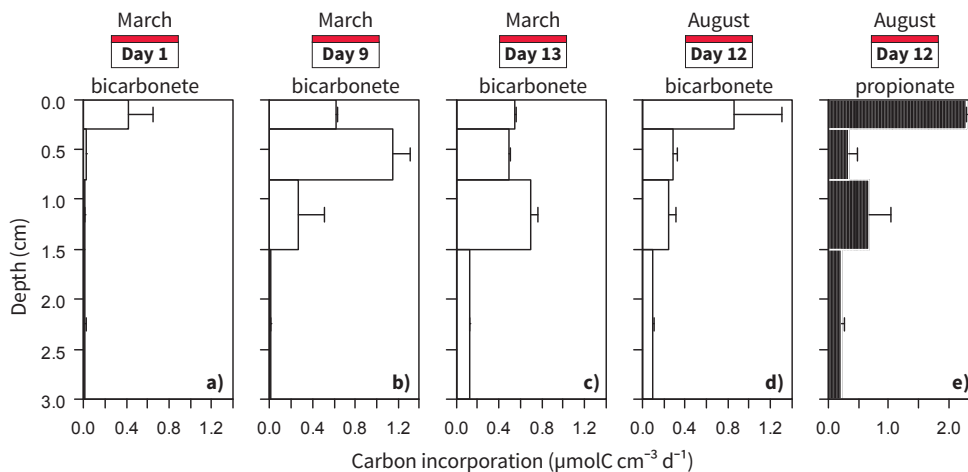


Figure 4. Depth profiles of inorganic carbon incorporation rates in bacterial biomass for March day 1 (a), 9 (b), 13 (c) and August day 12 (d) as well as propionate uptake rates for August day 12 (e). Average (\pm SD) rates were calculated from PLFA-SIP labeling, corrected for source labeling levels and converted to total biomass as described in the methods ($n=2$).

3.3.4 Targeted manipulation experiments

Manipulation experiments had clear effects on the geochemical fingerprint, and the carbon uptake rates (Fig. 5). In the anoxic treatment the characteristic subsurface pH peak decreased from 8.4 to 7.7 after 24 hours of incubation indicating a strong decline in cathodic proton consumption (Fig. 5a). In parallel, both inorganic and organic carbon uptake were almost completely inhibited throughout the sediment (Fig. 5d, g), demonstrating that most of the microbial activity in the suboxic and sulfidic zones was linked to the presence of oxygen at the sediment surface.

Shallow cutting of the sediment (0.3 cm depth) induced an immediate geochemical response: within 1 hour, the pH maximum decreased from 8.4 to 7.8, the oxygen penetration depth doubled (Fig. 5b), and the DOU showed an almost 4-fold decrease (from 81 ± 2 to 24 ± 13 $\text{mmol O}_2 \text{ m}^{-2} \text{ d}^{-1}$). However, after 24 hours of incubation, the pH peak (8.3) as well as the DOU (61 ± 5 $\text{mmol O}_2 \text{ m}^{-2} \text{ d}^{-1}$) had almost fully re-established. PLFA-SIP analysis showed a negative impact on both carbon assimilation rates with the strongest inhibition occurring in sediment zones below the cut (Fig. 5e, h, Fig. S3). In particular, propionate consumption decreased by 70% whereas bicarbonate uptake for both March and August experiments decreased on average 48%. However, the overall reduction in carbon uptake was substantially less in the cutting experiments compared to the anoxic treatment (Table 1), which may indicate a temporal rather than permanent halt of the e-SOx process. In the top oxic layer, propionate assimilation was variable with no change for one replicate and an increase of 45% for the

second core; mean inorganic carbon fixation however was always enhanced in the oxic zone with an increase of 40% for March and 73% for the August experiment.

When the sediment was cut half way through the suboxic zone (at 0.8 cm) the subsurface pH maximum disappeared and the oxygen consumption decreased dramatically post-cut (from 80 ± 20 to 28 ± 6 mmol O₂ m⁻² d⁻¹, Fig. 5c) and both parameters did not recover in the remainder of the experiment. Carbon uptake rates were strongly reduced (>80%) below the cut (Fig. 5f, i) with values comparable to those obtained for the anoxic treatment. Propionate uptake was not substantially altered above the cutting depth, but bicarbonate incorporation was somewhat inhibited in the suboxic layer directly above the cut and again stimulated in the top layer. The combined results, from all three manipulation experiments, suggest that both inorganic and organic carbon assimilation were tightly linked with the e-SOx process.

3.4 DISCUSSION

3.4.1 Electrogenic sulfur oxidation

The microsensor and FISH data obtained in our sediment incubations confirmed results obtained in a previous field study (Malkin et al., 2014) and laboratory experiments (Nielsen et al., 2010; Risgaard-Petersen et al., 2012; Schauer et al., 2014). The temporal development of the characteristic geochemical fingerprint of the e-SOx process is accompanied by the downward growth of a dense network of long filamentous cable bacteria, which span the suboxic zone (Schauer et al., 2014; Malkin et al., 2014). Cable bacteria densities at peak development were half of those recorded in a similar sediment incubation experiment (2380 m cm⁻², Schauer et al., 2014) but 3 to 6-fold higher than densities in the suboxic zone (0.3-0.8 cm) observed under field conditions (120 m cm⁻³, Malkin et al., 2014). Additionally, we estimate that e-SOx was responsible for approximately 70% of the sedimentary oxygen consumption given the steep increase in DOU from day 6 to 13 and the sharp decrease in DOU an hour after cutting the sediment. This estimate closely aligns with the contribution of 81% found by Schauer et al., (2014) and highlights the important role e-SOx can play in sedimentary geochemical cycling. The drastic geochemical effects observed in the manipulation experiments, with either induced anoxia or cutting of the sediment at 0.3 cm depth, were consistent with previous observations (Nielsen et al., 2010; Pfeffer et al., 2012) and confirm the current conceptual model of e-SOx, in which electrons are transported from anodic cells to cathodic cells along the longitudinal axis of cable bacteria filaments.

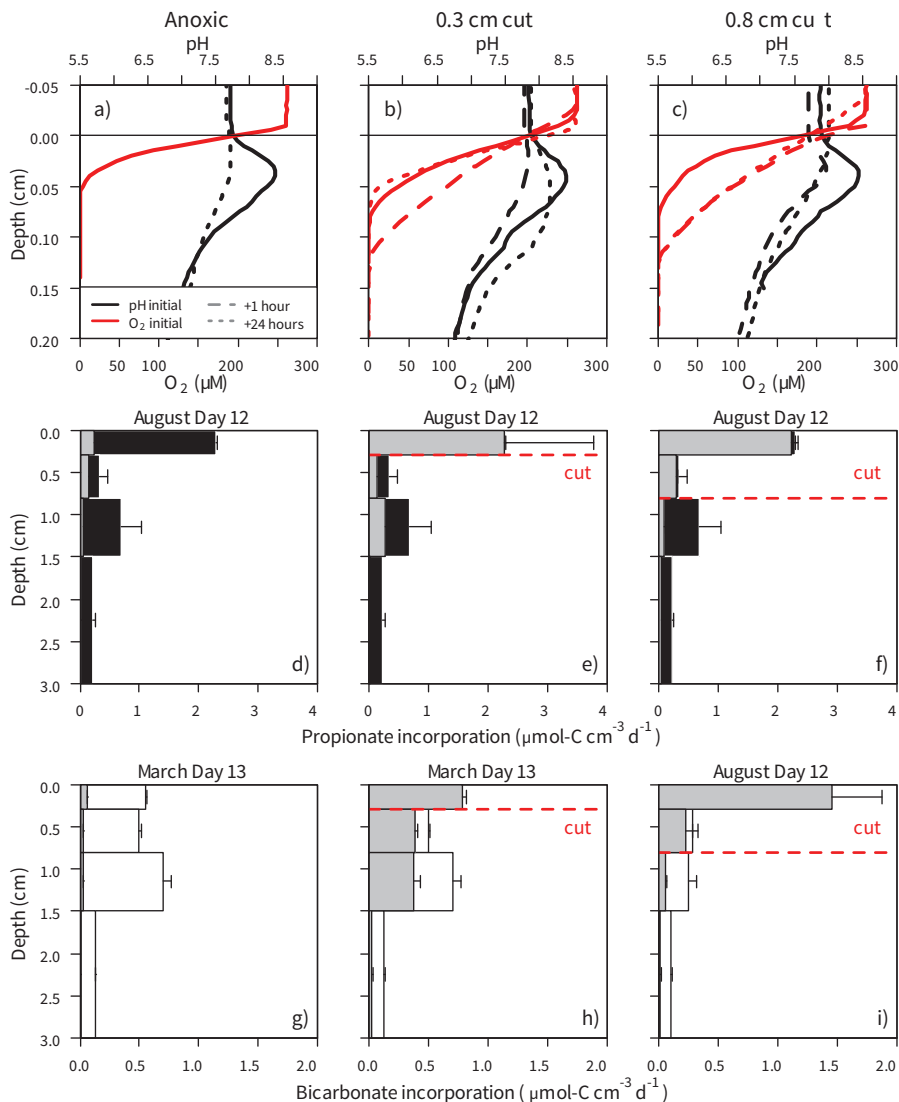


Figure 5. Effects of manipulation experiments on micro-sensor profiles and carbon incorporation in sediment with fully developed geochemical fingerprint of the e-SO_x process. Left column shows effects of anoxia, middle column corresponds to the 0.3 cm deep cut, and right column indicates results from the deeper 0.8 cm cut. Top row shows microsensor profiles of oxygen (red) and pH (black) for starting conditions and hours after manipulation are indicated in the legend. Only one representative replicate per treatment is shown for clarity ($n=3$), other replicates were similar. Carbon incorporation rates as calculated from ¹³C-PLFA analysis are represented in bar plots (d-i) with un-manipulated sediment in black (propionate) or white (bicarbonate) and rates obtained 24 hours after sediment was manipulated in grey. Averages (\pm SD) are plotted. Number of replicate cores was 2. Results of the shallow cut (0.3 cm deep) for August day 12 experiment can be found in SI (Fig. S3).

3.4.2 Carbon metabolism and growth of cable bacteria

We used two ^{13}C -stable isotope approaches (PLFA-SIP and nanoSIMS) to study the carbon metabolism of the fast growing cable bacteria. PLFA-SIP identified high incorporation of propionate in 15:0, 17:1 ω 6c and 17:1 ω 8c fatty acids, which we attributed to be biomarkers for cable bacteria given that those resemble the fatty acid composition of *Desulfobulbus* spp. (Taylor & Parkes 1983; Pagani et al., 2011) to which cable bacteria are most closely related (Pfeffer et al., 2012; Malkin et al., 2014). Propionate is steadily produced through mineralization of organic matter in sediments and serves as a major energy and carbon source for several Deltaproteobacteria (Sorensen et al., 1981; Purdy et al., 1997; Parkes et al., 1989). Rates of propionate assimilation measured with PLFA-SIP ($17 \text{ mmol C m}^{-2} \text{ d}^{-1}$) scale well with biomass accrument of the cable bacteria based on FISH counts ($16 \text{ mmol C m}^{-2} \text{ d}^{-1}$), which suggest the cable bacteria could successfully grow on propionate in the environment. Moreover, based on ^{13}C -DIC measurements obtained from pore water, we estimated that only 2% of the propionate assimilated was respired, indicating that propionate was mainly used as a carbon source by the cable bacteria rather than being respired by sulfate reducing bacteria. However, we found that propionate incorporation ($7 \text{ mmol C m}^{-2} \text{ d}^{-1}$) estimated by nanoSIMS explained 44% of the observed biomass increase (FISH). *Desulfobulbus* spp. can also grow on lactate, acetate, ethanol, propanol, and pyruvate (Laanbroek & Pfennig 1981; Widdel & Pfennig 1982; Parkes et al., 1993; Pagani et al., 2011) and therefore, it seems plausible that cable bacteria use other organic substrates besides propionate.

An autotrophic metabolism is unlikely as the biomass increase calculated from ^{13}C -inorganic carbon uptake (nanoSIMS) only explains $\sim 15\%$ of the observed cable bacteria growth. The limited incorporation of ^{13}C -bicarbonate measured in cable bacteria ($\sim 20\%$ of propionate uptake) is well within the range observed in heterotrophic micro-organisms (Roslev et al., 2004; Hesselsoe et al., 2005; Wegener et al., 2012) and inorganic incorporation can therefore most likely be attributed to anapleurotic reactions.

The fast expansion of the cable bacteria filament network, as observed in our incubations, has been previously explained by an exponential growth mechanism with high generation times, and continuous and uniform cell divisions throughout the filament (Schauer et al., 2014). When generation time is calculated based on ^{13}C -propionate incorporation (nanoSIMS) and FISH counts (using the same assumptions as Schauer et al., 2014 for the filament density at day 0), this provides the short generation time (20 hours) previously reported by Schauer et al., (2014). However, our ^{13}C -propionate incorporation (nanoSIMS) results indicate that the turnover of cathodic, oxygen respiring cells is twice as fast as that of anodic, sulfide-oxidizing cells. This suggests different energy yields from each half redox reactions that lead to rapid growing cathodic cells and less

efficient anodic cells. Moreover, estimation of growth efficiencies calculated from biomass increase ($16 \text{ mmol C m}^{-2} \text{ d}^{-1}$) and COC ($54 \text{ mmol O}_2 \text{ m}^{-2} \text{ d}^{-1}$) suggest an efficiency of 30%. Previously, a ratio of 1:1 of oxygen to carbon was reported for the cable bacteria (Schauer et al., 2014) but our results reveal higher energy dissipation from the transport of electrons along the centimetre-long filament. The metabolic differences between spatially and temporally distinct cable bacterial populations highlight the need for pure cultures to further study the growth characteristics of this recently discovered bacterium.

As observed previously (Pfeffer et al., 2012) the cutting manipulation at the 0.3 cm had an immediate and drastic response in the geochemistry of the sediment, suggesting an instant arrestment of e-SOx, presumably due to physical disruption of the electron transport by the cable bacteria filaments. Our manipulation experiments however indicate that under some conditions, this impediment of e-SOx may not be permanent. Unlike the cutting experiment of Pfeffer et al., (2012) we observed a partial restoration of the e-SOx geochemical signature 24 hours after the cut at 0.3 cm. Cable bacteria filament network below the cut (which were no longer in contact with oxygen) managed to regain or maintain part of their suboxic carbon uptake activity, which was substantially higher than in the anoxic treatment. The treatment with the deeper cutting depth at 0.8 cm did not show any sign of recovery of e-SOx activity after 24 hours. These distinct effects between the two cutting depths at 0.3 and 0.8 cm suggest that the recovery potential of the cable bacteria network depends on the location of disturbance with a critical threshold of a couple of millimetres within 24 hours. Re-establishment of e-SOx activity after cutting could be explained by fast regrowth at the upper terminal end of the cable filament, or perhaps, by reorientation, which implies some form of motility as proposed by Schauer et al., (2014). The mechanism by which the transport of electrons is re-established requires further study into chemotactic and motility capacities of the cable bacteria.

3.4.3 Associated chemoautotrophic community

Intriguingly, high rates of inorganic carbon fixation were measured in this study in concert with the downward development of the heterotrophic cable bacteria. Total inorganic carbon assimilation was 6-fold higher than those reported for subtidal environments (Enoksson & Samuelsson 1987; Thomsen & Kristensen 1997) and sandy intertidal sediments (Lenk et al., 2010) but are well within the range of rates obtained in sulfidic salt-marsh creek sediments (Chapter 2). Although inorganic carbon fixation was high in horizons dominated by e-SOx, this inorganic carbon is unlikely assimilated by the cable bacteria themselves, but rather by other chemoautotrophic bacteria. Clone libraries revealed that sulfur-oxidizing Epsilon- and Gammaproteobacteria were not

only present in the oxic zone, but persisted throughout the suboxic zone. PLFA analysis with ^{13}C -bicarbonate labeling also provided a biomarker fingerprint that was consistent with chemoautotrophic sulfur-oxidizing Epsilon- and Gammaproteobacteria (Inagaki et al., 2003; Takai et al., 2006; Li et al., 2007; Glaubitz et al., 2009; Sorokin et al., 2010; Labrenz et al., 2013). Hence both clone libraries and PLFA-SIP suggest that sulfur-oxidizing bacteria from the Epsilon- and Gammaproteobacteria may be the main chemoautotrophic organisms in sediments with e-SOx. The difference in depth distribution of inorganic carbon incorporation between the March and August experiments might be related to the initial conditions in the seasonal hypoxic marine Lake Grevelingen, where bottom waters were oxic in March (80% O_2 saturation) as opposed to anoxic in August (0% O_2 saturation). To conclude, the presence of the cable bacteria performing e-SOx process favoured the co-development of a strongly active chemoautotrophic community that extends down to centimetres of depth in the sediment.

Manipulation experiments provided further evidence of a tight coupling between subsurface chemoautotrophic organisms and the electron transport by the cable filament network. Induced anoxia demonstrated that chemoautotrophs in the suboxic zone directly depend on the oxygen in the overlying water given the almost complete inhibition of ^{13}C -bicarbonate uptake throughout the sediment. Likewise inorganic carbon incorporation drastically decreased below the cutting depth (in the 0.8 cm cutting depth treatment) and was only maintained in sediment layers where cable bacteria were still connected to oxygen. Inorganic carbon fixation was actually stimulated in the surface sediment layer after cutting, which could be due to an increased potential for reoxidation after the doubling in oxygen penetration once the cable network was disrupted. Finally, when the sediment was cut at 0.3 cm depth, bicarbonate uptake only slightly decreased (still maintained 50 to 70% of initial activity) as did propionate uptake by the cable bacteria, suggesting that chemoautotrophs partially recovered in synchrony with the re-establishment of the e-SOx process after 24 hours.

3.5 CONCLUSION

Our study therefore suggests that the complete oxidation of sulfide in e-SOx sediments may be a two-step process, regulated by a consortium of bacteria composed of chemo-organotrophic cable bacteria and sulfur-oxidizing chemo-lithoautotrophs, rather than by the cable bacteria alone. Given that in the deeper layers, oxygen and nitrate are absent (Risgaard-Petersen et al., 2012; Marzocchi et al., 2014) chemo-lithoautotrophs have to use other electron acceptors to oxidize reduced sulfur compounds. Although these chemo-lithoautotrophs may disproportionate sulfur (Grote et al., 2012; Wright et al., 2013) their metabolic link to the cable bacteria indicates they use the cable bacteria possibly as an electron acceptor by tapping on to the electron

transport network via nanowires, nanotubes, or fimbriae (Widdel & Pfennig 1982; Reguera et al., 2005; Dubey & Ben-Yehuda 2011). Clearly, further studies are needed to confirm key autotrophic players and to target the exact mechanisms by which the observed activity of the chemo(litho)autotrophic bacteria is coupled to the electron transport network of the cable bacteria. Our results suggest that other bacteria may benefit directly from the electron transport by the cable bacteria.

ACKNOWLEDGMENTS

WE THANKFULLY ACKNOWLEDGE THE ASSISTANCE WITH STABLE ISOTOPE ANALYSIS BY PETER VAN BREUGEL AND MARCO HOUTEKAMER, MICHIEL KIENHUIS FOR TECHNICAL ASSISTANCE WITH NANOSIMS ANALYSIS, MOLECULAR WORK OF BEKIR FAYDACI AND SINEM ATLI, AND THE HELP OF ANTON TRAMPER AND PIETER VAN RIJSWIJK DURING SEDIMENT COLLECTION. THIS WORK WAS FINANCIALLY SUPPORTED BY THE DARWIN CENTRE FOR GEOSCIENCE (H.T.S.B. AND F.J.R.M.), ERC GRANT TO F.J.R.M, DANISH COUNCIL FOR INDEPENDENT RESEARCH-NATURAL SCIENCES (R.S.), THE NETHERLANDS EARTH SYSTEM SCIENCE CENTRE (J.J.M.) AND AN NWO LARGE INFRASTRUCTURE SUBSIDY TO J.J.M.

3.6 SUPPLEMENTARY INFORMATION

3.6.1. *Material & Methods**Microsensor profiling*

Depth profiling was done with microsensors (Unisense A.S., Denmark) for H₂S (50- μ m tip diameter), O₂ (50- μ m tip) and pH (100 or 200 μ m tip) after calibration (H₂S: 5 point calibration curve using Na₂S standards; O₂: 2 point calibration using 100% in air bubbled seawater and 0% in the anoxic zone of the sediment; pH: 3 NBS standards and TRIS buffer, pH values reported on the total pH scale).

Porosity (0.89 \pm 0.01) was determined from water content and solid phase density upon drying sediment samples to a constant weight at 60°C, accounting for the salt content of the pore water. Solid phase dry density (2.60 \pm 0.03 g ml⁻¹) was measured as the volume displacement after adding a known mass of dry sediment to a graduated cylinder.

The diffusive oxygen uptake was calculated from the oxygen depth profile near the sediment water interface using Fick's First law.

$$J_i = \phi / (1 - 2 \ln \phi) D_i (S, T) \partial C_i / \partial x$$

where ϕ is the measured porosity, and the modified Wiessberg expression $\theta^2 = 1 - 2 \ln(\phi)$ is used to relate tortuosity to porosity (Boudreau, 1996). The diffusion coefficients D_i is calculated from salinity (S) and temperature (T) using the R package *marelac* (Soetaert, Petzoldt, & Meysman, 2014). The cathodic proton consumption (CPC) is the proton consumption corresponding to the cathodic half-reaction, O₂ + 4e⁻ + 4H⁺ \rightarrow 2H₂O. The CPC was calculated as the sum of the upward and downward alkalinity fluxes immediately above and below the pH maximum in the oxic zone. Alkalinity fluxes were calculated as the sum of the fluxes of the major individual pore water compounds that contribute to the alkalinity:

$$J_{TA} = J_{HCO_3^-} + 2J_{CO_3^{2-}} + J_{B(OH)_4^-} + J_{HS^-} + J_{OH^-} - J_{H^+}$$

The speciation of individual ions (carbonate, borate, sulfide and water equilibria) was calculated from H₂S and pH microsensor data using the R package *AquaEnv* (Hofmann, Soetaert, Middelburg, & Meysman, 2010). For this calculation, the measured depth profile of dissolved inorganic carbon and a constant depth profile for borate were assumed (proportional to salinity). The contribution of other macronutrients (ammonium, silicate) to alkalinity fluxes are likely small and were not considered. The concentration gradient dCi/dx for each individual species was estimated

by a noise robust numerical differentiation using the Savitsky–Golay algorithm, optimized with a $n=21$ point stencil (Savitzky & Golay, 1964). The current density was calculated from the CPC using a conversion factor of one electron per proton ($1 \text{ A m}^{-2} = 1.036 \times 10^{-5} \text{ mole m}^{-2} \text{ s}^{-1}$). The oxygen consumed by the cathodic half reaction (cathodic oxygen consumption: COC), was calculated based on 4 protons consumed for each oxygen molecule $\text{COC} = 0.25\text{CPC}$.

PLFA-SIP analysis

^{13}C -labeled substrate injections (100 μl) were made from 0 to 2 cm at depth intervals of 0.25 cm, and beyond this, every 0.5 cm down to 8 cm. Finally 100 μL was distributed on to the sediment surface. Labeled cores were kept in a tank with ^{13}C -labeled filtered seawater in the dark for 24 hours with continuous aeration at 16°C. To avoid stripping of the labeled CO_2 from the cores during incubations, the overlying seawater was bubbled with ^{13}C -saturated air during incubation. To this end, air was guided through a set-up with dual washing bottles. The first bottle contained a 1M sodium hydroxide solution to trap CO_2 , while the second bottle contained artificial seawater labeled with ^{13}C -bicarbonate. Propionate uptake rates were not corrected for pore water concentrations given that ^{13}C -substrate was added in high concentrations to ensure complete labeling of the propionate pool in the sediment. Bicarbonate incorporation rates were corrected considering a 60% dilution of ^{13}C -labeling levels in pore water DIC. Background isotopic values in pore water of dissolved inorganic carbon (DIC) were analysed in two cores without substrate addition. Pore water was obtained by centrifugation (4500 rpm for 5 minutes) and ^{13}C -DIC was measured by the head space technique with an elemental analyser-IRMS equipped with a gas injection port (Chapter 2).

For statistical analysis PLFA patterns of reference bacteria cultures from *Desulfobulbus* spp., Gamma- and Epsilonproteobacteria were added to PCA analysis (Donachie et al., 2005; Inagaki et al., 2004; Pagani et al., 2011; Suzuki et al., 2007; Takai et al., 2006; Taylor & Parkes, 1983; Zhang et al., 2005).

NanoSIMS

All analysed fields were first pre-sputtered with Cs^+ ions to stabilize secondary ion intensity. Analysis was done by rastering the primary Cs^+ ion beam (current 1–2 pA, energy 16 keV, focused to a nominal spot size of 130 nm) over the sample in 128x128 pixels with a dwelling time of 1 ms per pixel. The imaged areas had a size between 5x5 μm and 10x10 μm . Secondary ions were extracted from the sample surface and mass-separated in the magnetic sector of the instrument's mass detector. Quality of

data collected on different days was ensured by tuning the instrument before each analysis. Quasi-simultaneous arrival (QSA) correction was avoided by keeping the secondary ion intensities sufficiently low. Data processing was done using the Look@NanoSIMS freeware program (Polerecky et al., 2012). For each individual cell, relative ^{13}C abundance defined as $^{13}\text{C}/(^{12}\text{C}+^{13}\text{C})$, was determined based on the total ^{12}C and ^{13}C counts accumulated over all detected planes and pixels in the regions of interest (ROI) drawn around the cable bacterial filaments. ROIs for which the ^{13}C abundance varied significantly with depth were not included in the final analysis.

3.6.2 Supplementary figures and table

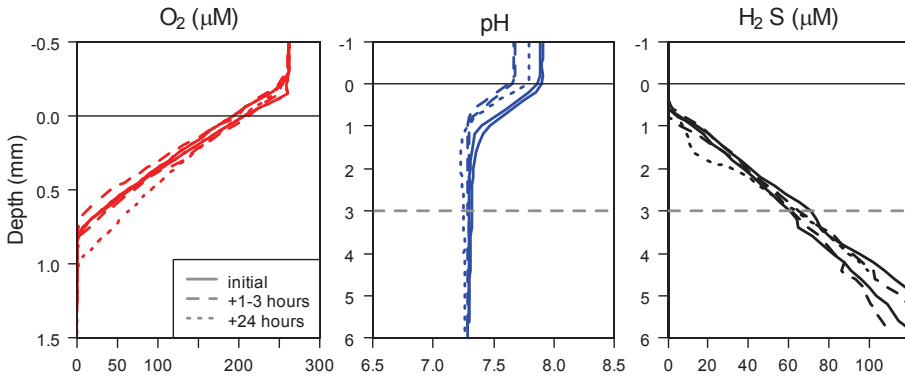
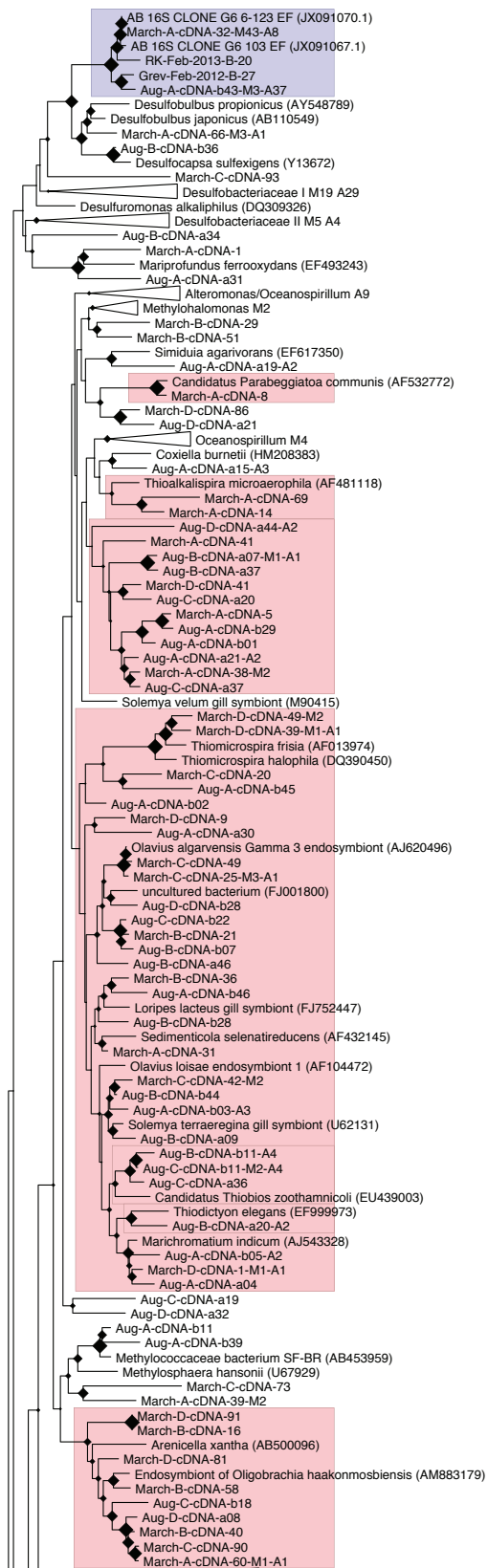
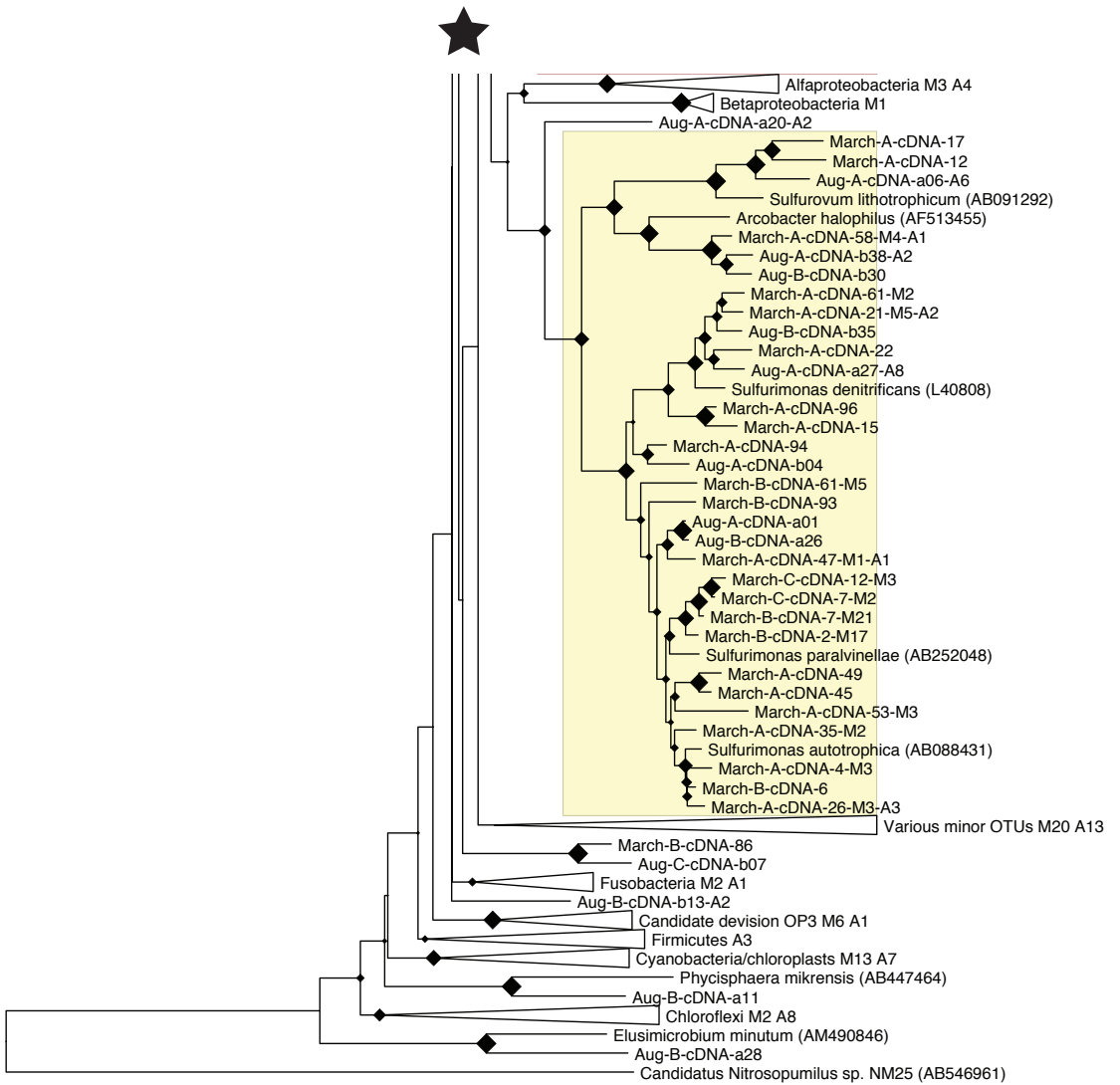


Figure S1. Sediment without the e-SOx geochemical fingerprint was used to determine possible effects of cutting at 0.3 cm depth (grey dotted line) on pore water chemistry. Controls were microprofiled (O₂, pH, H₂S) before the cut, 1 to 3 hours and 24 hours after incubation (n=2).

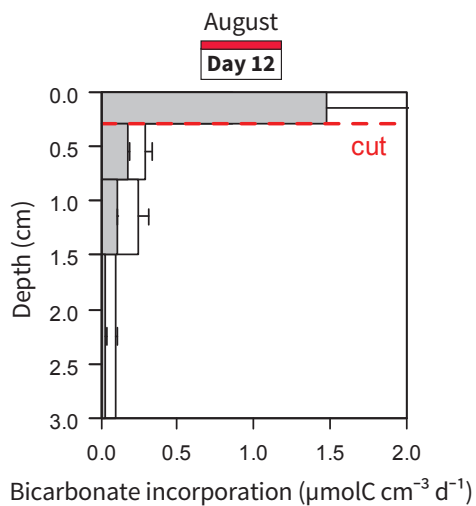
Figure S2. Phylogenetic tree of 16S cDNA clone library combining results from both the March (day 13) and August (day 12) 2012 experiments. Operational taxonomic units (OTU) group sequences with >97% similarity. Cable bacteria OTUs related to the Desulfobulbaceae are highlighted in blue, Epsilonproteobacteria OTUs in yellow and sulfur-oxidizing Gammaproteobacteria OTUs in red. Coding used for each OTU indicates the month (March or August), layer (A=0-0.3 cm, B=0.3-0.8 cm, C=0.8-1.5 cm, D=1.5-3.0 cm), cDNA, representative clone number, and finally a letter (M=March or A=August) followed by a number indicating the total number of clones in the OTU for each month.





0.03

Figure S3. Bicarbonate incorporation rates for shallow cut (0.3 cm deep) for August day 12. Rates were calculated from ^{13}C -PLFA analysis and are represented in bar plot with un-manipulated sediment in white and rates for manipulated sediment in grey. Averages (\pm SD) are plotted. Number of replicate core is 2.



*YVONNE A. LIPSEWERS, *DIANA VASQUEZ-CARDENAS,
DORINA SEITAJ, REGINA SCHAUER, SILVIA HIDALGO MARTINEZ,
JAAP S. SINNINGHE DAMSTÉ, FILIP J.R. MEYSMAN,
LAURA VILLANUEVA, HENRICUS T.S. BOSCHKER

* Equal contributors

Impact of seasonal hypoxia on activity, diversity and community structure of chemoautotrophic bacteria in a coastal sediment (Lake Grevelingen, The Netherlands)

ABSTRACT

In seasonal hypoxic coastal systems the availability of electron acceptors in the bottom water drastically changes throughout the year. This may induce shifts in reoxidation of reduced sulfur intermediates in the sediment, which then could impact sedimentary chemoautotrophic bacteria communities. To test this hypothesis, we used a multidisciplinary approach to examine the diversity and activity of the chemoautotrophic bacterial community in the sediments of the seasonally hypoxic marine Lake Grevelingen during two seasons (oxic spring and hypoxic summer). Combined 16S rRNA gene amplicon sequencing and phospholipid derived fatty acids (PLFA) analysis indicated major shift in total community structure due to hypoxia. Aerobic sulfur-oxidizing Gammaproteobacteria (Thiotrichales) and Epsilonproteobacteria (Campylobacterales) were prevalent during spring, whereas Deltaproteobacteria (Desulfobacterales) related to sulfate reducing bacteria prevailed during the summer. Dark CO₂ fixation rates in the surface sediment were three times higher in spring compared to summer hypoxia. At each site geochemical profiling enabled a clear linkage between the depth distribution of chemoautotrophy and the dominant sulfur oxidation mechanism, *i.e.*, electrogenic sulfur oxidation by cable bacteria or sulfide oxidation coupled to nitrate reduction by nitrate-accumulating Beggiatoaceae. The appearance of chemoautotrophic Epsilonproteobacteria was closely associated with the activity of chemoautotrophic, nitrate-accumulating Beggiatoaceae. When (heterotrophic) cable bacteria were present, the chemoautotrophic community was more diverse, and included sulfur-oxidizing Gamma- and Epsilonproteobacteria alongside sulfur disproportionating Deltaproteobacteria. The metabolic diversity of the sulfur-oxidizing bacterial community suggests a complex niche partitioning within the sediment probably driven by the availability of sulfur species (H₂S, S⁰, S₂O₃²⁻) and electron acceptors (both O₂, NO₃⁻) which are regulated by seasonal hypoxia.

4.1 INTRODUCTION

The reoxidation of reduced intermediates formed during anaerobic mineralization of organic matter is a key process in the biogeochemistry of coastal sediments (Soetaert et al., 1996; Jørgensen & Nelson 2004). Many of the micro-organisms involved in the reoxidation of reduced compounds are chemoautotrophs, *i.e.*, they fix inorganic carbon using the chemical energy derived from reoxidation reactions. In coastal sediments, sulfate reduction forms the main respiration pathway, accounting for 50% to 90% of the organic matter mineralization (Soetaert et al., 1996). The reoxidation of the pool of reduced sulfur compounds (dissolved free sulfide, thiosulfate, elemental sulfur, iron monosulfides and pyrite) produced during anaerobic mineralization hence forms the most important pathway sustaining chemoautotrophy in coastal sediments (Howarth 1984; Jørgensen & Nelson 2004).

Various lineages from the Alpha-, Gamma-, Delta- and Epsilonproteobacteria, including recently identified groups such as particle associated Gammaproteobacteria and large sulfur bacteria, couple dark CO₂ fixation to the oxidation of reduced sulfur compounds in marine sediments (Brüchert et al., 2003; Lavik et al., 2009; Sorokin et al., 2011; Grote et al., 2012). In sulfide-rich intertidal sediments, chemoautotrophic sulfur-oxidizers belonging to the Gammaproteobacteria have been identified to play a major role in the sulfur and carbon cycling (Lenk et al., 2010; Chapter 2). Accordingly, different types of chemoautotrophic sulfur-oxidizing communities appear to be present in coastal sediments, but it is presently not clear as to which environmental factors are actually determining the chemoautotrophic community composition at a given site.

More and more coastal systems are currently impacted by hypoxia, *i.e.* the depletion of oxygen in bottom waters ($< 65 \mu\text{mol O}_2 \text{ L}^{-1}$), which has a large impact on the biogeochemical cycling and ecological functioning of the underlying sediments (Diaz & Rosenberg 2008). At present, the prevalence of chemoautotrophy and the associated microbial communities have not been thoroughly investigated in coastal sediments of seasonal hypoxic basins. Yet, such sediments could be particularly useful to better understand the environmental factors determining sedimentary chemoautotrophy. The absence of suitable soluble electron acceptors in the bottom water in summer should theoretically result in a complete inhibition of sedimentary sulfur reoxidation, thus strongly reducing chemoautotrophy. Hence, in sediments underlying seasonal hypoxic basins, one expects a strong seasonality in both the chemoautotrophy activity as well as a marked change in the community structure of chemoautotrophy microbes.

However, the availability of soluble electron acceptors (O₂, NO₃⁻) in the bottom water is likely not the only determining factor of sulfur oxidation. A recent study by Seitaj et al., (2015) described the succession of sulfur oxidation mechanisms in the sediments of the seasonally hypoxic marine Lake Grevelingen via four dominant

mechanisms: (1) heterotrophic cable bacteria (*Desulfobulbaceae*) conducting electrogenic sulfur oxidation from late winter to spring, (2) sulfur oxidation by an intermediate iron shuttle, sustained by down mixing of iron-oxides into the sediment occurring in spring; (3) reoxidation of free sulfide in the sediment during summer catalyzed by a large pool of FeOOH formed in spring by the activity of cable bacteria and, (4) nitrate-accumulating *Beggiatoaceae* coupling nitrate reduction to sulfide oxidation after the summer hypoxia. Accordingly, we hypothesize that the presence of these particular sulfur oxidation regimes could be governing the community structure of chemoautotrophic microbes.

To examine the above hypothesis, we conducted a multidisciplinary study, involving both geochemistry and microbiology, to document the seasonal and spatial variations in the diversity and activity of chemoautotrophic bacteria in the sediments of the seasonal hypoxic Lake Grevelingen. Field sampling was conducted during spring (oxygenated bottom waters) and summer (oxygen depleted bottom waters). Sediment microsensor profiling of oxygen, free sulfide and pH was performed to characterize the geochemistry and identify the specific fingerprints of main sulfur oxidation mechanisms (Seitaj et al., 2015). General bacterial diversity was assessed by 16S rRNA gene amplicon sequencing and the analysis of phospholipid derived fatty acids (PLFA). Biovolumes of the two important sulfur oxidizing bacteria namely *Beggiatoaceae* and cable bacteria were determined by microscopy. PLFA analysis combined with ^{13}C stable isotope probing (PLFA-SIP) provided the activity and community composition of chemoautotrophs in the sediment. This approach was complemented by the analysis of genes involved in dark CO_2 fixation, *i.e.*, characterizing the abundance and diversity of the genes *cbbL* and *aclB* that code for key enzymes in Calvin-Benson Bassham (CBB) and reductive tricarboxylic acid (rTCA) carbon fixation pathways, respectively (Nigro & King 2007; Kovaleva et al., 2011; Hügler & Sievert 2011).

4.2 MATERIAL & METHODS

4.2.1 Study site and sediment sampling

Lake Grevelingen is a former estuary located within the Rhine-Meuse-Scheldt delta area of the Netherlands, which became a closed saline reservoir (salinity ~ 30) by dam construction at both the land side and sea side in the early 1970s. Due to an absence of tides and strong currents, Lake Grevelingen experiences a seasonal stratification of the water column, which in turn, leads to a gradual depletion of the oxygen in the bottom waters (Hagens et al., 2015). Bottom water oxygen at the deepest stations typically starts to decline in April, reaches hypoxic conditions by end of May ($\text{O}_2 < 63 \mu\text{M}$), further decreasing to anoxia in August ($\text{O}_2 < 1 \mu\text{M}$), while the overturning of the water

column and the associated re-oxygenation of the bottom water takes place in September (Seitaj et al., 2015). To study the effects of the bottom water oxygenation on the benthic chemoautotrophic community, we performed a field sampling campaign on March 13th, 2012 (before the start of the annual O₂ depletion) and August 20th, 2012 (at the height of the annual O₂ depletion). Detailed water column, pore water and solid sediment chemistry of Lake Grevelingen over the year 2012 have been previously reported in Hagens et al., (2015), Seitaj et al., (2015) and Sulu-Gambari et al., (2015).

Sediments were recovered at three stations along a depth gradient within the Den Osse basin, one of the deeper basins in marine Lake Grevelingen: Station 1 (S1) was located in the deepest point of the basin at 34 m water depth (51.747°N, 3.890°E), Station 2 (S2) at 23 m (51.749°N, 3.897°E) and Station 3 (S3) at 17 m (51.747°N, 3.898°E). Intact sediment cores were retrieved with a single core gravity corer (UWITEC) using PVC core liners (6 cm inner diameter, 60 cm length). All cores were inspected upon retrieval and only cores with a visually undisturbed surface were used for further analysis.

Thirteen sediment cores for microbial analysis were collected per station and per time point: two cores for phospholipid-derived fatty acid analysis (PLFA), two cores for nucleic acid analysis, four cores for ¹³C-bicarbonate labeling, three cores for microelectrode profiling, one core for quantification of cable bacteria, and one core for quantification of Beggiatoaceae. Sediment cores for PLFA extractions were sliced manually on board the ship (5 sediment layers; sectioning at 0.5, 1, 2, 4, and 6 cm depth). Sediment slices were collected in Petri dishes, and replicate depths were pooled and thoroughly mixed. Homogenized sediments were immediately transferred to centrifuge tubes (50 ml) and placed in dry ice until further analysis. Surface sediments in August consisted of a highly porous “fluffy” layer that was first left to settle after core retrieval. Afterwards, the top 1 cm thick layer was recovered through suction (rather than slicing). Sediment for nucleic acid analysis was collected by slicing manually at a resolution of 1 cm up to 5 cm depth. Sediment samples were frozen in dry ice, transported to the laboratory within a few hour and placed at -80°C until further analysis.

4.2.2 Microsensor profiling

Oxygen depth profiles were recorded with commercial microelectrodes (Unisense, Denmark; tip size: 50 µm) at 25–50 µm resolution. For H₂S and pH (tip size: 50 and 200 µm), depth profiles were recorded at 200 µm resolution in the oxic zone, and at 400 or 600 µm depth resolution below. Calibrations for O₂, pH and H₂S were performed as described by Malkin et al., (2014) and Seitaj et al., (2015). ΣH₂S was calculated from H₂S based on pH measured at the same depth using the R package AquaEnv (Hofmann et al., 2010). The oxygen penetration depth (OPD) is operationally defined as the depth

below which $[O_2] < 1 \mu M$, while the sulfide appearance depth (SAD) is operationally defined as the depth below which $[H_2S] > 1 \mu M$. The diffusive oxygen uptake (DOU) was calculated from the oxygen depth profiles as described in detail in Chapter 3.

4.2.3 DNA extraction and 16S rRNA gene amplicon sequencing

DNA from 0 cm to 5 cm sediment depth (in 1 cm resolution) was extracted using the DNA PowerSoil® Total Isolation Kit (Mo Bio Laboratories, Inc., Carlsbad, CA). Nucleic acid concentrations were quantified spectrophotometrically (Nanodrop, Thermo Scientific, Wilmington, DE) and checked by agarose gel electrophoresis for integrity. DNA extracts were kept frozen at $-80^\circ C$.

Sequencing of 16S rRNA gene amplicons was performed on the first cm of the sediment (0–1 cm depth) in all stations in March and August as described in Moore et al., (2015). Further details are provided in the SI. The 16S rRNA gene amplicon reads (raw data) have been deposited in the NCBI Sequence Read Archive (SRA) under BioProject number PRJNA293286. The phylogenetic affiliation of the 16S rRNA gene sequences was compared to release 119 of the SILVA NR SSU Ref database (<http://www.arb-silva.de/>; Quast et al., 2013) using the ARB software package (Ludwig et al., 2004). Sequences were added to a reference tree generated from the Silva database using the ARB Parsimony tool.

4.2.4 Sediment incubations and PLFA-SIP analysis

Sediment cores were labeled with ^{13}C -bicarbonate to determine the chemoautotrophic activity and associated bacterial community by tracing the incorporation of ^{13}C into bacterial phospholipid derived fatty acids (PLFA). To this end, four intact cores were sub-cored with smaller core liners (4.5 cm inner diameter; 20 cm height) that had pre-made side ports to inject the ^{13}C -label. *In situ* bottom water was kept over the sediment and no gas headspace was present. Cores were kept inside a closed cooling box during transport to the laboratory.

Stock solutions of 80 mM of ^{13}C -bicarbonate (99% ^{13}C ; Cambridge Isotope Laboratories, Andover, Ma, USA) were prepared as in Chapter 2. ^{13}C -bicarbonate was added to the sediment from 3 cm above the surface to 8 cm deep in the sediment cores in aliquots of 100 μl through vertically aligned side ports (0.5 cm apart) with the line injection method (Jørgensen 1978). March sediments were incubated at $17 \pm 1^\circ C$ in the dark for 24 h and continuously aerated with ^{13}C -saturated air to maintain 100% saturated O_2 conditions as those found *in situ*, but avoiding the stripping of labeled CO_2 from the overlying water (for details of the procedure, see Chapter 3). In August, sediments were incubated at $17 \pm 1^\circ C$ in the dark for 40 h to ensure sufficient labeling

as a lower activity was expected under low oxygen concentrations. In August, oxygen concentrations in the overlying water were maintained near *in situ* O₂ levels measured in the bottom water (S1: 0–4% saturation, S2: 20–26%, S3: 35–80%). A detailed description of aeration procedures for the August incubations can be found in the SI.

At the end of the incubation period, sediment cores were sliced in five depth intervals (as described for PLFA sediment cores sliced on board) thus obtaining two replicate slices per sediment depth and per station. Sediment layers were collected in centrifuge tubes (50 ml) and wet volume and weight were noted. Pore water was obtained by centrifugation (4500 rpm for 5 min) for dissolved inorganic carbon (DIC) analysis, and sediments were lyophilized for PLFA-SIP analysis.

Biomarker extractions were performed on freeze dried sediment as in Guckert et al., (1985) and ¹³C-incorporation into PLFA was analyzed as in Chapter 2. Nomenclature of PLFA can be found in the SI. Detailed description of the PLFA-SIP calculations can be found in Boschker & Middelburg (2002) and Chapter 3. Total dark CO₂ fixation rates (mmol C m⁻² d⁻¹) are the depth-integrated rates obtained from the 0–6 cm sediment interval.

4.2.5 Quantitative PCR

To determine the abundance of chemoautotrophs we quantified the genes coding for two enzymes involved in dark CO₂ fixation pathways: the large subunit of the RuBisCO enzyme *cbbL* gene, and the ATP citrate lyase *aclB* gene. These gene sequences were subsequently used to study the diversity of chemoautotrophs by phylogenetic analysis. The quantification of *cbbL* and *aclB* genes via quantitative PCR (qPCR) was performed in 1 cm resolution for the sediment interval between 0–5 cm depth in all stations in both March and August. qPCR analyses were performed on a Biorad CFX96™ Real-Time System/C1000 Thermal cycler equipped with CFX Manager™ Software. Abundance of the RuBisCO *cbbL* gene was estimated by using primers K2f/V2r as described by Nigro & King (2007). The abundance of ATP citrate lyase *aclB* gene was quantified by using the primer set *aclB_F/aclB_R*, which is based on the primers 892F/1204R by Campbell et al., (2003) with several nucleotide differences introduced after aligning $n = 100$ sequences of *aclB* gene fragments affiliated to Epsilonproteobacteria (See Table S1 for details). All qPCR reactions were performed in triplicate with standard curves from 10⁰ to 10⁷ molecules per microliter. Standard curves and qPCR reactions were performed as previously described in Lipsewers et al., (2014). Melting temperature T_m, PCR efficiencies (E) and correlation coefficients for standard curves are listed in Table S2.

4.2.6 PCR amplification and cloning

Amplifications of the RuBisCO *cbbL* gene and the ATP citrate lyase *aclB* gene were performed with the primer pairs specified in Table S1. The PCR reaction mixture was the following (final concentration): Q-solution (PCR additive, Qiagen, Valencia, CA) 1×; PCR buffer 1×; BSA (200 µg ml⁻¹); dNTPs (20 µM); primers (0.2 pmol µl⁻¹); MgCl₂ (1.5 mM); 1.25 U Taq polymerase (Qiagen, Valencia, CA). PCR conditions for these amplifications were the following: 95°C, 5 min; 35 × [95°C, 1 min; T_m, 1 min; 72°C, 1 min]; final extension 72°C, 5 min. PCR products were gel purified (QIAquick gel purification kit, Qiagen, Valencia, CA) and cloned in the TOPO-TA cloning® kit (Life Technologies, Carlsbad, CA) and transformed in *E. coli* TOP10 cells following the manufacturer's recommendations. Recombinant plasmid DNA was sequenced using M13R primer by BASECLEAR (Leiden, The Netherlands).

Sequences were aligned with MEGA5 software (Tamura et al., 2011) by using the alignment method ClustalW. The phylogenetic trees of the *cbbL* and *aclB* genes were computed with the Neighbour-Joining method (Saitou & Nei 1987). The evolutionary distances were estimated using the Jukes-Cantor method (Jukes & Cantor 1969) for DNA sequences and with the Poisson correction method for protein sequences (Zuckerkanndl & Pauling 1965) with a bootstrap test of 1,000 replicates. Sequences were deposited in NCBI with the following accession numbers: KT328918–KT328956 for *cbbL* gene sequences and KT328957–KT329097 for *aclB* gene sequences.

4.2.7 Quantification of cable bacteria and Beggiatoaceae

Microscopic identification of cable bacteria was achieved by Fluorescence *in situ* Hybridization (FISH), using a Desulfobulbaceae-specific oligonucleotide probe (DSB706; 5'-ACC CGT ATT CCT CCC GAT-3'), according to Schauer et al., (2014). Cable bacteria biovolume per unit of sediment volume (mm³ cm⁻³) was calculated based on measured filament length and diameter. The areal biovolume of cable bacteria (mm³ cm⁻²) was obtained by depth integration over all sediment layers analyzed.

Beggiatoaceae were identified via inverted light microscopy (Olympus IM) within 24 h of sediment retrieval. Intact sediment cores were sectioned at 5 mm intervals over the top 4 cm from which subsamples (20–30 mg) were used to count living Beggiatoaceae (Seitaj et al., 2015). The biovolume was determined by measuring length and width of all filaments found in the subsample, following the counting procedure of Jørgensen et al., (2010).

4.2.8 Statistical analysis

All statistical analyses were performed using the CRAN: stats package in the open source software R. A two-way ANOVA (aov) was used to test the effect of station, season, and sediment depth on chemoautotrophic activity, and gene abundances. PLFA concentrations and ^{13}C -incorporation values were expressed as a fraction of the total bacterial biomass and ^{13}C -incorporation (respectively) per sediment sample. These relative PLFA values were first log-transformed ($\log(x+1)$) and subsequently analyzed with Principal Component Analysis (PCA: prcomp) to distinguish different bacterial and chemoautotrophic communities in the sediment.

4.3 RESULTS

4.3.1 Geochemical characterization

The seasonal variation of the bottom water oxygen concentration in marine Lake Grevelingen strongly influenced the pore water concentrations of O_2 and H_2S . In March, the bottom water was fully oxygenated at all three stations ($299\text{-}307\ \mu\text{mol L}^{-1}$), oxygen penetrated $1.8\text{-}2.6\ \text{mm}$ deep in the sediment, and no free sulfide was recorded in the first few centimeters (Table 1). The width of the suboxic zone, operationally defined as sediment layer located between the OPD and the SAD, varied between $16\text{-}39\ \text{mm}$ across the three stations in March 2012. In contrast, in August, the oxygen was strongly depleted in the bottom waters at S1 ($0\ \mu\text{mol L}^{-1}$) and S2 ($11\ \mu\text{mol L}^{-1}$), and no O_2 was detected by microsensor profiling in the surface sediment at these stations. At station S3, the bottom water O_2 remained higher ($88\ \mu\text{mol L}^{-1}$), and oxygen penetrated down to $1.1\ \text{mm}$. In August, free sulfide was present up to the sediment-water interface at all three stations, and the accumulation of sulfide in the pore water increased with water depth (Fig. 1a).

Depth pH profiles showed much larger variation between stations in March compared to August (Fig. 1a). Sediment pH profiles can be used to identify the main pathways of sulfur oxidation in sediments (Seitaj et al., 2015; Meysman et al., 2015). The pH profiles in S1 and S3 in March were similar characterized by maximum values (concave up inflection) in the oxic zone and lower pH values in the suboxic zone, which indicate the geochemical signature of electrogenic sulfur oxidation (e-SOx) by cable bacteria. In contrast, the pH depth profile in S2 showed a pH minimum (concave down inflection) in the oxic layer and a subsurface maximum below, indicative of sulfur oxidation by motile nitrate-storing Beggiatoaceae (Seitaj et al., 2015; Fig. 1a). In contrast, the pH profiles at S1 and S3 in August 2012 show a gradual decline of pH with depth, and are representative of sulfate reduction occurring

Table 1. Geochemical characterization, chemoautotrophy rates, and quantification of cable bacteria and Beggiatoaceae in the three stations in Lake Grevelingen for spring (March) and summer (August).

Station	°C	Bottom water*		DOU	OPD	SAD	Suboxic zone**	pH signature***	Chemoautotrophy rate	Cable bacteria biovolume	Beggiatoaceae biovolume
		$\mu\text{M O}_2$	$\mu\text{M NO}_3^-$	$\text{mmol O}_2 \text{ m}^{-2} \text{ d}^{-1}$	mm	mm	mm		$\text{mmol C m}^{-2} \text{ d}^{-1}$	$\text{mm}^3 \text{ cm}^{-2}$	$\text{mm}^3 \text{ cm}^{-2}$
March	1	5	299 (oxic)	28.2	18.2 ± 1.7	1.8 ± 0.04	17.5 ± 0.7	16	3.1 ± 0.5	2.55	0.02
	2	5	301 (oxic)	27.9	15.8 ± 3.1	2.6 ± 0.65	21.3 ± 2.5	19	1.9 ± 0.1	ND	0.11
	3	5	307 (oxic)	27.7	17.1 ± 5.7	2.4 ± 0.4	41.8 ± 8.6	39	1.4 ± 0.3	2.08	0.05
August	1	17	0 (anoxic)	1.7	0	0	0.9 ± 1.1	0.9	0.2 ± 0.1	0.11	0.001
	2	17	12 (hypoxic)	11.6	0	0	0.6 ± 0	0.6	0.8 ± 0.3	ND	3.24
	3	19	88 (hypoxic)	10.6	13.9 ± 2.1	1.1 ± 0.1	4.2 ± 2.7	3	1.1 ± 0.5	0.003	0.004

DOU: dissolved O_2 uptake; OPD: O_2 penetration depth; SAD: $\Sigma \text{H}_2\text{S}$ appearance depth; e-SOx: electrogenic sulfur oxidation; ND: not determined
 *Bottom water is classified as anoxic with O_2 concentration below 1 μM and hypoxic below 63 μM .

**The thickness of the suboxic zone is defined as the average SAD minus the average OPD.

***pH signature serves to indicate the sulfur oxidizing mechanism that dominates the pore water chemistry as described by Seitaj et al., 2015

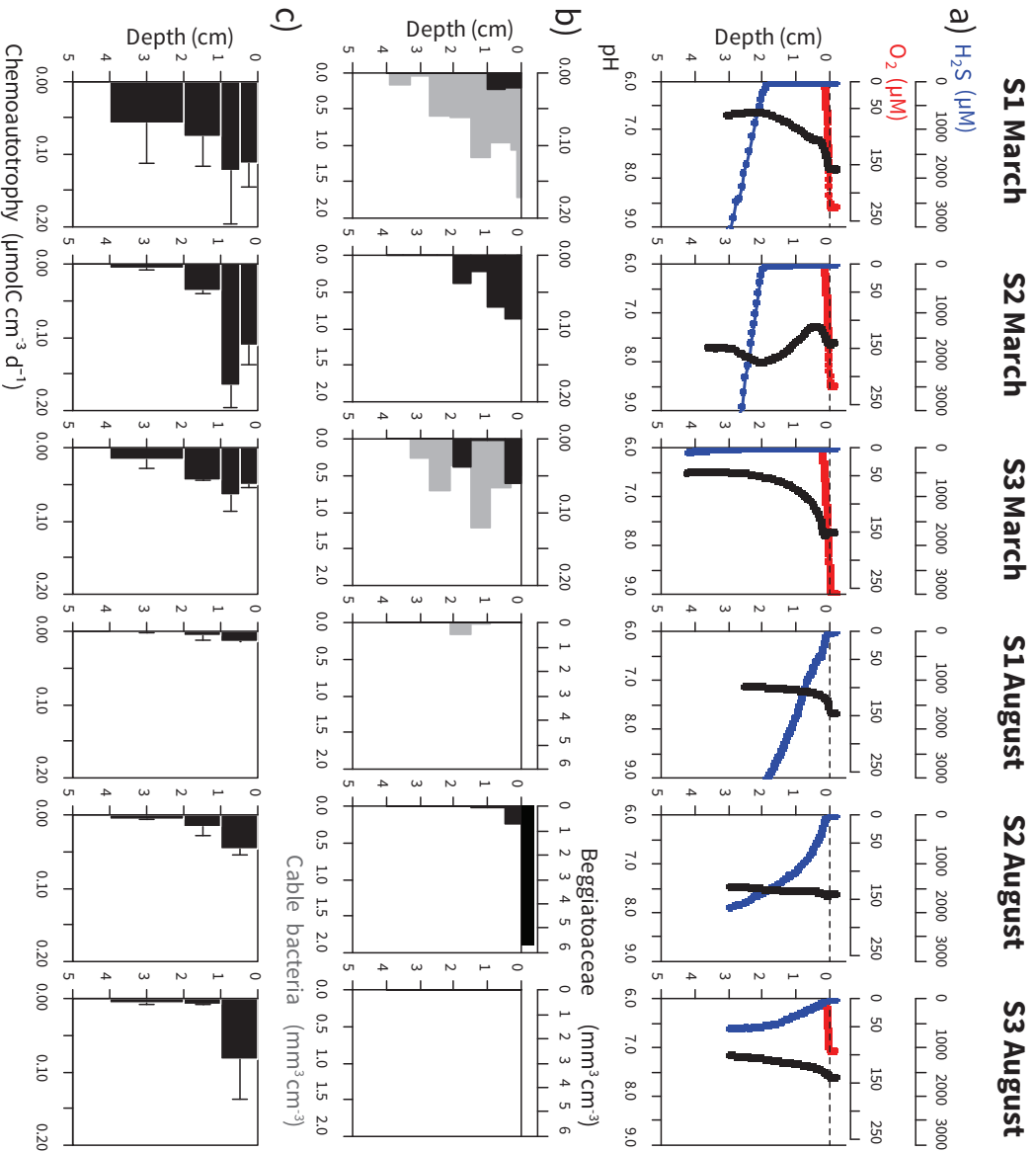


Figure 1. a) Geochemical fingerprint, b) biovolume of *Beggiatoaceae* (black) and cable bacteria (grey), c) chemoautotrophy depth profiles in sediment of Lake Grevelingen for March and August in all three stations. Note change in scale for *Beggiatoaceae* between March and August. S1: station 1 (34 m), S2: station 2 (23 m), S3: station 3 (17 m).

throughout the sediment (Meysman et al., 2015). The rather invariant pH profile at S2 in August could not be linked to any specific sulfur cycling mechanism.

4.3.2 Quantification of cable bacteria and Beggiatoaceae

We performed a detailed microscopy-based quantification of the biovolume of sulfur oxidizing cable bacteria and nitrate-storing Beggiatoaceae because they are likely to influence the chemoautotrophic community. In March, high biovolumes of cable bacteria were detected in S1 and S3 (Table 1) with filaments present throughout the suboxic zone until a maximum depth of 4 cm. At the same time, cable bacteria were absent in S2 (Fig. 1b). In August, cable bacteria were only detected between 1 and 2 cm deep at the deepest station, albeit at abundances that were close to the detection limit of the technique (S1). Beggiatoaceae were found in all three stations in March, although the biovolumes at S2 were one order of magnitude higher than in the other two stations (Table 1). In station S2, Beggiatoaceae were uniformly distributed up to the sulfidic appearance depth (Fig. 1b). During hypoxia, Beggiatoaceae were no longer detectable in stations S1 and S3 (Table 1) while at S2, filaments were no longer found in deeper sediment, but formed a thick mat at the sediment-water interface (Fig. 1b).

4.3.3 Bacterial diversity by 16S rRNA gene amplicon sequencing

The general diversity of bacteria was assessed by 16S rRNA gene amplicon sequencing analysis, which was applied to the surface sediment (0–1 cm) from all stations in both March and August. Approximately 50% of the reads could be assigned to three main clades: Gamma-, Delta-, and Epsilonproteobacteria (Fig. 2). The remaining reads were distributed amongst the order Bacteroidetes (14%), order Planctomycetes (6%), order Alphaproteobacteria (3%), the candidate phylum WS3 (2%), other orders (20%), and unassigned (5%).

Reads classified within the Gammaproteobacteria were the more abundant in March during oxygenated bottom water conditions than in August during hypoxia (Fig. 2). The majority of these reads could be assigned to the orders Alteromonadales, Chromatiales and Thiotrichales. The first order includes chemoheterotrophic bacteria that are either strict aerobes or facultative anaerobes (Bowman & McMeekin 2005). Additional phylogenetic comparison revealed that the reads assigned to the Chromatiales group were closely related to the Granulosicoccaceae, Ectothiorhodospiraceae, and Chromatiaceae families (Fig. S1). Reads in the Thiotrichales group were closely related to sulfur-oxidizing bacteria from the Thiotrichaceae family with 30% of the sequences related to the genera ‘*Candidatus Isobeggiatoa*’, ‘*Ca. Parabeggiatoa*’ and *Thiomargarita* (Fig. S2). It has been recently proposed that the genera *Beggiatoa*,

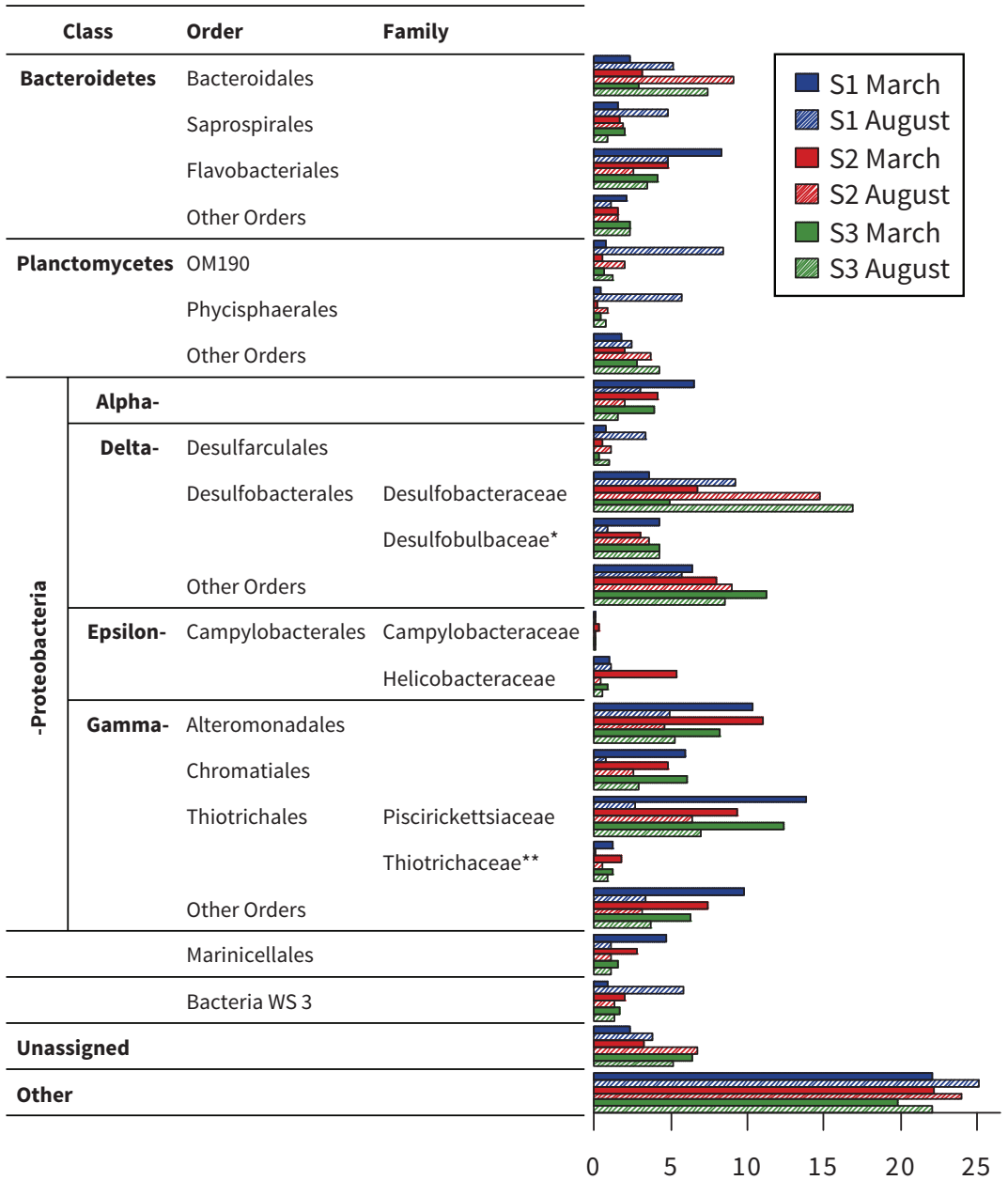


Figure 2. Percentage of total Bacteria 16S rRNA gene reads in the studied stations in March and August. Only the bacterial orders that had more than 3% of the total bacteria reads, in one or the other season, are reported (except in the case of the Thiotrichaceae family (Beggiatoaceae). * includes sequences closely related to cable bacteria; ** includes reads closely related to Beggiatoaceae

Thiomargarita and *Thioploca* should be reclassified into the originally published monophyletic family of Beggiatoaceae (Salman et al., 2011, 2013), and so here, these genera will be further referred to as Beggiatoaceae. Most of the reads assigned to the Beggiatoaceae came from station S2 where the geochemical fingerprint indicates active nitrate-storing Beggiatoaceae, and microscopy revealed high abundances of *Beggiatoa*-type filaments at this station. The percentage of reads assigned to sulfur-oxidizers from the order Thiotrichales decreased during August when oxygen concentrations in the bottom water declined.

Within the Deltaproteobacteria, reads were assigned to the order Desulfarculales, and Desulfobacterales (Fig. S3). Reads within the order of Desulfobacterales were mainly assigned to the families Desulfobacteraceae (between 10–20%) and Desulfobulbaceae (~5%) (Fig. 2). Additional phylogenetic comparison revealed that within the Desulfobulbaceae, 60% of the reads clustered within the genus *Desulfobulbus*, of which 30% were related to the electrogenic sulfur-oxidizing cable bacteria (Fig. S4). Overall, the number of reads assigned to the Desulfobulbaceae family was similar between the two seasons in S2 and S3, whereas in S1 the percentage of reads was approximately 4.5-fold higher in March compared to August (Fig. 2). In contrast, the number of reads assigned to the Desulfarculales and Desulfobacteraceae increased during hypoxia (Fig. 2), and phylogenetic analysis revealed a predominance in August of anaerobic metabolism related to the typical sulfate reducer genera *Desulfococcus*, *Desulfosarcina*, and *Desulfobacterium* (Fig. S5a–c).

Finally, all Epsilonproteobacteria reads were assigned to the order Campylobacteriales, such as the Campylobacteraceae and Helicobacteraceae families. Phylogenetic comparison showed that the reads were closely related to the genera *Sulfurovum*, *Sulfurimonas*, *Sulfurospirillum*, *Arcobacter* all capable of sulfur oxidation with oxygen or nitrate (Campbell et al., 2006; Fig. S6a–d). The percentage of reads in August was lower compared to March and highest numbers were present in S2 in March (~6%), (Fig. 2).

4.3.4 Bacterial community structure by PLFA analysis

The relative PLFA concentrations were used in a principal component analysis (PCA) to determine differences in bacterial community structure. A total of 22 PLFA, each contributing more than 0.1% to the total, were included in this analysis, while samples with too low bacterial biomass (less than one standard deviation below the mean of all samples) were excluded. The PCA analysis indicated that 73% of the variation within the dataset was explained by the first two axes. While the first PCA axis correlated with sediment depth (particularly for the March samples), the second PCA component clearly

water depth, while in August, the opposite trend was observed (Table 1). The chemoautotrophy activity at the deepest station (S1) varied strongly between seasons. The dark CO₂ fixation rate in March for S1 was the highest across all seasons and stations, but dropped by one order magnitude in August. In contrast, at the intermediate station (S2), the dark CO₂ fixation rate was only two times higher in March compared to August, while in the shallowest station (S3) the depth integrated rates were not significantly different between seasons ($p=0.56$).

The depth distribution of the chemoautotrophic activity also differed between seasons ($p=0.02$; Fig. 1c). In March, chemoautotrophic activity was found deep into the sediment (up to 4 cm) in stations S1 and S3 and had a more uniform depth distribution, whereas at station S2 chemoautotrophy only extended down to 2 cm and the highest activity was found in the top 1 cm. This distinction between the depth distributions of chemoautotrophy was consistent with the difference in sulfur oxidation regimes as detected by microsensor profiling (nitrate-storing Beggiatoaceae in S2 versus electrogenic sulfur oxidation by cable bacteria in S1 and S3). In August, the chemoautotrophic activity was restricted to the top cm of the sediment.

The PLFA ¹³C-fingerprints were analyzed by PCA to identify differences in chemoautotrophic community. Only PLFA that contributed more than 0.1% to the total ¹³C-incorporation and sediment layers that showed chemoautotrophy rates higher than 0.01 $\mu\text{mol C cm}^{-3} \text{d}^{-1}$ were used in the analysis. Because chemoautotrophy rates were low in August, the PCA analysis mainly analyzed the chemoautotrophic communities in March (Fig. 3b). Within the dataset, 64% of the variation was explained by the two principal axes. The first PCA axis showed a clear differentiation between station S2 on the one hand, and stations S1 and S3 on the other hand (Fig. 3b) in agreement with the sulfur oxidation regimes described above for March. Sediments from S2 showed a higher contribution of monounsaturated 16 and 18 carbon 7c fatty acids whereas sediments from S1 and S3 revealed an increased synthesis of fatty acids with iso and anti-iso 15 carbon PLFA, and saturated 14 carbon PLFA (Fig. S7c) indicating two diverging chemoautotrophic microbial assemblages. The three sediment samples from August that displayed sufficiently high activity, did not cluster in the PCA analysis and exhibited substantial variation in PLFA profiles.

4.3.6 Chemoautotrophic carbon fixation pathways

Different CO₂ fixation pathways are used by autotrophic bacteria (for detailed reviews see Berg 2011 and Hügler & Sievert 2011). The Calvin Benson-Bassham (CBB) cycle operates in many aerobic and facultative aerobic Alpha-, Beta- and Gammaproteobacteria, whereas the reductive tricarboxylic acid cycle (rTCA) operates in anaerobic or micro-aerobic members of the Delta- and Epsilonproteobacteria (amongst others). The

distribution of these two autotrophic carbon fixation pathways was studied by quantification of the abundance of *cbbL* gene (CBB pathway) and *aclB* gene (rTCA pathway) by qPCR down to 5 cm sediment depth (Fig. 4). Additionally, the diversity of *cbbL* and *aclB* gene sequences obtained from the surface sediment (0-1cm) was analyzed.

Significant differences were found between the abundance of the two genes ($p = 5.7 \times 10^{-7}$) and seasons ($p=0.002$), although not between stations (Fig. 4). The abundance of the *cbbL* gene copies was at least two-fold higher than that of the *aclB* gene in March and August in all stations ($p = 5 \times 10^{-5}$), which suggests a dominance of the CBB carbon fixation pathway in the sediments of Lake Grevelingen. In March, the depth distribution of both genes was differentiated between S2 and stations S1 and S3, in line with the previously noted segregation between geochemical fingerprints and PLFA-SIP patterns.

In March, the depth profiles of *cbbL* gene showed a similar trend in stations S1 and S3 with the gene abundance decreasing from the surface towards deeper layers, but the *cbbL* gene abundance was two-fold higher in S1 than in S3 (Fig. 4a). In line with the observed strong seasonal difference in chemoautotrophy and strong fluctuations in bottom water O_2 , the depth distribution of the *cbbL* gene in the deepest station (S1) differed between seasons ($p=0.004$), with lower gene copy abundances in the top 4 cm in August (Fig. 4a). In contrast, in the shallow station (S3) which experiences less dramatic seasonal fluctuations in bottom water O_2 , the *cbbL* gene copy number did not differ significantly between seasons ($p=0.4$), except for a sharp decrease in the top cm of the sediment. In station S2, abundance and depth distribution of *cbbL* gene copies was similar between the two seasons ($p=0.3$). All detected *cbbL* gene sequences clustered with uncultured Gammaproteobacteria clones, from the orders Chromatiales and Thiotrichales (both *cbbL1* and *cbbL2* clusters), found in intertidal sediment from Lowes Cove, Maine (Nigro & King 2007, Fig. 5a).

The abundance of the *aclB* gene significantly differed between months ($p=0.0004$) and stations ($p=0.04$). Similar depth profiles of the *aclB* gene were detected in stations S1 and S3, with subsurface maxima in deeper sediments (at 3-4 cm and 2-3 cm deep for S1 and S3 respectively, Fig. 4b). Station S2 showed the highest *aclB* gene abundance in March, which was uniformly distributed with sediment depth ($p=0.86$). In August, *aclB* gene abundance in S1 and S3 did not differ significantly from those found in March ($p=0.1$), whereas gene abundance decreased substantially in S2 ($p=9 \times 10^{-5}$). All stations showed a uniform distribution of the *aclB* gene abundance with depth in August. Bacterial *aclB* gene sequences in surface sediments (0–1 cm) of all stations were predominantly related to *aclB* sequences of Epsilonproteobacteria (Fig. 5b). Within the Epsilonproteobacteria, sequences clustered in six different subclusters and were mainly affiliated to bacteria in the order of Campylobacteriales, *i.e.* to the genera *Sulfuricurvum*, *Sulfurimonas*, *Thiovoluum*, *Arcobacter*, and macrofaunal endosymbionts. As observed for the *cbbL* gene, no clustering of sequences was observed according to station or season (Fig. 5b).

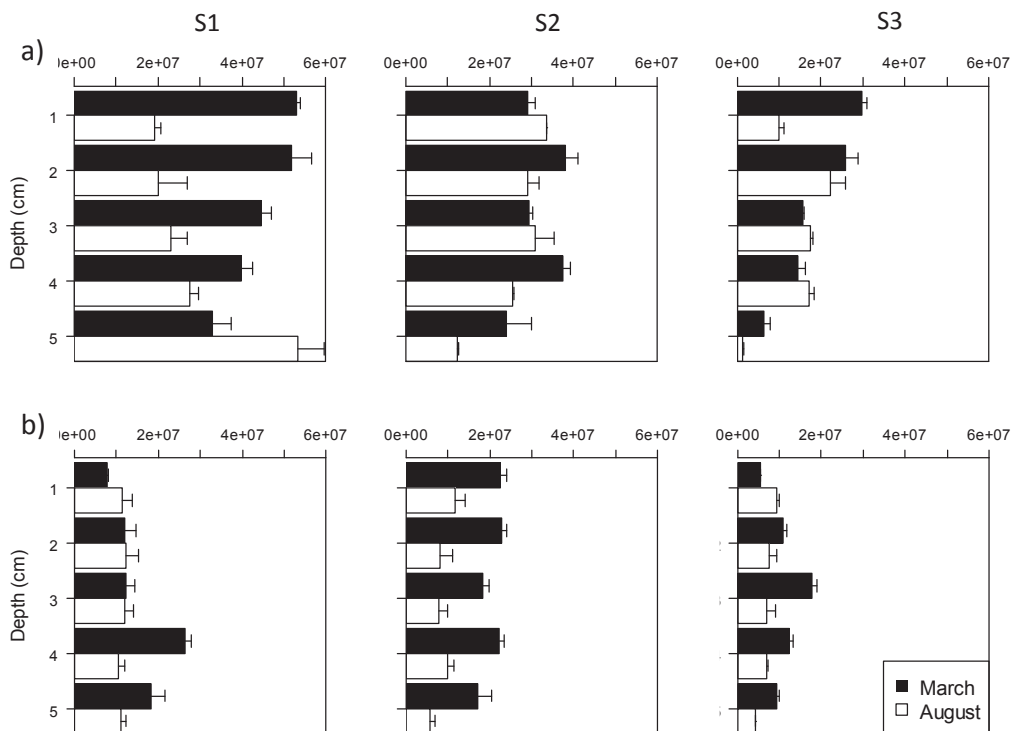


Figure 4. Abundance [copy g⁻¹] of two carbon fixation pathway genes with sediment depth [cm] for S1 (left), S2 (middle) and S3 (right) a) RuBisCO *cbbL* gene b) ATP citrate lyase *acfB* gene.

4.4 DISCUSSION

4.4.1 Seasonal shifts in the chemoautotrophy and associated bacterial assemblages

Together, our geochemical and microbiological characterization of the sediments of Lake Grevelingen indicates that the availability of electron acceptors (O₂, NO₃⁻) is an important environmental factor that controls the activity and community structure of chemoautotrophic bacterial community. In the deeper basins (S1), this electron acceptor availability changes on a seasonal basis by the establishment of summer hypoxia. In March, when the bottom waters had high oxygen levels, the chemoautotrophy rates were substantially higher than in August, when oxygen in the bottom water was depleted to low levels (Table 1). Moreover, in August, the chemoautotrophy rates showed a clear decrease with water depth, in line with the decrease of the bottom water oxygen concentration with depth (Table 1).

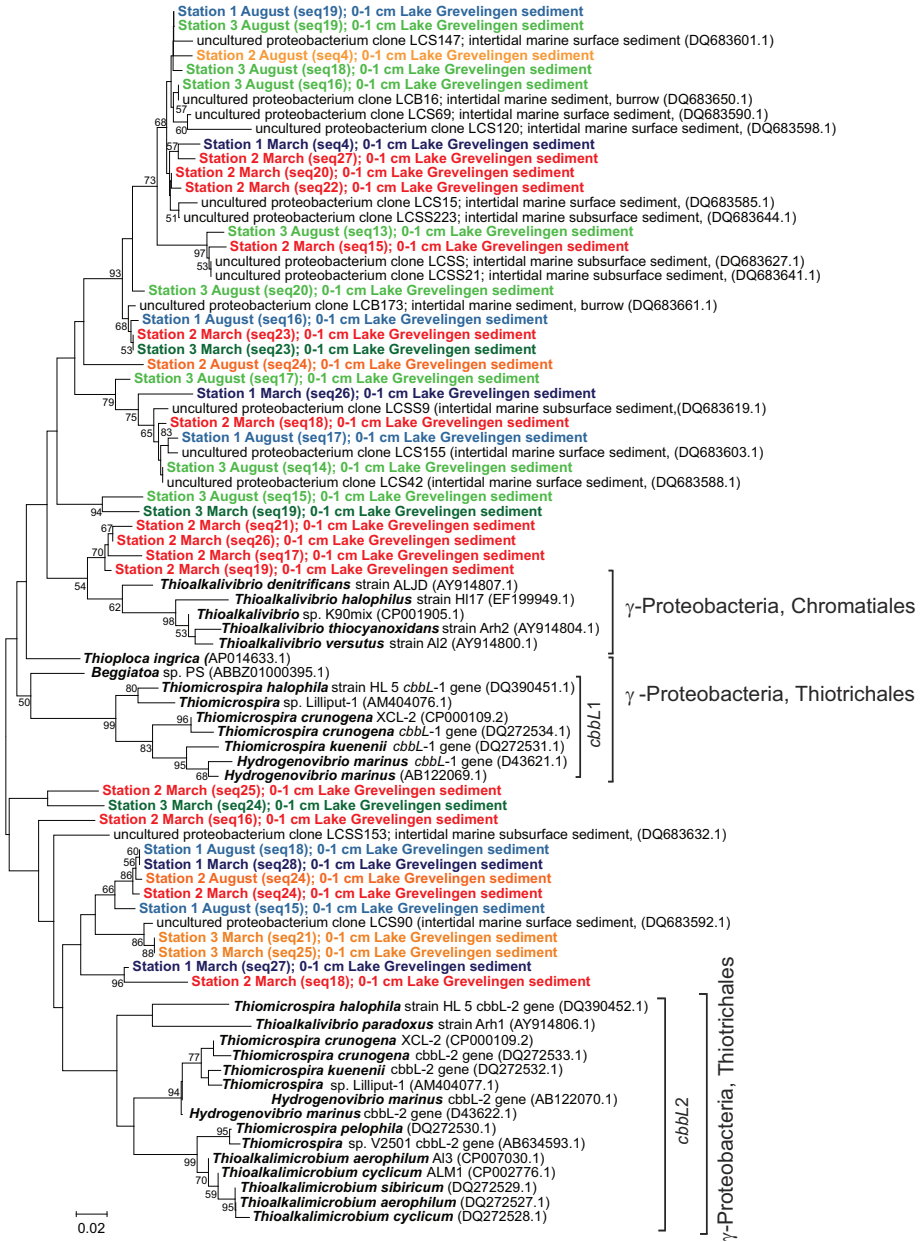
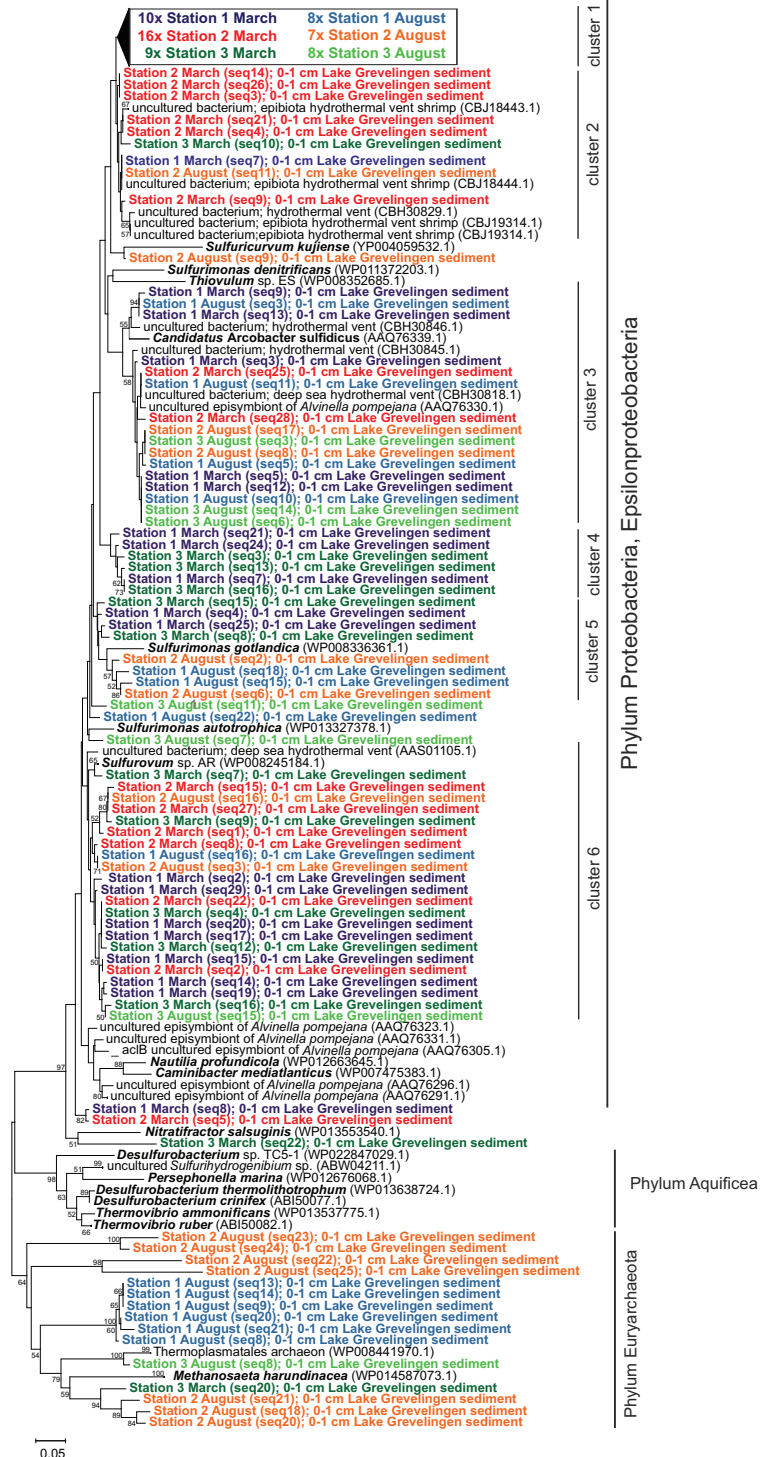


Figure 5. Phylogenetic tree (amino acid-based) of *cbbL* gene a) and *cbbL2* gene b) sequences retrieved in this study (S1, S2 and S3) and closest relatives (red: S1 March 2012; blue: S2 March 2012; orange: S3 March 2012; purple: S1 August 2012; green: S2 August 2012; brown: S3 August 2012). The scale bar indicates 2% a) and 5% b) sequence divergence.



The 16S rRNA gene amplicon sequencing analysis of our study reveals an associated response of the sulfur-oxidizing chemoautotrophic bacterial community in sediments of Lake Grevelingen to the seasonal changes in bottom water oxygen (Fig. 2). In March, when oxygen concentrations in the bottom water are high, the microbial community in the top centimeter at all three stations was characterized by Epsilon- and Gammaproteobacteria that are known chemoautotrophic sulfur-oxidizers (e.g. capable of oxidizing sulfide, thiosulfate, elemental sulfur and polythionates) using oxygen or nitrate as electron acceptor (Sorokin et al., 2001; Campbell et al., 2006; Takai et al., 2006; Labrenz et al., 2013; Kojima & Fukui 2003; Mußmann et al., 2003; Dobrinski et al., 2005; Salman et al., 2011). In August, the lack of electron acceptors (oxygen and nitrate) in the bottom water is accompanied by a decrease in the relative abundance of these Gammaproteobacteria. At the same time, there is a relative increase in the top centimeter of reads related to the Desulfobacteraceae family, and in particular, we observed a shift in the microbial community structure towards sulfate reducing bacteria from the genera *Desulfococcus* and *Desulfosarcina*. In coastal sediments, these genera are characteristic for deeper sediment layers experiencing anaerobic mineralization (Llobet-Brossa et al., 2002; Miyatake 2011; Muyzer & Stams 2008), and thus, they are not unexpected in surface sediments during strongly hypoxic (S2) and anoxic (S1) conditions encountered in August 2012. PLFA patterns further confirm the seasonal difference in the bacterial community (Fig. 3a), with more PLFA related to aerobic metabolism in March (*i.e.* 16:1 ω 7c and 18:1 ω 7c; Vestal & White 1989) as opposed to more PLFA related to anaerobic pathways in August (*i.e.* ai15:0, i17:1 ω 7c, 10Me16:0; Taylor & Parkes 1983; Boschker & Middelburg 2002; Edlund et al., 1985). However sediments below the OPD in March show more similar PLFA patterns as the sediments in August, indicating that anaerobic metabolisms such as sulfate reduction prevail in deeper anoxic sediments in March.

4.4.2 Activity and diversity of chemoautotrophic bacteria in spring

Although the availability of soluble electron acceptors (O_2 , NO_3^-) in the bottom water is important, our data show that it cannot be the only structuring factor of the chemoautotrophic communities. In March 2012, the three stations examined all experienced similar bottom water O_2 and NO_3^- concentrations (Table 1), but still substantial differences were observed in the chemoautotrophic communities (Fig. 3b) as well as in the depth distribution of the chemoautotrophy in the sediment (Fig. 1c). We attribute these differences to the presence of specific sulfur oxidation mechanisms that are active in the sediments of Lake Grevelingen (Seitaj et al., 2015). In March 2012, two separate sulfur oxidation regimes were active at the sites investigated: sites S1 and S3 were impacted by electrogenic sulfur oxidation by cable bacteria, while site S2

was dominated by sulfur oxidation via nitrate-storing *Beggiatoaceae*. Each of these two regimes is characterized by a specific sulfur-related microbial community and particular depth distribution of the chemoautotrophy. We now discuss these two regimes separately in more detail.

Cable bacteria

In March, stations S1 and S3 (Fig. 1a) showed the geochemical fingerprint of electrogenic sulfur oxidation (e-SOx) consisting of a centimeter-wide suboxic zone that is characterized by acidic pore waters ($\text{pH} < 7$) (Nielsen et al., 2010; Meysman et al., 2015). Electrogenic sulfur-oxidation is attributed to the metabolic activity of cable bacteria (Pfeffer et al., 2012), which are long filamentous bacteria that extend centimeters deep into the sediment (Schauer et al., 2014). The observed depth-distribution of cable bacteria at S1 and S3 (Fig. 1b) was congruent with the observed geochemical fingerprint of e-SOx. Cable bacteria couple the oxidation of sulfide in deeper layers to the reduction of oxygen near the sediment-water interface, by conducting electrons along their longitudinal axis (long-distance electron transport). Note that stations S1 and S3 also contained *Beggiatoa* filaments, even though these attained low biovolumes and were only found at certain depths, suggesting that they did not play a significant role in sulfur oxidation.

When e-SOx is present in the sediment (sites S1 and S3 in March), the chemoautotrophic activity penetrates deeply into the sediment and is evenly distributed throughout the suboxic zone (Fig. 1c). These field observations confirm previous laboratory results, in which cable bacteria developed in homogenized sediments, and a highly similar depth pattern of deep chemoautotrophy was noted (Chapter 3). This deep dark carbon fixation is surprising in two ways. Firstly, chemoautotrophy is generally dependent on reoxidation reactions, but there is no transport of oxygen or nitrate to centimeters depth in these cohesive sediments, and so the question is how chemoautotrophic reoxidation can go on in the absence of suitable electron acceptors. Secondly, although cable bacteria perform sulfur oxidization, a recent study has shown that cable bacteria are likely not responsible for the deep CO_2 fixation, as they have a heterotrophic metabolism (Chapter 3).

To reconcile these observations, it was proposed that in sediments with e-SOx, heterotrophic cable bacteria can form a sulfur-oxidizing consortium with chemoautotrophic Gamma- and Epsilonproteobacteria throughout the suboxic zone (Chapter 3). The results obtained here provide various lines of evidence that support the existence of such a consortium. The PLFA-SIP patterns in S1 and S3 (Fig. 3b) showed a major ^{13}C -incorporation in PLFA associated to sulfur-oxidizing Gamma- and Epsilonproteobacteria throughout the top 5 cm of the sediment (Inagaki et al., 2003; Donachie et al., 2005; Zhang et al., 2005;

Takai et al., 2006). In addition, the depth profiles of genes involved in dark CO₂ fixation (Fig. 4) revealed chemoautotrophic Gammaproteobacteria using the CBB cycle as well as Epsilonproteobacteria using the rTCA cycle, which confirms the potential dark carbon fixation by both bacterial groups deep in the sediment. The higher abundance of *cbbL* genes in S1 compared to S3 indicates a greater potential for Gammaproteobacteria, which may explain the two-fold higher total chemoautotrophy rate encountered in S1. Moreover, the peak in *aclB* gene abundance found in deeper sediment suggests that Epsilonproteobacteria could play an important role in sulfur oxidation in the deeper suboxic zone in both stations. Clearly, a consortium could sustain the high rates of chemoautotrophy throughout the suboxic zone, however the question still remains as to how the Gamma- and Epsilonproteobacteria are metabolically linked to the cable bacteria.

One hypothesis is that the chemoautotrophic Gamma- and Epsilonproteobacteria use the cable bacteria network as an electron acceptor (Chapter 3) while accessing sulfide in the suboxic zone produced through the dissolution of FeS caused by the low pH produced by e-SO_x or produced by sulfate reduction (Risgaard-Petersen et al., 2012; Fig. 6). A second hypothesis is that the metabolic connection goes through an intermediate sulfur compound such as elemental sulfur or thiosulfate: cable bacteria oxidize free sulfide to this intermediate, which is then further oxidized to sulfate by the consortium members (Fig. 6). Overall, we hypothesize that this diverse group of chemoautotrophic bacteria in the presence of cable bacteria suggests a complex niche partitioning between these sulfur-oxidizers (Gamma-, Epsilon-, and Deltaproteobacteria). In marine sediments, Gammaproteobacteria have been proposed to thrive on free sulfide, whereas Epsilonproteobacteria use elemental sulfur, and Deltaproteobacteria perform S⁰-disproportionation (Pjevac et al., 2014) possibly linked to the different sulfur oxidation pathways used by each group (Yamamoto & Takai 2011).

Nitrate-storing Beggiatoaceae

Nitrate-storing *Beggiatoa* filaments move through the sediment transporting their electron acceptor (intracellular vacuoles filled with high concentrations of NO₃⁻) into deeper sediment and electron donor (intracellular granules of elemental sulfur) up to the surface, and in doing so, they oxidize free sulfide to sulfate in a two-step process that creates a wide suboxic zone (Sayama et al., 2005; Seitaj et al., 2015; Fig. 6). In March, the microsensor depth profiles at S2 (Fig. 1a) revealed a cm-thick suboxic zone with a subsurface pH minimum at the OPD followed by a pH maximum at SAD, which is the characteristic geochemical fingerprint of sulfur oxidation by nitrate-storing *Beggiatoa* (Seitaj et al., 2015; Sayama et al., 2005). At the same time, microscopy revealed high biovolumes of *Beggiatoaceae* that were uniformly distributed throughout the suboxic zone (Fig. 1b), thus corroborating the information obtained from the geochemical fingerprint.

The chemoautotrophy depth profile at S2 in March (Fig. 1c) recorded higher activities in the top 1 cm and chemoautotrophic activity penetrated down to 2 cm (at the SAD). The alignment of depth distribution of Beggiatoaceae and chemoautotrophic activity suggest that CO₂ fixation was carried out by the nitrate-storing Beggiatoaceae themselves. *Beggiatoa* can indeed grow as obligate or facultative chemoautotrophs depending on the strain (Hagen & Nelson 1996). The PLFA-SIP analysis further supported chemoautotrophy by Beggiatoaceae as the PLFA patterns obtained at S2 resembled those of *Beggiatoa* mats encountered in sediments associated with gas hydrates (Zhang et al., 2005).

However, the CO₂ fixation by *Beggiatoa* could be complemented by the activity of other chemoautotrophs. Beggiatoaceae have previously been reported to co-occur with chemoautotrophic nitrate reducing and sulfur oxidizing Epsilonproteobacteria (*Sulfurovum* and *Sulfurimonas*) in the deep sea Guyamas basin (Bowles et al., 2012). Interestingly, station S2 in March showed the highest abundance of *acI*B gene copies of all stations and seasons (Fig. 4b), and in addition, it also had the highest relative percentage of 16S rRNA gene read sequences assigned to the Epsilonproteobacteria (Fig. 2). Therefore, the dark carbon fixation at station S2 is likely caused by both the motile, nitrate-storing Beggiatoaceae as well as the sulfur-oxidizing Epsilonproteobacteria. Yet, as was the case of the cable bacteria above, the metabolic link between Beggiatoaceae and the Epsilonproteobacteria remains currently unknown. One option is that Beggiatoaceae are transporting nitrate to deeper layers, and that this nitrate is somehow released to the pore water (e.g. by mortality and rupture which leaks nitrate out of the *Beggiatoa* filaments), after which the Epsilonproteobacteria can utilize the nitrate. Overall, the chemoautotrophic community associated with nitrate-storing Beggiatoaceae deserves additional study.

Clear differences in the chemoautotrophic community structure between S2 and the other two stations (S1 and S3) are additionally observed in the PLFA-SIP profiles (Fig. 3b). In particular, stations S1 and S3 showed an increase in the contribution of specific biomarkers linked to sulfate reducing Deltaproteobacteria (Taylor & Parkes 1983; Webster et al., 2006; Chapter 2). Deltaproteobacteria such as *Desulfobacterium autotrophicum* and *Desulfocapsa* sp., as identified by 16S rRNA gene sequencing, are known to grow as chemoautotrophs by performing H₂ oxidation or S⁰-disproportionation (Finster et al., 1998; Böttcher et al., 2005; Fig. 6), and are important contributors to the chemoautotrophic activity in coastal sediments (Thomsen & Kristensen 1997, Chapter 2). However, a further identification of the chemoautotrophic Deltaproteobacteria through the functional genes related to carbon fixation pathways was not performed in this study. Although it is known that autotrophic Deltaproteobacteria mainly use the reductive acetyl-CoA pathway (see Hügler 2011 for review), further development of the functional gene approach is necessary to determine and clarify the diversity of Deltaproteobacteria involved in the chemoautotrophic activity.

4.4.3 Activity and diversity of chemoautotrophic bacteria in summer

In August, when the O₂ levels in the bottom water were low, a third geochemical regime was observed at all stations, which was different from the regimes associated with cable bacteria or nitrate-storing *Beggiatoa*. The microsensor profiling revealed an upward diffusive transport of free sulfide, produced in deeper sediment horizons through sulfate reduction (Fig. 1a). This resulted in a uniform decrease in pH with depth, which is consistent with sediments dominated by sulfate reduction (Meysman et al., 2015). As noted above, the chemoautotrophy rates showed a close relation with the bottom water oxygen concentration. The number of gene copies of the two carbon fixation pathways investigated (CBB and rTCA) also decreased under hypoxic conditions (Fig. 4), suggesting a strong dependence of subsurface chemoautotrophy on the availability of oxygen in bottom waters.

The highest chemoautotrophy rate was recorded at the shallower station (S3) which still had substantial O₂ in the bottom water (Table 1), thus supporting sulfur oxidation at a shallow oxic-sulfidic interface in the sediment (canonical sulfur oxidation *sensu* Meysman et al., 2015). Several studies have shown that chemoautotrophy ceases in the absence of oxygen in the overlying water column (Thomsen & Kristensen 1997; Miyatake 2011; Chapter 3). Such full anoxia occurred in the deepest station (S1), but still limited chemoautotrophic activity was recorded in the top layer of the sediment. A possible explanation is that some residual aerobic sulfur oxidizing bacteria were supported by the very low oxygen levels as recorded in our incubations. However, Seitaj et al., (2015) showed that cable bacteria activity at S1 in spring leads to a buildup of FeOOH in the top of the sediments, which prevents sulfide diffusion to the bottom water during anoxia in summer ($3\text{H}_2\text{S} + 2\text{FeOOH} \rightarrow 2\text{FeS} + \text{S}^0 + 4\text{H}_2\text{O}$). The elemental sulfur formed in this reaction may support chemoautotrophic sulfur disproportionating bacteria (Finster et al., 1998). At station S2, *Beggiatoa* filaments were found forming a mat at the sediment surface in S2 (Fig. 1b) and chemoautotrophy rates were limited to this mat. *Beggiatoaceae* can survive hypoxic periods by using stored nitrate as electron acceptor (Schulz & Jørgensen 2001) which is thought to be a competitive advantage that leads to their proliferation in autumn in S1 (Seitaj et al., 2015). Such survival strategies may be used to produce energy for maintenance rather than growth under hypoxic conditions which would in combination with the low oxygen concentrations explain the low chemoautotrophy to biovolume ratio observed in S2 in August compared to March.

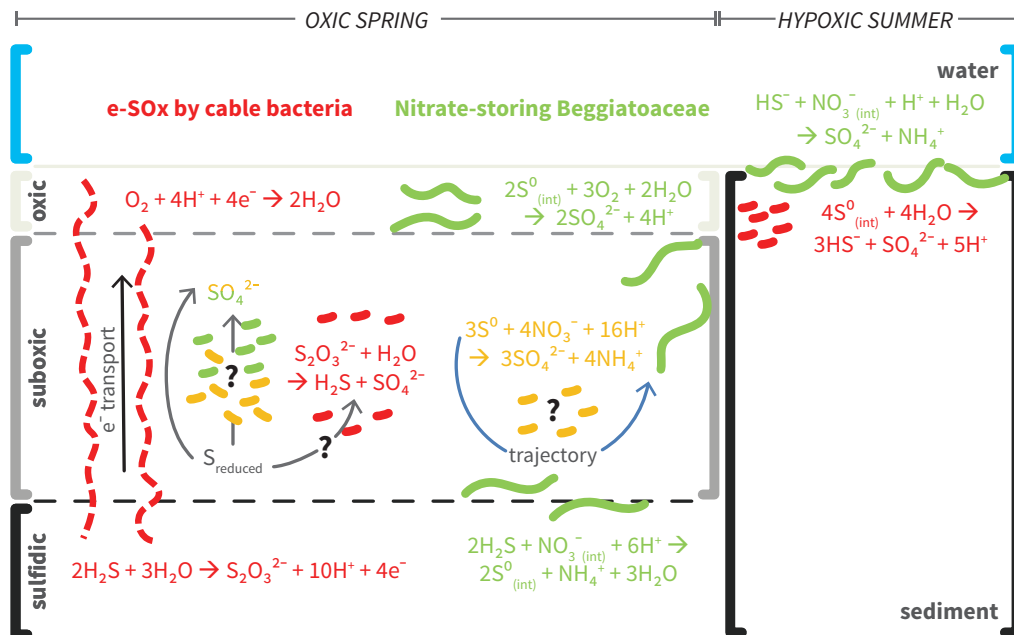


Figure 6. Schematic representation of the main sulfur oxidation mechanisms by chemoautotrophic bacteria under oxic conditions in spring and hypoxic conditions in summer in marine Lake Grevelingen. Single-cell and filamentous sulfur-oxidizing bacteria are shown as follows, yellow: Epsilonproteobacteria, green: Gammaproteobacteria, red: Deltaproteobacteria. Grey arrows represent possible reoxidation processes by chemoautotrophic bacteria and the color of the reaction indicates the bacterial group involved. Blue arrow indicates the trajectory of Beggiatoaceae (thick green lines) from the surface to the sulfide horizon and back up to the surface. Black arrow indicates the long-distance electron transport by cable bacteria (red broken lines).

4.5 CONCLUSION

In conclusion, the sediments of Lake Grevelingen harbors a great potential for chemoautotrophic activity given the high sulfide production rates in these organic rich sediments that is however strongly affected by summer hypoxia. This results in a diverse community of chemoautotrophic bacteria in the sediment. Niche partitioning between sulfur-oxidizing Gamma-, Epsilon- and Deltaproteobacteria is hypothesized to be driven by the availability of sulfur species (H_2S , S^0 , $S_2O_3^{2-}$, FeS) and electron acceptors (O_2 , NO_3^- ; Pjevac et al., 2014; Macalady et al., 2008; Grünke et al., 2011). In addition, the amount of dark carbon fixed, the depth distribution of chemoautotrophy as well as the structure of chemoautotrophic bacteria appears to be strongly dependent on specific sulfur oxidation regimes, characterized by dense populations of specific groups of filamentous sulfur oxidizing bacteria (cable bacteria or

nitrate-accumulating Beggiatoaceae). These keystone sulfur oxidizing bacteria seem to act as true microbial ecosystem engineers that strongly influence the chemical environment of the sediment, and thereby have a large impact on the microbial community structure. There seems to be close metabolic interactions between filamentous sulfur-oxidizers and the co-occurring chemoautotrophic community, but the actual mechanisms of these interactions remain presently unresolved, and require further study. An in depth study on the availability of different sulfur species in the sediment in relation to the presence of cable bacteria and Beggiatoaceae could shed light on these interactions. These tight metabolic relationships may ultimately regulate the cycling of sulfur, carbon and even nitrogen in Lake Grevelingen and in similar seasonally hypoxic sediments.

ACKNOWLEDGMENTS

WE THANKFULLY ACKNOWLEDGE THE CREW OF THE R/V LUCTOR (PETER COOMANS AND MARCEL KRISTALIJN) AND PIETER VAN RIJSWIJK FOR THEIR HELP IN THE FIELD DURING SEDIMENT COLLECTION, MARCEL VAN DER MEER AND SANDRA HEINZELMANN FOR SUPPORT ONBOARD AND ASSISTANCE WITH INCUBATIONS, PETER VAN BREUGEL AND MARCO HOUTEKAMER FOR THEIR ASSISTANCE WITH STABLE ISOTOPE ANALYSIS, AND ELDA PANOTO FOR TECHNICAL SUPPORT. THIS WORK WAS FINANCIALLY SUPPORTED BY SEVERAL GRANTS FROM DARWIN CENTRE FOR BIOGEOSCIENCES TO HTSB (GRANT NO: 3061), LV (GRANT NO: 3062) AND FJRM (GRANT NO: 3092), F.J.R.M. RECEIVED FUNDING FROM THE EUROPEAN RESEARCH COUNCIL UNDER THE EUROPEAN UNION'S SEVENTH FRAMEWORK PROGRAMME (FP7/2007-2013) VIA ERC GRANT AGREEMENT N° [306933], AND RS RECEIVED SUPPORT FROM DANISH COUNCIL FOR INDEPENDENT RESEARCH-NATURAL SCIENCES.

4.6 SUPPLEMENTARY INFORMATION

4.6.1 Materials & Methods

Aeration of ¹³C- incubations

To maintain the low oxygen levels found in August at S2 and S3, 30 ml of *in situ* overlying water was removed and cores were closed with rubber stoppers. Headspace was then flushed with N₂ through a needle inserted between the core liner and the rubber stopper without disturbing the water surface. After several minutes, N₂ flushing was stopped and 10 and 35% of the headspace was replaced with air using a syringe for S2 and S3, respectively. No air was added to S1 cores. All cores were gently mixed (0.2 rpm) on a shacking plate to homogenize oxygen concentration in headspace with those in overlying water. At the end of the experiment oxygen saturation in overlying water were verified with oxygen optodes (PreSens Fibox 3 LCD) obtaining anoxic conditions for S1 (0–4% air saturation), hypoxic for S2 (20–26%) and S3 (35–80%).

PLFA nomenclature

The shorthand nomenclature used for phospholipid derived fatty acids is as follows. The number before the colon indicates the number of carbon atoms, while the number after represents the number of double carbon bonds in the fatty acids chain. The position of the initial double bond is then indicated by the last number after the number of carbons from the methyl end (ω). The double bond geometry is designated by cis (c) or trans (t). Methyl branching (Me) is described as being in the second carbon iso (i), third carbon anteiso (a) or a number followed by Me is used to indicate the position relative to the carboxyl end (e.g. 10Me16:0). Further details can be found in Vestal & White (1989).

PCR 16S rRNA gene amplicon library preparation for pyrosequencing and analysis

PCR reactions were performed with the universal (Bacteria and Archaea) primers S-D-Arch-0519-a-S-15 (5'-CAG CMG CCG CGG TAA-3') and S-D-Bact-785-a-A-21 (5'-GAC TAC HVG GGT ATC TAA TCC-3') (Klindworth et al., 2013) adapted for pyrosequencing by the addition of sequencing adapters and multiplex identifier (MID) sequences. To minimize bias three independent PCR reactions were performed containing: 16.3 μ L H₂O, 6 μ L HF Phusion buffer, 2.4 μ L dNTP (25 mM), 1.5 μ L forward and reverse primer (10 μ M; each containing an unique MID tail), 0.5 μ L

Phusion Taq and 2 μL DNA (6 ng/ μL). The PCR conditions were following: 98 °C, 30 s; 25 \times [98 °C, 10 s; 53 °C, 20 s; 72 °C, 30 s]; 72 °C, 7 min and 4 °C, 5 min.

The PCR products were loaded on a 1% agarose gel and stained with SYBR® Safe (Life technologies, Netherlands). Bands were excised with a sterile scalpel and purified with Qiaquick Gel Extraction Kit (QIAGEN, Valencia, CA) following the manufacturer's instructions. PCR purified products were quantified with Quant-iT™ PicoGreen® dsDNA Assay Kit (Life Technologies, Netherlands). Equimolar concentrations of the barcoded PCR products were pooled and sequenced on GS FLX Titanium platform (454 Life Sciences) by Macrogen Inc. Korea.

Samples were analyzed using the QIIME pipeline (Caporaso et al., 2010). Raw sequences were demultiplexed and then quality-filtered with a minimum quality score of 25, length between 250–350, and allowing maximum two errors in the barcode sequence. Sequences were then clustered into operational taxonomic units (OTUs, 97% similarity) with UCLUST (Edgar 2010). Reads were aligned to the Greengenes Core reference alignment (DeSantis et al., 2006) using the PyNAST algorithm (Caporaso et al., 2010). Taxonomy was assigned based on the Greengenes taxonomy and a Greengenes reference database (version 12_10) (McDonald et al., 2012; Werner et al., 2012). Representative OTU sequences assigned to the specific taxonomic groups were extracted through `classify.seqs` and `get.lineage` in Mothur (Schloss et al., 2009) by using the greengenes reference and taxonomy files.

In order to determine a more accurate taxonomic classification of the bacterial groups with high percentage of reads and known to contain members with chemotrophic metabolism, sequence reads of the order Chromatiales and Thiotrichales (Fig. S1, S2), reads of the order Desulfarculales (Fig. S3), the family of Desulfobulbaceae (Fig. S4a) and the genus *Desulfubulbus* (Fig. S4b), reads of the family Desulfobacteraceae (Fig. S5a–c), and additionally reads of the orders Campylobacteriales (Fig. S6a–d) were extracted from the dataset and added to a phylogenetic tree as described in the Experimental procedures.

FISH quantification

The minimum limits of quantification via FISH for single cells were 1.5×10^6 cells cm^{-3} , taken as the FISH count with the negative control probe NON338; a minimum of 1000 4,6-diamidino-2-phenylindole-stained cells was evaluated for this count. The FISH detection limit for cable bacteria was lower than for single cells, and was calculated to be 10 cm filament cm^{-3} (corresponding to <1 filament in 0.1 ml of sediment).

4.6.2 *Supplementary figures and tables*

Table S1. Primer pairs described in the text, PCR conditions and amplicon size used in this study.

Table S1: Primer pairs described in the text, PCR conditions and amplicon size used in this study.

Assay	Target	Primer pair	T _m [°C]	Amplicon size [b]	Reference
qPCR + PCR/cloning	<i>cbbL</i> gene	K2f (5'-ACCAACAAGCCSAAGCTSGG-3') V2r (5'-GCCTTCSAGCTTGCCSACCRC-3')	qPCR 57 PCR 62	492-495	Nigro and King, 2007
qPCR + PCR/cloning	<i>acIB</i> gene	<i>acIB</i> F (5'-TGGACHATGGTDGCHGGKGGT-3') <i>acIB</i> R (5'-ATARTTKGGBCCACCKCKTC-3')	qPCR 54 PCR 53	312	Campbell et al., 2003

PCR conditions: 95°C 5 min; 40 x [95°C 1 min, T_m 40 s, 72°C 1 min]; 72°C 5 min. qPCR conditions: 95°C 4 min; 40 x [95°C 30 s, T_m 40 s, 72°C 30 s]; 80°C 25 s.

Table S2. PCR efficiencies (E) and coefficients of determination of the quantitative PCR standard curves.

qPCR assay	target molecule	T _m [°C]	March		August	
			E [%]	R ²	E [%]	R ²
RubisCO <i>cbbL</i> gene (K2f - V2r)	DNA	57	82.0	0.988	82.2	0.999
ATP citrate lyase <i>acIB</i> gene (<i>acIB</i> F - <i>acIB</i> R)	DNA	54	71.7	0.996	70.4	0.994

qPCR conditions: 95°C 4 min; 40 × [95°C 30 s, T_m 40 s, 72 °C 30 s]; 80 °C 25 s

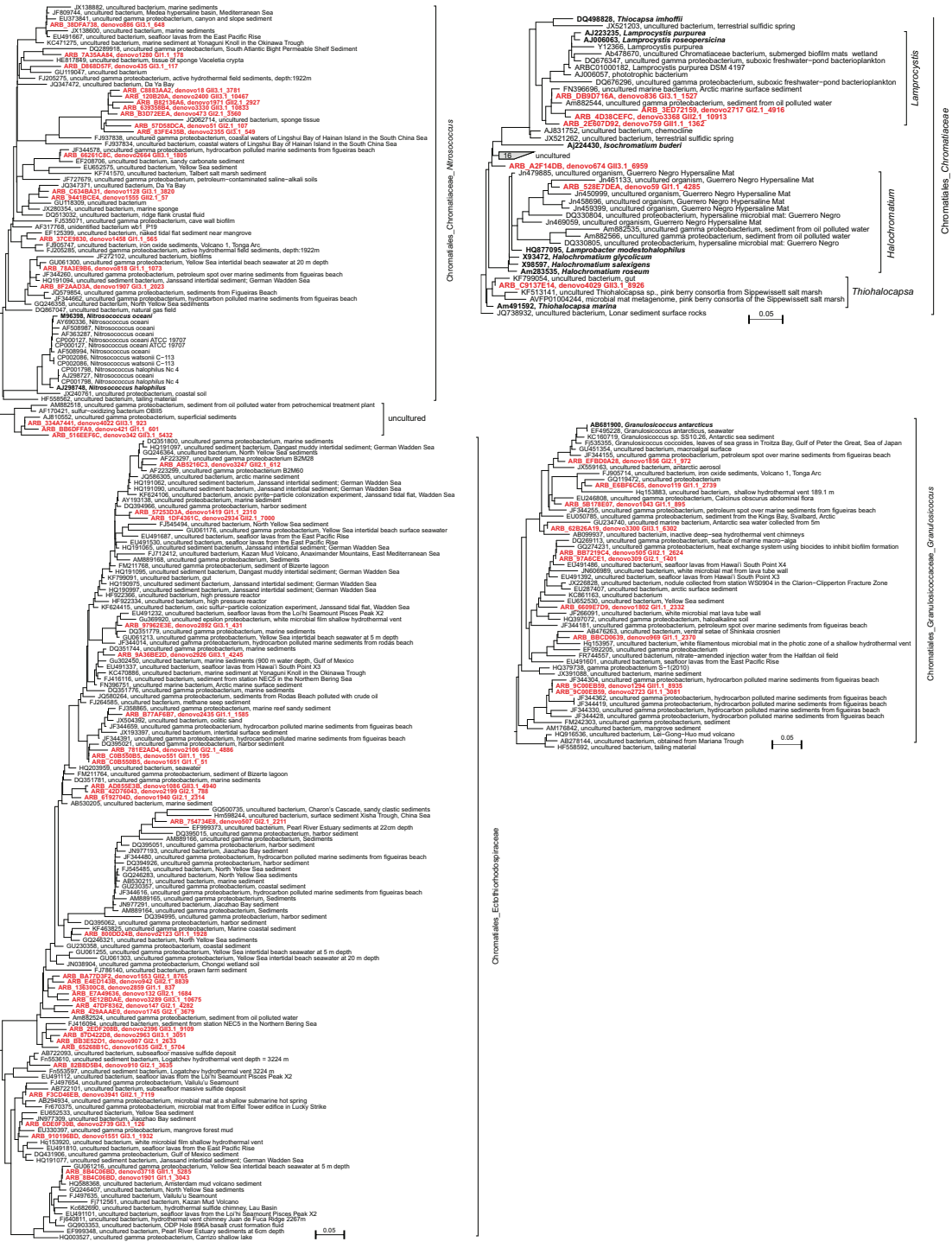


Figure S1. Gammaproteobacteria; order Chromatiales

CHEMOAUTOTROPHY IN SEASONALLY HYPOXIC SEDIMENTS

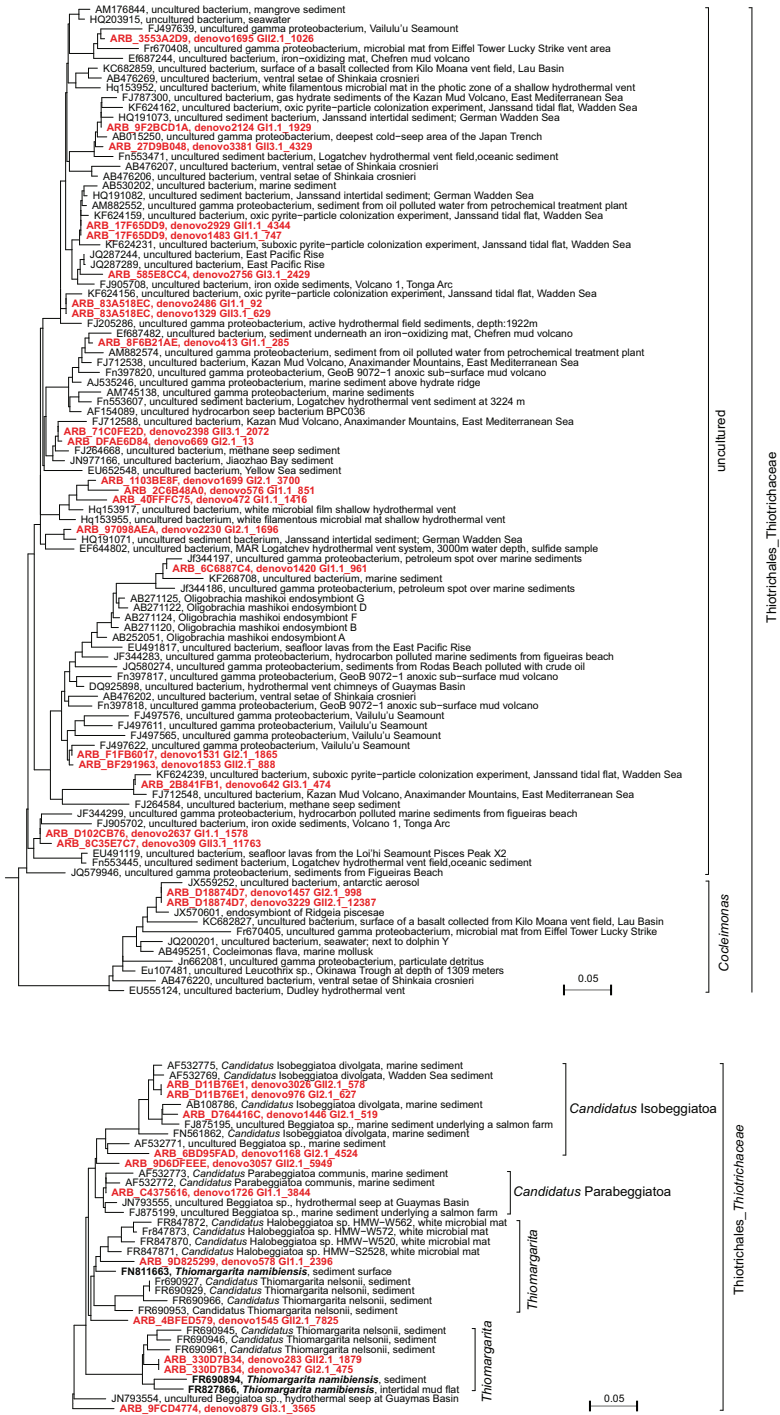


Figure S2. Gammaproteobacteria; family Thiotrichaceae

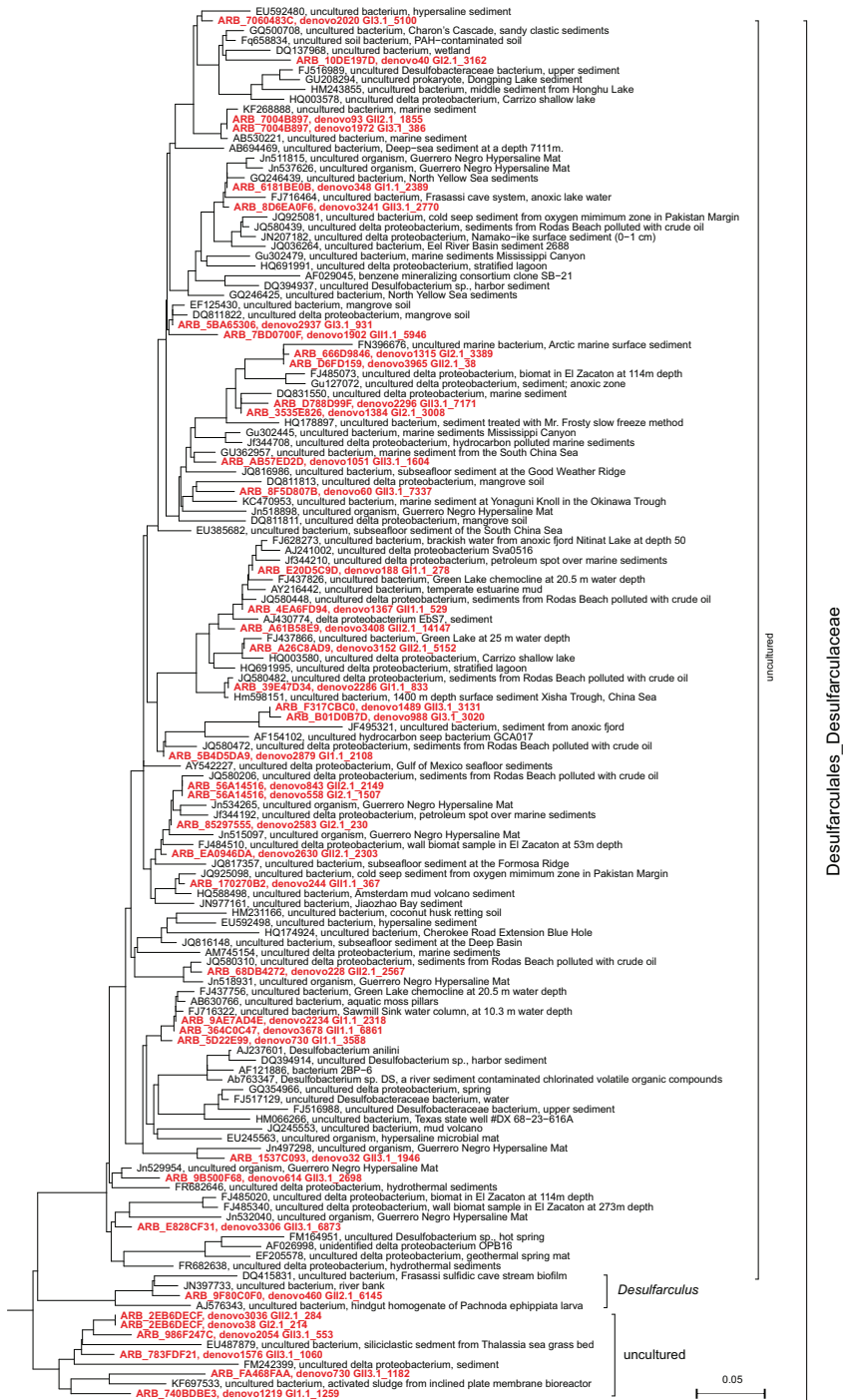


Figure S3. Deltaproteobacteria; order Desulfurales

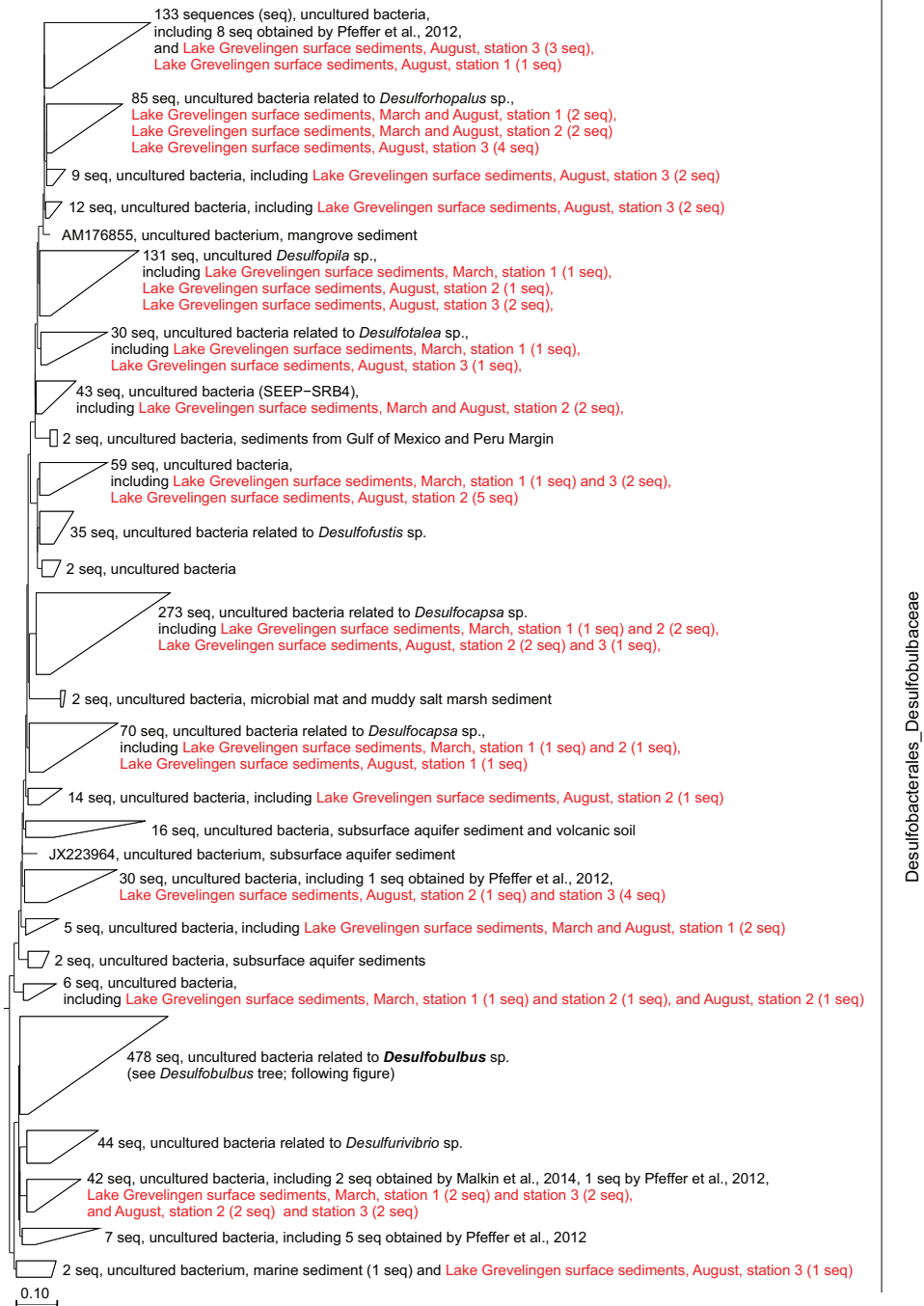


Figure S4a. Deltaproteobacteria; order Desulfubacterales, family Desulfubulbaceae



Figure S4b. Deltaproteobacteria; order Desulfobacteriales, family Desulfubulbaceae, genus *Desulfubulbus*

CHEMOAUTOTROPHY IN SEASONALLY HYPOXIC SEDIMENTS

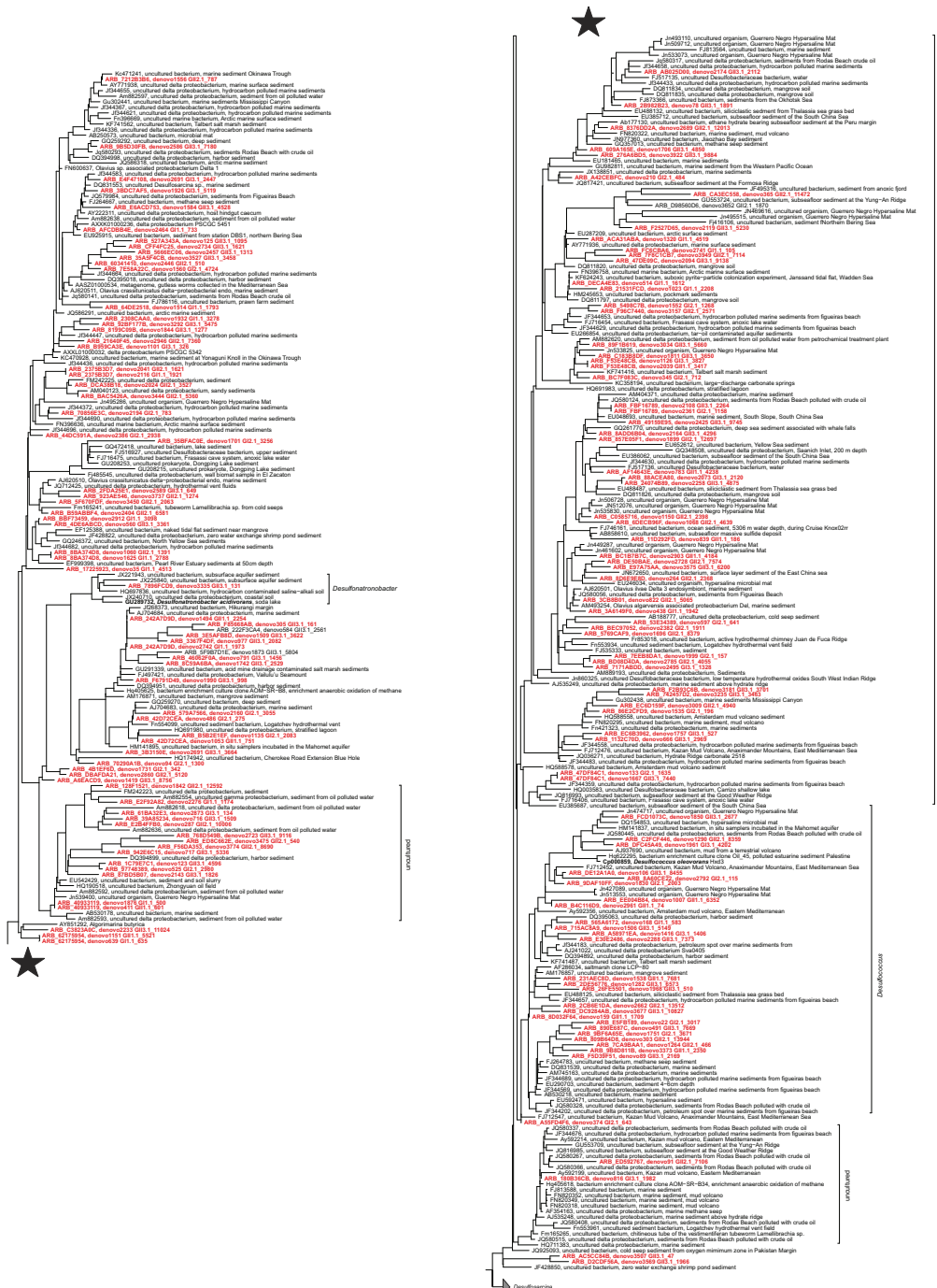


Figure S5a. Deltaproteobacteria; order Desulfobacterales, family Desulfobacteraceae

CHEMOAUTOTROPHY IN SEASONALLY HYPOXIC SEDIMENTS

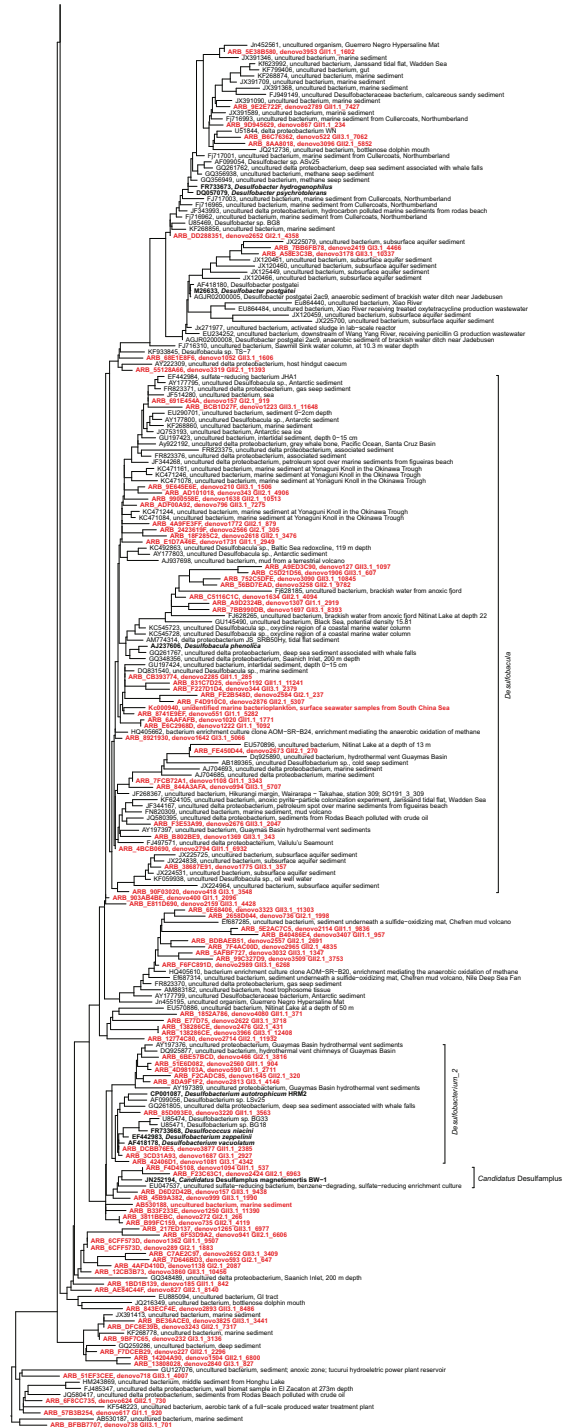
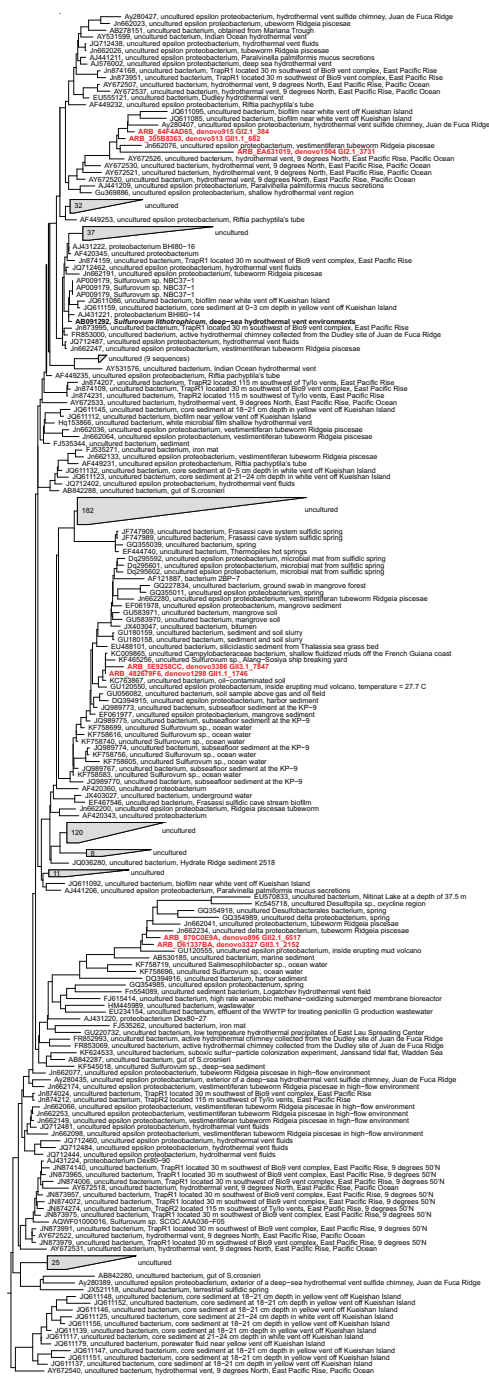


Figure S5c. Deltaproteobacteria; order Desulfobacterales, family Desulfobacteraceae



Campylobacteriales_Helicobacteraceae_Sulfurovum

Figure S6a. Epsilonproteobacteria; order Campylobacteriales, family Helicobacteraceae, genus *Sulfurovum*

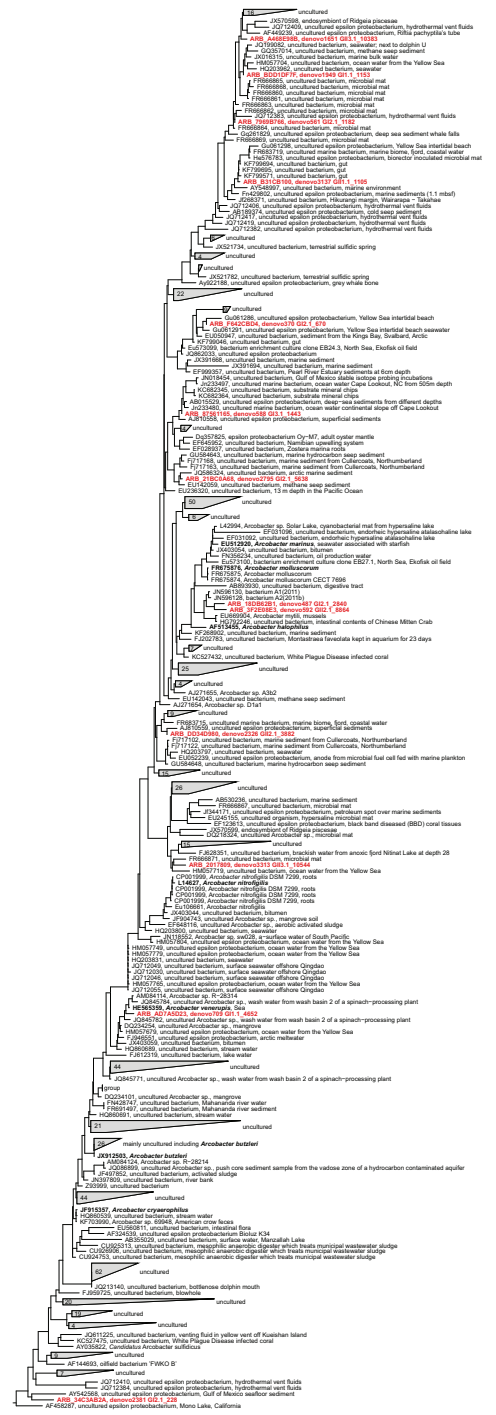


Figure S6b. Epsilonproteobacteria; order Campylobacterales, family Campylobacteraceae, genus *Acrobacter*



Figure S6c. Epsilonproteobacteria; order Campylobacterales, family Campylobacteraceae, genus *Sulfurimonas*

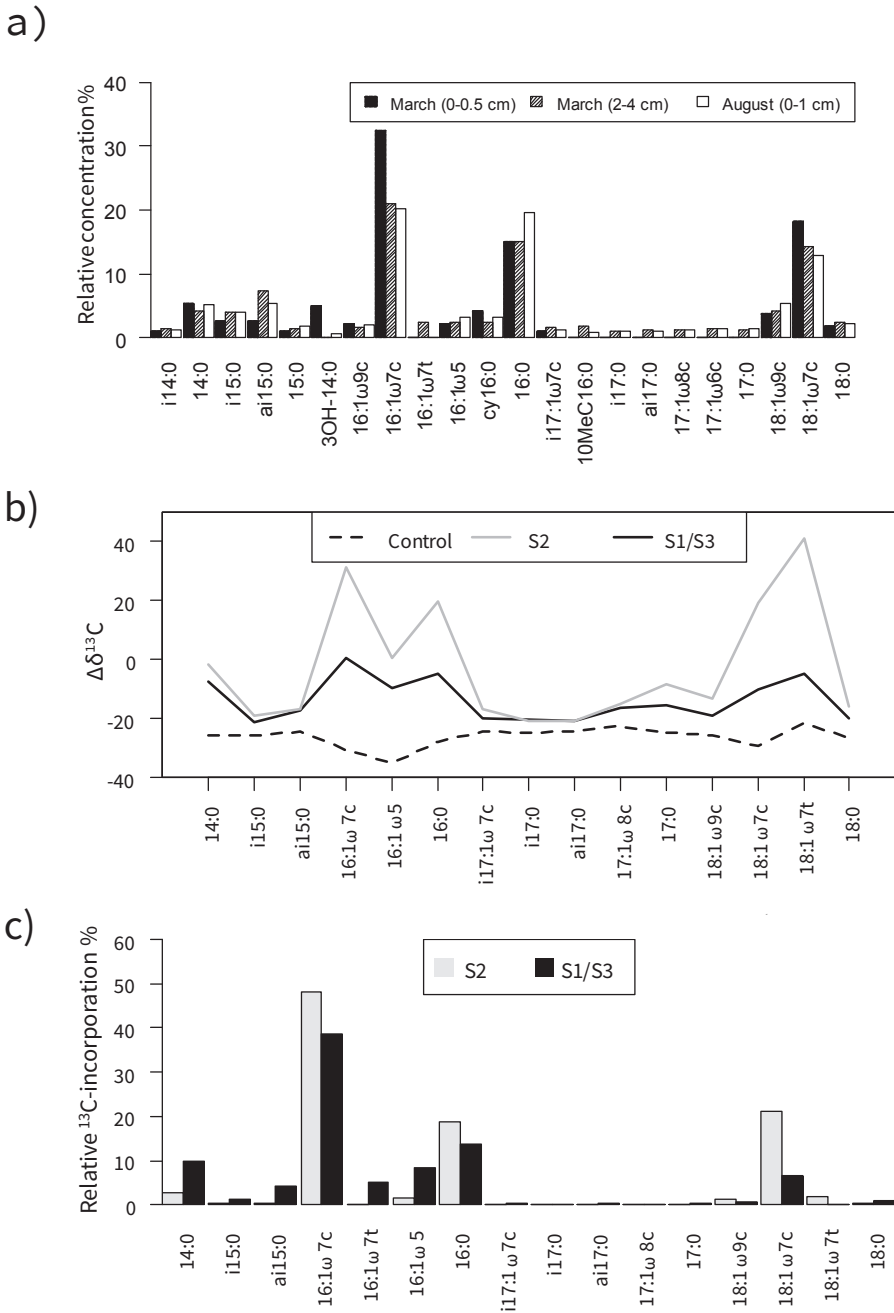


Figure S7. Characteristic PLFA profiles of a) the average relative concentration of PLFAs for March (0-0.5 cm and 2-4 cm) and August (0-1 cm), b) the average $\Delta\delta^{13}\text{C}$ values and c) relative ^{13}C incorporation of PLFAs for S2 and S1/S3 March (0-1 cm). Grouping of samples was determined by PCA analysis (see Figure 3).

DIANA VASQUEZ-CARDENAS, CINTIA ORGANO QUINTANA,
FILIP J.R. MEYSMAN, ERIK KRISTENSEN,
HENRICUS T.S. BOSCHKER

MAR. ECOL. PROG. SER. (DOI: 10.3354/MEPS11679)

*Species-specific effects of two
bioturbating polychaetes on sediment
chemoautotrophic bacteria*

ABSTRACT

Bioturbation has major impacts on sediment biogeochemistry, which can be linked to the functional traits of the macrofauna involved. *Nereis (Hediste) diversicolor* and *Marenzelleria viridis* are two functionally different bioturbating polychaetes that strongly affect the ecology and biogeochemistry of coastal sediments. However, the different effects of these polychaetes on the activity and composition of microbial communities and on chemoautotrophic bacteria have not been extensively studied. We performed experiments with sediment aquaria that contained each species separately as well as a non-bioturbated control. Bacterial communities in different sediment zones (surface, burrow, subsurface) were characterized by phospholipid derived fatty acid analysis combined with stable isotope labeling (^{13}C -bicarbonate) to quantify the dark CO_2 fixation by chemoautotrophic bacteria. Pore water chemistry ($\Sigma\text{H}_2\text{S}$ and DIC) was additionally assessed in each treatment. The strong ventilation but low bioirrigation capacity in the open-ended burrows of *N. diversicolor* resulted in enhanced aerobic chemoautotrophic activity potentially by sulfur oxidizing and nitrifying bacteria along the burrow. In contrast, slower ventilation and higher irrigation by *M. viridis* induced an advective mode of pore water transport. This promotes anaerobic chemoautotrophy around the blind-ended burrow and within the subsurface sediment. Sulfate-reducing bacteria were the dominant anaerobic chemoautotrophs that probably disproportionate sulfur. In conclusion, our analysis shows that bioturbating fauna influence the microbial community and chemoautotrophic activity in sediments, but that the effect strongly depends on the structure of the burrow and on species-specific ventilation behavior and irrigation capacity.

5.1 INTRODUCTION

Ideally, marine sediments are characterized by a predictable vertical zonation of electron donors and acceptors, but in the presence of benthic fauna this typical one-dimensional redox zonation is disturbed through particle reworking and solute transport induced by burrow formation and ventilation, a process known as bioturbation (Aller 1988; Meysman et al., 2006; Kristensen et al., 2012). Bioturbation creates steep chemical gradients along burrows, which may modify the spatial distribution of various microbial metabolic pathways such as sulfate reduction, sulfide oxidation, denitrification and nitrification (Aller 1988; Kristensen & Kostka 2005; Bertics & Ziebis 2010). The manner in which chemical gradients and subsequently microbial assemblages vary in the sediment have been linked to the functional traits of the bioturbating fauna such as burrow properties (e.g. shape, depth, and residence time), ventilation behavior, feeding habits and/or sediment mixing intensity (Marinelli et al., 2002; Papaspyrou et al., 2006; Bertics & Ziebis 2009; Laverock et al., 2010). Bioturbation therefore has a major impact on sediment biogeochemistry, which differs depending on the ecology and behavior of the macrofaunal organisms involved (Braeckman et al., 2010; Mermillod-Blondin 2011; Kristensen et al., 2014).

Nereis (Hediste) diversicolor and *Marenzelleria viridis* are two burrow-dwelling polychaetes that have contrasting effects on the ecosystem functioning of coastal areas in the Baltic Sea (Kristensen et al., 2014). Both species are surface deposit feeders, but *N. diversicolor* is also a suspension feeder (Christensen et al., 2000). In regards to bioturbation activities, both *N. diversicolor* and *M. viridis* promote limited amount of particle reworking, which consists of a random downward transport of sediment particles over short distances, known as gallery biodiffusion (Kristensen et al., 2012). However, the burrow morphology and ventilation mode (*i.e.* flushing of the burrow with oxygenated water) is strongly different between the two polychaetes, which induce distinct modes of bioirrigation (*i.e.* biologically enhanced transport of pore water and solutes) that create divergent geochemical conditions. *N. diversicolor* inhabits a mucus-lined open-ended burrow (typically U or Y shaped, up to 20 cm deep) that is regularly flushed by undulatory body movements (Kristensen & Kostka 2005). This intense burrow ventilation results in diffusion-based radial solute transport into the surrounding sediment pore water, but creates only limited advective pore water movement in the surrounding sediment (Pischedda et al., 2011; Kristensen et al., 2014). *N. diversicolor* has twice as much oxygenated sediment surrounding the burrows than *M. viridis* (5 cm³ versus 1.8 cm³ respectively) creating more oxidized conditions in deeper sediments (Kristensen et al., 2011, Jovanovic et al., 2014). In contrast, *M. viridis* creates deep burrows (up to 30 cm deep) which are typically straight down and blind-ended. *M. viridis* ventilates its burrow slowly through ciliar and muscular movements that promote advective flow of

anoxic pore water in the surrounding sediment (Kristensen et al., 2011; Jovanovic et al., 2014; Quintana et al., 2011). *M. viridis* activity therefore simultaneously maintains reduced conditions in the deeper sediment which stimulate sulfate reduction, and can potentially enhance sulfide oxidation in surface sediments given the upward flow of solutes (Quintana et al., 2007; Kristensen et al., 2011, 2014).

The distinct impacts of *N. diversicolor* and *M. viridis* on the sediment geochemistry suggest substantial differences in the bacterial community composition and function. One microbial metabolism considered to be affected by bioturbation is chemoautotrophy given the steep chemical gradients and the potential overlap of electron acceptors and donors along the burrow structure (Aller 1988; Kristensen & Kostka 2005). Burrow walls are ideal environments for chemoautotrophic bacteria which fix inorganic carbon by obtaining energy from the oxidization of reduced compounds (e.g. sulfide, ammonium) produced in the sediment. The specific effects of bioturbation on the microbial community composition have occasionally been studied (Steward et al., 1996; Papaspyrou et al., 2006; Cuny et al., 2007; Kunihiro et al., 2011), including only one study that quantified the impact on chemoautotrophic growth (Reichardt 1988). Reichardt (1988) found a substantial increase of dark CO₂ fixation along the burrow of the lugworm *Arenicola marina* when compared to the surface sediment. Therefore, we expect an enhanced chemoautotrophic activity along the burrow of *N. diversicolor* and *M. viridis* compared to the adjacent sediment. However, given the contrasting functional traits of these two polychaete species, we hypothesize that the bacterial community in these burrow environments could be species-specific. To test this hypothesis, we used phospholipid derived fatty acid analysis combined with stable isotope probing (PLFA-SIP). This approach allows simultaneous characterization of the total bacterial and chemoautotrophic community composition as well as the quantification of dark CO₂ fixation rates (Chapter 2). We also determined the effects of polychaetes on sediment pore water chemistry. The impact on chemoautotrophic activity and differences in microbial composition were then linked to the functional traits of *N. diversicolor* and *M. viridis*.

5.2 MATERIALS & METHODS

5.2.1 Experimental set up

Sediment incubations were performed consisting of three treatments: with addition of *Nereis (Hediste) diversicolor* (Nd), with addition of *Marenzelleria viridis* (Mv), and without addition of polychaetes (Control). Sediment (top 25 cm), polychaetes and overlying water for incubations were collected at Bregner Bay, Denmark (55.48118° N, 10.61002° E) in September 2012 (water depth: 50 cm, water temperature: 18°C, salinity: 20). The sediment at the sampling location has been previously described as organic-poor median sand with a porosity of 0.40±0.03 (Quintana et al., 2007;

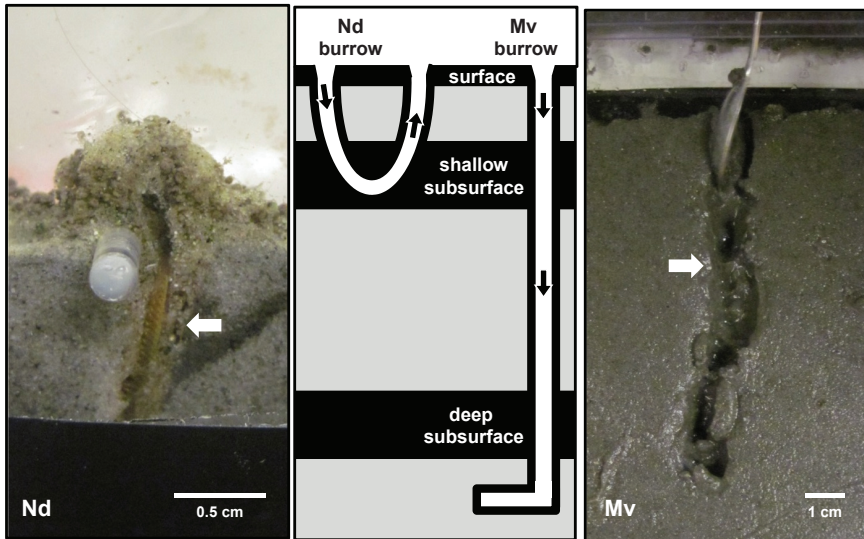


Figure 1. The left image shows *Nereis diversicolor* (Nd) and its burrow surrounded by an oxidized halo seen against the side of the flat aquarium. Right image shows the sampled burrow area of *Marenzelleria viridis* (Mv). White arrows indicate the position of the burrow structure. The central panel provides a schematic representation of the burrow geometry, burrow water flow (black arrows) and the 4 sediment zones sampled in black (burrow, surface 0-0.5 cm, shallow subsurface 2-4 cm, deep subsurface 12-14 cm).

Jovanovic et al., 2014). Sediment was gently sieved at the location through a 1 mm mesh and later homogenized in the laboratory. Active individuals of *M. viridis* and *N. diversicolor* were collected for experiments during sieving, and were kept in buckets with aerated seawater (15°C) and a thin layer of sieved sediment.

For the sediment incubations, we used flat aquaria (height: 35 cm, length: 20 cm, width: 1 cm) which had one removable side panel that was adapted with injection ports distributed on a two-dimensional grid (distance every of 2 cm between ports). Before assembling the flat aquaria, plastic foil was placed against the inside wall of the removable side panel. This decreased the disturbance of the sediment when the aquarium was opened. Ten aquaria (Nd: 3, Mv: 3, and Control: 4) were filled with homogenized sediment to obtain a ~28 cm sediment depth layer. Aquaria were wrapped in aluminum foil so that only the sediment surface was exposed to light, limiting the development of photosynthetic communities along the walls of the aquaria during incubation. Aquaria were submerged into 90 L water tanks filled with *in situ* seawater at 16 ± 2 °C and exposed to 12 h light/12 h dark cycle for 7 days. Water circulation in the flat aquaria was ensured by aerating each aquarium separately with air pumps and tubing adapted with needles.

Polychaetes were weighed and transferred to the aquaria after a 24 h settling period of the sediment. Only motile, visibly undamaged individuals were used in the experiments. Average wet weight was 0.11 ± 0.02 g for *N. diversicolor* (n=3) and 0.37 ± 0.03 g for *M. viridis* (n=3). Only one individual was added to each flat aquarium to facilitate the identification and collection of burrow sediment for further analysis. The resulting faunal densities (500 ind. m⁻²) were within the range observed in Odense Fjord of 14-3013 ind m⁻² for *N. diversicolor* and 0-1174 ind m⁻² for *M. viridis* (Delefosse et al., 2012).

5.2.2 Biomarker analysis

Six days after the addition of individual polychaetes to the flat aquaria we evaluated the effect of bioturbation on the microbial composition and chemoautotrophic activity by analyzing the phospholipid derived fatty acids combined with stable isotope probing (PLFA-SIP, Boschker et al., 1998). First, we employed PLFA fingerprinting, which allows the study of the composition and abundance of the total bacterial community. Second, the composition of the chemoautotrophic community and its activity (*i.e.* dark CO₂ fixation rate) was characterized by the incorporation of ¹³C-labeled dissolved inorganic carbon (DIC) into bacterial PLFA. A stock solution of ¹³C-sodium bicarbonate of 60 mM (99% ¹³C; Cambridge Isotope Laboratories, Andover, Ma, USA) was prepared in artificial seawater free of Ca⁺² and Mg⁺² to prevent carbonate precipitation. Shortly before use, the bicarbonate solution was bubbled with N₂ in order to remove the O₂. The line injection method (Jørgensen 1978) was used to introduce ¹³C-labeled substrate in to the sediment. The substrate was injected through the ports in the side wall of the aquaria in 20 µl aliquots from the bottom to the top. Finally, 180 µl substrate was added to the ~2 cm thick layer of overlying water. The top of the aquaria was covered with Parafilm to prevent evaporation and then returned to the water tanks (16±2 °C). The aquaria were kept elevated above the water line to prevent mixing of overlying water with tank water. Overlying water was bubbled with ¹³C-CO₂ saturated air to avoid stripping of the label from the overlying water during incubations as described in Chapter 3. Incubations were performed in the dark to exclude ¹³C-incorporation by photosynthetic micro-organisms. Two of the four Control aquaria did not receive ¹³C-substrate and were used to measure the natural abundance δ¹³C.

Stable isotope labeling was terminated after 45 h. Overlying water was removed with a syringe and the sediment surface was examined to locate burrow openings. Aquaria were then placed on their side and the lateral panel was removed. For Nd treatment more than one burrow was present, in which case only the burrow containing the polychaete was considered. The coloration of the sediment surrounding the burrow, burrow diameter and length were recorded. The burrow sediment was

defined as the 3 mm thick layer surrounding the burrow wall. In the case of *N. diversicolor* the burrow sediment also included the mucoid burrow lining. The sediment from the active burrows was collected with a sterile spatula. Organisms were carefully extracted from their burrows using pincers. The remaining sediment matrix in the aquaria was then sectioned in horizontal layers of 0.5 cm intervals in the top centimeter, followed by 1 cm intervals to 4 cm depth, and 2 cm intervals to 18 cm depth. Four sediment zones were selected to compare the effects of the burrowing activity on the PLFA fingerprint and ^{13}C -labeling of the microbial community: burrow (sampled as explained above), surface (0-0.5 cm), shallow subsurface (2-4 cm), and deep subsurface (12-14 cm, Fig. 1). Sediment was collected in pre-weighed 50 ml double centrifuge tubes and placed on ice until further processing. The bottom of the inner tube was equipped with a GF/C filter to facilitate the collection of pore water. Tubes with sediment were centrifuged at 500 g for 15 min. and pore water was collected from the outer tube while the sediment in the inner tube was frozen overnight and subsequently lyophilized.

PLFA extractions were performed on dry sediment according to Guckert et al., (1985) and Boschker et al., (1998) and analyzed by gas chromatography – isotope ratio mass spectrometry (GC-IRMS, Thermo, Germany) on an apolar analytical column (ZB5-MS Phenomenex). The precision of the GC-IRMS is $\sim 0.3\text{‰}$ $\delta^{13}\text{C}$ which corresponds to a variation in ^{13}C content of $\sim 0.0003\%$ (Boschker & Middelburg 2002). PLFA concentrations are expressed in carbon units (nmol C-PLFA g dw $^{-1}$). Total bacterial biomass was determined as the sum of the concentrations of all bacterial fatty acids (C12:0 to C20:0) converted to biomass assuming PLFA constitute 5.5% of the carbon present in the total bacterial carbon biomass (Middelburg et al., 2000). Sediment dry weight was converted to bulk sediment volume using a dry sediment density of 2.55 g dw cm $^{-3}$ and the measured sediment porosity (see Pore water analysis). Characterization of the chemoautotrophic community was based on ^{13}C -incorporation into PLFA. Briefly, PLFA ^{13}C -label incorporation (pmol ^{13}C cm $^{-3}$ of bulk sediment) is calculated as the product of each bacterial PLFA concentration and its ^{13}C fraction after labeling (corrected for natural ^{13}C fraction of unlabeled samples). Dark CO_2 fixation rates (nmol C cm $^{-3}$ d $^{-1}$) were calculated by summation of the PLFA incorporation data for each sediment sample, which was then converted to total biomass incorporation and divided by the length of the incubation period. Dark CO_2 fixation rates were corrected for $\delta^{13}\text{C}$ -DIC values in pore water relative to natural $\delta^{13}\text{C}$ -DIC. A detailed description of the PLFA-SIP calculations can be found in Boschker & Middelburg (2002).

5.2.3 Label transfer

To determine the possible grazing on chemoautotrophic bacteria, we measured the ^{13}C -labeling of the polychaetes recovered from the aquaria. Polychaetes were collected at the end of the incubation period, weighed, frozen and then lyophilized. Dried individuals were subsequently pulverized and analyzed by an elemental analyzer-isotope ratio mass spectrometer (EA-IRMS, Finnigan Delta S). Precision of the technique is in the order of $\pm 0.1\%$ $\delta^{13}\text{C}$ for carbon isotopic values. The natural carbon isotopic composition was determined for two individuals of each species taken directly from the sampling site and analyzed as described above.

5.2.4 Pore water analysis

Pore water collected from flat aquaria at the end of the incubation was analyzed for dissolved inorganic carbon (DIC) and total free sulfide ($\sum\text{H}_2\text{S} = [\text{H}_2\text{S}] + [\text{HS}^-] + [\text{S}^{2-}]$). DIC samples (0.5 ml) were collected in gas-tight vials and preserved with 30 μl of a saturated HgCl_2 solution. Total DIC and $\delta^{13}\text{C}$ -DIC were measured by the headspace technique using an EA-IRMS equipped with a gas injection port (Chapter 2). Background carbon isotopic values were analyzed on pore water in parallel samples from the two Control aquaria without ^{13}C -substrate addition. $\sum\text{H}_2\text{S}$ samples (0.5 ml) were fixed with 50 mL of a 1 M zinc acetate solution and analyzed following Cline (1969, precision of $\pm 2\%$ and sensitivity at pH 0.35 of $29.5 \times 10^3 \text{ L mole}^{-1} \text{ cm}^{-1}$). Weight loss of wet sediment subsamples after drying at 60°C for 48 h was used for porosity determination.

5.2.5 Statistical analysis

All statistical analyses were performed using the extension package CRAN: stats in the open source software R. Normal distribution (Shapiro-Wilk test) and homogeneity of variance (Barlett's test) were tested for each data set, and data were log-transformed when necessary to fulfill the assumptions of ANOVA. A two-way ANOVA (aov) was used to test the effect of polychaete treatments and sediment depths, on bacterial biomass and chemoautotrophic activity. Depth integrated pore water DIC and $\sum\text{H}_2\text{S}$ were tested with one-way ANOVA for treatment effects. Significant differences were further analyzed using a Tukey's multiple comparisons of means (TukeyHSD). Both PLFA concentrations and ^{13}C -incorporation values were expressed as a fraction of the total per sediment sample. Relative PLFA values were log-transformed as $(\log(x+1))$ and analyzed with Principal Component Analysis (prcomp) to determine differences in the microbial assemblage and within the chemoautotrophic community among layers and treatments. Only PLFAs contributing more than 0.1% to the total sediment activity were included in the PCA analysis.

5.3 RESULTS

5.3.1 *Sediment appearance*

The surface sediment in all treatments had similar appearance after 6 days of acclimatization, and consisted of a light brown surface sediment layer indicative of oxidized conditions, while the sediment below showed a dark grey coloration suggesting reduced conditions. The oxidized surface layer was ~4 mm deep in the Control, 3-4 mm in Nd, and only ~1.5 mm in the Mv sediments. However, on closer inspection, Nd and Mv sediments exhibited several physical differences. The surface sediment in Nd aquaria was loose and fluffy (indicating surface reworking) and detritus accumulations were present around burrow openings whereas surface sediment in Mv aquaria appeared more compact (Fig. 1). Sediment surrounding the burrow in the Nd aquaria had a brownish coloration similar to the oxidized surface layer (Fig. 1). Nd burrows were typically U-shaped and reached between 2 and 4 cm into the sediment. One aquarium contained one burrow, whereas the other two aquaria had several burrows, yet only the active and inhabited burrow was sampled for analysis. Each Mv aquarium had only one burrow, which was straight, penetrating up to 18 cm deep and had a similar grey coloration as the subsurface sediment (Fig. 1). One of the three Mv aquaria was discarded because the worm was found outside of the aquarium at the end of the incubation. The burrows of *N. diversicolor* and *M. viridis* both had an average burrow diameter of 3 mm.

The porosity ranged from 0.31 to 0.47 between treatments and depths, with an overall mean depth-integrated porosity value of 0.39 ± 0.05 which was in agreement with previous analyses of the same sediment (Quintana et al., 2007; Jovanovic et al., 2014).

5.3.2 *Total bacterial community*

Surface, burrow, and two subsurface depths (shallow and deep) were examined using phospholipid-derived fatty acid (PLFA) analysis. A total of 39 PLFA were identified of which 29 were considered as bacterial biomarkers. The PLFA not used in our data analysis were polyunsaturated fatty acids (PUFA) that are considered to be eukaryote biomarkers (Vestal & White 1989). These PUFAs were mostly present in the surface samples and accounted for 6% of the total PLFA. A subset of 14 out of 29 bacterial fatty acids represented more than 90% of the total bacterial biomass per sample (Fig. 2). Major bacterial PLFAs were 16:1 ω 7c (25 \pm 0.3%), 18:1 ω 7c (22 \pm 0.9%), 16:0 (19 \pm 0.6%), 18:1 ω 9c (5 \pm 0.2%), 14:0 (5 \pm 0.3%), ai15:0 (4 \pm 0.3%), 16:1 ω 7t (2 \pm 0.9%), i15:0 (2 \pm 0.1%), and 18:0 (2 \pm 0.1%), whereas minor fatty acids (1-2%) included 15:0, 16:1 ω 5, 17:1 ω 8c, 17:1 ω 6c and 17:0.

Table 1. Bacterial biomass and chemoautotrophy rates (mean±SD) for the different treatments and sediment depths studied. Number of replicates is stated in parenthesis next to the treatment code: Control: no bioturbation, Nd: *Nereis diversicolor*, Mv: *Marenzelleria viridis*, na: not applicable, nd: not detected. Ranges are stated when there were only 2 replicates.

	Bacterial biomass $\mu\text{mol C cm}^{-3}$			Chemoautotrophy rates $\text{nmol C cm}^{-3} \text{d}^{-1}$		
	Control (4)	Nd (3)	Mv (2)	Control (2)	Nd (3)	Mv (2)
Surface	20 ± 8	15 ± 2	13-16	43-145	49 ± 9	52-76
Burrow	na	13 ± 4	9-12	na	59 ± 68	10-11
Shallow subsurface	11 ± 2	9 ± 1	9-11	1.6-1.9	2 ± 0.3	3.6-4.0
Deep subsurface	9 ± 2	na	8-10	< 1	na	nd

Two-way ANOVA (Shapiro-Wilk $p=0.39$, Bartlett test $p=0.56$) on log-transformed bacterial biomass data showed a statistically significant effect of sediment depth ($F_{(3,24)}=10.95$, $p=0.0001$) rather than treatment ($F_{(2,24)}=0.189$, $p=0.83$). TukeyHSD showed differences occurred mainly between the higher bacterial abundance in surface sediments compared to the lower values in both subsurface sediments (shallow subsurface $p=0.0009$, deep subsurface $p=0.00009$). In general, subsurface bacterial biomass represented 55-65% of the surface biomass (Table 1). One-way ANOVA for the bacterial biomass in Control, showed statistical differences between layers ($F_{(2,11)}=4.421$, $p=0.039$) with the surface sediment not significantly different from that in shallow subsurface (TukeyHSD $p=0.52$) but significantly higher than in deep subsurface (TukeyHSD $p=0.05$). In the Nd treatment one-way ANOVA ($F_{(2,6)}=6.961$, $p=0.027$) showed that the bacterial biomass in the burrow was not statistically different from that in the surface sediment (TukeyHSD $p=0.53$), whereas for the Mv treatment (one-way ANOVA, $F_{(3,7)}=7.923$, $p=0.012$) the bacterial biomass in the burrow was lower from that in the surface (TukeyHSD $p=0.07$) but not statistically different from subsurface biomass (TukeyHSD $p>0.6$).

The bacterial community composition characterized through PLFA fingerprinting showed differences between depth layers along the first principal component axis, with a total of 53% of the variation between samples explained by the first two principal components (Fig. 2a). Surface samples for all treatments showed a clear differentiation from deeper layer with a higher contribution of 16:1 ω 7c, 18:1 ω 7c/9c, and 14:0. Two of the three Nd burrow samples also clustered with the surface samples whereas Mv burrows resembled PLFA patterns of the subsurface. Deeper sediments increased by ~15% in the relative contribution of ai15:0 compared to surface samples and 16:1 ω 7t was only present in deeper layers.

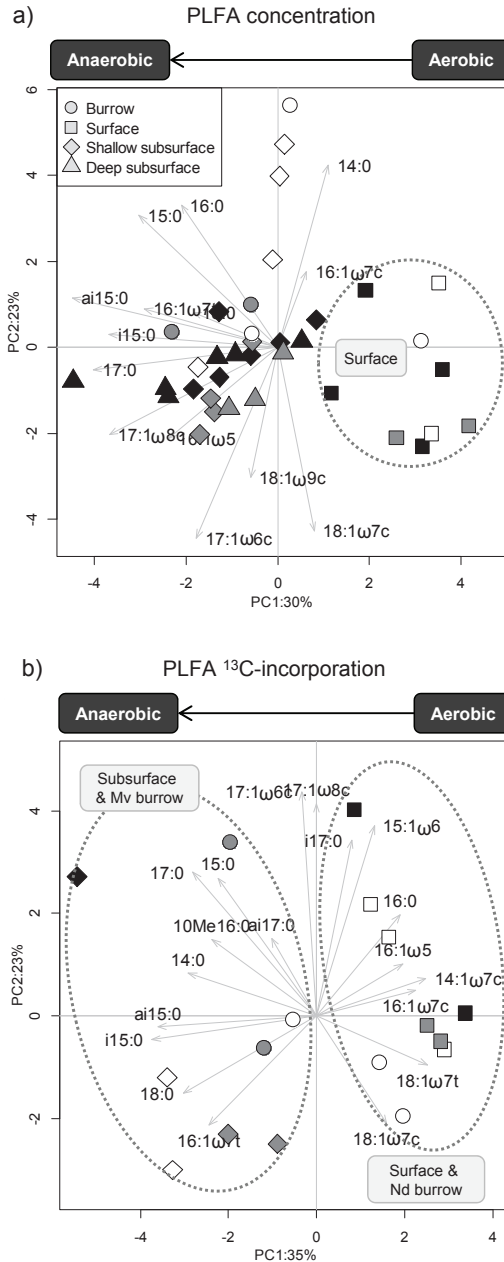


Figure 2. Principal component analysis (PCA) of a) PLFA concentrations (nmol C-PLFA g dw⁻¹) and b) ^{13}C -incorporation (pmol ^{13}C g dw⁻¹) for each sediment depth. Values were log transformed prior to analysis. The percent of variation amongst samples explained by each of the first two principal components (PC) can be found on the corresponding axis. Grey arrows represent the proportion of total variance explained by each PLFA. Treatments are identified by color scheme: black for Control (without bioturbation), white for *N. diversicolor*, and grey for *M. viridis*. Sediment depths are represented by different symbols as noted in legend.

5.3.3 Chemoautotrophic community

Combining the PLFA fingerprint technique with stable isotope probing allows for a targeted study of the active chemoautotrophic bacterial community. The incorporation of ^{13}C label could be determined for 20 bacterial fatty acids. Three PLFAs consistently displayed the highest ^{13}C -assimilation: 16:1 ω 7c ($34\pm 4\%$), 18:1 ω 7c ($26\pm 5\%$), and 16:0 ($17\pm 2\%$). However, principal component analysis (PCA) showed a clear divergence in the composition of the chemoautotrophic bacterial community between surface and subsurface samples (Fig. 2b). Surface samples were characterized by more label uptake into even numbered mono-unsaturated fatty acids, while synthesis of branched and saturated fatty acids prevailed in subsurface samples. Burrow sediments exhibited a specific PLFA fingerprint for each polychaete treatment (Fig. 2b). Nd burrow samples showed the highest relative ^{13}C -incorporation into 16:1 ω 7c ($36\pm 2\%$) and 18:1 ω 7c ($30\pm 5\%$), which was similar to that observed for surface samples. Nonetheless, one replicate of Nd burrow had less 18:1 ω 7c (25%) and thus clustered towards the subsurface PLFA fingerprint in the PCA (Fig. 2b). Mv burrows showed at least 3 times higher ^{13}C incorporation into ai15:0 (8%) and i15:0 (2.5%) than surface sediments, therefore closely resembling subsurface PLFA patterns. Moreover, monounsaturated fatty acid 16:1 ω 7t was prevalent in subsurface sediment but differed between treatments with an average incorporation of 10% for Nd and 4% for Mv and the Control treatment.

Overall, highest chemoautotrophy rates were found in the surface and the lowest in the subsurface sediments (Table 1). Very low chemoautotrophic activities were detected within the deep subsurface layer of all treatments (12 to 14 cm deep) and, therefore, these data were not considered for further analysis. The two-way ANOVA (Shapiro-Wilk $p=0.053$, Bartlett test $p=0.55$) performed on log-transformed (volumetric) chemoautotrophy rates showed significant differences between all sediment zones ($F_{(2,11)}=47.432$, $p=3.9\times 10^{-6}$). However, Nd burrow and surface rates were the only pair that were not significantly different (TukeyHSD $p=0.857$) and were on average 20 times higher than subsurface rates. In contrast, the mean dark CO_2 fixation rate of Mv burrow was only 15% of the surface rate and 2.5-times higher than subsurface activity. Subsurface chemoautotrophic activity was 2-folds higher in Nd and 4-folds higher in Mv when compared to the subsurface activity in the Control treatment.

5.3.4 Trophic interactions

Isotope results from field-collected specimens revealed a natural $\delta^{13}\text{C}$ signal of -15 to -14 ‰ for *N. diversicolor* and -14 to -13‰ for *M. viridis*. All polychaetes retrieved from ^{13}C labeled incubations were alive and motile at the end of the incubation period and were used to determine possible ^{13}C enrichment. All polychaetes were enriched in ^{13}C and $\delta^{13}\text{C}$ values were more pronounced for *M. viridis*, (-1 to -2‰) than for *N. diversicolor* (-11 to -7‰), suggesting a higher grazing of chemoautotrophic bacteria by *M. viridis* than by *N. diversicolor*.

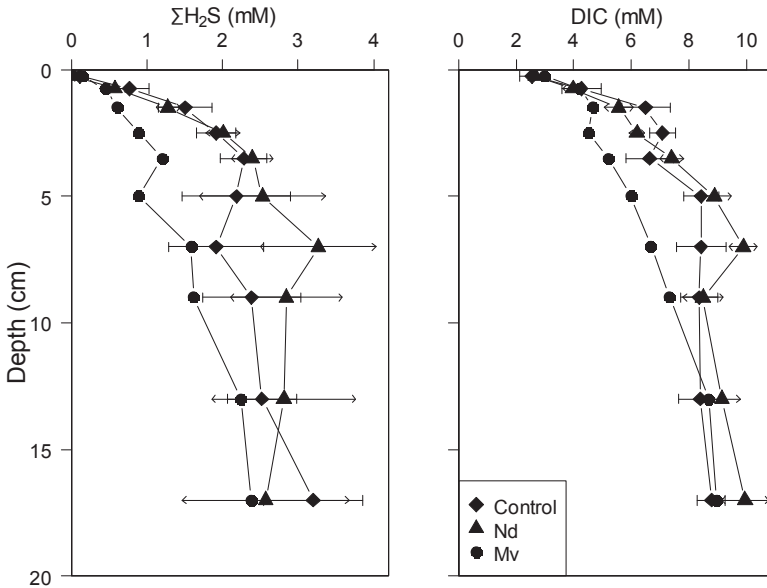


Figure 3. Sediment pore water profiles for ΣH_2S and DIC for the different treatments (Control: no bioturbation, Nd: *Nereis diversicolor*, Mv: *Marenzelleria viridis*). The error bars show SE (Control n = 4, Nd n = 3, Mv n = 2).

5.3.5 Pore water chemistry

Free sulfide (ΣH_2S) concentrations in the pore water of the Control and Nd treatment were low at the surface (~ 0.1 mM) increasing to 2.5 mM at 5 cm depth, remaining fairly constant deeper down (Fig. 3). The increase in ΣH_2S for Mv was less pronounced only reaching 1 mM at 5 cm depth and then gradually increasing to 3 mM at 17 cm depth. However, one-way ANOVA test (Shapiro-Wilk $p=0.74$, Bartlett test $p=0.94$) showed that the pore water ΣH_2S inventories (depth integrated ΣH_2S up to 20 cm) were not statistically different ($F_{(2,6)}=0.592$, $p=0.582$) between treatments (Nd: 82 ± 38 , Mv: $29-69$, C: 73 ± 32 mmol m^{-2}). DIC showed a pattern similar to that of ΣH_2S with a rapid increase in the Control and Nd treatment from overlying water values (~ 2 mM) at the sediment surface to ~ 9 mM at 5 cm depth (Fig. 3). One-way ANOVA (Shapiro-Wilk $p=0.65$, Bartlett test $p=0.19$) showed that depth integrated DIC was statistically different between treatments ($F_{(2,6)}=6.839$, $p=0.028$) with DIC inventory of 223-224 mmol m^{-2} for Mv, 276 ± 15 mmol m^{-2} for Nd and 260 ± 19 mmol m^{-2} for Control treatment. The Mv treatment showed a more gradual increase in DIC which was significantly different from Nd (TukeyHSD $p=0.02$) and to a lesser degree from Control (TukeyHSD test $p=0.08$).

5.4 DISCUSSION

5.4.1 Bacterial community

Sediment bioturbated by *N. diversicolor* and *N. virens* have shown 4 - 5 times higher bacterial abundance at the surface and burrow when compared to subsurface sediment (Papaspyrou et al., 2006). Likewise, Dobbs & Guckert (1988) observed an enrichment of bacterial biomass associated with the burrow lining of deep-burrowing shrimp (*Callinassa trilobata*) while sediment from the burrow wall had a similar bacterial biomass to that of subsurface sediment. PLFA analysis of sediment bioturbated by three polychaete species (*Notomastus lobatus*, *Branchioasychus americana*, *Balanoglossus aurantiacus*) showed a 20 - 75% species-dependent decrease in bacterial biomass from surface to the burrow (Steward et al., 1996). The Mv and Nd treatments followed a similar trend with ~36% higher bacterial biomass in the surface sediment than in the subsurface, while bacterial biomass in Mv and Nd burrows were only 13% and 26%, respectively, lower than surface bacterial abundances.

The biomarker patterns revealed distinct differences in microbial communities between surface and subsurface sediments. Furthermore, PLFA patterns in burrow and surface sediment were alike for Nd, whereas in the Mv treatment, the biomarker fingerprint of the burrow resembled that of the subsurface sediment. Nd burrow and surface sediment contained higher quantities of 16:1 ω 7c and 18:1 ω 7c, and although these compounds are ubiquitous amongst bacteria, they are typically more abundant in aerobic environments (Vestal & White 1989). The dominance of an aerobic microbial community in the Nd burrow is in line with our observation of oxidized conditions (light brown halo around the burrow lining) and the known intense ventilation (*i.e.* pumping of burrow with oxygenated waters) performed by *N. diversicolor* (Pischedda et al., 2011). In contrast, the burrow of *M. viridis* and subsurface sediments showed increased concentrations of ai15:0 and i15:0, which are compounds that indicate a high proportion of anaerobic metabolism (Findlay et al., 1990; Bühring et al., 2005). The enhancement of anaerobic activity in burrow sediments of *M. viridis* rather than *N. diversicolor* are consistent with the known impact of *M. viridis* bioturbation on sediment geochemistry, which boosts anaerobic processes such as sulfate reduction (Kristensen et al., 2011; Quintana et al., 2013).

A decrease in the concentration of 16:1 ω 7c combined with an increase in its trans form (16:1 ω 7t) observed in the subsurface of all treatments may be linked to ambient stress on the bacteria (Findlay et al., 1989; Vestal & White 1989). Manipulated sediments can take between 5 days and 2 weeks to reach a steady state or resemble natural biogeochemical conditions (Findlay et al., 1990; Kristensen 2001; Porter et al., 2006; Stocum & Plante 2006). As such it is possible that the week-long acclimatization of the microbial community in our incubations may have not allowed

for a complete recovery of the microbial community after the initial disturbance of the sediment (*i.e.* sieving and homogenization). Nevertheless sieving compared to freezing or asphyxiation, has been found to be the least disruptive method in regards to the magnitude of the effect and recovery time, both of the microbial community and the geochemical conditions (Porter et al., 2006; Stocum & Plante 2006).

5.4.2 Chemoautotrophic community

PLFA-SIP analysis showed that the chemoautotrophic bacteria associated with the Nd burrow sediment grouped with surface sediments, whereas chemoautotrophs from the Mv burrow clustered with subsurface samples. Prevalence of aerobic or anaerobic bacterial communities in burrow environments has previously been linked to the functional traits of the macrofauna (Dobbs & Guckert 1988; Steward et al., 1996; Pappaspyrou et al., 2006; Laverock et al., 2010) and our results confirm this species-specific bioturbation effect.

N. diversicolor intermittently ventilates its U-shaped burrow in regular cycles of ~10 min. ventilation and ~5 min. resting periods (Pischedda et al., 2011). The final result is a strong oxygenation of the burrow, with a mean oxygen concentration of ~70% saturation in the burrow. The O₂ concentration in the inhalant opening matches that of the overlying water which decreases toward the exhalant opening, encountering the lowest O₂ values at the bottom of the burrow (Pischedda et al., 2011). From the oxygenated burrow, oxygen diffuses into the sediment sustaining oxidized conditions (over 0.5 to 3 mm) generating steep chemical gradients radially from the center of the burrow towards the surrounding sediment. This radial transport of oxygen stimulates the aerobic reoxidation of reduced compounds by bacteria within the burrow (Banta et al., 1999). Strong aerobic activity is also inferred from the high chemoautotrophic labeling of even numbered monounsaturated 16- and 18-carbon fatty acids in the Nd burrow sediment, similar to the aerobic PLFA pattern noted in the surface sediment of all treatments. These mono-unsaturated PLFA are also highly abundant in sulfur-, nitrite- and ammonium-oxidizing chemoautotrophic bacteria (Blumer et al., 1969; Lipski et al., 2001; Knief et al., 2003; Inagaki et al., 2004; Labrenz et al., 2013; Chapter 2). The nitrification potential of *Nereis* spp. burrows substantially exceeds that of surface sediments (Kristensen & Kostka 2005), yet, here chemoautotrophy rates in the burrow and surface sediment of the Nd treatment were similar. Nitrifying bacteria have generally lower growth yields than sulfur-oxidizing bacteria (Chapter 2) and thus their activity may be underrepresented by the PLFA-SIP technique. Nonetheless, biomarker analysis of Nd burrows and surface sediments points to an aerobic chemoautotrophic community composed of sulfur-oxidizing and nitrifying bacteria.

Chemoautotrophy rates in Nd burrows were variable, with one replicate exceeding the other two by more than 80%, possibly due to the distinct burrowing behavior in the replicate aquaria. Several burrow openings were observed in the aquaria with the lowest chemoautotrophy rates, while only one burrow was found in the most active aquarium. In the aquaria with more than one burrow, Nd individuals apparently rebuilt and changed burrow over the course of the experiment. PCA analysis further showed that the less active Nd burrow had a larger contribution of anaerobic bacterial biomarkers (ai15:0 and i15:0) suggesting that the burrow was only shortly occupied before sampling. In fact, the residence time of burrows is an important factor determining the succession and maturation of the microbial community (Marinelli et al., 2002). Therefore, the higher aerobic chemoautotrophy found in the aquarium with one Nd burrow suggests that stable burrows with steady ventilation strongly affect the chemoautotrophic bacterial community.

Effects of burrowing by *M. viridis* on the geochemistry and microbial community are opposite to those of *N. diversicolor*. *M. viridis* ventilates its blind-ended burrow 10 times less than *N. diversicolor* which results in 75% air saturation at the burrow opening, which quickly decreases with depth along the burrow axis until anoxic conditions are obtained, interrupted by sporadic bursts of faint oxygenation (~8% air saturation) at the burrow end (Quintana et al., 2011; Jovanovic et al., 2014). Nonetheless, *M. viridis* has a stronger irrigation capacity due to deep burrowing and the percolation of return water through the sediment, which tends to dilute the pore water chemistry as seen in the DIC and $\Sigma\text{H}_2\text{S}$ depth profiles over the top 10 cm (Fig. 3). Pore water is injected from the burrow into the surrounding sediment and is pushed upwards to the sediment-water interface through advective transport, which increases the efflux of pore water solutes (Quintana et al., 2007; Jovanovic et al., 2014). This transport induced by *M. viridis* translates into a 10-fold increase of the chemoautotrophic activity in the burrow compared with Control subsurface sediment, but the chemoautotrophic activity remains still lower than that at the sediment surface. In agreement with the overall anaerobic conditions in the Mv burrow, the burrow sediment was characterized by biomarkers typical for sulfate reduction such as, i15:0, ai15:0, i17:1, 10Me16:0, 17:1, 16:1 (Taylor & Parkes 1983; Edlund et al., 1985; Boschker & Middelburg 2002; Webster et al., 2006). A chemoautotrophy study by Miyatake (2011) found similar PLFA-SIP patterns as in our Mv sediment, which were attributed to sulfate-reducing bacteria from the Deltaproteobacteria performing sulfur-disproportionation. The enhanced chemoautotrophic anaerobic activity in presence of *M. viridis* therefore could be attributed to such Deltaproteobacteria.

5.4.3 Chemoautotrophy rates

A long held notion is that burrows are interfaces between oxic and anoxic sediments and serve as hot spots of reoxidation processes and hence of chemoautotrophic activity (Aller 1988; Kristensen & Kostka 2005). Apart from our study, only Reichardt (1988) has directly quantified chemoautotrophic growth in the burrow of the lugworm *Arenicola marina* ($\sim 500 \text{ nmol C cm}^{-3} \text{ d}^{-1}$). These high chemoautotrophy rates are 8-times higher than the rates from Nd burrow and 48-times higher than the Mv treatment of our study. *A. marina* is a strong bioturbator, both in regards to particle reworking and burrow ventilation (Meysman et al., 2005) thus higher reoxidation rates would be expected in burrows of lugworms rather than in Mv and Nd burrows.

Aerobic chemoautotrophy rates obtained in our study ($40\text{-}145 \text{ nmol C cm}^{-3} \text{ d}^{-1}$) are in the lower range reported for coastal sediments characterized by non-mat forming sulfur-oxidizers ($100\text{-}200 \text{ nmol C cm}^{-3} \text{ d}^{-1}$ from 0 to 2 cm deep; Thomsen & Kristensen 1997; Lenk et al., 2010; Chapter 2). In organic-poor permeable sediments, $\sim 70\%$ of the total dark CO_2 fixation can be attributed to sulfur-oxidizing Gammaproteobacteria not related to filamentous morphotypes (Lenk et al., 2010). However, much higher *in situ* chemoautotrophy rates ($900\text{-}7000 \text{ nmol C cm}^{-3} \text{ d}^{-1}$) have been found in surface sediments colonized by white mats of filamentous sulfur-oxidizers (Chapter 2). White bacterial mats have been observed at Mv burrow openings in several studies (Kristensen et al., 2011; Quintana et al., 2013; Renz & Forster 2014) and white patches appeared on the surface of some of our incubations. It is plausible that the upward flow of sulfide and ammonium-rich pore water to the sediment-water interface, induced by advective mode of pore water irrigation by *M. viridis*, favors the development of these microbial mats of filamentous sulfur-oxidizers at the surface.

Alternatively, sulfate-reducers, within the Deltaproteobacteria, capable of sulfur-disproportionation or H_2 oxidation have been proposed as key players of anaerobic chemoautotrophy in subsurface sediments (Thomsen & Kristensen 1997; Miyatake 2011; Chapter 2). Anaerobic dark carbon fixation ($10\text{-}40 \text{ nmol C cm}^{-3} \text{ d}^{-1}$) is usually lower than aerobic chemoautotrophy as seen in intact sediments with limited bioturbation (Enoksson & Samuelsson 1987; Lenk et al., 2010; Chapter 2) and in laboratory incubations with sieved or homogenized sediment (Thomsen & Kristensen 1997; Chapter 3). Higher subsurface chemoautotrophic activity than in surface sediment has been observed in heavily bioturbated sediment by lugworm *A. marina* (Reichardt 1988) plausibly as a result of the intense injection of oxic overlying water into the subsurface sediment (Meysman et al., 2005). However, we found limited chemoautotrophic activity in subsurface sediments ($1\text{-}4 \text{ nmol C cm}^{-3} \text{ d}^{-1}$) which accounted for less than 1% of the surface activity in non-bioturbated Controls and $\sim 5\%$ in bioturbated sediments. *N. diversicolor* and *M. viridis* bioirrigate to a much lesser degree than *A. marina* (Kristensen et al., 2014) and thus only slightly stimulate subsurface chemoautotrophic activity compared to non-bioturbated subsurface sediments.

5.4.4 Trophic interaction

Hylleberg (1975) first introduced the concept of bacterial gardening in lugworms, where bacterial biomass is enhanced for feeding purposes by the lugworms as a result of particle mixing, excretion of fecal pellet, breakdown of particles through grazing or transport of solutes by ventilation (Aller & Yingst 1985). A study of the potential carbon sources of the head-down deposit feeder *Heteromastus filiformis* indicated a large dietary contribution by heterotrophic rather than chemoautotrophic bacteria (Clough & Lopez 1993). Alternatively, an increased survival of the polychaete *Capitella* sp.I has been reported in organic rich, sulfidic coastal sediments, which was linked to the ingestion of chemoautotrophic bacteria (Tsutsumi et al., 2001). Our stable isotope analysis also suggests that both *M. viridis* and *N. diversicolor* graze on chemoautotrophic bacteria in the sediment given the observed ^{13}C -enrichment. Comparison of excess ^{13}C fraction of the polychaetes with the corresponding chemoautotrophic activity showed that *M. viridis* can assimilate $0.017+0.003 \text{ d}^{-1}$ of the chemoautotrophic production while *N. diversicolor* had a lower uptake rate of $0.010+0.002 \text{ d}^{-1}$. These results suggest a stronger grazing capacity by *M. viridis* on chemoautotrophic bacteria than *N. diversicolor*. Additionally, growth rates of *N. diversicolor* ($0.020-0.035 \text{ d}^{-1}$; Kristensen 1984, Christensen et al., 2000) suggest that 30 to 50% of its diet could be supplemented by chemoautotrophs. However, *N. diversicolor* can switch from filter to deposit feeding when phytoplankton concentrations are low in overlying water (Christensen et al., 2000) therefore the high grazing of benthic chemoautotrophic bacteria observed in our incubations may be a consequence of depleted phytoplankton stocks in the water reservoir. Conversion of our uptake rates to biomass increment resulted in $2.8+0.9 \text{ mg C indiv}^{-1} \text{ d}^{-1}$ for *M. viridis* and six times less for *N. diversicolor* ($0.5 +0.1 \text{ mg C indiv}^{-1} \text{ d}^{-1}$). *M. viridis* has been shown to have turnover rates twice as high as *N. diversicolor*, which is in agreement with the opportunistic behavior exhibited by *Marenzelleria* spp. (Sarda et al., 1995).

5.5 CONCLUSION

In the absence of bioturbating fauna, chemoautotrophic activity and reoxidation processes such as sulfur oxidation are primarily limited to the surface oxic-anoxic interface given the depletion of oxidants in anoxic sediments (Fig. 4). In contrast, the two bioturbating polychaetes studied induce complex O_2 and H_2S dynamics in the sediment modulating the composition of the microbial community and the associated metabolic activity. Strong ventilation by *N. diversicolor* extends the oxic microenvironments into the sediment where aerobic dark carbon fixation through sulfide oxidation and nitrification are mainly promoted along the burrow. Whereas the slower pumping behavior combined with deeper burrows of *M. viridis* enhance anaerobic microbial metabolism (*i.e.* sulfate reduction and sulfur disproportionation) in subsurface sediment. Concomitantly, the upward pumping of

sulfidic and nutrient-rich pore water by *M. viridis* may potentially promote the development of sulfur-oxidizing microbial mats on the surface as seen in field observations (Kristensen et al., 2011; Quintana et al., 2013; Renz & Forster 2014). More targeted food web studies are necessary to determine the potential gardening of these microbial mats by *M. viridis*. In conclusion, the spatial distribution and magnitude of microbial processes, such as chemoautotrophy, can be strongly regulated by the species-specific functional traits of macrofauna and the extent of these effects should be examined in intact coastal sediments.

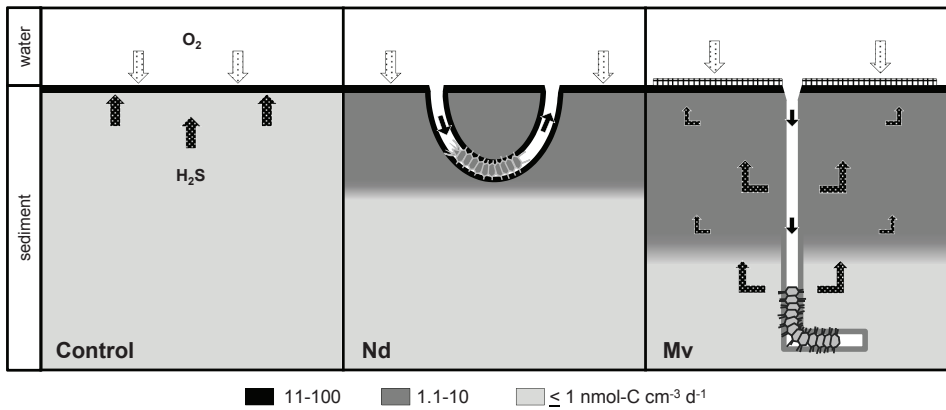


Figure 4. A conceptual scheme summarizing the distribution of chemoautotrophic activity in the three treatments: Control (no bioturbation), *Nereis diversicolor* (Nd) and *Marenzelleria viridis* (Mv). Color scale is in accordance with three ranges of chemoautotrophic activity as indicated below the scheme. Black arrows in the sediment represent the direction of $\Sigma\text{H}_2\text{S}$ flux and white arrows in the overlying water indicate O_2 flux in the Control sediment. Burrows are U-shaped for *N. diversicolor* and L-shaped for *M. viridis*. Polychaetes are represented at the bottom of the burrow. Solid black arrows in burrows indicate the direction of pore water flow. Meshed areas at the burrow opening of *M. viridis* denote sulfur-oxidizing bacterial mat formations.

ACKNOWLEDGMENTS

WE THANKFULLY ACKNOWLEDGE ZELJKO JOVANOVIĆ FOR FIELDWORK ASSISTANCE AND SUPPORT DURING THE PREPARATION OF THE EXPERIMENTS, PETER VAN BREUGEL AND MARCO HOUTEKAMER FOR THEIR ASSISTANCE WITH THE STABLE ISOTOPE ANALYSIS, DICK VAN OEVELEN FOR HIS INSIGHT ON TROPHIC INTERACTIONS, FRANCESCO MONTSERRAT FOR FRUITFUL DISCUSSIONS ON BIOTURBATION AND LUCAS STAL FOR HIS COMMENTS ON THE MANUSCRIPT. THIS WORK WAS FINANCIALLY SUPPORTED BY A GRANT FROM THE DARWIN CENTRE FOR GEOSCIENCE (TO HTSB AND FJRM), ERC GRANT 306933 (FJRM), AND GRANT #12-127012 FROM THE DANISH COUNCIL FOR INDEPENDENT RESEARCH/NATURAL SCIENCES (EK).

DIANA VASQUEZ-CARDENAS, FILIP J.R. MEYSMAN, PETER VAN BREUGEL,
LORENZ MEIRE, HEIDI L. SØRENSEN, HENRICUS T.S. BOSCHKER

Bacterial chemoautotrophy in coastal sediments

ABSTRACT

In coastal sediments, chemoautotrophy is known to occur widely, but the regulation, global importance nor the depth distribution of dark carbon fixation have been systematically investigated. Here, we surveyed nine coastal sediments by means of stable isotope probing (^{13}C -DIC) and bacterial biomarker analysis (phospholipid derived fatty acids), thus increasing the number of sedimentary chemoautotrophy observations by 60%. Together with values compiled from literature, this provides a dataset on dark carbon fixation rates ranging from 0.07 to 36 $\text{mmol C m}^{-2} \text{d}^{-1}$. A power-law relation between chemoautotrophy and benthic oxygen uptake translated into a nearly linear relation between dark carbon fixation and water depth. In addition, the CO_2 fixation efficiency also showed a decreasing trend with water depth: salt marshes (21%), near-shore (9%) and continental shelf sediments (3%). Furthermore, five characteristic depth distributions of chemoautotrophy are identified based on the mode of pore water transport (advective, diffusive, bioturbated), and the dominant mode of sulfur oxidation. Highest dark carbon fixation rates were found in diffusion-driven cohesive sediments, where high chemoautotrophic activity takes place near the sediment surface at the O_2 - H_2S overlap. Lowest chemoautotrophy rates were found in advective-driven permeable sediments with deep oxygen penetration while bioturbated sediments showed intermediate dark carbon fixation rates. Extrapolated to the global coastal ocean, we estimated a chemoautotrophic production of 0.06 Pg C y^{-1} , which is a two-and-a-half times lower than previous estimates, and yet still one order of magnitude higher than the potential chemoautotrophic production of hydrothermal vents ($0.002 \text{ Pg C y}^{-1}$) where chemoautotrophs are the main primary producers.

6.1 INTRODUCTION

Chemoautotrophic micro-organisms obtain their metabolic energy by the oxidation of various inorganic substrates, such as ammonium, ferrous iron, and sulfide, and they use this energy to synthesize organic bio-molecules from carbon dioxide. Chemoautotrophic microbes hence typically thrive in redox gradient systems, *i.e.*, transitions between reduced and oxidized environments, such as the chemocline of permanently stratified water bodies or the interface between oxic and sulfidic horizons in marine sediments (Jørgensen 1982; Labrenz et al., 2005). In terms of seafloor environments, hydrothermal vents form the most conspicuous ecosystems, as both symbiotic and free-living chemoautotrophic bacteria are the main primary producers there, obtaining their energy from the oxidation of sulfide and other reduced compounds that are enriched in the expelled vent fluids (Cavanaugh et al., 1981; Nakagawa & Takai 2008). Globally however, the total sulfide production by sulfate reduction in coastal marine sediments is roughly one order of magnitude higher than the sulfide output from hydrothermal vents, and thus coastal sediments have a much greater potential for chemoautotrophy-based primary production than deep sea ecosystems (Howarth 1984). Yet, the prevalence and magnitude of chemoautotrophy in coastal sediments remains poorly documented.

In coastal sediments, sulfate reduction is the main respiration pathway, accounting for 50% to 90% of the organic matter mineralization (Soetaert et al., 1996), and produces a large sedimentary pool of reduced sulfur compounds, such as dissolved free sulfide, thiosulfate, elemental sulfur, iron monosulfide and pyrite (Jørgensen & Nelson 2004). Only a small fraction (3-10%) of this reduced sulfur is buried into deeper horizons, and so, a large amount of energy within the reduced sulfur reservoir remains available for chemoautotrophic micro-organisms that catalyze the oxidation of these reduced sulfur compounds through a variety of pathways. The microbial biomass that is newly produced by dark CO₂ fixation becomes available in the microbial food web and eventually adds to the pool of organic matter in the sediment (Tsutsumi et al., 2001; Chapter 2 & 5).

The importance of chemoautotrophy in sedimentary carbon cycling can be assessed by evaluating the so-called CO₂ fixation efficiency, *i.e.*, the ratio of the CO₂ fixed by chemoautotrophy over the total CO₂ released in the mineralization of organic matter. Based on crude electron balance considerations, this dark CO₂ fixation efficiency has been estimated to be ~7% for a “typical” coastal sediment (Jørgensen & Nelson 2004), although recently and following a similar approach, it has been argued that chemoautotrophy could possibly account for more than 30% of the sediment carbon cycling in coastal sediments (Middelburg 2011). These diverging estimates

partially reflect the paucity of empirical data on coastal sediment chemoautotrophy, as only a handful of studies have experimentally determined and compared benthic respiration rates (e.g. sedimentary CO₂ production or O₂ consumption as a proxy for the mineralization rate of organic matter) with dark carbon fixation rates (Enoksson & Samuelsson 1987; Bauer et al., 1988; Thomsen & Kristensen 1997; Lenk et al., 2010; Santoro et al., 2013; Dyskma et al., 2016; Chapter 2 & 3). Overall, the dark CO₂ fixation rate in these studies varies between 0.02 mmol C m⁻² d⁻¹ (hydrocarbon seeps) and 36 mmol C m⁻² d⁻¹ (salt marshes), while the associated CO₂ fixation efficiency ranges between 1.5% (brackish lake) and 32% (intertidal sediments). Accordingly, there appears to be a lot of variability between sites and habitats, and so the question arises as to which environmental factors drive the chemoautotrophic activity at a given site, and also generate the observed variation in the CO₂ fixation efficiency. At present, only one study has addressed this issue experimentally, but detected no significant relationship between chemoautotrophy and bacterial production, sediment respiration or organic matter content (Santoro et al., 2013). In a similar fashion, the depth distribution of chemoautotrophic activity may vary greatly between geochemically distinct sediment habitats (Lenk et al., 2010; Thomsen & Kristensen 1997; Enoksson & Samuelsson 1987; Chapters 2, 3 & 4), but also this aspect has not been studied systematically.

In the present study, we provide a round-up of the current knowledge about chemoautotrophy in coastal sediments, by combining the available literature data with a set of newly collected field data. The principal objectives were: (1) to expand the existing dataset of dark carbon fixation rates in marine sediments, (2) to examine the link between sediment characteristics (e.g. water depth, porosity, organic matter content, benthic oxygen consumption) and chemoautotrophic production in coastal sediments, (3) to estimate the overall importance of chemoautotrophy in the sedimentary carbon cycle of the coastal ocean, and (4) to characterize the depth distribution of the chemoautotrophic activity in coastal sediments. To accomplish these goals, a set of coastal sediments were surveyed experimentally, spanning a range of habitats (salt marsh, estuarine, continental shelf and subpolar fjord sediments). Intact sediment cores were injected with ¹³C-bicarbonate, and ¹³C-incorporation into bacterial phospholipid derived fatty acids were measured to determine total chemoautotrophic production as described in Chapters 2 & 3. These new data were subsequently combined with existing literature data to enable a cross-system comparison of the total dark CO₂ fixation rate as well as CO₂ fixation efficiency in coastal sediments. Based on the biogeochemistry of the sediment, five depth distribution models for chemoautotrophic activity are proposed, each pertaining to a specific sediment habitat type.

6.2 METHODS & MATERIALS

6.2.1 Study sites and sampling

Chemoautotrophy was investigated at nine coastal sites that cover a range in water depth (0-107 m), porosity (0.3-0.8), organic matter content (0.08-7.4%), and oxygen consumption rates (3.4-86 mmol O₂ m⁻² d⁻¹). This field survey included four intertidal sites in the Rhine-Meuse-Scheldt Delta area (The Netherlands), which represented distinct habitats (oyster reef, sand flat, salt marsh) in terms of their depositional and biogeochemical regimes. All sediment was sampled from unvegetated areas (salt marsh sediments were recovered from creek beds). In addition, four subtidal shelf sites were sampled along a transect off-shore in the North Sea, and one high latitude site (Kobbefjord, Greenland) was surveyed seasonally over one year. Site characteristics are summarized in Table 1 and a detailed description of the sites, as well as the sediment sampling procedure is provided in the Supplementary Material. In addition to these new field data, the available literature data on coastal benthic chemoautotrophy were compiled, which provided data on 10 additional sites (20 observations). An “observation” refers to the determination of the dark CO₂ fixation rate at a particular site at a particular time; some sites hence have multiple time points. For all sites (field sites evaluated here as well as literature sites), we compiled the following information where available (Table 1, Table S1): chemoautotrophy rates, total oxygen uptake (TOU), dissolved oxygen uptake (DOU), porosity (p), organic carbon content (OC), *in situ* temperature (T), oxygen penetration depth (OPD), and CO₂ fixation efficiency (C:O₂).

6.2.2 PLFA-SIP analysis

To assess the chemoautotrophic activity, we combined the analysis of phospholipid derived fatty acids with stable isotope probing (PLFA-SIP) (Boschker et al., 1998). For all sites, the same method was employed (see Chapter 2 & 3 for details), where ¹³C-bicarbonate was added to the pore water with the line injection method, adding label through vertically aligned side ports in the core liners (0.5 cm apart; 100 µl of label per hole). A 20 mM stock solution of labeled NaHCO₃ (99% ¹³C; Cambridge Isotope Laboratories, Andover, Ma, USA) was prepared in calcium- and magnesium-free artificial seawater in order to prevent carbonate precipitation. The stock solution was bubbled with N₂ shortly before use to remove oxygen (thus preventing spurious reoxidation upon introduction in anoxic pore water). Labeled cores were kept for 24 hours at *in situ* temperature (±2°C) in a darkened incubator to prevent phototrophic CO₂ fixation. High

latitude sediments (site KF) were incubated for ~48 hours due to low activity, except for June 2011. Cores were incubated with *in situ* seawater and the overlying water was continuously bubbled with air as described in Chapter 3.

At the end of the incubation period, sediment cores were sectioned in intervals (0.3, 0.5, 0.8, 1 or 2 cm slicing pattern was site dependent) to a maximum depth of 6 cm (average maximum depth was 5 cm). Sediment layers were collected in centrifuge tubes (50 ml), pore water was obtained by centrifugation (4500 rpm for 5 minutes) and sediments were lyophilized for PLFA-SIP analysis as in Guckert et al., (1985) and Boschker et al., (1998). ^{13}C -incorporation into PLFA was analyzed by gas chromatography – isotope ratio mass spectrometry (GC-IRMS, Thermo, Bremen, Germany) on an apolar analytical column (ZB5-MS Phenomenex). Two additional cores without ^{13}C -label were used as controls and treated in the same manner as described above.

6.2.3 Chemoautotrophy rates

Incorporation rates of ^{13}C into individual PLFA (expressed in $\mu\text{mol PLFA-C per g of dry sediment d}^{-1}$) were calculated for each sediment layer as the product of individual bacterial fatty acid concentrations ($\mu\text{mol PLFA-C g}^{-1}$) and its ^{13}C fraction corrected for background values, divided by the incubation time. Incorporation rates were summed over all bacterial PLFA (12:0 to 20:0) and converted to biomass carbon using a conversion factor of $55 \text{ mmol PLFA-C (mol biomass C)}^{-1}$ (Chapter 2). To arrive at volumetric dark CO_2 fixation rates (*i.e.* $\mu\text{mol biomass-C per cm}^{-3}$ of bulk sediment per day), rates were multiplied with the conversion factor $\rho(1-\phi)$, where ϕ is porosity and ρ is the solid sediment density; ρ was set equal to 2.60 g cm^{-3} for cohesive or 2.55 g cm^{-3} for permeable sediment. Rates were corrected for ^{13}C -DIC enrichment in the pore water, which was measured by the head space technique with an elemental analyzer-IRMS equipped with a gas injection port (Chapter 2). Total chemoautotrophy rates ($\text{mmol C m}^{-2} \text{ d}^{-1}$) were calculated as the cumulative activity in all depth layers (integration to a depth of 4 to 6 cm). Detailed description of the PLFA-SIP analysis and calculations can be found in Boschker & Middelburg (2002) and Boschker (2004). Note that anapleurotic reactions, *i.e.*, CO_2 fixation by heterotrophic bacteria utilized to replenish carbon intermediates in metabolic pathways, may account for 1.5% to 33% of the biomass production by heterotrophs (Wegener et al., 2012). However the PLFA-SIP method used here does not measure CO_2 fixation through anapleurotic reactions, because the fixed CO_2 is not directly utilized in the synthesis of phospholipid fatty acids (Chapter 2). Accordingly, calculated dark CO_2 fixation rates represent the “true” metabolism of chemoautotrophs.

Table 1. List of coastal field sites from the present study where chemoautotrophy was evaluated. Chemoautotrophy rates, total (TOU) and dissolved oxygen uptake (DOU) are reported as $\text{mmol m}^{-2} \text{d}^{-1}$. ϕ : porosity, OC: organic carbon content, T: *in situ* temperature in Celsius, αCO_2 : CO_2 fixation efficiency, OPD: oxygen penetration depth. See text for the description of the different sediment habitats (SOx: sulfur oxidation).

Site	Code	Latitud	Longitud	Date	T (°C)	Depth (mbsl)	ϕ	OC %	Sediment habitat
Rattekaai Salt Marsh Oosterschelde, the Netherlands	RK11	N 51°26'21"	E 04°10'11"	Jun-11	16	0	0.74	3	Electrogenic SOx
Zandkreek (Oosterschelde) the Netherlands	ZK11	N 51°32'41"	E 03°53'22"	Feb-11	4	0	0.54	0.4	Bioturbated
Oosterschelde sand flat the Netherlands	OSF	N 51°26'52"	E 04°05'47"	May-11	15	0	0.42	0.2	Bioturbated
Westerschelde mud flat (Kapellebank), the Netherlands	WMF	N 51°27'31"	E 03°58'48"	Jul-11	18	0	0.72	2	Bioturbated
SE Frisian Front (station 15) North Sea	NS.15	N 53°43'01"	E 04°59'08"	Aug-11	18	33	0.50	0.2	Bioturbated
Dutch coast (station 13) North Sea	NS.13	N 53°26'21"	E 05°19'55"		18	9	0.37	0.03	Advective
SE Dogger Bank (station 8) North Sea	NS.8	N 54°45'56"	E 03°41'52"		9	50	0.40	0.1	Advective
NW Dogger Bank (station 4) North Sea	NS.4	N 55°55'54"	E 03°36'52"		8	53	0.31	0.1	Advective
Kobbefjord, SW Greenland	KFjun	N 64°10'48"	W 51°31'27"	Jun-11	2	107	0.78	7.4 ^a	Bioturbated
	KFsept			Sep-11	3		0.75	5.2 ^a	
	KFdec			Dec-11	1		0.79	6.5 ^a	
	KFmay			May-12	0		0.78	6.4 ^a	

^a Malkin et al., 2014; ^b Lohse et al., 1996; ^c Sørensen et al., 2015

NA: Not applicable

CHEMOAUTOTROPHY IN COASTAL SEDIMENTS

Total chemoautotrophy mean±SD	Relative contribution of surface chemoautotrophy (0-1 cm)	TOU mean±SD	α CO ₂ TOU	DOU mean±SD	α CO ₂ DOU	OPD (mm)
8.6±2.6	0.75	82±22	0.11	30±4 ^a	0.22	0.7 ^a
2.5±0.9	0.50	55±12	0.05	14±3	0.18	1.8
1.5±0.5	0.60	38±16	0.04	5±1.6	0.19	1.6 ^a
1.8±0.5	0.38	86±4	0.02	17±6	0.04	2
0.9±0.06	0.46	23±3	0.04	6.7-8.9 ^b	NA	3-15 ^b
0.07±0.02	0.46	8±1.6	0.01			
0.2±0.09	0.19	8±0.3	0.03			
0.07±0.02	0.40	3.4±0.6	0.02			
0.5±0.07	0.32	11±1.8 ^c	0.05	5±3.3 ^c	0.03	8 ^c
0.6±0.04	0.20	12±0.6 ^c	0.05	6±1.3 ^c	0.02	6 ^c
0.4±0.2	0.41	7±1.7 ^c	0.06	7±1.2 ^c	0.03	6 ^c
0.08±0.05	0.29	7±1.3 ^c	0.01	5±0.9 ^c	0.005	6 ^c

6.2.4 Sediment characteristics

Porosity was determined from water content and wet density of sediment slices used for PLFA-SIP analysis. Lyophilized surface sediment was ground to a fine powder to determine the organic carbon content (OC) for each site using an elemental analyzer (Thermo Scientific; precision $\pm 0.18\%$). To determine the total oxygen uptake (TOU) in intertidal and North Sea sediments, cores were sealed with gas tight lids equipped with a central stirrer. Fiber optical oxygen sensors (FireSting OXF1100) were inserted through the lid and secured with rubber stoppers. TOU rates were determined from linear regression of oxygen concentrations in the overlying water versus incubation time. Incubations were stopped after a decrease of $\sim 30\%$ in O_2 air saturation. Microsensor profiling of O_2 on intertidal sediments was performed using micro-electrodes (Unisense A.S., Aarhus, Denmark) to obtain the oxygen penetration depth (OPD) and dissolved oxygen uptake (DOU) rates as described in Malkin et al., (2014). All parameters were measured in triplicates per station. Methods used for TOU, DOU, and OPD determination for the KF site are described in Sørensen et al., (2015).

6.2.5 Statistical analysis

The 12 observations on chemoautotrophy obtained in the present study, in addition to the 23 observations reported in literature, as well as the associated environmental characteristics recorded, are listed in Tables 1 and S1. This dataset formed the basis of the statistical analysis. Pearson's correlation coefficient (r) was calculated to investigate the linear dependence between environmental parameters (porosity, OC content, TOU, DOU) and chemoautotrophic activity. Chemoautotrophy rates and oxygen fluxes (DOU, TOU) were log transformed prior to linear regression analysis.

6.3 RESULTS & DISCUSSION

6.3.1 A survey of benthic chemoautotrophy rates

The field survey of chemoautotrophy in coastal sediments ($n=12$ observations; Table 1) revealed dark carbon fixation rates varying from 0.07 to 8.2 $\text{mmol C m}^{-2} \text{d}^{-1}$. Higher rates have been reported before in literature (36 $\text{mmol C m}^{-2} \text{d}^{-1}$), but the lowest value reported here (0.07 $\text{mmol C m}^{-2} \text{d}^{-1}$) is considerably smaller than the previously reported minimum value in literature (0.2 $\text{mmol C m}^{-2} \text{d}^{-1}$). Accordingly, the current study has expanded the coverage of the natural activity range by surveying sediments with low activity (Table S1). The total range of dark CO_2 fixation rates is broad (0.07 to 36 $\text{mmol C m}^{-2} \text{d}^{-1}$), and so, the question becomes as to what environmental factors

determine such wide-ranging chemoautotrophic activity? Santoro et al., (2010) examined chemoautotrophic activity in relation to sediment oxygen uptake, bacterial production (^3H -leucine incorporation), and organic carbon content in 11 freshwater and brackish lakes from boreal and tropical locations. They found no significant correlation between area-based chemoautotrophy rates and the selected environmental variables. Our study does also not find any significant correlation between dark carbon fixation and organic carbon content ($r=0.26$, $p=0.16$, $n=30$) and porosity ($r=0.17$, $p=0.37$, $n=32$; Fig. S1). However, the current dataset does reveal a strong correlation between sedimentary O_2 consumption and dark CO_2 fixation. Accordingly, the chemoautotrophy rate in the top centimeter of the sediment was compared to the DOU, assuming that reoxidation in the surface is fueled by O_2 diffusion from the sediment-water interface, and the depth-integrated chemoautotrophy rate to the TOU, assuming that non-local injection of O_2 at depth (e.g. by burrow ventilation) can stimulate deep chemoautotrophy. Total chemoautotrophic activity (0-6 cm) was significantly correlated to TOU ($r=0.87$, $p= 1.23 \times 10^{-7}$, $n=23$; Fig. 1a) as was the surface chemoautotrophy (0-1 cm) to DOU ($r=0.82$, $p= 6.693 \times 10^{-6}$, $n=20$; Fig. 1b). Log-log regression analysis of the chemoautotrophic activity with either TOU or DOU provides a power law relation ($r^2=0.73$ for TOU and $r^2=0.67$ for DOU), which signifies that chemoautotrophy is relatively more important in sediments with high oxygen uptake rates, typically found in near shore sediments (Glud 2008; Fig. 1c).

The general trend of increasing chemoautotrophy from intertidal areas to the continental shelf in the current dataset can be explained by decomposing the dark carbon fixation rate (DCF) as $\text{DCF} = \alpha_{\text{CO}_2} * \text{R}_{\text{min}}$, where R_{min} represents the mineralization rate (the CO_2 production by the decomposition of sedimentary organic matter) and α_{CO_2} is the CO_2 fixation efficiency of the chemoautotrophic community (the ratio of the CO_2 fixed by chemoautotrophy over the total CO_2 released by mineralization). Note that direct measurement of the mineralization rate is difficult, and so, R_{min} values are typically not recorded in marine sediments (and hence are lacking in the dataset here). However, the TOU is typically accepted as a suitable proxy for organic carbon mineralization rate in the sediment, and a recent meta-analysis of oxygen consumption in marine sediments shows that both TOU and DOU decrease with water depth in the coastal ocean (Glud 2008; Fig. 1c). Therefore, a first reason why DCF decreases with water depth, is because R_{min} decreases with water depth. Sediments at greater water depths are less reactive than shallower sediments, because primary production tends to decline offshore as nutrients are supplied by terrestrial runoff, and organic matter is degraded more extensively the larger distance it travels through the water column before reaching the sediment (Glud 2008). To express the dependency of chemoautotrophy on water depth more quantitatively, the power law relation between oxygen uptake rates and total chemoautotrophic production can be

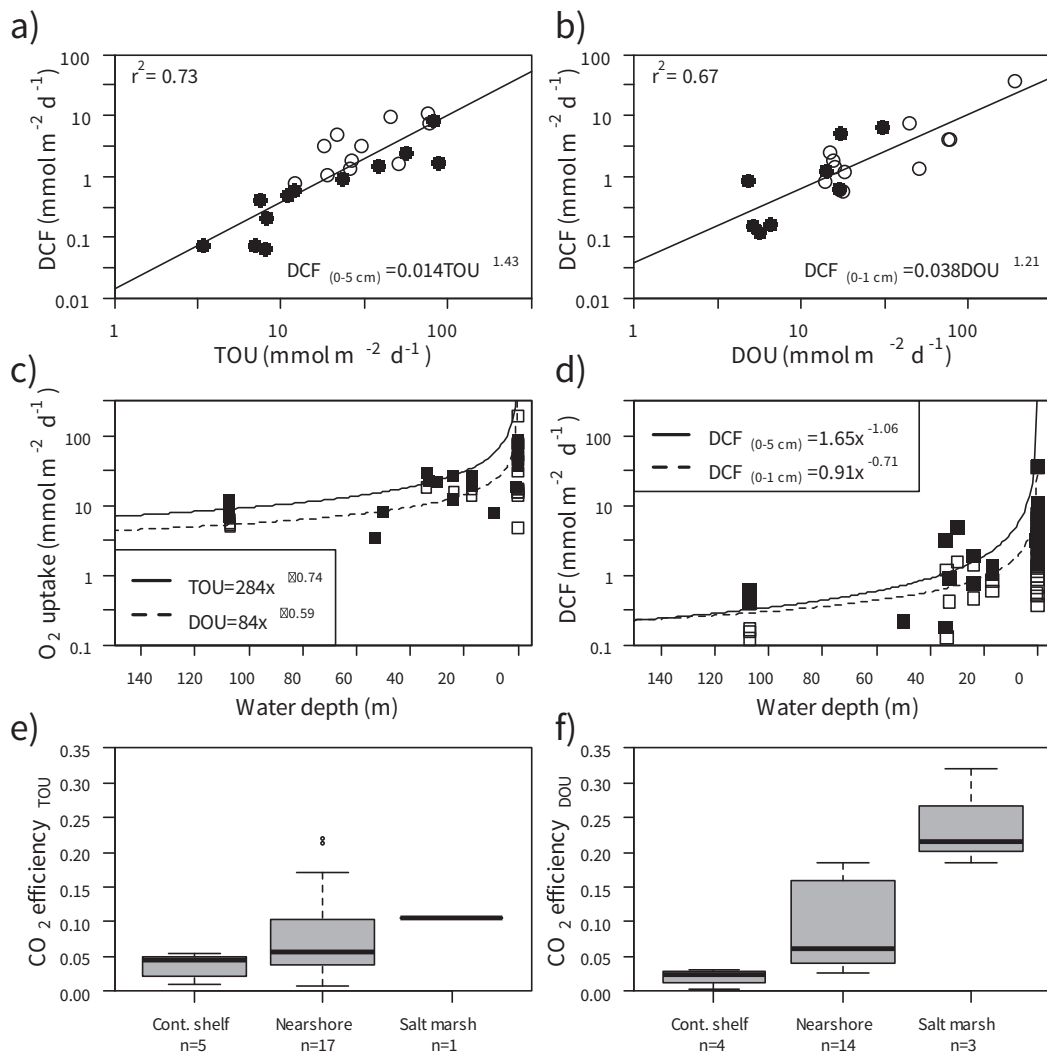


Figure 1. a) Comparison of the total (0-5 cm) dark carbon fixation (DCF) and the total oxygen uptake (TOU) of the sediment. b) Comparison of the surface chemoautotrophy rate (0-1 cm) to the dissolved oxygen uptake (DOU) of the sediment. c) Plot of sediment oxygen uptake against water depth; regression models as reported by Glud (2008). Data from the present study are plotted in black symbols and data from literature are white. d) Regression models for the chemoautotrophic activity ($\mu\text{mol C m}^{-2} \text{d}^{-1}$) in coastal sediments (0-150 m water depth). Black squares are based on TOU rates and total chemoautotrophy (0-5 cm), whereas white squares are based on DOU and surface chemoautotrophy (0-1 cm). Boxplot of CO₂ fixation efficiencies of chemoautotrophs (αCO_2) for three different coastal sediment zones using TOU e) and DOU f) as a proxy for mineralization.

combined with the regressions reported by Glud (2008). The TOU and DOU scales with water depth with an exponent of -0.74 and -0.59 (respectively), and chemoautotrophy scales with TOU and DOU with an exponent of +1.43 and +1.21 (respectively), thus the chemoautotrophy overall scales with water depth with an exponent of -1.05 and -0.71 (respectively; Fig. 1d). Accordingly, we find that the sedimentary chemoautotrophy is approximately inversely related to the water depth within the coastal ocean.

The fact that the exponent of the power between oxygen uptake and DCF exceeds one (Fig. 1a, 1b) indicates that an increase in the mineralization rate results in a more than proportional increase of the chemoautotrophy rate, and therefore, the CO₂ fixation efficiency α_{CO_2} should also decrease with water depth. Across the dataset, CO₂ fixation efficiencies (calculated as the ratio of DCF over TOU or DOU) were found to range from 0.01 to 0.32 with a median of ~0.06, which corresponds well with the typical CO₂ fixation efficiency of 0.07 that has been previously estimated for coastal sediments based on simplified electron balance calculations (Jørgensen & Nelson 2004). In general, the CO₂ fixation efficiency can be expressed as

$$\alpha_{CO_2} = \sum_i \mu_i \lambda_i \gamma_i \quad (23)$$

For each chemoautotrophic pathway, the CO₂ fixation efficiency scales as the product of three factors: (1) the production efficiency γ_i , which scales the production rate of a given electron donor to the mineralization rate, (2) the reoxidation efficiency λ_i of the electron donor (*i.e.*, how much is effectively used for microbial respiration and not diverted to abiotic oxidation), and (3) the CO₂ fixation yield μ (e.g., the moles of CO₂ fixed per mole of electron donor oxidized). For example, the estimate of Jørgensen & Nelson (2004) was based on the assumptions that (1) coastal chemoautotrophy is dominated by sulfide oxidation (only one pathway, $i = 1$) (2) half the carbon respired is mineralized by sulfate reduction ($\gamma=0.50$), (2) 90% of the sulfide produced via sulfate reduction is oxidized by sulfur-oxidizing chemoautotrophs ($\lambda=0.9$), and (3) a growth yield of 15% for sulfur-oxidizers ($\mu=0.15$). This way one directly arrives at $\alpha_{CO_2} = 0.50 \times 0.90 \times 0.15 = 0.07$.

When differentiating between three depth zones in the coastal ocean, we find a $3 \pm 2\%$ CO₂ fixation efficiency in continental shelf sediments (50-200 m water depth), $9 \pm 6\%$ for near-shore sediments (0-50 m water depth, including intertidal sediments and excluding brackish lagoons), and $21 \pm 9\%$ for salt marshes (Fig. 1e, f). These values agree well with previous estimates by Howarth (1984) that were based on a much smaller dataset (3-6% for continental shelf, 7-13% for near-shore sediments, and 10-18% for salt marshes). This depth dependency can be explained by evaluating the different components contributing to the CO₂ fixation efficiency (see Eq (23)). Salt marsh sediments are typically fine-grained, organic-rich sediments with high mineralization rates,

where sulfate reduction is the dominant respiration pathway (75%-90%), and nearly all sulfide is reoxidized by means of microbial metabolism (85%-95%; Howarth 1984). Furthermore, high growth yields of aerobic sulfur-oxidizers (0.16-0.56; Klatt & Polerecky 2015) are expected in such sulfide-rich environments. As a result, CO₂ fixation efficiencies are high in salt marsh sediments, and hence, chemoautotrophy is a potentially underestimated source of labile organic matter in salt marsh and other active near-shore sediments. At the opposite end, continental shelf sediments are often characterized by coarse-grained, organic-poor sediments, but still, these sediments sustain sizeable mineralization rates via the catalytic bed filter effect (Huettel et al., 2014). The low chemoautotrophy rates in these sediments are hence due to low CO₂ fixation efficiencies, caused by the centimeter deep penetration of oxygen in these sediments through advective pore water flow (Lohse et al., 1996; Huettel et al., 2003), which favors aerobic mineralization of organic matter and heterotrophy and hence a low prevalence of anaerobic respiration (low production efficiency γ). Furthermore, strong pore water flushing can flush electron donors out of the sediment thus preventing reoxidation in the sediment (low reoxidation efficiency λ). Due to the low production of sulfide in these sediments, ammonium becomes the primary electron donor for chemoautotrophic bacteria. However, nitrifying bacteria typically exhibit low growth yields of approximately 0.1 (low μ ; Middelburg 2011) that are substantially lower than for sulfur-oxidizing bacteria (Klatt & Polerecky 2015). Overall, the combination of these factors strongly diminishes the CO₂ fixation efficiency and explains the rapid drop of the chemoautotrophy as a function of water depth (Fig. 1d-f).

With these mean CO₂ fixation efficiencies for the two coastal depth zones (near-shore and salt marsh sediments together form the 0-50 m zone, average efficiency 10 \pm 8%) we can further estimate the importance of chemoautotrophy in the global ocean. Adopting the global sediment respiration for continental shelf (0.29 Pg C y⁻¹) and near-shore (0.53 Pg C y⁻¹) sediments (Dunne et al., 2007), chemoautotrophy would contribute an average of 0.01 Pg C y⁻¹ and 0.05 Pg C y⁻¹ for each depth regimes respectively. Our calculated chemoautotrophic production of 0.06 Pg C y⁻¹ is thus two-and-a-half times lower than the conservative estimates of benthic chemoautotrophic production in coastal sediments (0.15-0.29 Pg C y⁻¹; Middelburg 2011), which suggests that values calculated in Middelburg (2011) severely overestimate the contribution of chemoautotrophy in the coastal ocean.

6.3.2 Biogeochemical sediment regimes

A biogeochemistry-oriented conceptual model of chemoautotrophy in coastal sediments was developed by making a distinction between three sediment regimes, each of which represents a different mode of geochemical cycling determined by the

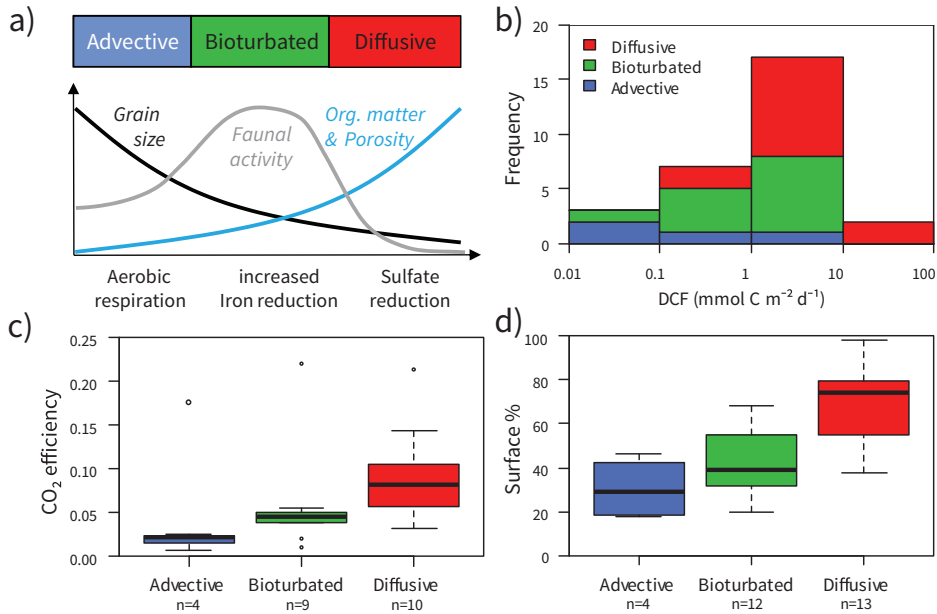


Figure 2. a) Classification of three biogeochemical regimes where chemoautotrophy rates (dark carbon fixation: DCF) are reported. This classification takes into account grain size, organic matter content, porosity, bioturbation intensity the distribution of oxygen and free sulfide in the pore water. Mode of organic matter mineralization are also indicated (aerobic respiration, iron reduction, sulfate reduction). b) Frequency distribution of chemoautotrophy rates, c) boxplot of the CO_2 fixation efficiencies for chemoautotrophs (αCO_2) and d) the relative contribution of chemoautotrophy occurring in the surface layer (0-1 cm) for the three biogeochemical sediment regimes.

dominant physical transport regime: “advective”, “bioturbated”, or “diffusive” (Fig. 2a). The underlying rationale is that chemoautotrophy is principally enabled by reoxidation reactions between energetically favorable electron acceptors (O_2 , NO_3^-) and suitable electron donors (H_2S , Fe^{2+} , NH_4^+), and hence, we expect the transport mode of electron acceptors/donors to be a key determinant of the magnitude and location of chemoautotrophy in coastal sediments. In general, the transport mode suitably co-varies with sediment characteristics (grain size, porosity) and the principal mode of organic matter mineralization (aerobic respiration, enhanced iron reduction, sulfate reduction) - see review by Aller 2014 (Fig. 2a). Permeable sediments consist of highly porous coarse-grained sands, with low organic matter content and a relative low level of faunal reworking (Fig. 2a). Physical advection, induced by

waves and bottom current strongly influence sands due to the high permeability which allows a deep intrusion of oxygenated bottom water into the sediment, thus favoring aerobic over anaerobic mineralization pathways (Huettel et al., 2014). Bioturbated sediments are typically found at intermediate porosities and organic matter levels (Fig. 2a), and are inhabited by large macrofauna that sustain a high intensity of bioturbation, both inducing solid phase transport (bio-mixing) as well as solute transport (bio-irrigation) (Meysman et al., 2006; Kristensen et al., 2012). These bioturbated sediments are typically characterized by a shallow oxygen penetration, but at the same time, they also show an absence of free sulfide in the pore water, as the sediment geochemistry is typically dominated by strong iron cycling and ferruginous pore water conditions (free sulfide is removed from the pore water by ferrous iron and sequestered into iron sulfides; Kristensen & Kostka 2005; Meysman et al., 2006). Consequently in addition to sulfate reduction, a part of the mineralization will occur through dissimilatory iron reduction. Finally, diffusive sediments are cohesive sediments with a low median grain size, high porosity and high organic matter content (Fig. 2a), which are characterized by high rates of sulfide production through sulfate reduction, and hence, these sediments are characterized by strong accumulation of free sulfide in the pore water at depth. Diffusive sediments are not impacted by bioturbation due to the toxic effects of sulfide on macrofauna (Rosenberg et al., 2002), and are neither impacted by physical advection due to their impermeability (Huettel et al., 2014).

Highest chemoautotrophy rates were typically found in diffusive sediments (RK, MLG) due to the high availability of both free sulfide in pore water and electron acceptors. In particular, two sulfidic sediments in the dataset had dark carbon fixation rates exceeding $10 \text{ mmol C m}^{-2} \text{ d}^{-1}$ (Fig. 2b); these correspond to a field observation in a salt marsh creek ($36 \text{ mmol C m}^{-2} \text{ d}^{-1}$; Chapter 2) and for laboratory incubated sediments from a seasonal hypoxic reservoir ($11 \text{ mmol C m}^{-2} \text{ d}^{-1}$; Chapter 3). More than half of all the chemoautotrophy measurements ($n=17$) fell within the range of $1\text{-}10 \text{ mmol C m}^{-2} \text{ d}^{-1}$ either from diffusive or bioturbated sediments (Fig. 2b). Chemoautotrophy observations within the range of $0.1\text{-}1 \text{ mmol C m}^{-2} \text{ d}^{-1}$ were fewer ($n=7$) and were dominated by bioturbated sediments, while sediments with very low chemoautotrophy rates (range of $0.01\text{-}01 \text{ mmol C m}^{-2} \text{ d}^{-1}$; $n=3$) were dominated by advective sediments.

Additionally we estimated the CO_2 fixation efficiencies (based on TOU values) for these three sediment regimes obtaining a mean ($\pm\text{SD}$) CO_2 fixation efficiency of $2\pm 0.9\%$ for advective sediments, $4\pm 2\%$ for bioturbated sediments and $8\pm 3\%$ for diffusive sediments (Fig. 2c). Advective and bioturbated sediments make up the majority of the seafloor of the coastal ocean, although the relative prevalence of these regimes is presently not very well quantified. If we attribute 45% of the total benthic coastal respiration (0.82 Pg C y^{-1} ; Middelburg 2011) to advective sediments,

45% to bioturbated and 10% to diffusive sediments, and employ our estimated CO₂ fixation efficiency for these three regimes, we can calculate a second estimate for the global chemoautotrophic production, where advective sediments account for 0.007 Pg C y⁻¹ (0.82 x 0.45 x 0.02), bioturbated sediments 0.014 Pg C y⁻¹ (0.72 x 0.45 x 0.04), and diffusive sediments 0.007 Pg C y⁻¹ (0.82 x 0.10 x 0.08). The total chemoautotrophic production of 0.03 Pg C y⁻¹ is two times lower than the estimate above of 0.06 Pg C y⁻¹ based upon the water depth. This could either suggest that highly active sites with high chemoautotrophy rates are overrepresented in the water depth-based upscaling, or that bioturbated sediments are underrepresented. Given the uncertainties in the underlying calculations (see above), further investigations are necessary to more precisely constrain the global chemoautotrophy rate within the 0.03-0.06 Pg C y⁻¹ range.

6.3.3 Conceptual chemoautotrophy depth-distribution models

Firstly, we evaluated the relative contribution of chemoautotrophic activity occurring at the sediment surface (0-1 cm depth) in relation to the subsurface activity for all sites where information is available on the depth distribution on chemoautotrophy (n=29, Fig. 2d and Fig. S3). Diffusive sediments have a higher relative contribution of chemoautotrophy at the surface layer than bioturbated or permeable sediments. In diffusive sediments with high free sulfide in pore water a mean of 74% of the total chemoautotrophy occurred at the sediment surface. In these sediments, most chemoautotrophy occurs in relation to aerobic sulfur oxidation at the oxic-anoxic interface, which is typically located very shallow (~1-2 mm depth) in these organic-rich sediments with high sulfate reduction rates. In contrast, in advective sediments, where O₂ and NO₃⁻ are flushed into deeper sediment layers by physical advection, 70% of the dark carbon fixation occurred in subsurface sediments. In bioturbated sediments, 61% of the dark carbon fixation occurred beneath the surface layer, where O₂ and NO₃⁻ can diffuse into the sediment along the walls of animal burrows flushed by bio-irrigation, which likely enhances deep chemoautotrophic activity.

Overall, five distinct depth-distribution models were observed in the chemoautotrophy dataset related to the three main sediment categories described above with the diffusive sediments split into three subcategories. We made a final distinction between the three dominant modes of sulfur oxidation (Meysman et al., 2015; Seitaj et al., 2015) present in diffusive sediments: canonical sulfur oxidation by microbes positioned at an overlapping O₂-H₂S interface (e.g. *Thiobacillus*, *Thiovolum*, *Arcobacter*, non-vacuolate *Beggiatoa*), sulfur oxidation by motile, filamentous, nitrate accumulating bacteria (e.g. vacuolate *Beggiatoa*), and electrogenic sulfur oxidation (e-SOx) by the recently discovered cable bacteria. As further explained in detail below, these five

regimes cause the different interactions between electron donors and acceptors. It should be noted however that in reality, depth distributions are not always clear cut (e.g. sediments can be in transition between two biogeochemical regimes).

Canonical sulfide oxidation (Fig. 3a) – In cohesive, organic rich sediments, where the organic loading is so high that reactive metal oxides are all reduced, free sulfide may accumulate in the pore water, and migrate upward to the sediment surface, where it comes into contact with O_2 that diffuses from the overlying water into the sediment. This creates a narrow overlap between O_2 and H_2S , which is often only a few tens of micrometers thick (Jørgensen & Nelson 2004), and the sulfur oxidation that takes place is referred to as canonical sulfide oxidation ($H_2S + 2O_2 \rightarrow SO_4^{2-} + 2H^+$; Meyersman et al., 2015). Our data confirm that this diffusional reaction zone is a hotspot of sulfide oxidation associated with high dark carbon fixation rates (Fig. 3a). Most chemoautotrophic activity is strongly concentrated within the top layer of the sediment, but still, a small but measurable amount (~20%) of chemoautotrophic activity occurred below the oxic-anoxic interface (Fig. 3a). Chemoautotrophy in sediment horizons without O_2 and NO_3^- is possible through processes such as sulfur disproportionation (Bak & Pfennig 1987), and the oxidization of hydrogen through sulfate reduction (Thomsen & Kristensen 1997; Miyatake 2011). This chemoautotrophy depth pattern linked to canonical sulfur oxidation was repeatedly observed in creek bed sediments of a salt marsh (RK05, RK06; Chapter 2) and at various stations in the sediments of marine Lake Grevelingen during the summer hypoxia (MLG1a, MLG3a; Chapter 4). In some occasions (RK05, RK06, MLG2a), a white mat of filamentous sulfur bacteria was observed, likely non-vacuolate *Beggiatoa* (large gliding filamentous bacteria containing light refracting sulfur globules, but without intracellular NO_3^- storage; Jørgensen, 1982), but at other times no distinct biofilm was notable at the O_2 - H_2S interface, and hence chemoautotrophy may have been carried out by colourless sulfur bacteria (e.g. *Arcobacter*, *Sulfurimonas*; Campbell et al., 2006). The chemoautotrophy depth pattern linked to canonical sulfide oxidation was also seen in the early phase of laboratory sediment incubations, when sediment from Lake Grevelingen was homogenized and incubated with fully oxygenated overlying water (I.MLG1, Chapter 3).

Vacuolate Beggiatoa (Fig. 3b) - It has already been realized for quite long that the direct “canonical” reaction of H_2S with O_2 is rather exceptional form of sulfur oxidation in the coastal seafloor (Jørgensen 1982; Jørgensen and Nelson, 2004). Most coastal sediments generally exhibit a distinct separation between oxic and sulfidic horizons, a so-called suboxic zone, where neither O_2 nor H_2S are present in detectable concentrations. One mechanism to create such a suboxic zone is through vacuolate and motile colorless sulfur bacteria, such as *Thioploca* and some *Beggiatoa*, which are capable of intracellular redox shuttling between the oxic and sulfidic

horizons (Jørgensen & Nelson 2004; Sayama et al., 2005). These bacteria store nitrate intracellularly in a large central vacuole, and this nitrate reservoir is used at depth to oxidize free sulfide to elemental sulfur, which is also stored intracellularly ($2\text{H}_2\text{S} + \text{NO}_{3(\text{int})}^- + 6\text{H}^+ \rightarrow 2\text{S}_{(\text{int})}^0 + \text{NH}_4^+ + 3\text{H}_2\text{O}$). When migrating back to the surface this elemental sulfur is further oxidized to sulfate in the presence of O_2 or NO_3^- ($2\text{S}_{(\text{int})}^0 + 3\text{O}_2 + 2\text{H}_2\text{O} \rightarrow 2\text{SO}_4^{2-} + 4\text{H}^+$; Preisler et al., 2007). This cyclic movement and the associated transport of redox compounds then creates the suboxic zone (Fig. 3b). A suboxic zone (19 mm thick) induced by intracellular redox shuttling, in association with high densities of vacuolate *Beggiatoa*, was observed *in situ* in spring in the sediments of a seasonally hypoxic marine lake when bottom waters were oxygenated (MLG2m; Chapter 4). The associated depth distribution of chemoautotrophic activity rather than being limited to the oxic surface sediments as with canonical sulfur oxidation spans from the surface to the sulfide appearance depth, in accordance with the sediment layer where *Beggiatoa* glide through (Fig. 3b). Chemoautotrophic activity however decreases towards the sulfide horizon suggesting that most of the carbon fixed might be associated to the oxidation of elemental sulfur rather than the oxidation of sulfide to elemental sulfur with nitrate but detailed physiological studies are needed to confirm these findings.

Electrogenic sulfur oxidation (Fig. 3c)- Electrogenic sulfur oxidization (e-SOx) has only been recently discovered and provides a second mechanism to create a suboxic zone in diffusive coastal sediments. The process is performed by long filamentous bacteria, so-called cable bacteria belonging to the Deltaproteobacteria, which are capable of channeling electrons over cm scale distances along their longitudinal axis (Nielsen et al., 2010; Pfeffer et al., 2012; Meysman et al., 2015). Although the physiological details of electron transport are currently unknown, the e-SOx process involves two spatially segregated redox half-reactions, *i.e.*, anodic sulfide oxidation which occurs throughout the suboxic zone as well as in the top of the sulfidic zone ($\text{H}_2\text{S} + 4\text{H}_2\text{O} \rightarrow \text{SO}_4^{2-} + 10\text{H}^+ + 8\text{e}^-$) and cathodic oxygen reduction which occurs within the oxic zone ($\text{O}_2 + 4\text{H}^+ + 8\text{e}^- \rightarrow 2\text{H}_2\text{O}$). The necessary redox coupling between these two half reactions is ensured by transporting electrons from cell to cell along the filamentous cable bacteria. This proton production at depth and the proton consumption at the sediment surface induce a specific pH fingerprint upon the pore water, which serves to distinguish e-SOx from other sulfur oxidizing mechanisms (Meysman et al., 2015; Seitaj et al., 2015; Chapter 4).

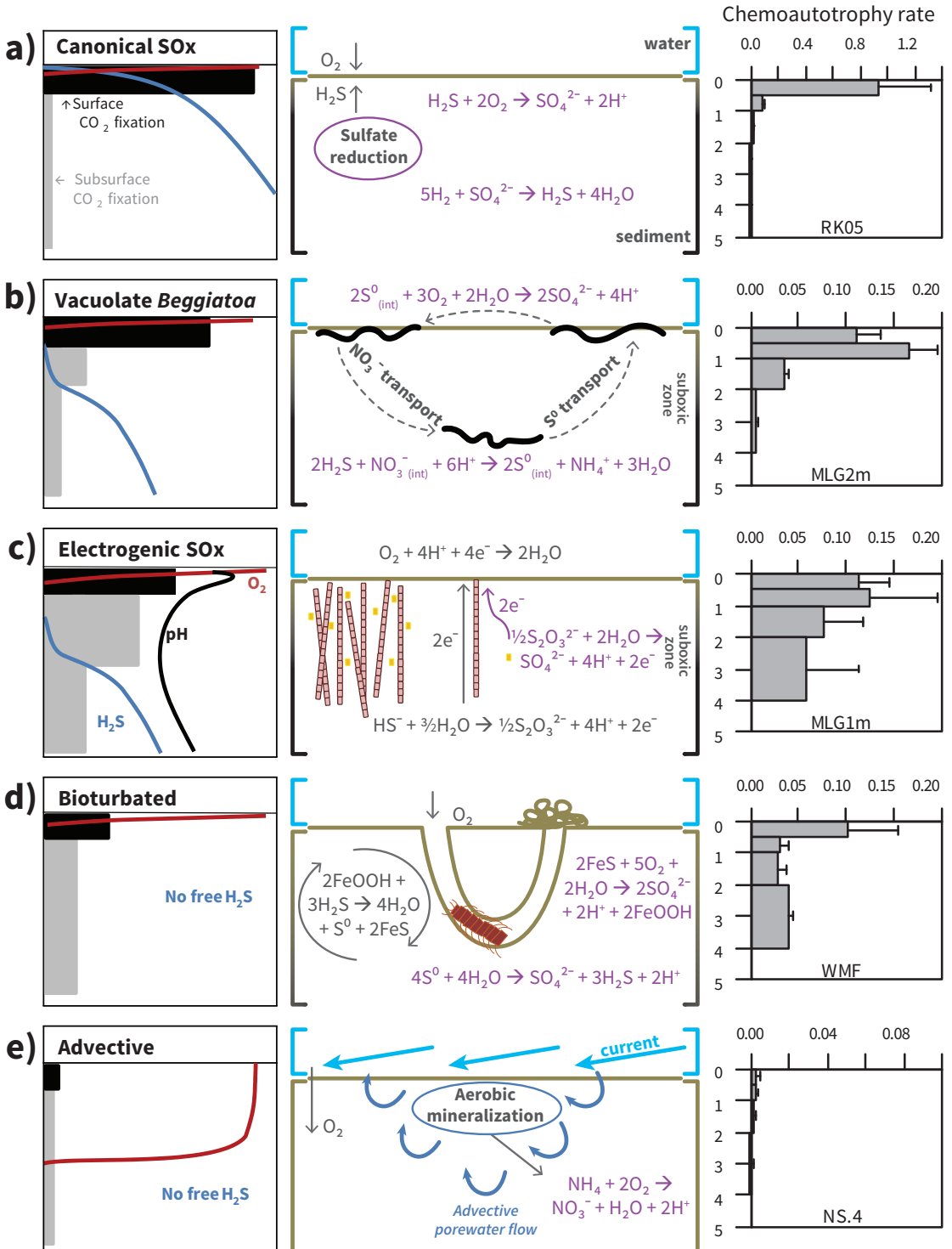
The chemoautotrophy depth profile associated with e-SOx is highly remarkable, as substantial rates of dark carbon fixation occur deep down in the sediment, where O_2 and NO_3^- are absent. The current survey of intertidal sediments, the e-SOx dependent chemoautotrophy depth profile was found in the salt marsh sediment in summer 2011 (RK11), which exhibited the distinct geochemical fingerprint of e-SOx

(Malkin et al., 2014) and high dark carbon fixation from the surface to below the sulfide horizon (~15 mm deep, Fig. S2). A second observation of this pattern under natural conditions comes from the seasonally hypoxic marine Lake Grevelingen, where the e-SOx geochemical fingerprint was observed and high densities of cable bacteria were confirmed by fluorescence *in situ* hybridization (MLG1m, MLG3m; Chapter 4).

In laboratory sediment incubations under controlled conditions (I.MLG9, I.MLG13, I.MLG12; Chapter 3) it was noted that the zone of chemoautotrophy develops in unison with the deepening of the suboxic zone, *i.e.*, the zone of intense dark CO₂ fixation expanded deeper as the cable bacteria network grew deeper into the sediment (Chapter 3). Remarkably, this strong chemoautotrophic activity could not be attributed directly to the cable bacteria, as targeted ¹³C-labeling experiments revealed that cable bacteria were incorporating propionate, and hence, have a heterotrophic metabolism. Instead, biomarker signatures in combination with 16S-rRNA gene sequencing indicated that the deep chemoautotrophy observed was most likely performed by other sulfur oxidizing bacteria belonging to the Epsilon- and Gammaproteobacteria (Chapter 3 & 4). We speculate that the deep chemoautotrophic activity occurs via a sulfur-oxidizing consortium, whereby cable bacteria oxidize sulfide to some sulfur intermediate and the associated chemoautotrophic bacteria then oxidize this intermediate further to sulfate by using the conductive structures of the cable bacteria as an electron acceptor (Fig. 3c).

Bioturbated sediments (Fig. 3d) – In sediments subject to bioturbation by macrofauna, geochemical gradients are regulated by both bio-irrigation of pore water solutes and bio-mixing of solid particles (Kristensen 1988; Meysman et al., 2006). During bio-irrigation, the injection

Figure 3. The depth distribution of chemoautotrophic activity in five idealized biogeochemical regimes in coastal sediments. Conceptual model depth distribution of oxygen, free sulfide and pH (left column); a schematic representation of the main biogeochemical reactions affecting the depth distribution of the chemoautotrophic activity (middle column); and the depth distribution of chemoautotrophic activity as measured in coastal sediments (right column). Chemoautotrophy rates in $\mu\text{mol C cm}^{-3} \text{ d}^{-1}$ - note the change in scale. a) Canonical sulfur oxidation in sediments with overlapping O₂ and H₂S. b) Sulfur oxidation driven by intracellular redox shuttling by motile, nitrate-storing, colorless sulfur bacteria (Beggiatoa, black filaments). c) Electrogenic sulfur oxidation by cable bacteria (red filaments) with a hypothetical consortium of sulfur-oxidizing chemoautotrophic bacteria (yellow single cells). Purple reactions denote chemoautotrophic reactions while grey reactions pertain to cable bacteria. d) Bioturbated sediments where particle reworking and ventilation of burrow structures alter the reoxidation zones in the sediment. Grey reaction denotes iron cycling by mixing of sediment particles through bioturbation. e) Advective driven sediments, mostly permeable, created by bottom water currents that produce deep O₂ penetration and high aerobic mineralization. It should be noted however that in reality, depth distributions are not always clear cut (e.g. sediments can be in transition between two biogeochemical regimes).



of overlying water into the sediment by macrofauna - for burrow ventilation or filter feeding purposes - provides a pulse of electron acceptors (O_2 and NO_3^-) to the subsurface. This deep injection of electron acceptors can increase the heterotrophic decomposition of organic matter, but also stimulate chemoautotrophic processes, such as nitrification along the burrow structure (Kristensen & Kostka 2005). Pore water rich in reduced compounds (e.g. elemental sulfur, thiosulfate and hydrogen) is also washed through the sediment during bio-irrigation of the burrow which may stimulate anaerobic chemoautotrophy via S-disproportionation and H_2 -oxidization in subsurface sediment (Chapter 5). Additionally bio-mixing, *i.e.*, particle reworking, strongly increases the iron cycling in the sediment, by stimulating the two-way interconversion between iron sulfides (FeS) and iron oxides (FeOOH) whereby iron oxides are transported downwards and reduced, and iron sulfides are transported upwards and oxidized (Canfield et al., 1993; Seitaj et al., 2015). The upward mixing of iron sulfides into the oxic zone potentially forms the main supply of reduced sulfur substrate for chemoautotrophs (Fig. 3d) although microbial oxidation of iron sulfides at circum-neutral pH has not been well studied (Schippers 2004).

The observed seasonal changes in the depth-distribution of chemoautotrophy at KF (Fig. S2) may be associated to iron cycling by sediment mixing since both the availability of oxygen in the sediment (OPD) and the production of sulfide via sulfate reduction showed no clear seasonal trend (Sørensen et al., 2015). Substantial sediment mixing was found in the upper 5 cm of the sediment (Sørensen et al., 2015) which would explain the even distribution of chemoautotrophy in June and September 2011 up to 6 cm deep. However the intensity of mixing must have decreased by December to the top 2 cm where chemoautotrophic activity was present. By the end of winter (May 2012) mixing of the sediment must have been minimal which would result in the depletion of the electron donor pool for chemoautotrophs.

However, the effect of macrofauna on the chemoautotrophic depth distribution and associated microbial community may largely depend on functional traits of the species that are present at a given site (Marinelli et al., 2002; Bertics & Ziebis 2009; Laverock et al., 2010; Chapter 5). The higher proportion of dark carbon fixation at ZK and OSF compared to the other bioturbated sediments (NS.15, WMF, JS06, StnL, KF) could be the result of different communities of bioturbating fauna (Fig. S2). For example, deeply bioturbating polychaetes such as the lugworm *Arenicola* spp. and *Nereis* spp. can significantly alter chemoautotrophy rates at the surface and along the burrow walls (Reichardt 1988; Kristensen & Kostka 2005; Chapter 5), while small oligochaetes and bivalves (*Macoma* sp.) do not heavily bio-irrigate or -mix sediments.

Advective sediments (Fig. 3c) – In permeable sediments (porosity < 0.4), water currents and wave action create an advective transport of pore water, which induces a centimeter deep penetration of oxygen, that enhances aerobic respiration rather than sulfate reduction (Huettel et al., 2014). Thus chemoautotrophic activity is likely fueled

by the oxidation of ammonium (*i.e.* nitrification) originating from aerobic mineralization unlike the previously described four scenarios (Fig. 3e). However, nitrifying bacteria have low growth yields (1 mole C fixed : 10 moles NH_4 oxidized; Middelburg 2011) which result in overall low dark carbon fixation activity. The North Sea area studied (station 4, 8 and 13) exhibits low sulfate reductions rates (up to $6.5 \text{ mmol C m}^{-2} \text{ d}^{-1}$; Upton et al., 1993) which in combination with the flushing of the porous sediment matrix by water movements, limit the availability of electron donors necessary for chemoautotrophic bacteria throughout the sediment. In accordance, chemoautotrophy was found at centimeter depth in permeable sediments from the North Sea where oxygen was present (Fig. S2), but chemoautotrophy rates were comparatively low in relation to the rest of the compiled dataset. Note that in sediment core incubations, it is difficult to mimic the *in situ* advective transport of pore water which may alter the depth-distribution of chemoautotrophy. The Thomsen and Kristensen (2008) work is also interesting in this respect as they incubated a permeable sandy sediment under laboratory conditions. As there was only limited water flow in these incubations, pore water flow was probably low, mineralization was mainly by anaerobic processes and chemoautotrophy rates and efficiencies were relatively high for a permeable sediment (Table S2).

6.4 CONCLUSION

Here we show that chemoautotrophic activity varies broadly in coastal sediments related to mineralization rates, water depth, pore water transport mechanisms, and sulfur oxidation pathways. Dark carbon fixation tended to be highest in diffusion-driven intertidal sediments with high anaerobic mineralization activity and lowest in permeable continental shelf sediments driven by advective pore water transport and aerobic mineralization. Overall our global estimates of chemoautotrophy based on CO_2 fixation efficiencies for near-shore and continental shelf sediments indicate that coastal sediments indeed do have a much greater potential for chemoautotrophic production than deep sea hydrothermal vents where primary production is mainly fueled by chemoautotrophy. Hence, the renewal of labile organic matter by chemoautotrophs may be more important in carbon budgets of the coastal ocean than currently considered. The compiled dataset also revealed distinct depth distribution patterns of dark carbon fixation for five biogeochemical regimes related to pore water transport and sulfur oxidation mechanisms. However more biogeochemical studies including chemoautotrophy rates are necessary to consolidate these conceptual models and precisely determine the global chemoautotrophy rate (0.03-0.06 Pg C y^{-1} range).

ACKNOWLEDGEMENTS

WE THANK SAIRAH MALKIN, SILVIA HIDALGO MARTINEZ, AND PIETER VAN RIJSWIJK FOR FIELD ASSISTANCE ON THE INTERTIDAL FLATS, THE CAPTAIN AND CREW OF THE PELAGIA ON THE NORTH SEA CRUISE, KARL ATTARD, MARTIN BLICHER, ANNI GLUD, ANNA HAXEN AND THOMAS KROGH FOR FIELD AND LABORATORY ASSISTANCE IN GREENLAND, AND MARCO HOUTEKAMER FOR HIS ASSISTANCE WITH STABLE ISOTOPE ANALYSIS. THIS WORK WAS FINANCIALLY SUPPORTED BY THE DARWIN CENTRE FOR GEOSCIENCE (HTSB AND FJRM), AND AN ERC STARTING GRANT TO FJRM.

6.5 SUPPLEMENTARY INFORMATION

6.5.1 Material & Methods

Site description

To determine chemoautotrophy in intertidal sediments, four sites (ZK, OSF, RK, WMF) were selected in the Delta area (The Netherlands), which represented habitats that were highly distinct in terms of their biogeochemistry (Table 1). Zandkreek (ZK) has a porosity of 0.54 and organic carbon content (OC) of 0.4%, that is characterized by Pacific oyster beds (*Crassostrea gigas*) that induce a high sedimentation of cohesive, organic rich material, which accumulates by biodeposition of the bivalves. Hence, the ZK site sustains high organic matter mineralization rates (Dauwe et al., 2001; Chapter 2) and supports significant chemoautotrophic activity (Chapter 2). Still, the sediments are non-sulfidic (*i.e.* no free sulfide accumulates in the pore water) in the top 5 cm, and the sediments show high densities of macrofauna, thus indicating strong bioturbation (Chapter 2). The Oosterschelde Sand Flat (OSF) site is located in a tidal inlet, and supports medium sands with a porosity of 0.42 and OC of 0.2%. At the time of sampling, there was no free sulfide detected in the top 2.5 cm of sediment, and sediments were heavily bioturbated by high densities ($> 50 \text{ m}^{-2}$) of the lugworm *Arenicola marina* (Malkin et al., 2014). The third intertidal site, Rattekaai (RK), is a salt marsh with cohesive sediment (porosity 0.74) with high organic matter loads (OC:3%) promoting high rates of sulfate reduction (Pallud & Van Cappellen 2006). The sediment in the salt marsh creek is generally black and sulfidic (*i.e.* detectable free sulfide in the pore water) up to the depth of oxygen penetration, and is often covered by a white mat of *Beggiatoa*-like sulfur oxidizing bacteria, although cable bacteria have also been recently found at the site (Malkin et al., 2014). The highest chemoautotrophy rates up to now in literature were reported at the RK site (Chapter 2). The Westerschelde Mud Flat (WMF) site is a highly bioturbated site, characterized by benthic fauna such as *Hydrobia*, *Macoma*, *Heteromastus*, and *Pygospio* and high microphytobenthos densities in summer (Weerman 2011); sediment had high silt content and free sulfide was not detected in the pore water. All four intertidal sites were visited between February and July 2011. Undisturbed sediment was collected during low tide using polycarbonate core liners (5 cm outer diameter and 20 cm in length; $n=3$), which was incubated to measure chemoautotrophy rates (as detailed in main text). Large core liner (10 cm outer diameter and 30 cm in length) was used to collect intact sediment for total O_2 consumption (TOU, $n=3$). A third set of cores liners (4 cm in diameter and 10 in length) were used to sample sediment for O_2 microprofiling ($n=3$).

To determine chemoautotrophy in subtidal shelf sediments, a transect perpendicular to the coast was surveyed in the southern North Sea (NS). This transect included four stations (NS.4, NS.8, NS.13, NS.15) running from the Wadden island of Terschelling (Dutch coast) to the Dogger Bank in the central North Sea. All stations had low organic matter input and silt content (Table 1). Stations NS.4, NS.8 and NS.13 are categorized as non-depositional, in comparison station NS.15 on the Frisian front, receives a higher organic matter input and has a higher silt content (Stoeck et al., 2002). Sediment was collected during a cruise onboard the RV Pelagia using a Reineck box corer. Subsequently polycarbonate core liners (5 cm outer diameter and 20 cm in length) were inserted into the box corer and used for chemoautotrophy measurements ($n=3$). A second set of cores (10 cm outer diameter and 30 cm in length) was also sampled from the box corer and was used for TOU measurements ($n=3$). No microprofiling was performed for these sites due to the high risk of breaking micro-sensors due the high content of shell fragments. Bioturbating macrofauna was observed at all stations. Fauna included sand tubeworms and brittle stars at the Dogger bank stations (NS.4 and NS.8), and sea urchins, razor clams, and polychaetes towards the Frisian front (NS.15) and near the Dutch coast (NS.13).

To examine chemoautotrophy in a high latitude depositional area, the Kobbefjord (KF) site was selected, which is located in SW Greenland near the city of Nuuk and part of the Marine Basic Nuuk monitoring program operated by the Nuuk Ecological Research Operations (NERO). Kobbefjord contains numerous basins and sills, has a maximum water depth of 140 m and receives freshwater inputs from rivers and melting of glaciers (Sørensen et al., 2015). The sampling site was located in the central basin at a water depth of 110 m which was sampled on four occasions from June 2011 to May 2012 (Table 1) to determine seasonal variations of the benthic chemoautotrophy. Sediment cores were retrieved in Plexiglas liners (6 cm outer diameter and 50 cm in length) using a Kajak sampler (KC Denmark). On board, cores were subsampled with polycarbonate core liners (4 cm outer diameter and 20 cm in length) for chemoautotrophy incubations ($n=3$). A separate set of cores was used to measure CO_2 and O_2 benthic fluxes, as well as O_2 microsenor profiling as described in (Sørensen et al., 2015). Small worms were found in sediment cores throughout the year.

6.5.2 Supplementary tables and figures

Table S1. List of coastal areas in literature where chemoautotrophy has been evaluated. Chemoautotrophy rates, total (TOU) and dissolved oxygen uptake (DOU) are reported as $\text{mmol m}^{-2} \text{d}^{-1}$. ϕ : porosity, OC: organic carbon content, T: *in situ* temperature in Celsius, αCO_2 : CO_2 fixation efficiency, OPD: oxygen penetration depth. See text for the description of the different sediment habitats (SOx: sulfur oxidation). *Table S1 continues.*

Site	Code	Date	T (°C)	Depth (mbsl)	ϕ	OC %	Sediment habitat	Reference
Gullmar Fjord SW Sweden	StnL	Sept-81	NR	30	0.5	3.1	Bioturbated	Enoksson & Samuelsson 1987 ++
Marine lagoon Faellesstrand NE Fyn Island, Denmark (incubated sediment for 24 days)	I.MLF24	Aug-94	NR	0.4	0.32	0.5	Advective	Thomsen & Kristensen 1997 ++
Janssand sandflat (upper flat), German Wadden Sea	JS06	Oct-06	6	0	0.45	0.7 d	Bioturbated	Lenk et al., 2010 ++
Rattekaai Salt Marsh Oosterschelde, the Netherlands	RK05	Apr-05	14	0	0.6	NR	Canonical SOx	Chapter 2 (Boschker et al., 2014) +
	RK06	May-06	17	0	0.6	2		
Zandkreek (Oosterschelde) the Netherlands	ZK05	Apr-05	14	0	0.5	NR	Bioturbated	
	ZK07	Oct-06	13	0	0.5	0.6		
Marine Lake Grevelingen, the Netherlands (time series incubation experiment)	I.MLG1	Mar-12	16	34	0.9	3.4	Canonical SOx	Chapter 3 (Vasquez-Cardenas et al., 2015) +
	I.MLG9						Electrogenic SOx	
	I.MLG13							
	I.MLG12	Aug-12						
Marine Lake Grevelingen, the Netherlands	MLG1m	Mar-12	5	34	0.89	4	Electrogenic SOx	Chapter 4 (Lipsewers et al.) +
	MLG2m			24			Vacuolated Beggiatoa	
	MLG3m			17			Electrogenic SOx	
	MLG1a	Aug-12		34		3.7	Canonical SOx	
	MLG2a			24				
	MLG3a			17				
Brackish lagoon, Brazil	Br1	Sep-08	25	2	NR	0.2	NA	Santoro et al., 2013 ++
	Br2			1.8	NR	8		
	Br3			1.8	NR	9.4		
Intertidal sand, France	CS	Jul-13	19	0	NR	NR	NA	Dyskma et al., 2016 +++
	CA	Jul-13	21	0	NR	NR	NA	
	JS13	Apr-13	13	0	0.35	0.11	Bioturbated	

Table S1 cont.

Code	Total chemoautotrophy mean \pm SD (sediment layer cm)	Relative contribution of surface chemoautotrophy (0-1 cm)	TOU mean \pm SD	α_{CO2} TOU	DOU mean \pm SD	α_{CO2} DOU	OPU (mm)	Reference
StnL	4.8 (0-4)	0.32	22	0.22	NR	NA	NR	Enoksson & Samuelsson 1987 ++
I.MLF24	3.1 (0-3.5)	0.18	18	0.17	18*	0.03	NR	Thomsen & Kristensen 1997 ++
JS06	3 (0-3)	0.32	~145 e	~0.02	~47 e	~0.02	<20 e (low tide)	Lenk et al. 2010 ++
RK05	5.5 \pm 1.9 (0-5)	0.93	NR	NA	17 \pm 3	0.32	0.45	Chapter 2 (Boschker et al., 2014) +
RK06	36.3 \pm 4.8 (0-5)	0.98	NR		192 \pm 41	0.19	0.23	
ZK05	2.6 \pm 0.3 (0-5)	0.92	NR		15 \pm 0.4	0.17	1.7	
ZK07	2.9 \pm 0.2 (0-5)	0.61	NR		16 \pm 2	0.18	0.95	
I.MLG1	1.6 \pm 0.5 (0-3)	0.84	51*	0.03	51 \pm 4	0.03	0.5	Chapter 3 (Vasquez-Cardenas et al., 2015) +
I.MLG9	9.6 \pm 2.4 (0-3)	0.79	45*	0.21	45 \pm 3	0.17	0.4	
I.MLG13	10.9 \pm 0.9 (0-3)	0.38	76*	0.14	76 \pm 4	0.05	0.6	
I.MLG12	7.3 \pm 2.2 (0-3)	0.55	78*	0.09	78 \pm 18	0.05	0.2	
MLG1m	3.1 \pm 0.5 (0-5)	0.38	30 \pm 0.6 f	0.10	18 \pm 2 f	0.07	1.8	Chapter 4 (Lipsewerts et al.) +
MLG2m	1.9 \pm 0.1 (0-5)	0.74	26 \pm 0.2 f	0.07	16 \pm 3 f	0.09	2.6	
MLG3m	1.4 \pm 0.3 (0-5)	0.44	26 \pm 2 f	0.05	17 \pm 6 f	0.04	2.4	
MLG1a	0.2 \pm 0.07 (0-5)	0.72	0.5 \pm 0.5 f	NA	0 f	NA	0	
MLG2a	0.8 \pm 0.3 (0-5)	0.59	12 \pm 1.2 f	0.06	0 f	NA	0	
MLG3a	1.1 \pm 0.5 (0-3)	0.78	19 \pm 1 f	0.06	14 \pm 2 f	0.06	1.1	
Br1	1.0 \pm 0.4 (0-1)	NA	37 \pm 5 f	0.03	NR	NA	NR	Santoro et al., 2013 ++
Br2	1.4 \pm 2.6 (0-1)		97 \pm 7 f	0.01				
Br3	0.8 \pm 0.2 (0-1)		51 \pm 3 f	0.02				
CS	0.38 (0-1)	NA	NR	NA	NR	NA	NR	Dyskma et al., 2016 +++
CA	0.50 (0-1)							
JS13	1.1 (0-1)							

Technique used to measure chemoautotrophy rates (*i.e.* dark carbon fixation) in sediments: + ^{13}C PLFA-SIP method / ++ ^{14}C total / +++ ^{14}C - FISH - FACS - Scintillography

d) Billerbeck et al., 2006 ; e) Jansen et al., 2009; f) Seitaj et al., 2015

*TOU and DOU are considered equal in incubated sediments as sediments were homogenized and fauna removed.

NR: Not reported; NA: Not applicable

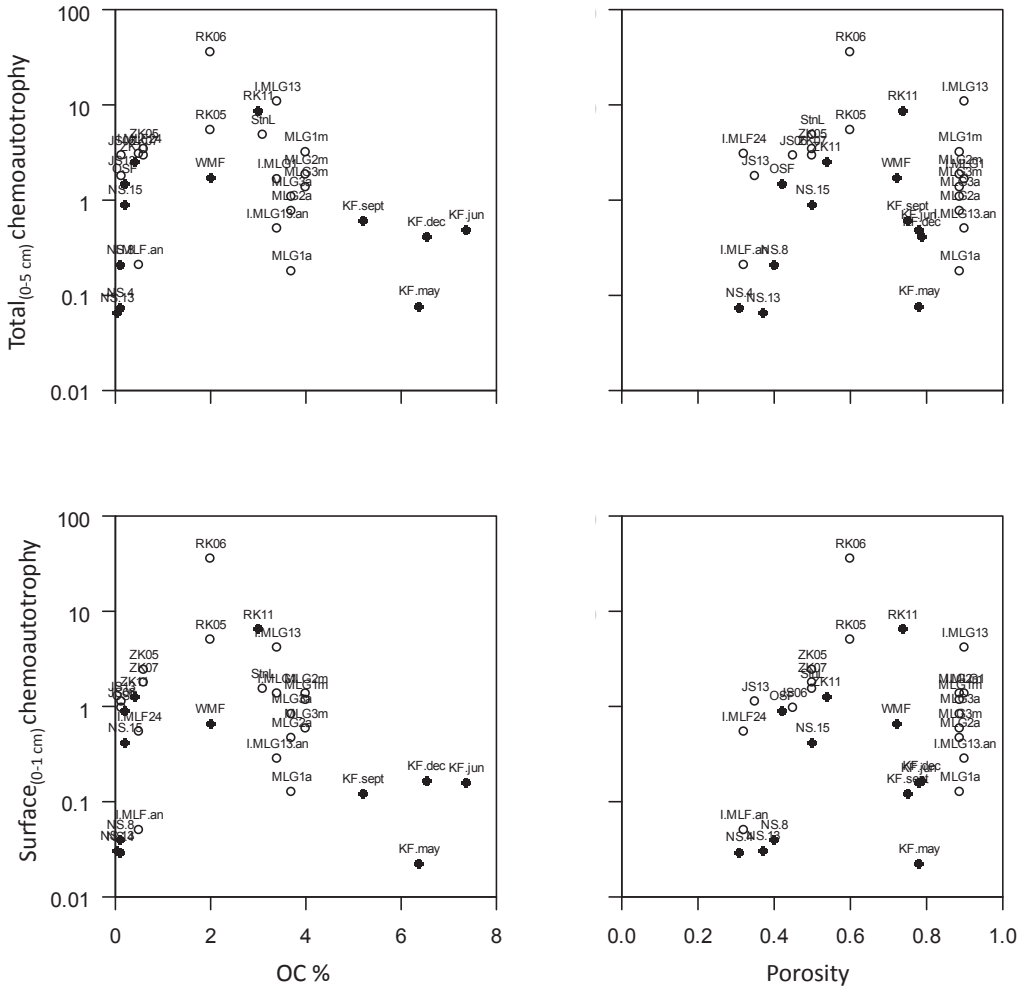


Figure S1. Total (top row) and surface chemoautotrophy rates (bottom row) in relation to organic carbon (OC) content (left column) and porosity (right column). Black circles are data from this study and white circles are from literature. Abbreviation of the site names can be found in Table 1 and Table S1.

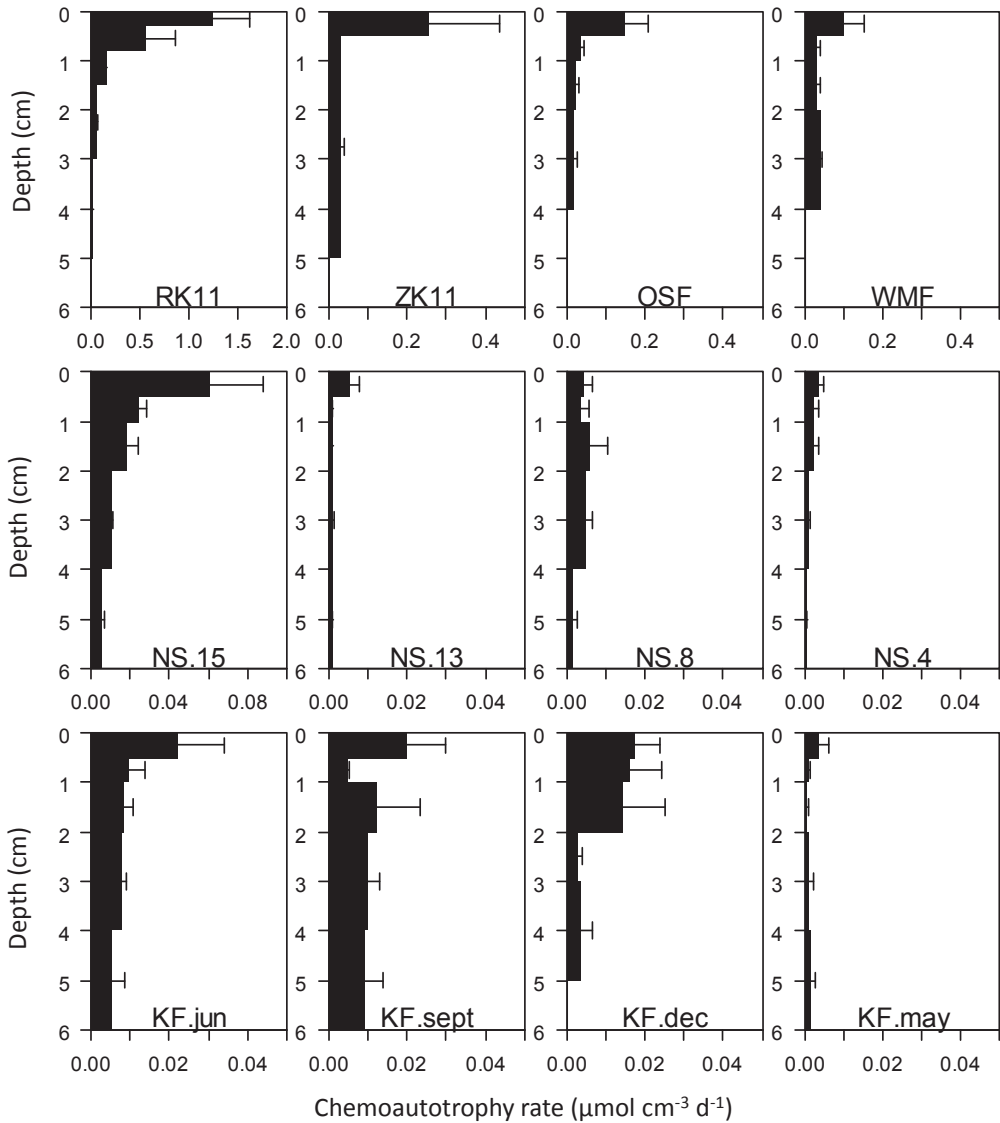


Figure S2. Depth distribution of chemoautotrophic activity from four intertidal sites in the Netherlands (top row), four sites along a transect in the southern North Sea (middle row), and Greenland site during four sampling campaigns (bottom row). Abbreviation of the site names can be found in Table 1. Note change of scale for chemoautotrophy rates.

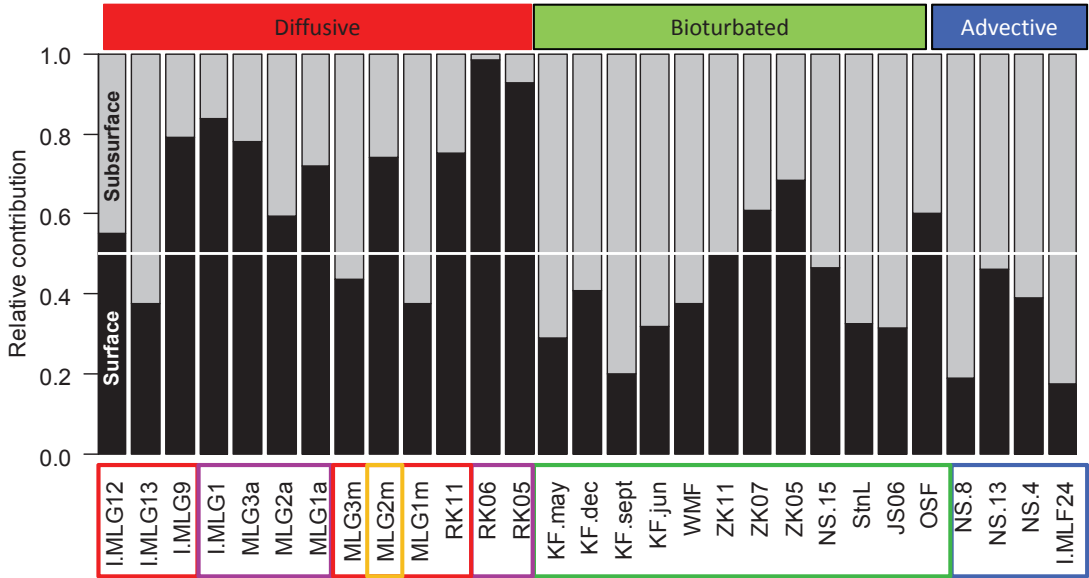


Figure S3. Relative contribution of surface layer (0-1 cm; black) and subsurface layer (1-5 cm; grey) to the chemoautotrophic activity for the coastal sediments in the dataset. Sediments are organized (left to right) based on porosity in a decreasing order (Table 1 and S1). The white horizontal line indicates an equal contribution of surface and subsurface activity. Abbreviations of sampling sites are listed in Table 1 and S1. (red: electrogenic sulfur oxidation, purple: canonical sulfur oxidation, orange: nitrate-storing Beggiatoaceae, green: bioturbated, blue: advective)

Discussion

Chemoautotrophy is normally associated to extreme environments such as hydrothermal vents where chemoautotrophic bacteria are the primary producers. However chemoautotrophy is considered to be a minor process in coastal sediments although it has not been thoroughly studied. This thesis increased the number of chemoautotrophy measurements from 6 (in the literature) to 32 across a broad range of coastal sediments, and in doing so, shows the great potential for chemoautotrophic production in coastal areas. This final chapter thus synthesizes the collective findings of this research project and points out unresolved issues regarding the three main objectives of the thesis: key microbial players performing chemoautotrophy, regulatory factors, and the importance of chemoautotrophy in the coastal ocean.

7.1 Niche differentiation between chemoautotrophic bacteria

In this thesis, a broad range of coastal sediments were surveyed spanning cohesive and permeable sediments, bioturbated and non-bioturbated, from intertidal areas to the continental shelf, including temperate and subpolar sediments. DNA-based techniques were used to identify potential key players as well as biomarker analysis (PLFA-SIP) to quantify chemoautotrophic activity throughout the sediment. The majority of the chemoautotrophic bacteria identified in the sediments surveyed were sulfur-oxidizers from the Gamma- and Epsilonproteobacteria groups, while a minority of Deltaproteobacteria sequences were identified from bacteria capable of S-disproportionation (Chapter 2, 3, 4). Abundant sulfur-oxidizers are not unexpected in coastal sediments, as most of the energy produced through mineralization is bound in reduced sulfur compounds (Howarth 1984). Moreover, the incorporation of bicarbonate in to biomarkers (*i.e.* PLFA-SIP) resembled PLFA-SIP patterns of sulfur-oxidizing Gamma- and Epsilonproteobacteria, indicating that not only were these bacteria present but they were also active in the sediment. PLFA signatures similar

to sulfate reducing bacteria from the Deltaproteobacteria were also distinguished indicative of an active group of anaerobic chemoautotrophic bacteria in anoxic sediments (Chapter 2, 4, 5). This diverse group of sulfur-dependent chemoautotrophic bacteria suggests a complex niche differentiation linked to different biogeochemical sediment types. Three biogeochemical sediment regimes were defined based on pore water transport mechanisms: advective, bioturbated and diffusive (Chapter 6). (Advective sediments will be discussed latter on in this chapter.)

Diffusive sediments exhibit small grain size, high organic matter content, low porosity, and high free sulfide content in pore water (in the top 5 cm) with little to no bioturbation. Diffusive sediments were found in a seasonally hypoxic marine lake and a salt marsh which were characterized by sulfur-oxidizing Gamma- and Epsilonproteobacteria (Chapters 2, 3, 4). Filamentous Gammaproteobacteria and Epsilonproteobacteria are frequently found in sulfidic environments due to their unique metabolic capacities. On the one hand, filamentous members of the Beggiatoaceae family (Gammaproteobacteria) have a high affinity for H_2S and high uptake rates that allow them to compete with chemical sulfide oxidation at O_2 - H_2S interfaces, resulting in chemoautotrophic sulfur oxidation accounting up to 90% of the benthic O_2 -consumption (Jørgensen 1982). Furthermore, vacuolated Beggiatoaceae can out-compete other sulfur-oxidizers because they are capable of storing nitrate intracellularly and oxidizing sulfide to sulfate in two spatially separated reactions which lead to the formation of a cm-thick suboxic zone, *i.e.* sediment devoid of both oxygen and free sulfide in pore water (Sayama et al., 2005; Seitaj et al., 2015; Fig.1). On the other hand, Epsilonproteobacteria are metabolically versatile micro-organisms that can oxidize sulfide, thiosulfate and elemental sulfur under micro-aerobic and anaerobic conditions (Campbell et al., 2006; Takai et al., 2006; Labrenz et al., 2013; Fig. 1). They usually characterize oxic-anoxic interfaces in deep-sea vents, sulfidic cave waters, and chemoclines but are rarely reported in coastal sediments (Campbell et al., 2006) although they have recently been found in tidal pools and intertidal sediments where they oxidize S^0 aerobically or with nitrate (Pjevac et al., 2014). Niche differentiation between these two Proteobacteria groups has been attributed to 1) the ratio between oxygen and sulfide in cave waters and cold seeps (Macalady et al., 2008; Grünke et al., 2011), 2) sulfur substrate preference, *i.e.* Gammaproteobacteria thrive on free sulfide while Epsilonproteobacteria prefer elemental sulfur, in sulfidic intertidal sediments of the German Wadden Sea (Pjevac et al., 2014), 3) different sulfur oxidizing pathways as speculated for deep sea vents (Nakagawa & Takai 2008; Yamamoto & Takai 2011). Interestingly, the study on the chemoautotrophic community in the seasonally hypoxic marine lake suggests that Epsilonproteobacteria may interact metabolically with nitrate-storing Beggiatoaceae (Chapter 4) whereas Epsilonproteobacteria were apparently not present in salt marsh sediments alongside the Beggiatoaceae

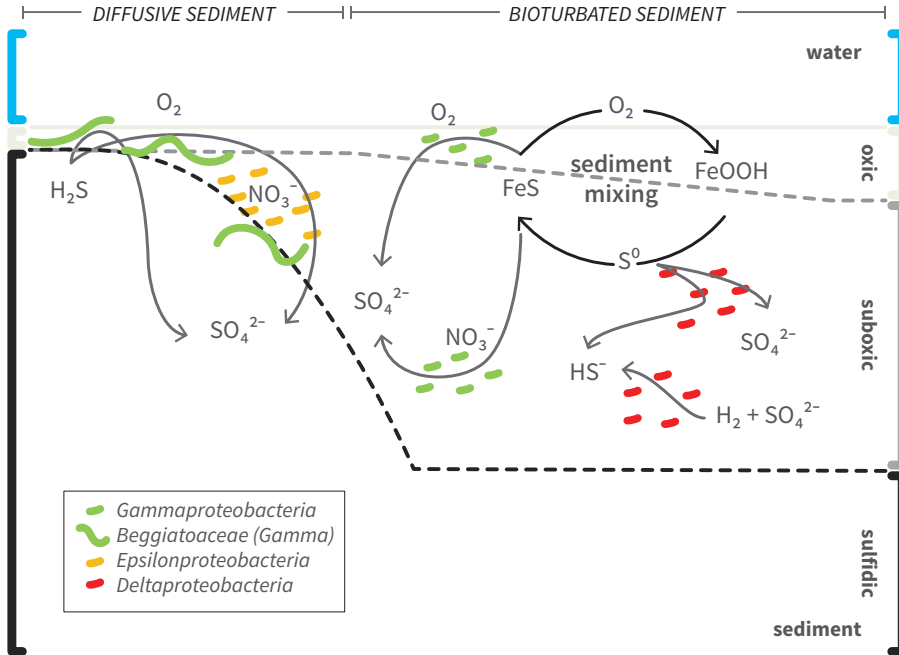


Figure 1. Potential niche differentiation amongst chemoautotrophic bacteria in coastal sediments. Electron donors (reduced S-species) and acceptors (O_2 , NO_3^- , H_2S , SO_4^{2-}) are shown. Black arrows represent abiotic reactions and grey arrows indicate sulfur-oxidation. Light grey area indicates the oxic zone, grey area indicates the suboxic zone, and black indicates sediment rich in free-sulfide.

mats (Chapter 2). Hence could fluctuating oxygen conditions such as those occurring in seasonally hypoxic basins favor the development of Epsilonproteobacteria? Or could Beggiatoaceae release nitrate while diving into deeper anoxic sediments which would serve as electron donor for Epsilonproteobacteria? This thesis thus raises questions as to what environmental factors promote the co-occurrence of filamentous Gamma- and Epsilonproteobacteria in diffusive sediments, and hence which possible metabolic mechanism may drive this interaction.

Contrary to diffusive sediments, mostly single-cell sulfur-oxidizing Gammaproteobacteria were found in bioturbated sediments. Sediment mixing by macrofauna promotes iron cycling between FeOOH and FeS which prevents the accumulation of free sulfide in pore water (Seitaj et al., 2015), thus iron sulfide becomes the main sulfur oxidation pathway for chemoautotrophic bacteria in these sediments. Accordingly, single-cell Gammaproteobacteria identified in bioturbated sediments were closely related to bacteria capable of oxidizing reduced sulfur compounds with either oxygen or nitrate/nitrite (Ghosh & Dam 2009; Fig. 1). In the Janssand intertidal

sandflat (German Wadden Sea) single-cell Gammaproteobacteria were identified as the main chemoautotrophic bacteria in the sediment accounting for 40-70% of the total chemoautotrophic production measured (Lenk et al., 2010). In deeper anoxic sediments however Deltaproteobacteria were also active (Fig.1). Anaerobic chemoautotrophy in bioturbated intertidal sediments (Zandkreek) can account for up to 90% of the dark carbon fixation which was attributed mainly to Deltaproteobacteria and to a lesser degree to Gammaproteobacteria (Miyatake 2011). Chemoautotrophic Deltaproteobacteria have been found to mainly disproportionate elemental sulfur in coastal sediments (Pjevac et al., 2014). Deltaproteobacteria from the Desulfobulbaceae family such as *Desulfocapsa* sp. and *Desulfobulbus propionicus*, identified in this study (Chapter 2) are capable of autotrophic growth via H₂-oxidation or disproportionation of elemental sulfur, thiosulfate, and sulfite (Dannenberg et al., 1992; Finster et al., 1998; Pagani et al., 2011). Hence in bioturbated sediments there appears to be a clear separation between the main chemoautotrophic groups (Gamma- and Deltaproteobacteria) mainly driven by the availability of oxygen and nitrate rather than by reduced sulfur compounds.

Overall this thesis shows that chemoautotrophic community assemblages differ between coastal sediments given the availability and transport (diffusive, bioturbated, advective) of electron donors (H₂S, S⁰, FeS) and acceptors (O₂, NO₃⁻, S⁰) determined by the biogeochemical characteristic of the sediment. Further characterization of the chemoautotrophic community composition across diverse coastal sediments should thus focus on reduced sulfur, oxygen, and nitrate availability in the sediment in relation to the sulfur oxidation pathways present in the main bacterial groups to link metabolic function with habitat preference among Epsilon-, Delta-, filamentous and single-cell Gammaproteobacteria.

7.2 Regulatory factors of chemoautotrophic activity

Chemoautotrophy studies of coastal sediments are scarce in literature, with only four studies reporting dark carbon fixation rates: two for subtidal sediments in the Baltic Sea (Enoksson & Samuelsson 1987; Thomsen & Kristensen 1997), one intertidal sandflat in the German Wadden sea (Lenk et al., 2010), and three tropical brackish lakes in Brazil (Santoro et al., 2013), accordingly the environmental factors that control chemoautotrophy are largely unknown. Only Santoro et al., (2013) had studied the possible correlation between dark carbon fixation and bacterial production, sediment respiration or organic matter content. However they found no clear correlations amongst their dataset (including freshwater, brackish and marine lakes, 11 observations in total). On the contrary, the analysis performed here on the 6 observations from the literature plus the 26 observations in this thesis, resulted in a clear power relation between chemoautotrophy and benthic oxygen consumption (TOU

and DOU) which translates into an inverse relationship between chemoautotrophy and water depth (Chapter 6). Although this thesis more than quadruples the number of chemoautotrophy observations in literature, the compiled chemoautotrophy dataset is still missing more observations from continental shelf sediments and lower latitudes which are necessary to precise the correlation between chemoautotrophy and benthic oxygen consumption.

Nonetheless, the strong correlation between benthic oxygen consumption and dark carbon fixation, using the TOU as a proxy for mineralization rates, allowed the estimation of CO₂ fixation efficiencies of the chemoautotrophic community. CO₂ fixation efficiencies tended to increase from continental shelf sediments towards intertidal areas, as well as from advective to diffusive-driven sediments (Chapter 6). These trends led us to identify three determining factors of CO₂ fixation efficiencies: (1) the production efficiency γ , which scales the production rate of a given electron donor to the mineralization rate, (2) the reoxidation efficiency λ of the electron donor (*i.e.*, how much is effectively used for microbial respiration and not diverted to abiotic oxidation), and (3) the CO₂ fixation yield μ (e.g., the moles of CO₂ fixed per mole of electron donor oxidized). In diffusive-driven salt marsh sediments for example, high mineralization rates are observed where sulfate respiration can represent 70% of the organic matter mineralized ($\gamma=0.70$) with only ~5% of the sulfide buried in the sediment ($\lambda=0.95$, Howarth 1984). Some of the sulfidic sediments studied in this thesis presented abundant chemoautotrophic *Beggiatoa*-like filaments that can present energetic efficiencies of at least 21% ($\mu=0.21$, Howarth 1984). Thus the resulting chemoautotrophic production accounts for 14% of the carbon respired ($0.70 \times 0.95 \times 0.21 = 0.14 \times 100 = 14\%$). In the case of Rattekaai salt marsh sampled in 2006 with respiration rates of 197 mmol C m⁻² d⁻¹, chemoautotrophic production would be estimated at 28 mmol C m⁻² d⁻¹ (Fig. 2a). Higher rates (36 mmol C m⁻² d⁻¹) were measured which indicate higher efficiencies by *Beggiatoa* (up to 0.37) or a higher contribution of sulfate reduction to the total respiration (up to 90%, Howarth 1984). In contrast, advective-driven sediments such as those found in the North Sea, present respiration rates of ~11.5 mmol C m⁻² d⁻¹ (Brenner et al., 2015) and sulfate reduction rates ranging from 0.5 to 3.2 mmol SO₄⁻² m⁻² d⁻¹ (Upton et al., 1993) which suggest a low percentage of the total respiration mediated by anaerobic mineralization in these permeable sediments. Considering this estimated 16% contribution from sulfate reduction to the benthic respiration ($\gamma=0.16$) for the North Sea sediments near Dogger Bank (respiration rate: ~3.8 mmol C m⁻² d⁻¹), with limited burial of sulfide (~5%, $\lambda=0.95$) given the high flushing of the sediment and a low growth yield of 10% for chemoautotrophic bacteria ($\mu=0.10$, mostly nitrifying bacteria; Middelburg 2011) then the potential chemoautotrophy production (0.06 mmol C m⁻² d⁻¹) scales well with the measured activity (0.07 mmol C m⁻² d⁻¹; Fig. 2b).

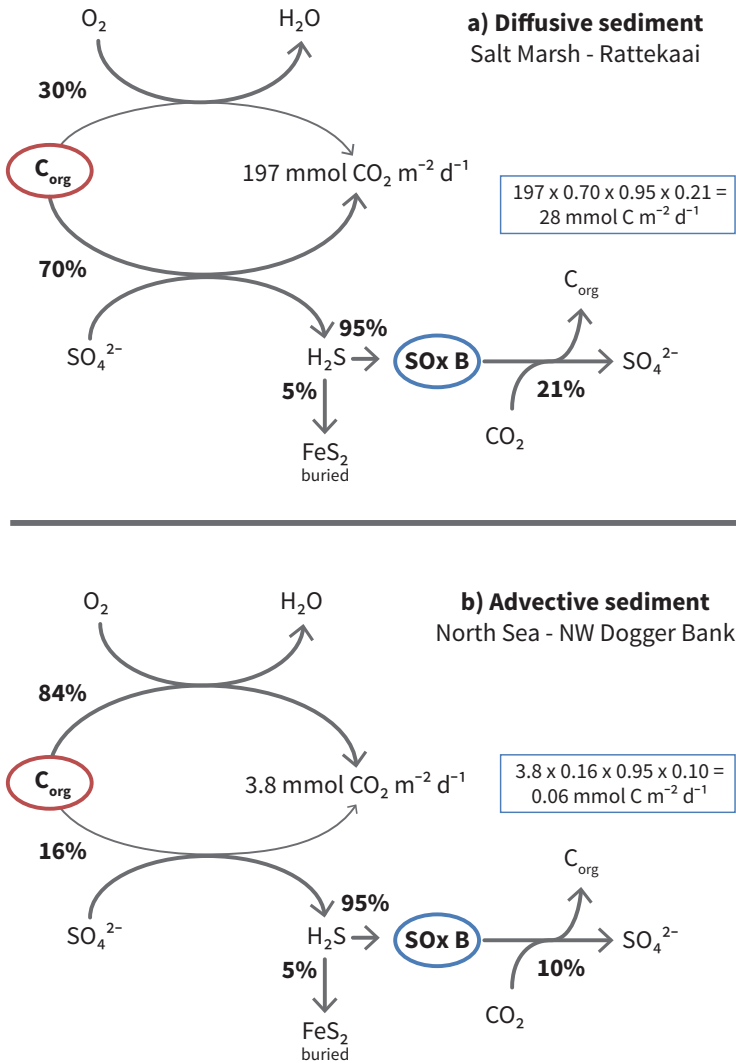


Figure 2. Coupling of carbon and sulfur cycles, and the potential rates of chemoautotrophic production in sediments based on CO₂ fixation efficiencies. Two biogeochemical sediment regimes are depicted: diffusive driven (a) and advective-driven (b). C_{org}: organic carbon, SOx B: sulfur-oxidizing chemoautotrophic bacteria.

7.3 Depth-distribution of chemoautotrophy

This thesis describes for the first time five distinct depth-distribution patterns for chemoautotrophy in biogeochemically different sediments: advective-driven sediments, canonical sulfur oxidation, vacuolate Beggiatoaceae, bioturbated and electrogenic sulfur oxidation (Chapter 6). Firstly, uniformly distributed low chemoautotrophic activity with sediment depth was found in advective sediments characterized by large grain size and low organic matter content. In these sediments, bottom water movements continuously flush the sediment matrix which results in deep oxygen penetration that can sustain high mineralization rates via aerobic pathways (Huettel et al., 2003). The low production of sulfide via sulfate reduction thus prevents high rates of reoxidation by chemoautotrophs throughout the sediment. The second scenario is the classical depth-distribution of chemoautotrophy whereby high chemoautotrophy occurs through canonical sulfur oxidation (Meysman et al., 2015) at the sediment surface where both electron acceptors and donors are abundant when O_2 - H_2S overlap. In deeper sediment reoxidation is limited because below the first few millimeters of the sediment oxygen and nitrate are not present. In the third scenario, deeper chemoautotrophic activity is apparent in the presence of nitrate-storing Beggiatoaceae. These chemoautotrophic bacteria glide through the sediment to oxidize sulfide and thus can exhibit growth in anoxic sediment.

In the fourth biogeochemical scenario, bioturbated sediments, variable subsurface enhancement of chemoautotrophy was found. Bioturbation has long been considered to create a secondary reoxidation area along burrow structures through ventilation of the burrow by the fauna that pump electron acceptors into deep sediment where reduced compounds are abundant (Aller 1988; Kristensen & Kostka 2005). However, given the different modes of irrigation and ventilation capacities between polychaetes, bivalves and other bioturbating fauna typical of marine sediments (Kristensen et al., 2012), the effect of bioturbation on the reoxidizing chemoautotrophic bacterial community may vary depending on the macrofauna involved. This thesis shows that the effects on the chemoautotrophic community in fact differed depending on the functional traits of two bioturbating polychaetes; *Nereis diversicolor* and *Marenzelleria viridis* (Chapter 5). The strong ventilation but low bioirrigation capacity in the open-ended burrows of *N. diversicolor* resulted in enhanced aerobic chemoautotrophic activity (e.g. sulfur oxidizing and nitrifying bacteria) along the burrow, whereas the slower ventilation and higher irrigation by *M. viridis* induced an advective mode of pore water transport that promoted anaerobic chemoautotrophy around the blind-ended burrow and within the subsurface sediment. Thus on a small-scale (e.g. burrow environment) bioturbating fauna can have a species-specific enhancement on the chemoautotrophic activity. However the limited number of studies in literature quantifying the effects

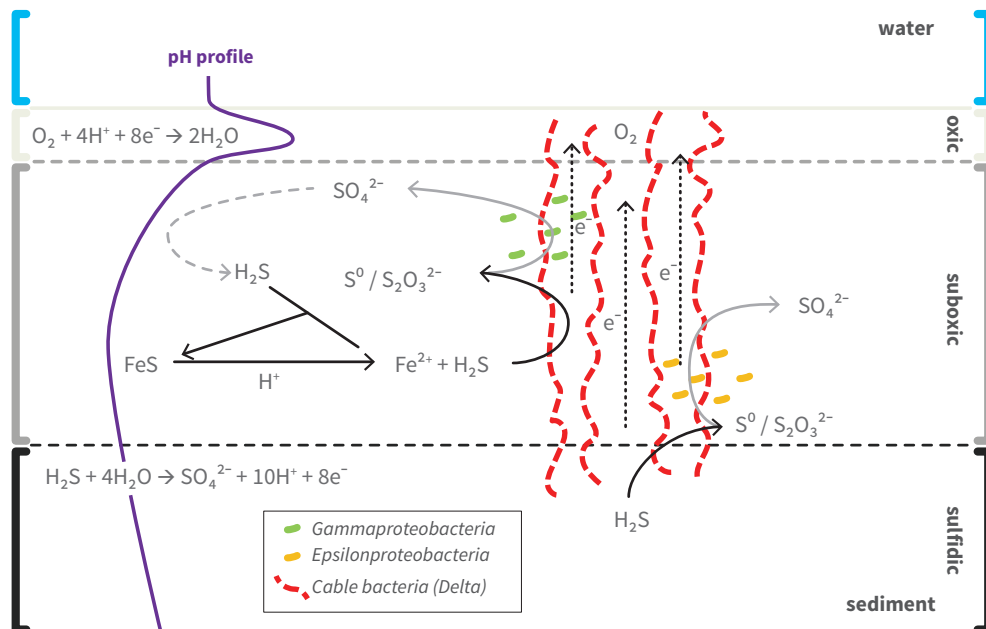


Figure 3. Potential scenario for a SO_x-consortium between electrogenic sulfur-oxidizing cable bacteria and chemoautotrophic sulfur-oxidizing bacteria (Gamma- and Epsilonproteobacteria). Cable bacteria perform the initial oxidation of sulfide to elemental sulfur or thiosulfate (curved black arrows) which is then oxidized to sulfate by chemoautotrophic bacteria using the cable bacteria network as electron acceptor (curved grey arrows). pH profile of electrogenic sulfur oxidation is shown in purple. Straight black arrows represent abiotic reactions and broken grey arrow indicates sulfide production through sulfate reduction. Light grey area indicates the oxic zone, grey area indicates the suboxic zone, and black indicates sediment rich in free-sulfide.

of bioturbating fauna of the depth distribution of chemoautotrophy in combination with the diverse types of ventilation of burrows and irrigation (Kristensen et al., 2012) raises the question: are the effects of bioturbation on chemoautotrophy species-specific or can they be grouped by functional traits (type-specific)?

The final scenario was an unexpected finding as uniformly distributed high chemoautotrophic activity was observed from the surface to cm-depth in diffusive sediments that presented electrogenic sulfur oxidation (e-SO_x) by cable bacteria. Even more remarkable was the fact that dark carbon fixation activity developed in unison with the deepening of the cable bacteria network (Chapter 3). Dedicated laboratory experiments (Chapter 3) and seasonal observations in *in situ* marine lake sediments (Chapter 4) suggested a tight metabolic link between the cable bacteria and chemoautotrophic bacteria closely related to sulfur-oxidizing Gamma- and Epsilonproteobacteria (Fig. 3). The cm-deep chemoautotrophic activity, in the absence of both electron

acceptors and donors is speculated to occur via a SO_x-consortium with the cable bacteria. The complete oxidation of sulfide in e-SO_x sediments may thus be controlled by this bacterial consortium whereby the initial oxidation of sulfide to sulfur intermediates (elemental sulfur or thiosulfate) is performed by the cable bacteria. These sulfur oxidation intermediates then become readily available as electron donors for the surrounding chemoautotrophic sulfur-oxidizers which use the cable bacteria filaments as an electron acceptor potentially by connecting to the periplasm via nanowires, nanotubes, or fimbriae (Widdel & Pfennig 1982; Reguera et al., 2005; Dubey & Ben-Yehuda 2011). In addition, within the suboxic zone sulfide is not only produced through sulfate reduction but also from the dissolution of iron sulfide due to the high pH caused by the electrogenic sulfur oxidation (Risgaard-Petersen et al., 2012). To date, the precise mechanism by which this newly recognized coupling of chemoautotrophic and cable bacteria activity remains elusive. Moreover, it is unknown, if this potential metabolic link between the cable bacteria and sulfur-oxidizing chemoautotrophs holds true for other marine and freshwater sediments or other types of microbial metabolisms.

7.4 Importance of chemoautotrophy in carbon and sulfur cycling

Chemoautotrophy has largely been ignored in coastal carbon budgets as it is estimated to account for less than 10% of the carbon respired (Jørgensen & Nelson 2004). Although the mean CO₂ fixation efficiency of 6% is in line with previous estimations, CO₂ fixation efficiency found for near-shore sediment (9%) and salt marshes (21%) indicate a much greater chemoautotrophic potential in these areas. Thus chemoautotrophic production can contribute substantially to the carbon cycling, especially in salt marshes, which had not been previously quantified (Chapter 2, 6).

Moreover, the estimated yearly production of dark carbon fixation in coastal sediments (0.06 Pg C y⁻¹) in this thesis exceeds the autotrophic production of deep-sea vent ecosystems by one-order of magnitude (Raven 2009). In hydrothermal vents chemoautotrophs are the main primary producers (Howarth 1984; Nakagawa & Takai 2008) and they sustain numerous symbiotic relationships with invertebrates (Dubilier et al., 2008), thus chemoautotrophic bacteria in coastal sediments have the potential to sustain an even greater community of macrofauna. However, the role of chemoautotrophic production as an alternative food source for invertebrates in coastal sediments has not been thoroughly studied. One study showed that the diet of head-down deposit feeder *Heteromastus filiformis* largely depends on heterotrophic rather than chemoautotrophic bacteria (Clough & Lopez 1993) whereas the polychaete *Capitella* sp. showed a selective utilization of chemoautotrophs as food source in sulfide-rich sediments under laboratory conditions (Tsutsumi et al., 2001). Incubation experiment with polychaetes

Nereis diversicolor and *Marenzelleria viridis* also suggests consumption of chemoautotrophic organic matter by both polychaetes, with a potentially greater contribution to the diet of *M. viridis* (Chapter 5). Hence targeted stable isotope studies should be performed to determine the extent of the contribution of chemoautotrophs to the diet of different species and to the coastal food web in general.

The diverse group of sulfur-oxidizing bacteria found also contributes to the sulfur cycling in coastal sediments which has a considerable effect on the functioning of the ecosystem. In the study on the effects of seasonal hypoxia on the benthic chemoautotrophic community, sulfur-oxidizing Gamma- and Epsilonproteobacteria were found to potentially work together with cable bacteria to reoxidize pore water sulfide (Chapter 4). Electrogenic sulfur-oxidizing cable bacteria have been proposed to create a buffering area of iron oxides in spring that binds to sulfide in summer preventing the diffusion of sulfide into bottom waters (Seitaj et al., 2015). Likewise, the episodic occurrence of sulfide in bottom waters of the southwest African shelf has been reported to disappear in unison with a bloom of chemoautotrophic Gamma- and Epsilonproteobacteria (Lavik et al., 2009). Assuming that the SO_x-consortium between cable bacteria and chemoautotrophic Gamma- and Epsilonproteobacteria is mutually beneficial then one could hypothesize that this SO_x-consortium is responsible for the absence of sulfide in bottom water in marine Lake Grevelingen during the summer hypoxia. The environmental controls of euxinia (*i.e.* build-up of sulfide) in low oxygen bottom waters are largely unknown but sulfur-oxidizing chemoautotrophic bacteria may play a pivotal role in detoxifying sulfidic sediments.

Summary

Chemoautotrophy is the process by which micro-organisms fix CO₂ by obtaining energy from the oxidation of reduced compounds such sulfide and ammonium (e.g. sulfur oxidation and nitrification). This metabolism is widespread in nature and is vastly studied in extreme environments such as hydrothermal vents and chemoclines in hypoxic basins where it contributes greatly to primary production. However, chemoautotrophs are easily overlooked in coastal areas where the photoautotrophic organisms are the main primary producers. Moreover, chemoautotrophs are estimated to have CO₂ fixation efficiencies of less than 10% (*i.e.*, the ratio of chemoautotrophic CO₂ fixation over the total CO₂ released from the mineralization of organic matter), which results in the exclusion of chemoautotrophic carbon production from coastal carbon budgets. Nonetheless, the production of sulfide (the main electron donor for chemoautotrophic bacteria in sediments) is much higher in coastal sediments than in hydrothermal vent systems, which suggests a greater potential for chemoautotrophic sulfur oxidizers in coastal sediments. In fact, chemoautotrophs have been shown to fix up to 22% of the carbon respired in subtidal sediments, and sulfur oxidation by large filamentous bacteria (Beggiatoaceae) can account for up to 90% of the oxygen respiration in sediments with overlapping O₂ and H₂S. Thus the aim of this thesis was to assess chemoautotrophic activity in a range of coastal environments by identifying potential key players, determining regulatory factors of the process and evaluating the importance of chemoautotrophic activity in coastal ocean sediments.

The majority of chemoautotrophic bacteria identified through sequencing (16S rRNA gene and 16S rRNA, and carboxylation genes of two carbon fixation pathways: the Calvin Benson-Bassham and the reductive tricarboxylic acid cycles) was related to sulfur oxidizing bacteria, from the Gamma-, Epsilon- and Deltaproteobacteria clades (Chapters 2, 3, 4). The co-occurrence of these diverse groups of sulfur-oxidizing chemoautotrophic bacteria may be attributed to a complex niche differentiation driven most likely by the availability of different sulfur species (free sulfide, iron sulfide, thiosulfate, elemental sulfur) in the different sediment types. For example, filamentous Beggiatoaceae (Gammaproteobacteria) are characteristic for cohesive, sulfur-rich sediments because they have a high affinity for H₂S and high uptake rates that allow them to compete with chemical sulfide oxidation at O₂-H₂S

interfaces (Chapter 2). Furthermore, vacuolated Beggiatoaceae can outcompete other sulfur-oxidizers because they are capable of storing nitrate intracellularly and oxidizing sulfide to sulfate in two spatially separated reactions (Chapter 4). Metabolically versatile Epsilonproteobacteria were also found in this sediment type where they probably oxidize elemental sulfur aerobically or with nitrate. The research described in this thesis suggests that these Epsilonproteobacteria may depend on the activity of filamentous sulfur oxidizers such as vacuolated-Beggiatoaceae and heterotrophic cable bacteria (Chapter 3, 4). Unicellular, sulfur-oxidizing Gammaproteobacteria also appear to be metabolically linked to cable bacteria in cohesive sediments but the exact mechanism remains elusive (Chapter 3, 4). In contrast, in bioturbated sediments unicellular Gammaproteobacteria potentially use iron sulfide as their main electron donor (Chapter 2). Lastly, chemoautotrophic Deltaproteobacteria related to sulfate reducers that can disproportionate sulfur were prevalent in deeper anoxic sediment layers and during hypoxic bottom water conditions (Chapter 2, 4).

Rates of bacterial dark carbon fixation by bacteria were surveyed in a variety of coastal sediments covering intertidal flats, a marine lake, nearshore and continental shelf sediments by means of stable isotope probing (^{13}C -DIC) and bacterial biomarker analysis (phospholipid derived fatty acids, PLFA-SIP). In total we report 26 new observations that more than quadruple the existing number (6) of sedimentary chemoautotrophy rates available in the literature. Dark carbon fixation rates ranged from 0.07 to 36 mmol C m⁻² d⁻¹ with highest activity found in cohesive salt marsh sediments, while lowest rates were found in advective-driven continental shelf sediments. The majority of the dark carbon fixation rates (n=17) fell within 1 and 10 mmol C m⁻² d⁻¹. A correlation analysis to determine possible environmental factors that influence the dark carbon fixation rate resulted in a significant power-law correlation between chemoautotrophy rates and the benthic oxygen consumption (Chapter 6). This correlation indicates that as benthic oxygen consumption increases, dark carbon fixation increases more than proportionally with the highest values towards shallower water depth. Using the sediment oxygen uptake rate as a proxy for sediment mineralization we were able to estimate the CO₂ fixation efficiency for the different sediments. Across the dataset, we found a CO₂ fixation efficiency ranging from 0.01 to 0.32 with a median of ~0.06, which corresponds well with the CO₂ fixation efficiency of 0.07 that has been estimated for coastal sediments based on simplified electron balance calculations. When differentiating between three depth zones in the coastal ocean, we found 3% CO₂ fixation efficiency in continental shelf sediments (50-200 m water depth), 9% for nearshore sediments (0-50 m water depth, including intertidal sediments), and 21% for salt marshes (Chapter 6). Thus, chemoautotrophic activity plays a more prevalent role in the carbon cycling in reactive intertidal sediments (especially in salt marshes) than in deeper continental shelf

sediments. With these mean CO₂ fixation efficiencies for the different water depths we estimated for coastal sediments a global chemoautotrophic production of 0.06 Pg C y⁻¹ (Chapter 6). This is two-and-a-half times lower than the conservative estimate of 0.15 Pg C y⁻¹ indicating that previous studies have severely overestimated the contribution of chemoautotrophy in coastal sediments.

Furthermore, five distinct depth-distribution patterns of chemoautotrophy are described that could be linked to three sediment types that differ in the main mode of pore water transport: advective, bioturbated, and diffusive, which align well with sediment characteristics such as grain size, porosity, organic matter content and fauna activity (Chapter 6). In the case of diffusive sediments, the prevalent mode of sulfur oxidation was used to distinguish between three additional categories: electrogenic sulfur oxidation by cable bacteria, sulfide by motile, nitrate accumulating *Beggiatoaceae* and canonical sulfide oxidation within an overlapping O₂-H₂S interface. (1) Sediments with canonical sulfide oxidation had most of the chemoautotrophic activity at the sediment surface where electron donor (H₂S) and acceptor (O₂ or NO₃⁻) overlap (Chapters 2, 3, 4). (2) Nitrate-storing *Beggiatoaceae* create a suboxic zone in the sediment by gliding up and down between the surface and the sulfide horizon depth. In this scenario *Beggiatoa* is the main contributor to chemoautotrophic activity, which is found at the surface and throughout the suboxic zone (Chapter 4). (3) Electrogenic sulfur oxidation by cable bacteria also creates a suboxic zone in sediments but has a distinct pH profile, which distinguishes it from that of the nitrate-storing *Beggiatoaceae*. In this case, dark carbon fixation is evenly distributed from the surface to below the sulfide horizon potentially by means of a sulfur-oxidizing consortium between chemoautotrophic bacteria and the heterotrophic cable bacteria (Chapters 3, 4). (4) Bioturbating activity results in the intrusion of electron acceptors into deep anoxic sediments via intense bio-irrigation whereas strong particle mixing supports iron cycling. Thus chemoautotrophic activity is enhanced in deeper sediments and along the burrow walls, as well as at the surface compared to non-bioturbating sediments (Chapter 5, 6). Moreover, the effects of bioturbation on chemoautotrophic bacteria are species-specific and thus vary between sites with differing macrofaunal communities (Chapter 5). (5) In advective-driven permeable sediments, the constant flushing of the sediment produces deep oxygen penetration which enhances aerobic respiration that favors nitrifying bacteria with low growth yields (0.10), but diminishes anaerobic sulfate reduction and thus sulfide oxidation. This results in a minimum chemoautotrophic activity throughout the sediment matrix (Chapter 6).

In accordance with the three main objectives of this thesis it is concluded that 1) chemoautotrophy in coastal sediments is conducted by a diverse group of sulfur-oxidizing bacteria which co-occur either through complex sulfur-niche differentiation in bioturbated sediments or by way of a bacterial consortium when filamentous sulfur

oxidizers are present in diffusive sediments, but the exact mechanisms involved remain to be determined. 2) Chemoautotrophy rates vary depending on the main mode of pore water transport, which affects the sediment mineralization rate and the availability of electron donors and acceptors. Five distinct depth-distribution patterns of the dark carbon fixation are described that are linked to the main mode of sulfur oxidation. 3) Globally, chemoautotrophic production is one order of magnitude higher than that found in hydrothermal vents where chemoautotrophic bacteria are responsible for most of the primary production. Coastal benthic chemoautotrophy may therefore be an important source of renewed labile organic matter, especially in intertidal sediments, which should not be overlooked in future food web and biogeochemical studies.

Samenvatting

Chemoautotrofie is het proces waarbij micro-organismen CO₂ vastleggen en tegelijkertijd energie winnen uit de oxidatie van gereduceerde producten zoals sulfide en ammonium (bijvoorbeeld zwaveloxidatie en nitrificatie). Dit metabolisme is wijdverspreid in de natuur en is intensief bestudeerd in extreme milieus zoals hydrothermale bronnen op de oceaanbodem en chemoclines in hypoxische bassins waar het in grote mate bijdraagt aan de primaire productie. In kustgebieden, waar de foto-autotrofe organismen de belangrijkste primaire producenten zijn, worden chemoautotrofe bacteriën al snel over het hoofd gezien. Bovendien schat men de efficiëntie van chemoautotrofe bacteriën op minder dan 10% (dat wil zeggen, de verhouding tussen chemoautotrofe CO₂-fixatie en de totale CO₂-vrijzetting uit de mineralisatie van organisch materiaal), waardoor chemoautotrofe koolstofproductie in de berekening van koolstofbudgetten voor kustgebieden wordt uitgesloten. Niettemin is de productie van sulfide (de belangrijkste elektrondonor voor chemoautotrofe bacteriën in sedimenten) in kustsedimenten veel hoger dan in hydrothermale systemen, wat een groter potentieel voor chemoautotrofe zwavel-oxiderende organismen in kustsedimenten suggereert. Er is dan ook aangetoond dat chemoautotrofe bacteriën in sublittorale sedimenten tot wel 22% van de verademde koolstof fixeren en zwavel-oxidatie door grote filamenteuze bacteriën (Beggiatoaceae) verantwoordelijk is voor 90% van het zuurstofverbruik in sedimenten met overlappende O₂ en H₂S. Het doel van dit proefschrift was dan ook de chemoautotrofe activiteit in een reeks van kustgebieden te bestuderen door mogelijke bacteriële hoofdrolspelers te identificeren, het bepalen van proces-regulerende factoren en het belang van chemoautotrofe activiteit in de marine sedimenten van kustgebieden te evalueren.

Het merendeel van de chemoautotrofe bacteriën, welke zijn geïdentificeerd door middel van *sequenzen* (16S rRNA-gen en 16S rRNA en carboxylering genen van twee carbon fixatie cycli: de Calvin Benson-Bassham en de reductieve tricarbonzuur cyclus), was gerelateerd aan zwavel-oxiderende bacteriën, afkomstig uit de *clades* van Gamma-, Epsilon- en Delta-proteobacteria (hoofdstukken 2, 3, 4). Het gezamenlijk voorkomen van deze verschillende groepen van zwavel-oxiderende chemoautotrofe bacteriën kan worden toegeschreven aan een complexe niche-differentiatie die waarschijnlijk voortkomt uit de beschikbaarheid van verschillende zwavelverbindingen

(vrij sulfide, ijzersulfide, thiosulfaat, elementair zwavel) in de verschillende typen zeebodems. Filamenteuze *Beggiatoaceae* (Gammaproteobacteria) bijvoorbeeld, zijn kenmerkend voor cohesieve, zwavelrijke sedimenten omdat ze een hoge affiniteit voor H_2S en een hoge opnamesnelheden hebben waarmee ze goed kunnen concurreren met chemische sulfide-oxidatie in de O_2 - H_2S grensvlakken (hoofdstuk 2). Bovendien zijn er *Beggiatoaceae* met vacuolen die hen in staat stellen om andere zwavel-oxiderende bacteriën te verdringen, doordat ze nitraat intracellulair kunnen opslaan en de oxidatie van sulfide naar sulfaat in twee ruimtelijk gescheiden reacties (hoofdstuk 4) kunnen uitvoeren. In dit type sediment werden tevens metabolisch veelzijdige Epsilon-proteobacteria gevonden, welke elementaire zwavel waarschijnlijk aëroob of met behulp van nitraat oxideren. Het in dit proefschrift beschreven onderzoek suggereert dat deze Epsilon-proteobacteria afhankelijk zijn van de activiteit van filamenteuze zwavel-oxiderende bacteriën, zoals *Beggiatoaceae* met vacuolen en heterotrofe kabelbacteriën (hoofdstuk 3, 4). Eéncellige, zwavel-oxiderende Gamma-proteobacteria lijken ook metabolisch te kunnen worden gekoppeld aan kabelbacteriën in cohesieve sedimenten, maar het exacte mechanisme is nog steeds onduidelijk (hoofdstuk 3, 4). Daarentegen maken ééncellige Gamma-proteobacteria in gebioturbeerde sedimenten waarschijnlijk gebruik van ijzersulfide als belangrijkste elektronendonor (hoofdstuk 2). Tenslotte komen chemoautotrofe Delta-proteobacteria, gerelateerd aan sulfaat-reducerende bacteriën, overwegend voor in diepere, zuurstofloze sedimentlagen en tijdens hypoxische bodemwatercondities (hoofdstuk 2, 4).

De snelheid van “donkere” bacteriële koolstoffixatie (d.w.z. niet afhankelijk van zonlicht) is onderzocht in een verscheidenheid aan kustsedimenten, zoals intergetijdenplaten, een zoutwatermeer en sedimenten van zowel de diepere kustzone als het continentaal plat, door middel van een stabiele isotoop *probing* (^{13}C -DIC) en de analyse van bacteriële biomarkers (fosfolipide-vetzuren, PLFA-SIP). In totaal dragen wij 26 nieuwe waarnemingen aan, welke het bestaand aantal in de literatuur (6) van sedimentaire chemoautotrofie-snelheden meer dan verviervoudigen. Donkere koolstoffixatie varieerde tussen 0.07 en 36 mmol C $m^{-2}d^{-1}$, waarbij de hoogste activiteit werd gevonden in cohesieve sedimenten van schorren (kwelders), terwijl de laagste snelheden werden gevonden in advectie-gedreven sedimenten van het continentale plat. De meerderheid van de gevonden snelheden voor donkere koolstoffixatie ($n = 17$) bevond zich binnen 1 en 10 mmol C $m^{-2} d^{-1}$. Een correlatie-analyse om de mogelijke invloed van milieu-factoren op de koolstoffixatie te bepalen, leidde tot een significante *power law*-correlatie tussen chemoautotrofie-snelheden en het benthische zuurstofverbruik (hoofdstuk 6). Deze correlatie geeft aan dat, als door benthische respiratie het zuurstofverbruik toeneemt, de donkere koolstoffixatie meer dan proportioneel stijgt met de hoogste waarden in de richting van het ondiepe water. Door de snelheid van de zuurstofopname van het sediment te gebruiken als een *proxy* voor

mineralisatie in het sediment, waren we in staat om de CO₂-fixatie efficiëntie te schatten voor de verschillende sedimenten. Over de hele dataset beschouwd, varieert de efficiëntie van CO₂-fixatie van 0.01 tot 0.32, met een mediane waarde van ~ 0.06, hetgeen goed overeenkomt met de voor kustsedimenten geschatte efficiëntie van 0.07, gebaseerd op vereenvoudigde elektronenbalans-berekeningen. Wanneer onderscheid wordt gemaakt tussen drie dieptezones in de kustzee, vonden we 3% efficiëntie voor CO₂-fixatie in continentaal plat sedimenten (50-200 m waterdiepte), 9% voor kustzone-sedimenten (0-50 m waterdiepte, met inbegrip van intertidale sedimenten) en 21% voor de kweldersedimenten (hoofdstuk 6).

Chemoautotrofe activiteit speelt dus een meer prominente rol in de koolstofcyclus in de reactieve sedimenten van intergetijdengebied (vooral in schorren), dan in de dieper gelegen sedimenten van het continentaal plat. Met deze gemiddelde efficiënties van CO₂-fixatie voor de verschillende waterdieptes, komen wij voor kustsedimenten op een geschatte wereldwijde chemoautotrofe productie van 0.06 Pg C y⁻¹ (hoofdstuk 6). Dit is twee-en-een-half keer lager dan de voorzichtige raming van 0.15 Pg C y⁻¹, wat aangeeft dat eerdere studies de bijdrage van chemoautotrofie in kustsedimenten ernstig hebben overschat.

Bovendien worden er vijf verschillende diepte-distributiepatronen van chemoautotrofie beschreven, die kunnen worden gekoppeld aan drie sedimenttypes die verschillen in de belangrijkste manier van poriewater-transport: advectief, door bioturbatie en diffuus, welke op hun beurt goed aansluiten bij sedimentkarakteristieken zoals korrelgrootte, porositeit, het organische stof gehalte en bodemfauna-activiteit (hoofdstuk 6). Bij diffuse sedimenten is de belangrijkste manier van zwaveloxidatie gebruikt om onderscheid te maken tussen drie extra categorieën: elektrogene zwaveloxidatie door kabelbacteriën, sulfide door beweeglijke, nitraat-accumulerende *Beggiatoaceae* en canonical sulfide-oxidatie in een overlappend O₂-H₂S grensvlak. (1) Sedimenten met *canonical* sulfide-oxidatie hadden de meeste chemoautotrofe activiteit aan het sedimentoppervlak waar elektronendonoren (H₂S) en acceptoren (O₂ of NO₃⁻) met elkaar overlappen (hoofdstuk 2, 3, 4). (2) Nitraat-accumulerende *Beggiatoaceae* creëren een sub-oxische zone in het sediment door op en neer te glijden tussen het oppervlak en de sulfide horizon-diepte. In dit scenario levert *Beggiatoa* de belangrijkste bijdrage aan chemoautotrofe activiteit, zowel aan de oppervlakte als in de sub-oxische zone (hoofdstuk 4). (3) Elektrogene zwavel-oxidatie door kabelbacteriën creëert ook een sub-oxische zone in sedimenten, maar heeft een duidelijke pH-profiel, waardoor het zich onderscheidt van die van de nitraat-accumulerende *Beggiatoaceae*. In dit geval is de donkere koolstoffixatie gelijkmatig verdeeld van het sedimentoppervlak tot onder de sulfide horizon, door middel van een zwavel-oxiderend consortium tussen chemoautotrofe bacteriën en heterotrofe kabelbacteriën (hoofdstuk 3, 4). (4) Bioturbatie-activiteit leidt, via intense bio-irrigatie, tot het doordringen van elektronenacceptoren in

diepe, anoxische sedimenten, terwijl de sterke fysische menging van sedimentdeeltjes de ijzercyclus bevordert. Op deze manier wordt chemoautotrofe activiteit versterkt in diepere sedimenten en langs de wanden van (worm)gangen, evenals aan het sedimentoppervlak in vergelijking met niet-gebioturbeerde sedimenten (Hoofdstuk 5, 6). Bovendien zijn de effecten van bioturbatie op chemoautotrofe bacteriën soort-specifiek en variëren dus tussen locaties met verschillende macrofaunagemeenschappen (hoofdstuk 5). (5) In advectie-gedreven, permeabele sedimenten zorgt het constante doorspoelen van het sediment voor doordringing van zuurstof in diepere sedimentlagen, hetgeen aërobe ademhaling bevordert, wat weer ten gunste werkt van nitrificerende bacteriën met lage groeiopbrengsten (0.10) verbetert, maar tegelijkertijd anaërobe sulfaat-reductie -en dus sulfide-oxidatie- vermindert. Dit resulteert in een minimale chemoautotrofe activiteit door de gehele sediment-matrix (hoofdstuk 6).

In overeenstemming met de drie hoofddoelstellingen van dit proefschrift kan worden geconcludeerd dat 1) Chemoautotrofie in kustsedimenten wordt uitgevoerd door een diverse groep van zwavel-oxiderende bacteriën welke samen voorkomen, hetzij door middel van complexe zwavel-niche differentiatie in gebioturbeerde sedimenten, hetzij door middel van een bacterieel consortium wanneer filamenteuze zwavel-oxiderende bacteriën aanwezig zijn in diffuse sedimenten, maar hiervan dienen de exacte mechanismen nog worden vastgesteld. 2) Snelheden van chemoautotrofie variëren afhankelijk van de belangrijkste wijze van poriewatertransport, wat weer de mineralisatiesnelheid van het sediment en de beschikbaarheid van elektronendonoren en -acceptoren beïnvloedt. Vijf verschillende diepte-distributie patronen van de donkere koolstoffixatie zijn beschreven, welke zijn gekoppeld aan de belangrijkste manier van zwavel-oxidatie. 3) Wereldwijde chemoautotrofie-productie is één orde van grootte hoger dan die bij onderzeese hydrothermale bronnen, waar chemoautotrofe bacteriën verantwoordelijk zijn voor het grootste deel van de primaire productie. Chemoautotrofie in kustsedimenten kan daarom een belangrijke bron zijn van vernieuwd labiel organisch materiaal -met name in intertidale sedimenten-, welke in toekomstige voedselweb- en biogeochemische studies niet over het hoofd moeten worden gezien.

References

- Aida M, Kanemori M, Kubota N, Matada M, Sasayama Y, et al., (2008) ***Distribution and population of free-living cells related to endosymbiont harbored in *Oligobranchia mashikoi* (a Siboglinid Polychaete) inhabiting Tsukumo Bay.*** Microb. Environ. 23: 81-88.
- Aller RC, Yingst JY (1985) ***Effects of the marine deposit-feeders *Heteromastus filiformis* (Polychaeta), *Macoma baltica* (Bivalva), and *Tellina texana* (Bivalva) on average sedimentary solute transport, reaction rates, and microbial distributions.*** J Mar. Res. 43: 615-645.
- Aller RC. (1988). ***Benthic fauna and biogeochemical processes in marine sediments : The role of burrow structures.*** In: Blackburn, T. & Sørensen, J. (eds) Nitrogen cycling in coastal marine environments. John Wiley & Sons Ltd. p 301-338
- Aller RC. (2014). ***Sedimentary diagenesis, depositional environments, and benthic fluxes.*** In: Holland H.D. and Turekian K.K. (eds) Treatise on Geochemistry, 2nd ed. Oxford: Elsevier Ltd. 8: 293-334.
- Bak F, Pfennig N (1987) ***Chemolithotrophic growth of *Desulfovibrio sulfodismutans* sp. nov.*** by disproportionation of inorganic sulfur compounds Arch. of Microbiology 147: 184-189.
- Banfield JF, Nealson KH. (1997). ***Geomicrobiology: Interactions between microbes and minerals.*** Ribbe, P. (eds). Mineralogical Society of America, Washington D.C. pp 448
- Banta G, Holmer M, Jensen M, Kristensen E. (1999). ***Effects of two polychaete worms, *Nereis diversicolor* and *Arenicola marina*, on aerobic and anaerobic decomposition in a sandy marine sediment.*** Aqua.Micro. Eco. 19:189–204.
- Bauer JE, Montagna P a., Spies RB, Prieto MC, Hardin D. (1988). ***Microbial biogeochemistry and heterotrophy in sediments of a marine hydrocarbon seep.*** Limnol. Oceanogr. 33:1493–1513.
- Behrens S, Lösekann T, Pett-Ridge J, Weber PK, Ng WO, Stevenson BS, et al., (2008). ***Linking microbial phylogeny to metabolic activity at the single-cell level by using enhanced element labeling-catalyzed reporter deposition fluorescence in situ hybridization (EL-FISH) and NanoSIMS.*** Appl. Environ. Microbiol. 74:3143–3150.

- Belsler LW. (1984). *Bicarbonate uptake by nitrifiers: Effects of growth rate, pH, substrate concentration, and metabolic inhibitors*. Appl Env. Microbiol 48: 1100–1104.
- Berg IA. (2011). *Ecological aspects of the distribution of different autotrophic CO₂ fixation pathways*. Appl. Environ. Microbiol. 77:1925–36.
- Bertics VJ, Ziebis W. (2009). *Biodiversity of benthic microbial communities in bioturbated coastal sediments is controlled by geochemical microniches*. ISME J. 3:1269–85.
- Billerbeck M, Werner U, Polerecky L, Walpersdorf E, de Beer D, et al., (2006) *Surficial and deep pore water circulation governs spatial and temporal scales of nutrient recycling in intertidal sand flat sediment*. Mar. Eco. Prog. Ser. 326: 61-76.
- Blumer M, Chase T, Watson SW (1969) *Fatty acids in lipids of marine and terrestrial nitrifying bacteria*. J Bacteriol. 99: 366-370.
- Boschker HTS, Middelburg JJ. (2002). *Stable isotopes and biomarkers in microbial ecology*. FEMS Microbiol. Ecol. 40:85–95.
- Boschker HTS, Nold SC, P W, Bos D, de Graaf W, Pel R, et al., (1998). *Direct linking of microbial populations to specific biogeochemical processes by ¹³C-labeling of biomarkers*. Lett. to Nat. 392:801–805.
- Boschker HTS. (2004). *Linking microbial community structure and functioning: stable isotope (¹³C) labeling in combination with PLFA analysis*. In: Kowalchuk, G, De Bruijn, F, Head, I, Akkermans, A, & Van Elsas, J, eds (ed). Molecular Microbial Ecology Manual II. Kluwer Academic Publishers: Dordrecht, the Netherlands, pp. 1673–1688.
- Böttcher ME, Thamdrup B, Gehre M, Theune A. (2005). *³⁴S/³²S and ¹⁸O/¹⁶O fractionation during sulfur disproportionation by *Desulfobulbus propionicus**. Geomicrobiol. J. 22:219–226.
- Boudreau BP, Meysman FJR (2006) *Predicted tortuosity of muds*. Geology 34: 693-696.
- Boudreau BP. (1996). *The diffusive tortuosity of fine-grained unlithified sediments*. Geochim. Cosmochim. Acta 60:3139–3142.
- Bowles MW, Nigro LM, Teske AP, Joye SB. (2012). *Denitrification and environmental factors influencing nitrate removal in Guaymas Basin hydrothermally altered sediments*. Front. Microbiol. 3:1–11.
- Bowman JP, McMeekin TA. (2005). *Alteromonadales ord. nov.* In: Brenner, D, Krieg, N, Staley, J, Garrity, G, Boone, D, De Vos, P, et al., eds (ed), Bergey's Manual® of Systematic Bacteriology SE - 10, Springer US, pp. 443–491.
- Braeckman U, Provoost P, Gribsholt B, Van Gansbeke D, Middelburg J, Soetaert K, et al., (2010). *Role of macrofauna functional traits and density in biogeochemical fluxes and bioturbation*. Mar. Ecol. Prog. Ser. 399:173–186.

- Brenner H, Braeckman U, Le Guitton M, Meysman FJR. (2015). *The impact of sedimentary alkalinity release on the water column CO₂ system in the North Sea*. Biogeosciences Discuss. 12:12395–12453.
- Brinch-Iversen J, King GM (1990) *Effects of substrate concentration, growth state, and oxygen availability on relationships among bacterial carbon, nitrogen and phospholipid phosphorus content*. FEMS Microbiol. Ecol. 74: 345-355.
- Brüchert V, Jørgensen BB, Neumann K, Riechmann D, Schlösser M, Schulz H. (2003). *Regulation of bacterial sulfate reduction and hydrogen sulfide fluxes in the central Namibian coastal upwelling zone*. Geochim. Cosmochim. Acta 67:4505–4518.
- Bühning SI, Elvert M, Witte U. (2005). *The microbial community structure of different permeable sandy sediments characterized by the investigation of bacterial fatty acids and fluorescence in situ hybridization*. Environ. Microbiol. 7:281–293.
- Campbell BJ, Craig Cary S. (2004). *Abundance of reverse tricarboxylic acid cycle genes in free-living micro-organisms at deep-sea hydrothermal vents*. Appl. Environ. Microbiol. 70:6282–6289.
- Campbell BJ, Engel AS, Porter ML, Takai K. (2006). *The versatile Epsilonproteobacteria: Key players in sulfidic habitats*. Nat. Rev. Microbiol. 4:458–68.
- Campbell BJ, Stein JL, Cary SC. (2003). *Evidence of chemolithoautotrophy in the bacterial community associated with Alvinella pompejana, a hydrothermal vent polychaete*. Appl. Environ. Microbiol. 69:5070–5078.
- Canfield D, Jørgensen B, Fossing H, Glud R, Gundersen J, Ramsing N, et al., (1993). *Pathways of organic carbon oxidation in three continental margin sediments*. Mar. Geol. 113:27–40.
- Canfield DE, Kristensen E, Thamdrup B. (2005). *Aquatic geomicrobiology*. Elsevier Academic Press, London pp.640
- Caporaso JG, Kuczynski J, Stombaugh J, Bittinger K, Bushman FD, Costello EK, et al., (2010). *Correspondence QIIME allows analysis of high-throughput community sequencing data intensity normalization improves color calling in SOLiD sequencing*. Nat. Publ. Gr. 7:335–336.
- Cavanaugh C, Gardiner S, Jones M, Jannasch H, Waterbury J. (1981). *Prokaryotic cells in the hydrothermal vent tube worm Riftia pachyptila Jones: Possible chemoautotrophic symbionts*. Science 213:340–342.
- Cavanaugh CM (1983) *Symbiotic chemoautotrophic bacteria in marine-invertebrates from sulfide-rich habitats*. Nature 302: 58-61.
- Christensen B, Vedel A, Kristensen E. (2000). *Carbon and nitrogen fluxes in sediment inhabited by suspension-feeding (Nereis diversicolor) and non-suspension-feeding (N. virens) polychaetes*. Mar. Ecol. Prog. Ser. 192:203–217.

- Cline J. (1969). *Spectrophotometric determination of hydrogen sulfide in natural waters*. Limnol. Oceanogr. 14:454–458.
- Clough LM, Lopez GR. (1993). *Potential carbon sources for the head-down deposit-feeding polychaete *Heteromastus filiformis**. J. Mar. Res. 51:595–616.
- Cuny P, Acquaviva M, Miralles G, Stora G, Grossi V, Gilbert F. (2007). *Influence of bioturbation by the polychaete *Nereis diversicolor* on the structure of bacterial communities in oil contaminated coastal sediments*. Mar. Pollut. Bull. 54:452–459.
- Dale AW, Sommer S, Haeckel M, Wallmann K, Linke P, Wegener G, et al., (2010). *Pathways and regulation of carbon, sulfur and energy transfer in marine sediments overlying methane gas hydrates on the Opouawe Bank (New Zealand)*. Geochim. Cosmochim. Acta 74:5763–5784.
- Damste JSS, Rijpstra WIC, Geenevasen JAJ, Strous M, Jetten MSM (2005) *Structural identification of ladderane and other membrane lipids of planctomycetes capable of anaerobic ammonium oxidation (anammox)*. FEBS Journal 272: 4270-4283.
- Dannenberg S, Kroder M, Dilling W, Cypionka H. (1992). *Oxidation of H_2 , organic compounds and inorganic sulfur compounds coupled to reduction of O_2 or nitrate by sulfate-reducing bacteria*. Microbiology 158:93–99.
- Dauwe B, Middelburg JJ, Herman PMJ. (2001). *Effect of oxygen on the degradability of organic matter in subtidal and intertidal sediments of the North Sea area*. Mar. Ecol. Ser. 215:13–22.
- de Bie MJM, Starink M, Boschker HTS, Peene JJ, Laanbroek HJ (2002) *Nitrification in the Schelde estuary: methodological aspects and factors influencing its activity*. FEMS Microbiol. Ecol. 42: 99-107.
- del Giorgio PA, Cole JJ (1998) *Bacterial growth efficiency in natural aquatic systems*. Annu. Rev. Ecol. Syst. 29: 503-541.
- Delefosse M, Banta G, Canal-Vergés P, Penha-Lopes G, Quintana C, Valdemarsen T, et al., (2012). *Macrobenthic community response to the *Marenzelleria viridis* (Polychaeta) invasion of a Danish estuary*. Mar. Ecol. Prog. Ser. 461:83–94.
- DeSantis TZ, Hugenholtz P, Larsen N, Rojas M, Brodie EL, Keller K, et al., (2006). *GreenGenes, a chimera-checked 16S rRNA gene database and workbench compatible with ARB*. Appl. Environ. Microbiol. 72:5069–5072.
- Diaz RJ, Rosenberg R. (2008). *Spreading dead zones and consequences for marine ecosystems*. Science 321:926–929.
- Dijkhuizen L, Harder W (1985) *Microbial metabolism of carbon dioxide*. In: Dalton H (ed), Comprehensive biotechnology. Oxford: Pergamon Press. pp. 409-423.

- Dijkman NA, Kromkamp JC (2006) *Phospholipid-derived fatty acids as chemotaxonomic markers for phytoplankton: Application for inferring phytoplankton composition*. Mar. Ecol. Prog. Ser. 324: 113-125.
- Dobbs FC, Guckert JB. (1988). *Callianassa trilobata (Crustacea: Thalassinidea) influences abundance of meiofauna and biomass, composition, and physiologic state of microbial communities within its burrow*. Mar. Ecol. Prog. Ser. 45:69–79.
- Dobrinski KP, Longo DL, Scott KM. (2005). *The carbon-concentrating mechanism of the hydrothermal vent chemolithoautotroph Thiomicrospira crunogena*. J Bacteriol. 187:5761–5766.
- Donachie SP, Bowman JP, On SLW, Alam M. (2005). *Arcobacter halophilus sp. nov., the first obligate halophile in the genus Arcobacter*. Int. J. Syst. Evol. Microbiol. 55:1271–7.
- Dubey GP, Ben-Yehuda S. (2011). *Intercellular nanotubes mediate bacterial communication*. Cell 144:590–600.
- Dubilier N, Bergin C, Lott C. (2008). *Symbiotic diversity in marine animals: The art of harnessing chemosynthesis*. Nat. Rev. Microbiol. 6:725–740.
- Dunne JP, Sarmiento JL, Gnanadesikan A. (2007). *A synthesis of global particle export from the surface ocean and cycling through the ocean interior and on the seafloor*. Global Biogeochem. Cy. 21:1–16.
- Dyksma S, Bischof K, Fuchs BM, Hoffmann K, Meier D, Meyerdierks A, et al., (2016). *Ubiquitous Gammaproteobacteria dominate dark carbon fixation in coastal sediments*. ISME J. in press.
- Edgar RC. (2010). *Search and clustering orders of magnitude faster than BLAST*. Bioinformatics 26:2460–2461.
- Edlund A, Nichols PD, Roffey R, White DC (1985) *Extractable and lipopolysaccharide fatty-acid and hydroxy acid profiles from Desulfovibrio species*. J Lipid Res. 26: 982-988.
- Elferink SJWH, Boschker HTS, Stams AJM (1998) *Identification of sulfate reducers and Syntrophobacter sp. in anaerobic granular sludge by fatty-acid biomarkers and 16S rRNA probing*. Geomicrobiol. J 15: 3-17.
- Elsaied HE, Kimura H, Naganuma T (2007) *Composition of archaeal, bacterial, and eukaryal RuBisCO genotypes in three Western Pacific arc hydrothermal vent systems*. Extremophiles 11: 191-202.
- Engel AS, Lee N, Porter ML, Stern LA, Bennett PC, Wagner M. (2003). *Filamentous Epsilonproteobacteria dominate microbial mats from sulfidic cave springs*. Appl. Environ. Microbiol. 69:5503–5511.

- Enoksson V, Samuelsson MO (1987) *Nitrification and dissimilatory ammonium production and their effects on nitrogen flux over the sediment-water interface in bioturbated coastal sediments*. Mar. Ecol. Prog. Ser. 36: 181-189.
- Evershed RP, Crossman ZM, Bull ID, Mottram H, Dungait J a J, Maxfield PJ, et al., (2006). *¹³C-Labeling of lipids to investigate microbial communities in the environment*. Curr. Opin. Biotechnol. 17:72–82.
- Feisthauer S, Wick LY, Kastner M, Kaschabek SR, Schlomann M, et al., (2008) *Differences of heterotrophic ¹³CO₂ assimilation by Pseudomonas knackmussii strain B13 and Rhodococcus opacus ICP and potential impact on biomarker stable isotope probing*. Environ. Microbiol. 10: 1641-1651.
- Findlay RH, King GM, Watling L. (1989). *Efficacy of phospholipid analysis in determining microbial biomass in sediments*. Appl. Environ. Microbiol. 55:2888–2893.
- Findlay RH, Trexler MB, Guckerte JB, White DC. (1990). *Laboratory study of disturbance in marine sediments: Response of a microbial community*. Mar. Ecol. Prog. Ser. 62:121–133.
- Finster K, Liesack W, Thamdrup B. (1998). *Elemental sulfur and thiosulfate disproportionation by Desulfocapsa sulfoexigens sp. nov., a new anaerobic bacterium isolated from marine surface sediment*. Appl. Environ. Microbiol. 64:119–125.
- Fry B. (2006). *Stable isotope ecology*. Springer Science+Business Media: New York.
- Fuseler K, Cypionka H. (1995). *Elemental sulfur as an intermediate of sulfide oxidation with oxygen by Desulfobulbus propionicus*. Arch. Microbiol. 164:104–109.
- Ghosh W, Dam B. (2009). *Biochemistry and molecular biology of lithotrophic sulfur oxidation by taxonomically and ecologically diverse bacteria and archaea*. FEMS Microbiol. Rev. 33:999–1043.
- Giri BJ, Bano N, Hollibaugh JT (2004) *Distribution of RuBisCO genotypes along a redox gradient in Mono Lake, California*. Appl. Environ. Microbiol. 70: 3443-3448.
- Glaubitiz S, Lueders T, Abraham W-R, Jost G, Jürgens K, Labrenz M. (2009). *¹³C-isotope analyses reveal that chemolithoautotrophic Gamma- and Epsilonproteobacteria feed a microbial food web in a pelagic redoxcline of the central Baltic Sea*. Environ. Microbiol. 11:326–337.
- Glud RN. (2008). *Oxygen dynamics of marine sediments*. Mar. Biol. Res. 4:243–289.

- Gottschal JC, Vries SD, Kuenen JG (1979) *Competition between the facultatively chemolithotrophic Thiobacillus A2, and obligately chemolithotrophic Thiobacillus and a heterotrophic Spirillum for inorganic and organic substrates*. Arch. Microbiol. 121: 241-249.
- Grote J, Schott T, Bruckner CG, Glöckner FO, Jost G, Teeling H, et al., (2012). *Genome and physiology of a model Epsilonproteobacterium responsible for sulfide detoxification in marine oxygen depletion zones*. Proc. Natl. Acad. Sci. U. S. A. 109:506–10.
- Grünke S, Felden J, Lichtschlag A, Girnth A-C, De Beer D, Wenzhöfer F, et al., (2011). *Niche differentiation among mat-forming, sulfide-oxidizing bacteria at cold seeps of the Nile Deep Sea Fan (Eastern Mediterranean Sea)*. Geobiology 9:330–48.
- Guckert JB, Antworth CP, Nichols PD, White DC. (1985). *Phospholipid, ester-linked fatty-acid profiles as reproducible assays for changes in prokaryotic community structure of estuarine sediments*. FEMS Microbiol. Ecol. 31:147–158.
- Gutierrez-Zamora M-L, Manefield M. (2010). *An appraisal of methods for linking environmental processes to specific microbial taxa*. Rev. Environ. Sci. Biotechnol. 9:153–185.
- Hadas O, Pinkas R, Erez J. (2001). *High chemoautotrophic primary production in Lake Kinneret, Israel: A neglected link in the carbon cycle of the lake*. Limnol. Oceanogr. 46:1968–1976.
- Hagen KD, Nelson DC (1996) *Organic carbon utilization by obligately and facultatively autotrophic Beggiatoa strains in homogeneous and gradient cultures*. Appl. Environ. Microbiol. 62: 947-953.
- Hagens M, Slomp CP, Meysman FJR, Seitaj D, Harlay J, Borges a V, et al., (2015). *Biogeochemical processes and buffering capacity concurrently affect acidification in a seasonally hypoxic coastal marine basin*. Biogeosciences 12:1561–1583.
- Hempflin WP, Vishniac W (1967) *Yield coefficients of Thiobacillus neapolitanus in continuous culture*. J Bacteriol 93: 874-878.
- Hesselsoe M, Nielsen JL, Roslev P, Nielsen PH. (2005). *Isotope labeling and microautoradiography of active heterotrophic bacteria on the basis of assimilation of ¹⁴C₂O₂*, *isotope labeling and microautoradiography of active heterotrophic bacteria on the basis of assimilation of ¹⁴C₂O₂*. Appl. Environ. Microbiol. 71:646–55.
- Hoehler TM, Alperin MJ, Albert DB, Martens CS (1998) *Thermodynamic control on hydrogen concentrations in anoxic sediments*. Geochim. Cosmochim. Acta 62: 1745-1756.
- Hofmann AF, Soetaert K, Middelburg JJ, Meysman FJR. (2010). *AquaEnv: An aquatic acid–base modelling environment in R*. Aquat. Geochemistry 16:507–546.

- Howarth WR. (1984). *The ecological significance of sulfur in the energy dynamics of salt marsh and coastal marine sediments*. Biogeochemistry 1:5–27.
- Huettel M, Berg P, Kostka JE. (2014). *Benthic exchange and biogeochemical cycling in permeable sediments*. Ann. Rev. Mar. Sci. 6:23–51.
- Huettel M, Røy H, Precht E, Ehrenhauss S. (2003). *Hydrodynamical impact on biogeochemical processes in aquatic sediments*. Hydrobiologia 494:231–236.
- Hügler M, Sievert SM. (2011). *Beyond the calvin cycle: Autotrophic carbon fixation in the Ocean*. Ann. Rev. Mar. Sci. 3:261–289.
- Hylleberg J. (1975). *Selective feeding by Abarenicola pacifica with notes on Abarenicola vagabunda and a concept of gardening in lugworms*. Ophelia 14:113–137.
- Inagaki F, Takai K, Kobayashi H, Nealson K, Horikoshi K. (2003). *Sulfurimonas autotrophica gen. nov., sp. nov., a novel sulfur-oxidizing Epsilonproteobacterium isolated from hydrothermal sediments in the Mid-Okinawa Trough*. Int. J. Syst. Evol. Microbiol. 53:1801–1805.
- Inagaki F, Takai K, Nealson KH, Horikoshi K. (2004). *Sulfurovum lithotrophicum gen. nov., sp. nov., a novel sulfur-oxidizing chemolithoautotroph within the Epsilonproteobacteria isolated from Okinawa Trough hydrothermal sediments*. Int. J. Syst. Evol. Microbiol. 54:1477–1482.
- Jannasch HW, Mottl MJ. (1985). *Geomicrobiology of deep-sea hydrothermal vents*. Science 229:717–25.
- Jannasch HW, Wirsén CO (1979) *Chemosynthetic primary production at east Pacific sea-floor spreading centers*. Bioscience 29: 592-598.
- Jansen S, Walpersdorf E, Werner U, Billerbeck M, Böttcher ME, de Beer D. (2009). *Functioning of intertidal flats inferred from temporal and spatial dynamics of O_2 , H_2S and pH in their surface sediment*. Ocean Dyn. 59:317–332.
- Jørgensen BB (1978) *Comparison of methods for the quantification of bacterial sulfate reduction in coastal marine-sediments 1. Measurement with radio-tracer techniques*. Geomicrobiol.J 1: 11-27.
- Jørgensen BB. (1982). *Ecology of the bacteria of the sulfur cycle with special reference to anoxic-oxic interface environments*. Philos. Trans. R. Soc. Lond. B. Biol. Sci. 298:543–61.
- Jørgensen BB, Bak F (1991) *Pathways and microbiology of thiosulfate transformations and sulfate reduction in a marine sediment (Kattegat, Denmark)*. Appl. Environ. Microbiol. 57: 847-856.
- Jørgensen BB. (2006). *Bacteria and marine biogeochemistry*. In: Shulz, HD & Zabel, M, eds (ed.), Marine Geochemistry, 2 ed, New York: Springer pp. 169–206.
- Jørgensen BB, Nelson DC (2004) *Sulfide oxidation in marine sediments: Geochemistry meets microbiology*. Geol. S Am S 379: 61-81.

- Jørgensen BB, Dunker R, Grünke S, Røy H. (2010). *Filamentous sulfur bacteria, Beggiatoa spp., in arctic marine sediments (Svalbard, 79 degrees N)*. FEMS Microbiol. Ecol. 73:500–13.
- Jovanovic Z, Larsen M, Organo Quintana C, Kristensen E, Glud R. (2014). *Oxygen dynamics and pore water transport in sediments inhabited by the invasive polychaete Marenzelleria viridis*. Mar. Ecol. Prog. Ser. 504:181–192.
- Jukes TH, Cantor CR. (1969). *Evolution of protein molecules. In: Munro HN (eds) Mammalian protein metabolism III*. Academic Press: New York. pp 21–132.
- Kelly DP (1999) *Thermodynamic aspects of energy conservation by chemolithotrophic sulfur bacteria in relation to the sulfur oxidation pathways*. Arch. Microbiol 171: 219-229.
- Kelly DP, Wood AP (2006) *The chemolithoautotrophic prokaryotes*. In: Dworkin M, Falkow S, Rosenberg E, Schleifer K-H, Stackebrandt E, (eds). The prokaryotes 2 ed. Berlin: Springer pp. 441-456.
- Kerger BD, Nichols PD, Antworth CP, Sand W, Bock E, et al., (1986) *Signature fatty-acids in the polar lipids of acid-producing Thiobacillus spp.: Methoxy, cyclopropyl, alpha-hydroxy-cyclopropyl and normal monoenoic fatty-acids*. FEMS Microbiol.Ecol. 38: 67-77.
- Kester DR, Duedall IW, Connors DN, Pytkowic.Rm (1967) *Preparation of artificial seawater*. Limnol. Oceanog. 12: 176-179.
- Klatt JM, Polerecky L. (2015). *Assessment of the stoichiometry and efficiency of CO₂ fixation coupled to reduced sulfur oxidation*. Front. Microbiol. 6:484
- Klindworth A, Pruesse E, Schweer T, Peplies J, Quast C, Horn M, et al., (2013). *Evaluation of general 16S ribosomal RNA gene PCR primers for classical and next-generation sequencing-based diversity studies*. Nucleic Acids Res. 4(1):2-11.
- Knief C, Altendorf K, Lipski A (2003) *Linking autotrophic activity in environmental samples with specific bacterial taxa by detection of ¹³C-labeled fatty acids*. Environ. Microbiol. 5: 1155-1167.
- Kojima H, Fukui M. (2003). *Phylogenetic analysis of Beggiatoa spp. from organic rich sediment of Tokyo Bay, Japan*. Water Res. 37:3216–3223.
- Kovaleva OL, Tourova TP, Muyzer G, Kolganova T V, Sorokin DY. (2011). *Diversity of RuBisCO and ATP citrate lyase genes in soda lake sediments*. FEMS Microbiol. Ecol. 75:37–47.
- Kristensen E. (1984). *Life cycle, growth and production in estuarine populations of the polychaetes Nereis virens and N. diversicolor*. Holartic Ecol. 7:249–256.
- Kristensen E. (1988). *Benthic fauna and biogeochemical processes in marine sediments: Microbial activities and fluxes*. In: Blackburn, T & Sorensen, J, eds (ed)., Nitrogen cycling in coastal marine environments. John Wiley & Sons Ltd., pp. 275–299.

- Kristensen E. (2001). *Impact of polychaetes (Nereis spp. and Arenicola marina) on carbon biogeochemistry in coastal marine sediments*. *Geochem. Trans.* 2:92.
- Kristensen E, Devol AH, Hartnett HE (1999) *Organic matter diagenesis in sediments on the continental shelf and slope of the eastern tropical and temperate North Pacific*. *Cont Shelf Res* 19: 1331-1351.
- Kristensen E, Kostka JE. (2005). *Macrofaunal burrows and irrigation in marine sediment: microbiological and biogeochemical interactions*. In: Kristensen, E, Haese, RR, & Kostka, JE, eds (ed), *Interactions between macro- and micro-organisms in marine sediments*. American Geophysical Union: Washington, D. C., pp. 125–158.
- Kristensen E, Hansen T, Delefosse M, Banta G, Quintana C. (2011). *Contrasting effects of the polychaetes Marenzelleria viridis and Nereis diversicolor on benthic metabolism and solute transport in sandy coastal sediment*. *Mar. Ecol. Prog. Ser.* 425:125–139.
- Kristensen E, Penha-Lopes G, Delefosse M, Valdemarsen T, Quintana C, Banta G. (2012). *What is bioturbation? The need for a precise definition for fauna in aquatic sciences*. *Mar. Ecol. Prog. Ser.* 446:285–302.
- Kristensen E, Delefosse M, Quintana CO, Flindt MR, Valdemarsen T. (2014). *Influence of benthic macrofauna community shifts on ecosystem functioning in shallow estuaries*. *Front. Mar. Sci.* 1:1–14.
- Kunihiro T, Takasu H, Miyazaki T, Uramoto Y, Kinoshita K, Yodnarasri S, et al., (2011). *Increase in Alphaproteobacteria in association with a polychaete, Capitella sp. I, in the organically enriched sediment*. *ISME J.* 5:1818–1831.
- Laanbroek HJ, Pfennig N. (1981). *Oxidation of short-chain fatty acids by sulfate-reducing bacteria in freshwater and in marine sediments*. *Arch. Microbiol.* 128:330–335.
- Labrenz M, Grote J, Mammitzsch K, Boschker HTS, Laue M, Jost G, et al., (2013). *Sulfurimonas gotlandica sp. nov., a chemoautotrophic and psychrotolerant Epsilonproteobacterium isolated from a pelagic redoxcline, and an emended description of the genus Sulfurimonas*. *Int. J. Syst. Evol. Microbiol.* 63:4141–4148.
- Labrenz M, Pohl C, Beckmann S, Martens-habbena W, Ju K. (2005). *Impact of different in vitro electron donor / acceptor conditions on potential chemolithoautotrophic communities from marine pelagic redoxclines*. *Appl. Environ. Microbiol.* 71:6664–6672.
- Langezaal A., Ernst S., Haese R., van Bergen P., van der Zwaan G. (2003). *Disturbance of intertidal sediments: The response of bacteria and foraminifera*. *Estuar. Coast. Shelf Sci.* 58:249–264.

- Laverock B, Smith CJ, Tait K, Osborn AM, Widdicombe S, Gilbert JA. (2010). *Bioturbating shrimp alter the structure and diversity of bacterial communities in coastal marine sediments*. ISME J. 4:1531–1544.
- Lavik G, Stührmann T, Brüchert V, Van der Plas A, Mohrholz V, Lam P, et al., (2009). *Detoxification of sulfidic African shelf waters by blooming chemolithotrophs*. Nature 457:581–4.
- Lenk S, Arnds J, Zerjatke K, Musat N, Amann R, et al., (2011) *Novel groups of Gammaproteobacteria catalyze sulfur oxidation and carbon fixation in a coastal, intertidal sediment*. Environ. Microbiol. 13: 758-774.
- Lever MA. (2012). *Acetogenesis in the energy-starved deep biosphere – A paradox?* Front. Microbiol. 2:1–18.
- Li Y, Peacock A, White D, Geyer R, Zhang C. (2007). *Spatial patterns of bacterial signature biomarkers in marine sediments of the Gulf of Mexico*. Chem. Geol. 238:168–179.
- Lichtschlag A, Felden J, Bru V. (2010). *Geochemical processes and chemosynthetic primary production in different thiotrophic mats of the Hakon Mosby Mud Volcano (Barents Sea)*. Limnol. Oceanogr. 55:931–949.
- Lipsewers YA, Bale NJ, Hopmans EC, Schouten S, Damsté JSS, Villanueva L. (2014). *Seasonality and depth distribution of the abundance and activity of ammonia oxidizing micro-organisms in marine coastal sediments (North Sea)*. Front. Microbiol. 5:1–12.
- Lipski A, Spieck E, Makolla A, Altendorf K (2001) *Fatty acid profiles of nitrite-oxidizing bacteria reflect their phylogenetic heterogeneity*. Syst.Appl. Microbiol 24: 377-384.
- Llobet-Brossa E, Rabus R, Böttcher ME, Könneke M, Finke N, Schramm A, et al., (2002). *Community structure and activity of sulfate-reducing bacteria in an intertidal surface sediment : A multi-method approach*. Aquat. Microb. Ecol. 29:211–226.
- Lohse L, Epping E, Helder W, van Raaphorst W. (1996). *Oxygen pore water profiles in continental shelf sediments of the North Sea: Turbulent versus molecular diffusion*. Mar. Ecol. Prog. Ser. 145:63–75.
- Ludwig W, Strunk O, Westram R, Richter L, Meier H, Yadhukumar, et al., (2004). *ARB: a software environment for sequence data*. Nucleic Acids Res. 32:1363–71.
- Macalady JL, Dattagupta S, Schaperdoth I, Jones DS, Druschel GK, Eastman D. (2008). *Niche differentiation among sulfur-oxidizing bacterial populations in cave waters*. ISME J. 2:590–601.
- Malkin SY, Rao AM, Seitaj D, Vasquez-Cardenas D, Zetsche E-M, Hidalgo-Martinez S, et al., (2014). *Natural occurrence of microbial sulfur oxidation by long-range electron transport in the seafloor*. ISME J. 8:1843–54.

- Manz W, Amann R, Ludwig W, Wagner M, Schleifer KH. (1992). *Phylogenetic oligodeoxynucleotide probes for the major subclasses of Proteobacteria - problems and solutions*. Syst. Appl. Microbiol. 15:593–600.
- Marinelli R, Lovell C, Wakeham S, Ringelberg D, White D. (2002). *Experimental investigation of the control of bacterial community composition in macrofaunal burrows*. Mar. Ecol. Prog. Ser. 235:1–13.
- Marzocchi U, Trojan D, Larsen S, Louise Meyer R, Peter Revsbech N, Schramm A, et al., (2014). *Electric coupling between distant nitrate reduction and sulfide oxidation in marine sediment*. ISME J. 8: 1682–1690.
- McDonald D, Price MN, Goodrich J, Nawrocki EP, DeSantis TZ, Probst A, et al., (2012). *An improved greengenes taxonomy with explicit ranks for ecological and evolutionary analyses of bacteria and archaea*. ISME J. 6:610–618.
- Mermillod-Blondin F. (2011). *The functional significance of bioturbation and biodeposition on biogeochemical processes at the water–sediment interface in freshwater and marine ecosystems*. J. North Am. Benthol. Soc. 30:770–778.
- Meysman FJR, Galaktionov O, Middelburg JJ. (2005). *Irrigation patterns in permeable sediments induced by burrow ventilation: A case study of Arenicola marina*. Mar. Ecol. Prog. Ser. 303:195–212.
- Meysman F, Middelburg J, Heip C. (2006). *Bioturbation: a fresh look at Darwin's last idea*. Trends Ecol. Evol. 21:688–695.
- Meysman FJR, Risgaard-Petersen N, Malkin SY, Nielsen LP. (2015). *The geochemical fingerprint of microbial long-distance electron transport in the seafloor*. Geochim. Cosmochim. Acta 152:122–142.
- Middelburg JJ, Barranguet C, Boschker HTS, Herman PMJ, Moens T, Heip CHR. (2000). *The fate of intertidal microphytobenthos carbon: An in situ ¹³C-labeling study*. Limnol. Oceanogr. 45:1224–1234.
- Middelburg JJ. (2011). *Chemoautotrophy in the ocean*. Geophys. Res. Lett. 38:1–4.
- Miyatake T. (2011). *Linking microbial community structure to biogeochemical function in coastal marine sediments*. PhD Dissertation, University of Amsterdam, Netherlands.
- Moodley L, Middelburg JJ, Soetaert K, Boschker HTS, Herman PMJ, et al., (2005) *Similar rapid response to phytodetritus deposition in shallow and deep-sea sediments*. J Mar. Res. 63: 457-469.
- Moore EK, Villanueva L, Hopmans EC, Rijpstra WIC, Mets A, Dedysh SN, et al., (2015). *Abundant trimethylornithine lipids and specific Gene sequences are indicative of Planctomycete importance at the oxic/anoxic interface in Sphagnum-dominated Northern Wetlands*. Appl. Environ. Microbiol. 81:6333–6344.

- Morono Y, Terada T, Nishizawa M, Ito M, Hillion F, Takahata N, et al., (2011). *Carbon and nitrogen assimilation in deep seafloor microbial cells*. Proc. Natl. Acad. Sci. U. S. A. 108:18295–18300.
- Musat N, Foster R, Vagner T, Adam B, Kuypers MMM. (2012). *Detecting metabolic activities in single cells, with emphasis on nanoSIMS*. FEMS Microbiol. Rev. 36:486–511.
- Musat N, Halm H, Winterholler B, Hoppe P, Peduzzi S, Hillion F, et al., (2008). *A single-cell view on the ecophysiology of anaerobic phototrophic bacteria*. Proc. Natl. Acad. Sci. U.S.A. 105:17861–17866.
- Mußmann M, Hu FZ, Richter M, de Beer D, Preisler A, et al., (2007) *Insights into the genome of large sulfur bacteria revealed by analysis of single filaments*. PloS Biol. 5: 1923-1937.
- Mußmann M, Schulz HN, Strotmann B, Kjær T, Nielsen LP, Rosselló-Mora RA, et al., (2003). *Phylogeny and distribution of nitrate-storing Beggiatoa spp. in coastal marine sediments*. Environ. Microbiol. 5:523–533.
- Muyzer G, Stams AJM. (2008). *The ecology and biotechnology of sulfate-reducing bacteria*. Nat. Rev. Microbiol. 6: 441-454
- Nakagawa S, Takai K. (2008). *Deep-sea vent chemoautotrophs: Diversity, biochemistry and ecological significance*. FEMS Microbiol. Ecol. 65:1–14.
- Nelson DC, Jannasch HW (1983) *Chemoautotrophic growth of a marine Beggiatoa in sulfide-gradient cultures*. Arch. Microb. 136: 262-269.
- Nelson DC, Jørgensen BB, Revsbech NP (1986) *Growth-pattern and yield of a chemoautotrophic Beggiatoa sp. in oxygen-sulfide microgradients*. Appl. Environ. Microbiol. 52: 225-233.
- Nielsen LP, Risgaard-Petersen N, Fossing H, Christensen PB, Sayama M. (2010). *Electric currents couple spatially separated biogeochemical processes in marine sediment*. Nature 463:1071–1074.
- Nigro LM, King GM (2007) *Disparate distributions of chemolithotrophs containing form IA or IC large subunit genes for ribulose-1,5-bisphosphate carboxylase/oxygenase in intertidal marine and littoral lake sediments*. FEMS Microbiol. Eco. 60: 113-125.
- Nilsson HC, Rosenberg R. (2000). *Succession in marine benthic habitats and fauna in response to oxygen deficiency: analysed by sediment profile-imaging and by grab samples*. Mar. Ecol. Prog. Ser. 197:139–149.
- Odintsova EV, Wood AP, Kelly DP (1993) *Chemoautotrophic growth of Thiotrix ramosa*. Arch. Microbiol. 160: 152-157.
- Orphan VJ, House CH, Hinrichs KU, McKeegan KD, DeLong EF (2001). *Methane-consuming archaea revealed by directly coupled isotopic and phylogenetic analysis*. Science 293:484–487.

- Pagani I, Lapidus A, Nolan M, Lucas S, Hammon N, Deshpande S, et al., (2011). **Complete genome sequence of *Desulfobulbus propionicus* type strain (1pr3)**. Stand. Genomic Sci. 4:100–110.
- Pallud C, Van Cappellen P. (2006). **Kinetics of microbial sulfate reduction in estuarine sediments**. Geochim. Cosmochim. Acta 70:1148–1162.
- Papaspyrou S, Gregersen T, Kristensen E, Christensen B, Cox RP. (2006). **Microbial reaction rates and bacterial communities in sediment surrounding burrows of two nereidid polychaetes (*Nereis diversicolor* and *N. virens*)**. Mar. Biol. 148:541–550.
- Parkes RJ, Dowling NJE, White D, Herbert R, Gibson G. (1993). **Characterization of sulfate-reducing bacterial populations with marine and estuarine sediments with different rates of sulfate reduction**. FEMS Microbiol. Ecol. 102:235–250.
- Parkes RJ, Gibson GR, Mueller-Harvey I, Buckingham WJ, Herbert RA. (1989). **Determination of the substrates for sulfate-reducing bacteria within marine and estuarine sediments with different rates of sulfate reduction**. J. Gen. Microbiol. 135:175–187.
- Perner M, Seifert R, Weber S, Koschinsky A, Schmidt K, Strauss H, et al., (2007). **Microbial CO₂ fixation and sulfur cycling associated with low-temperature emissions at the Lilliput hydrothermal field, southern Mid-Atlantic Ridge (9°S)**. Environ. Microbiol. 9:1186–201.
- Pfeffer C, Larsen S, Song J, Dong M, Besenbacher F, Meyer RL, et al., (2012). **Filamentous bacteria transport electrons over centimetre distances**. Nature 491:218–21.
- Pischedda L, Cuny P, Esteves JL, Poggiale J-C, Gilbert F. (2011). **Spatial oxygen heterogeneity in a *Hediste diversicolor* irrigated burrow**. Hydrobiologia 680:109–124.
- Pjevac P, Kamyshny A, Dyksma S, Mussmann M. (2014). **Microbial consumption of zero-valence sulfur in marine benthic habitats**. Environ. Microbiol. 16(11): 3416–3430.
- Polerecky L, Adam B, Milucka J, Musat N, Vagner T, Kuypers MMM. (2012). **Look@ NanoSIMS - a tool for the analysis of nanoSIMS data in environmental microbiology**. Environ. Microbiol. 14:1009–23.
- Porter ET, Owens MS, Cornwell JC. (2006). **Effect of sediment manipulation on the biogeochemistry of experimental sediment systems**. J. Coast. Res. 226:1539–1551.
- Preisler A, de Beer D, Lichtschlag A, Lavik G, Boetius A, Jørgensen BB. (2007). **Biological and chemical sulfide oxidation in a *Beggiatoa* inhabited marine sediment**. ISME J. 1:341–53.

- Prosser JI (1989) *Autotrophic nitrification in bacteria*. Adv. Microb. Physiol. 30: 125-181.
- Purdy KJ, Nedwill DB, Embley TM, Takii S. (1997). *Use of 16S rRNA-targeted oligonucleotide probes to investigate the occurrence and selection of sulfate-reducing bacteria in response to nutrient addition to sediment slurry microcosms from a Japanese estuary*. FEMS Microbiol. Ecol. 24:221–234.
- Quast C, Pruesse E, Yilmaz P, Gerken J, Schweer T, Yarza P, et al., (2013). *The SILVA ribosomal RNA gene database project: Improved data processing and web-based tools*. Nucleic Acids Res. 41:D590–6.
- Quintana CO, Tang M, Kristensen E. (2007). *Simultaneous study of particle reworking, irrigation transport and reaction rates in sediment bioturbated by the polychaetes Heteromastus and Marenzelleria*. J. Exp. Mar. Bio. Ecol. 352:392–406.
- Quintana CO, Hansen T, Delefosse M, Banta G, Kristensen E. (2011). *Burrow ventilation and associated pore water irrigation by the polychaete Marenzelleria viridis*. J. Exp. Mar. Bio. Ecol. 397:179–187.
- Quintana CO, Kristensen E, Valdemarsen T. (2013). *Impact of the invasive polychaete Marenzelleria viridis on the biogeochemistry of sandy marine sediments*. Biogeochemistry 115:95–109.
- Rabus R, Hansen TA, Widdel F (2006) *Dissimilatory sulfate- and sulfur-reducing prokaryotes*. In: Dworkin M, Falkow S, Rosenberg E, Schleifer K-H, Stackebrandt E, (eds). The Prokaryotes 2ed. Berlin: Springer. pp. 659–768.
- Raven J. (2009). *Contributions of anoxygenic and oxygenic phototrophy and chemolithotrophy to carbon and oxygen fluxes in aquatic environments*. Aquat. Microb. Ecol. 56:177–192.
- Redfield AC (1958) *The biological control of the chemical factors in the environment*. Am. Sci. 46: 205-221.
- Reguera G, McCarthy KD, Mehta T, Nicoll JS, Tuominen MT, Lovley DR. (2005). *Extracellular electron transfer via microbial nanowires*. Nature 435:1098–101.
- Reichardt WT. (1988). *Impact of bioturbation by Arenicola marina on microbiological parameters in intertidal sediments*. Mar. Ecol. Prog. Ser. 44:149–158.
- Renz J, Forster S. (2014). *Effects of bioirrigation by the three sibling species of Marenzelleria spp. on solute fluxes and pore water nutrient profiles*. Mar. Ecol. Prog. Ser. 505:145–159.
- Risgaard-Petersen N, Nielsen LP, Rysgaard S, Dalsgaard T, Meyer RL (2003) *Application of the isotope pairing technique in sediments where anammox and denitrification coexist*. Limnol.Oceanog. Methods 1: 63-73.

- Risgaard-Petersen N, Revil A, Meister P, Nielsen LP. (2012). *Sulfur, iron-, and calcium cycling associated with natural electric currents running through marine sediment*. Geochim. Cosmochim. Acta 92:1–13.
- Robertson LA, Kuenen JG (2006) *The colorless sulfur bacteria*. In: Dworkin M, Falkow S, Rosenberg E, Schleifer K-H, Stackebrandt E, (eds). The prokaryotes 2ed. Berlin: Springer. pp. 985-1011.
- Romanenko VI (1964) *Heterotrophic assimilation of CO₂ by bacterial flora of water*. Microbiologiya 33: 610-614.
- Romanova ND, Sazhin a. F. (2010). *Relationships between the cell volume and the carbon content of bacteria*. Oceanology 50:522–530.
- Rosenberg R, Agrenius S, Hellman B, Nilsson HC, Norling K. (2002). *Recovery of marine benthic habitats and fauna in a Swedish fjord following improved oxygen conditions*. Mar. Ecol. Prog. Ser. 234:43–53.
- Roslev P, Larsen M, Jorgensen D, Hesselsoe M. (2004). *Use of heterotrophic CO₂ assimilation as a measure of metabolic activity in planktonic and sessile bacteria*. J. Microbiol. Methods 59:381–393.
- Saitou N, Nei M. (1987). *The neighbor-joining method: A new method for reconstructing phylogenetic trees*. Mol. Biol. Evol. 4:406–25.
- Sakata S, Hayes JM, Rohmer M, Hooper AB, Seemann M (2008) *Stable carbon-isotopic compositions of lipids isolated from the ammonia-oxidizing chemoautotroph Nitrosomonas europaea*. Org. Geochem. 39: 1725-1734.
- Salman V, Amann R, Girth AC, Polerecky L, Bailey J V, Høglund S, et al., (2011). *A single-cell sequencing approach to the classification of large, vacuolated sulfur bacteria*. Syst. Appl. Microbiol. 34:243–259.
- Salman V, Bailey J V, Teske A. (2013). *Phylogenetic and morphologic complexity of giant sulfur bacteria*. Antonie van Leeuwenhoek, Int. J. Gen. Mol. Microbiol. 104:169–186.
- Santoro AL, Bastviken D, Gudasz C, Tranvik L, Enrich-Prast A (2013) *Dark carbon fixation: An important process in lake sediments*. PLoS One 8: e65813.
- Sarda R, Valiela I, and Foreman K. (1995). *Life cycle, demography, and production of Marenzelleria viridis in a salt marsh of southern New England*. J. Mar. Biol. Assoc. U.K. 75:725–738.
- Savitzky A, Golay M. (1964). *Smoothing and differentiation of data by simplified least squares procedures*. Anal. Chem. 36:1627–1639.
- Sayama M, Risgaard-petersen N, Nielsen LP, Fossing H, Christensen PB. (2005). *Impact of bacterial NO₃⁻ transport on sediment biogeochemistry*. Appl. Environ. Microbiol. 71:7575–7577.

- Schauer R, Risgaard-Petersen N, Kjeldsen KU, Tataru Bjerg JJ, B Jørgensen B, Schramm A, et al., (2014). *Succession of cable bacteria and electric currents in marine sediment*. ISME J. 8:1314–1322.
- Schippers A, Kock D, Höft C, Köweker G, Siebert M. (2012). *Quantification of microbial communities in subsurface marine sediments of the Black Sea and off Namibia*. Front. Microbiol. 3:1–11.
- Schippers A. (2004). *Biogeochemistry of metal sulfide oxidation in mining environments, sediments, and soils*. Geol. Soc. Am. Special Paper 379: 49–62.
- Schloss PD, Westcott SL, Ryabin T, Hall JR, Hartmann M, Hollister EB, et al., (2009). *Introducing mothur: Open-source, platform-independent, community-supported software for describing and comparing microbial communities*. Appl. Environ. Microbiol. 75:7537–7541.
- Schulz HN, Jørgensen BB. (2001). *Big bacteria*. Annu. Rev. Microbiol. 55:105–137.
- Seitaj D, Schauer R, Sulu-Gambari F, Hidalgo-Martinez S, Malkin SY, Laurine DW, et al., (2015). *Cable bacteria in the sediments of seasonally-hypoxic basins : a microbial 'firewall' against euxinia*. PNAS 43: 13278-13283.
- Skyring GW (1987) *Sulfate reduction in coastal sediments*. Geomicrobiol. J. 5: 295-374.
- Smaal AC, Kater BJ, Wijsman J (2009) *Introduction, establishment and expansion of the Pacific oyster Crassostrea gigas in the Oosterschelde (SW Netherlands)*. Helgoland Mar. Res. 63: 75-83.
- Soetaert K, Herman PMJ, Middelburg JJ (1996) *A model of early diagenetic processes from the shelf to abyssal depths*. Geochim. Cosmochim. Acta 60: 1019-1040.
- Soetaert K, Petzoldt T, Meysman FJR. (2014). *Marelac: Tools for aquatic sciences v2.1.3*. R Package.
- Sorensen J, Christensen D, Jørgensen BB. (1981). *Volatile fatty acids and hydrogen as substrates for sulfate-reducing bacteria in anaerobic marine sediment*. Appl. Environ. Microbiol. 42:5–11.
- Sørensen H, Meire L, Juul-Pedersen T, de Stigter HC, Meysman FJR, Rysgaard S, et al., (2015). *Seasonal carbon cycling in a Greenlandic fjord: An integrated pelagic and benthic study*. MEPS 539:1–17.
- Sorokin YI (1972) *Bacterial populations and processes of hydrogen sulfide oxidation in the Black Sea*. J. Du Conseil 34:423-454.
- Sorokin DY, Lysenko a. M, Mityushina LL, Tourova TP, Jones BE, Rainey FA., et al., (2001). *Thioalkalimicrobium aerophilum gen. nov., sp. nov. and Thioalkalimicrobium sibericum sp. nov., and Thioalkalivibrio versutus gen. nov., sp. nov., Thioalkalivibrio nitratis sp. nov. and Thioalkalivibrio denitrificans sp. nov., novel obligately alkaliphilic*. Int. J. Syst. Evol. Microbiol. 51:565–580.

- Sorokin DY, Kovaleva OL, Tourova TP, Muyzer G. (2010). *Thiohalobacter thiocyanaticus* gen. nov., sp. nov., a moderately halophilic, sulfur-oxidizing gammaproteobacterium from hypersaline lakes, that utilizes thiocyanate. *Int. J. Syst. Evol. Microbiol.* 60:444–50.
- Sorokin DY, Kuenen JG, Muyzer G. (2011). *The microbial sulfur cycle at extremely haloalkaline conditions of soda lakes.* *Front. Microbiol.* 2:44
- Steward CC, Nold SC, David B, Lovell CR. (1996). *Microbial biomass and community structures in the burrows of bromophenol producing and non-producing marine worms and surrounding sediments.* *Mar. Ecol. Prog. Ser.* 133:149–165.
- Stocum ET, Plante CJ. (2006). *The effect of artificial defaunation on bacterial assemblages of intertidal sediments.* *J. Exp. Mar. Bio. Ecol.* 337:147–158.
- Stoeck T, Kröncke I, Duineveld G, Palojärvi A. (2002). *Phospholipid fatty acid profiles at depositional and non-depositional sites in the North Sea.* *Mar. Ecol. Prog. Ser.* 241:57–70.
- Sulu-Gambari F, Seitaj D, Meysman FJR, Schauer R, Polerecky L, Slomp CP. (2015). *Cable bacteria control iron–phosphorus dynamics in sediments of a coastal hypoxic basin.* *Environ. Sci. Technol.* in press
- Suzuki D, Ueki A, Amaishi A, Ueki K. (2007). *Desulfobulbus japonicus* sp. nov., a novel Gram-negative propionate-oxidizing, sulfate-reducing bacterium isolated from an estuarine sediment in Japan. *Int. J. Syst. Evol. Microbiol.* 57:849–55.
- Swan BK, Martinez-Garcia M, Preston CM, Sczyrba A, Woyke T, Lamy D, et al., (2011). *Potential for chemolithoautotrophy among ubiquitous bacteria lineages in the dark ocean.* *Science* 333:1296–300.
- Tabita FR (1999) *Microbial ribulose 1,5-bisphosphate carboxylase/oxygenase: A different perspective.* *Photosynth. Res.* 60: 1-28.
- Takai K, Campbell BJ, Cary SC, Oida H, Nunoura T, Hirayama H, et al., (2005). *Enzymatic and genetic characterization of carbon and energy metabolisms by deep-sea hydrothermal chemolithoautotrophic isolates of Epsilonproteobacteria* *Appl. Environ. Microbiol.* 71:7310–7320.
- Takai K, Suzuki M, Nakagawa S, Miyazaki M, Suzuki Y, Inagaki F, et al., (2006). *Sulfurimonas paralvinellae* sp. nov., a novel mesophilic, hydrogen- and sulfur-oxidizing chemolithoautotroph within the Epsilonproteobacteria isolated from a deep-sea hydrothermal vent polychaete nest, reclassification of *Thiomicrospira denitrificans* as *Sulfurimonas denitrificans* comb. nov. and emended description of the genus *Sulfurimonas*. *Int. J. Syst. Evol. Microbiol.* 56:1725–33.
- Tamura K, Peterson D, Peterson N, Stecher G, Nei M, et al., (2011) *MEGA5: Molecular Evolutionary Genetics Analysis using maximum likelihood, evolutionary distance, and maximum parsimony methods.* *Molecular Biology and Evolution* 28: 2731-2739.

- Taylor J, Parkes RJ (1983) *The cellular fatty-acids of the sulfate-reducing bacteria, Desulfobacter sp, Desulfobulbus sp and Desulfovibrio desulfuricans*. J Gen Microbiol 129: 3303-3309.
- Thamdrup B, Canfield DE. (1996). *Pathways of carbon oxidation in continental margin sediments off central Chile*. Limnol. Oceanogr. 41:1629–50.
- Thomsen U, Kristensen E (1997) *Dynamics of ΣCO_2 in a surficial sandy marine sediment: The role of chemoautotrophy*. Aquat. Microb. Ecol. 12: 165-176.
- Timmer-Ten Hoor A (1981) *Cell yield and bioenergetics of Thiomicrospira denitrificans compared to Thiobacillus denitrificans*. Anton. Van Leeuw. 47: 231-243.
- Trimmer M, Nicholls JC, Deflandre B (2003) *Anaerobic ammonium oxidation measured in sediments along the Thames estuary, United Kingdom*. Appl. Environ. Microbiol. 69: 6447-6454.
- Tsutsumi H, Wainright S, Montani S, Saga M, Ichihara S, Kogure K. (2001). *Exploitation of a chemosynthetic food resource by the polychaete Capitella sp. I*. Mar. Ecol. Prog. Ser. 216:119–127.
- Tuttle JH, Jannasch HW (1979) *Microbial dark assimilation of CO_2 in the Cariaco Trench*. Limnol.Oceanog. 24: 746-753.
- Tuttle JH, Jannasch HW. (1973). *Sulfide and thiosulfate-oxidizing bacteria in anoxic marine basins*. Mar. Biol. 70:64–70.
- Upton AC, Nedwell DB, Parkes RJ, Harvey SM. (1993). *Seasonal benthic microbial activity in the southern North Sea: Oxygen uptake and sulfate reduction*. Mar Ecol Prog Ser 101:273–281.
- Van Frausum J, Middelburg JJ, Soetaert K, Meysman FJR (2010) *Different proxies for the reactivity of aquatic sediments towards oxygen: A model assessment*. Ecol. Model. 221: 2054-2067.
- Van Gaever S, Moodley L, Pasotti F, Houtekamer M, Middelburg JJ, et al., (2009) *Trophic specialisation of metazoan meiofauna at the Håkon Mosby mud volcano: Fatty acid biomarker isotope evidence*. Mar. Bio. 156: 1289-1296.
- Van Kessel MAHJ, Speth DR, Albertsen M, Nielsen PH, Op den Camp HJM, Kartal B, et al., (2015). *Complete nitrification by a single micro-organism*. Nature 528:555–559.
- Vaquier-Sunyer R, Duarte C. (2008). *Thresholds of hypoxia for marine biodiversity*. Proc. Natl. Acad. Sci. U.S.A. 105:15452–7.
- Vestal JR, White DC. (1989). *Lipid analysis in microbial ecology*. Bioscience 39:535–541.
- Webster G, Watt LC, Rinna J, Fry JC, Evershed RP, Parkes RJ, et al., (2006). *A comparison of stable-isotope probing of DNA and phospholipid fatty acids to study prokaryotic functional diversity in sulfate-reducing marine sediment enrichment slurries*. Environ. Microbiol. 8:1575–1589.

- Weerman E. (2011). *Spatial patterns in phototrophic biofilms: the role of physical and biological interactions*. PhD Dissertation. Radboud Universiteit Nijmegen.
- Wegener G, Bausch M, Holler T, Thang NM, Mollar XP, Kellermann MY, et al., (2012). *Assessing sub-seafloor microbial activity by combined stable isotope probing with deuterated water and ^{13}C -bicarbonate*. Environ. Microbiol. 14:1517–1527.
- Werner JJ, Koren O, Hugenholtz P, DeSantis TZ, Walters WA, Caporaso JG, et al., (2012). *Impact of training sets on classification of high-throughput bacterial 16S rRNA gene surveys*. ISME J. 6:94–103.
- Widdel F, Pfennig N. (1982). *Studies on dissimilatory sulfate-reducing bacteria that decompose fatty acids II. Incomplete oxidation of propionate by *Desulfobulbus propionicus* gen. nov., sp. nov.* Arch. Microbiol. 131:360–365.
- Williams L A., Reimers C. (1983). *Role of bacterial mats in oxygen-deficient marine basins and coastal upwelling regimes: Preliminary report*. Geology 11:267–269.
- Wirsen CO, Jannasch HW, Molyneux S. (1993). *Chemosynthetic microbial activity at mid-Atlantic ridge hydrothermal vent sites*. J. Geophys. Res. 98:9693–9703.
- Wright KE, Williamson C, Grasby SE, Spear JR, Templeton AS. (2013). *Metagenomic evidence for sulfur lithotrophy by Epsilonproteobacteria as the major energy source for primary productivity in a sub-aerial arctic glacial deposit, Borup Fiord Pass*. Front. Microbiol. 4:63.
- Wuchter C, Schouten S, Boschker HTS, Damste JSS (2003) *Bicarbonate uptake by marine Crenarchaeota*. Fems Microbiology Letters 219: 203-207.
- Yamamoto M, Takai K. (2011). *Sulfur metabolisms in Epsilon- and Gammaproteobacteria in deep-sea hydrothermal fields*. Front. Microbiol. 2:192.
- Zhang CL, Huang Z, Cantu J, Pancost RD, Brigmon RL, Lyons TW, et al., (2005). *Lipid biomarkers and carbon isotope signatures of a microbial (*Beggiatoa*) mat associated with gas hydrates in the Gulf of Mexico*. Appl. Environ. Microbiol. 71:2106–2112.
- Zopfi J, Ferdelman TG, Fossing H. (2004). *Thiosulfate, and elemental sulfur in marine sediments*. Geol. Soc. Am. 379:97–116.
- Zuckerandl E, Pauling L. (1965). *Evolutionary divergence and convergence in proteins*. In: V. Bryson and HJ Vogel (eds), Evolving Genes and Proteins. Acad. Press. New York 97–166.

Acknowledgements

The past years have been a steep learning curve both in life and research, mostly brought about by the numerous people that crossed my path. Now that my thesis is ending I wish to thank my family, friends, and colleagues without whom I would have never been able to achieve this feat.

I thank my supervisors, especially Eric for remembering that Colombian Masters student that oddly enough wanted to work on chemoautotrophy in Yerseke. It has been my pleasure to work alongside you from beginning to end of this research project, and I foresee this collaboration will not be our last. I thank Filip for inadvertently showing me the inner working of science and insisting until the end that when communicating science one must have a clear and interesting story which should take the reader by the hand (easier said than done). Finally I thank Lucas for his support during my PhD and for being living proof that in science “the world *is* our playground” and that it is up to us to play.

I thank my family: Sin el apoyo y enseñanzas de ti Ma y Pa para perseguir mis sueños nunca habría llegado tan lejos, gracias por inculcarme que era posible vivir de mi hobby, la ciencia. A mis hermanas, Margara y Ale, les agradezco su apoyo incondicional desde cada rincón del mundo; nuestras diferencias hacen posible que juntas-de-lejos, tengamos mas fuerza para conquistar nuestras metas. Muchas gracias especialmente a Ale por sus conocimientos editoriales, espíritu creativo, y largas noches detrás de su computador editando esta Tesis. Luna te agradezco tus sonrisas, canciones, arrebatos, abrazos y chistes, sin ti no habría logrado acabar esta tesis con calma y carcajadas, pues con tu llegada se pusieron en claro las prioridades de mi vida. Thea, Jaime y Moos I thank you for taking me into your family and making me feel at home amongst all the (back then) strange Dutch customs. Francesc, since the beginning we have been colleagues in science and allies in life, thank you for all your ramblings and silliness, but most of all for your endless desire to dream about everything, every time, everywhere. Happy anniversary Amor!

Moreover, I must thank my extended De Keete family, because you made my life in Yerseke interesting and dynamic, filled with fine European cuisine against all odds given the location of the NIOZ. Dorina, the quiet Albanian that had little to say in the beginning but soon had a tenacious opinion about the world, a strong scientific mind, wrapped around a sweet heart that quickly made you into more than just a friend. Christine, you were of

the few friendly faces in Amsterdam my first year in Holland, and after Curacao I think it was clear our lives would continue to cross paths. Eight years since then, 2 Masters degrees, 2 PhDs, 2 ½ munchkins and ever changing plans for our living situations, I thank you for your unconditional friendship. Silvia, gracias por tu gran voluntad, dulce gentiliza e inagotable buen humor pues con ello lograste ganarte mis abrazos y besitacos. Sven thank you for all the late-night talks trying to solve our “luxury” problems and decipher our uncertain existence, I hope your new path in life will bring you answers, and even more so, new questions to discuss together. Miche thank you for your smiles, your good humor, your uncensored stories and even your stubbornness, they make you unique and unforgettable, but most of all I thank you for not pursuing this PhD research project which has brought me so much satisfaction. And the lovely Juliette who always had something to do and somewhere to be, thank you for always being there even before we met in person; your good nature, never ending smiles and desire to try (have) everything are always a reminder that life is dynamic and we should dance with it, not against it. To all my other Keete roommates (Yayu, Heiko, Hélène, Vanessa, Kris, Tadao, Zhu, Zhigang, Hui, Lara, Roger) you have given me many colorful memories, it was truthfully *gezellig* and enriching to share my daily life with such a culturally diverse group of friends.

I would also like to thank all the Electro team members (past and present) for sharing your knowledge, curiosity and thoughts with each other to further science, it seems we may now be on our way to figuring out if the cable bacteria truly are responsible for this mysterious pH peak that had never been studied until the Danes came up with long distance electron transport. Yvonne thank you for your willingness to work together, I learned a lot about the molecular world alongside you and I am glad that in the end we had an interesting story to share. I also thank my students: Sinem, Bekir, Eefje, Casper, Yorick, because in their unique ways each one contributed to the making of this thesis. Moreover, I thank Peter van Breugel and Tanja M. for your insightful conversations about life, kids, travelling and gardening that did not merely make the tedious afternoons behind my computer bearable but mostly enriched my daily life outside of the NIOZ.

I lastly thank my Professors and friends back home. German, Gabriel y Juan Pablo sin su ejemplo y determinación como investigadores en un país como Colombia y su confianza en mis capacidades, no creo que me habría lanzado a perseguir un futuro como científica. A Mario, Mayra, y Diego les debo mas que mi amistad, nuestras largas tardes hablando sobre la vida y nuestros planes para el futuro, y las infinitas horas de trabajo de campo y detrás de un computador “haciendo ciencia”, sentaron la base para esta aventura que ahora culmina.

Gracias, Saludos, y hasta la próxima,

Diana Vasquez C.

Curriculum vitae

Email diana.vasquez@nioz.nl / dianavasquezcardenas@yahoo.com
Nationality Colombian
Date of birth April 28, 1980
Place of birth Bogotá, Colombia
Mobile phone +31-627402834

EDUCATION

2011 – 2016 **PhD student** - Marine Microbiology Department, Royal Netherlands Institute for Sea Research (NIOZ) – the Netherlands
2008 – 2010 **MSc Biological Sciences Cum Laude** in the program of Limnology and Oceanography at the University of Amsterdam – the Netherlands
2000 – 2006 **Bachelors in Marine Biology** with Academic Excellency awarded at the Universidad Jorge Tadeo Lozano – Colombia

PUBLICATIONS

Vasquez-Cardenas D, Quintana C, Meysman FJR, Kristensen E, Boschker HTS. Species-specific effects of two bioturbating polychaetes on sediment chemoautotrophic bacteria. MEPS (in press doi: 10.3354/meps11679)
Vasquez-Cardenas D, van de Vossenberg J, Polerecky L, Malkin SY, Schauer R, Hidalgo-Martinez S, et al., (2015). Microbial carbon metabolism associated with electrogenic sulfur oxidation in coastal sediments. ISME J. .
Boschker HTS, **Vasquez-Cardenas D**, Bolhuis H, Moerdijk-Poortvliet TWC, Moodley L. (2014). Chemoautotrophic carbon fixation rates and active bacterial communities in intertidal marine sediments. PLoS One 9:e101443.
Kunihiro T, Veuger B, **Vasquez-Cardenas D**, Pozzato L, Le Guitton M, Moriya K, et al., (2014). Phospholipid-derived Fatty acids and quinones as markers for bacterial biomass and community structure in marine sediments. PLoS One 9:e96219.
Malkin SY, Rao AM, Seitaj D, **Vasquez-Cardenas D**, Zetsche EM, Hidalgo-Martinez S, et al., (2014). Natural occurrence of microbial sulfur oxidation by long-range electron transport in the seafloor. ISME J. 8:1843–54.

CONFERENCES AND WORKSHOPS (Selection)

Session chair

Key players in benthic processes: micro vs macro. Co-chair: F. Montserrat ASLO 2015
Granada, Spain, 22-27 February 2015

Oral

Vasquez-Cardenas, D., Meysman, F.J.R., van Breugel, P., Boschker, H.T.S. Sediment chemoautotrophy in the coastal ocean. EGU. Vienna, Austria 17-22 April 2016.

Vasquez-Cardenas D, van de Vossenberg J, Polerecky L, Malkin SY, Schauer R, Hidalgo-Martinez S, et al., Microbial carbon metabolism associated with electrogenic sulfur oxidation in coastal sediments. EMBO Workshop on Microbial Sulfur Metabolism. Helsingør, Denmark 12-15 April 2015. (Prize for best student presentation)

Vasquez-Cardenas, D., Malkin, S., Faydaci, B., Meysman, F.J.R., Boschker, H.T.S. ¹³C-labelling of biomarkers: Unravelling a novel bacterial consortium in marine sediment. Benelux Association of Stable Isotope Scientists (BASIS) Gent, Belgium. 25-26 April 2013. (Prize for best student presentation)

Vasquez-Cardenas, D., Schauer, R., Hidalgo, S., Atli S., Confurius, V., Meysman, F.J.R., Boschker, H.T.S. Chemoautotrophy associated with microbial sulfide oxidation by long-distance electron transport in coastal sediment. Annual Conference of the Association for General and Applied Microbiology (VAAM) in collaboration with the Royal Netherlands Society for Microbiology (KNVM), Bremen, Germany. 10-13 March 2013

Poster

Vasquez-Cardenas, D., S. Malkin, S., Polerecky, L., Meysman, F.J.R., Boschker, H.T.S. Carbon metabolism in hypoxic sediments showing long-range microbial electron transport by cable bacteria. ASLO conference, Honolulu, Hawaii, USA. 23-28 February 2014

Vasquez-Cardenas, D., Malkin, S., Schauer, R., Hidalgo, S., Meysman, F.J.R., Boschker, H.T.S. Carbon metabolisms associated to electrogenic sulfide oxidation in coastal sediment. First EMBO Conference on Aquatic Microbial Ecology: SAME13 Stresa, Italy. 8-13 September 2013

Vasquez-Cardenas, D., Meysman, F.J.R., Boschker, H.T.S, Chemoautotrophy and reoxidation in coastal sediments. Marine Microbes Gordon Research Seminar. Lucca, Italy. 23-24 July 2012

Vasquez-Cardenas, D., Meysman, F.J.R., Boschker, H.T.S, Stal L. Reoxidation and chemoautotrophy in coastal sediment ecosystems: rates, regulation and microbial players Darwin days 2011. Darwin Center for Biogeosciences. Netherlands February 2011 (Prize for best poster)

